

IMPERIAL COLLEGE OF SCIENCE AND TECHNOLOGY

Department of Aeronautics,

Prince Consort Road, London, SW7 2BY

I.C Aero TN 87-102

June 1987

Vortex/Boundary-Layer Interactions: Data Report.

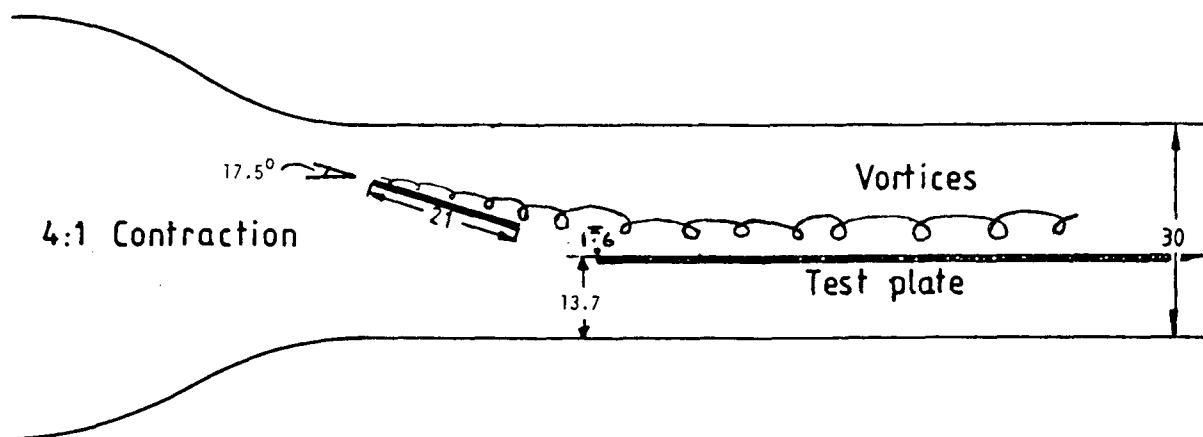
Final Report on NASA grant NAGw-581

A.D. Cutler and P. Bradshaw

Vol 2 of 2 (Figs.)

#### SUMMARY

This report summarizes the work done under NASA grant NAGw-581 "Vortex/Boundary-Layer Interactions" at the time of departure of the research assistant, Dr Cutler. The experimental methods are discussed in detail and the results are presented as a large number of figures, but are not interpreted in detail. This report should be useful to anyone who wishes to make further use of the data (which are available on floppy disc or magnetic tape) for the development of turbulence models or the validation of predictive methods. Journal papers are in course of preparation.



Dimensions in inches

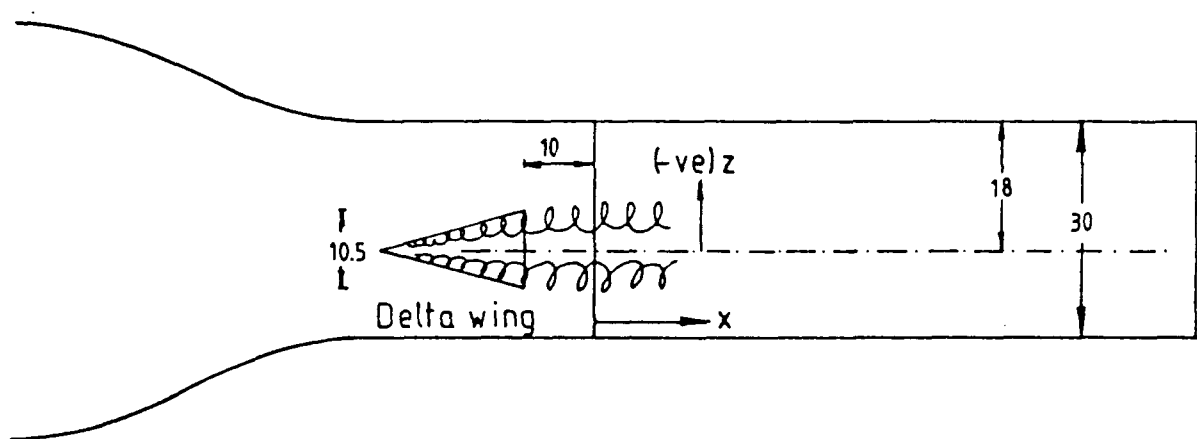
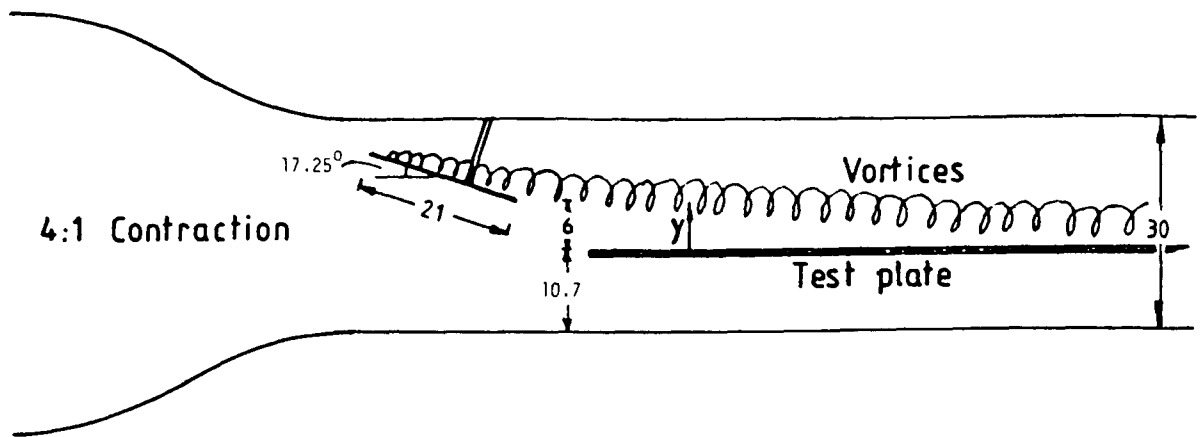
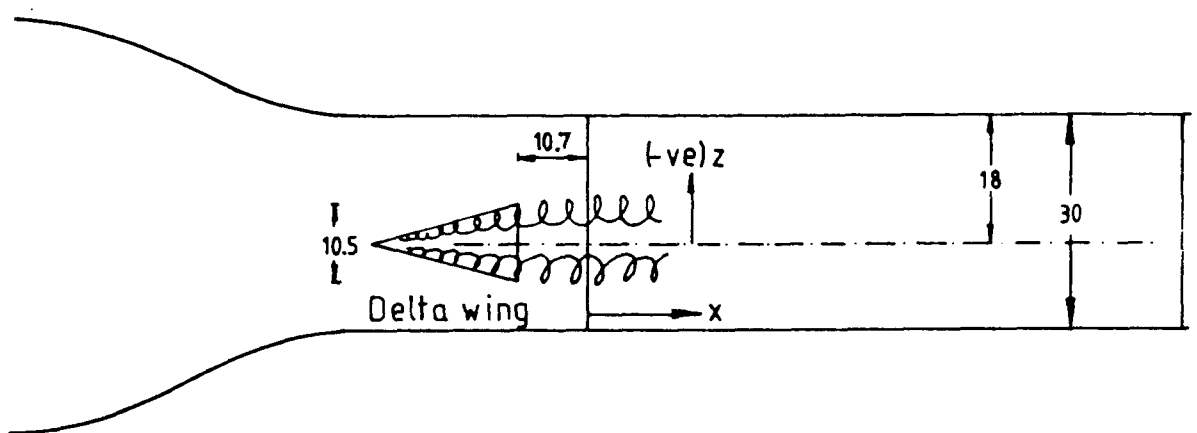


Figure 1. Wind tunnel working section with delta-wing vortex generator and test plate:

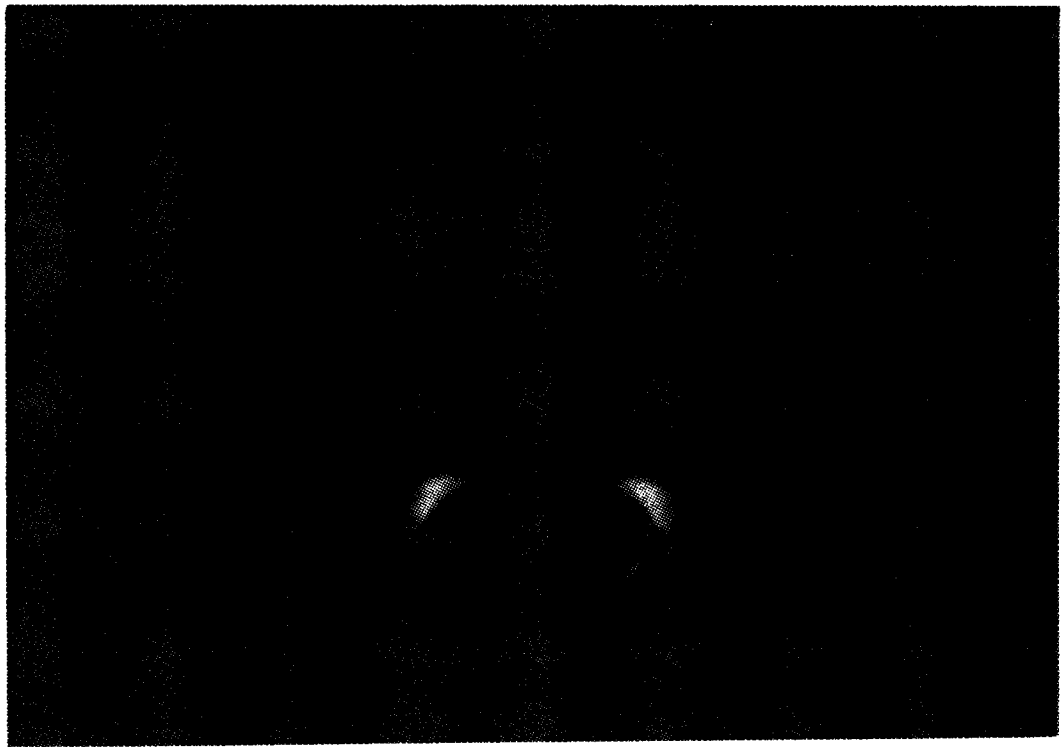
1(a) "delta-wing low" case



Dimensions in inches

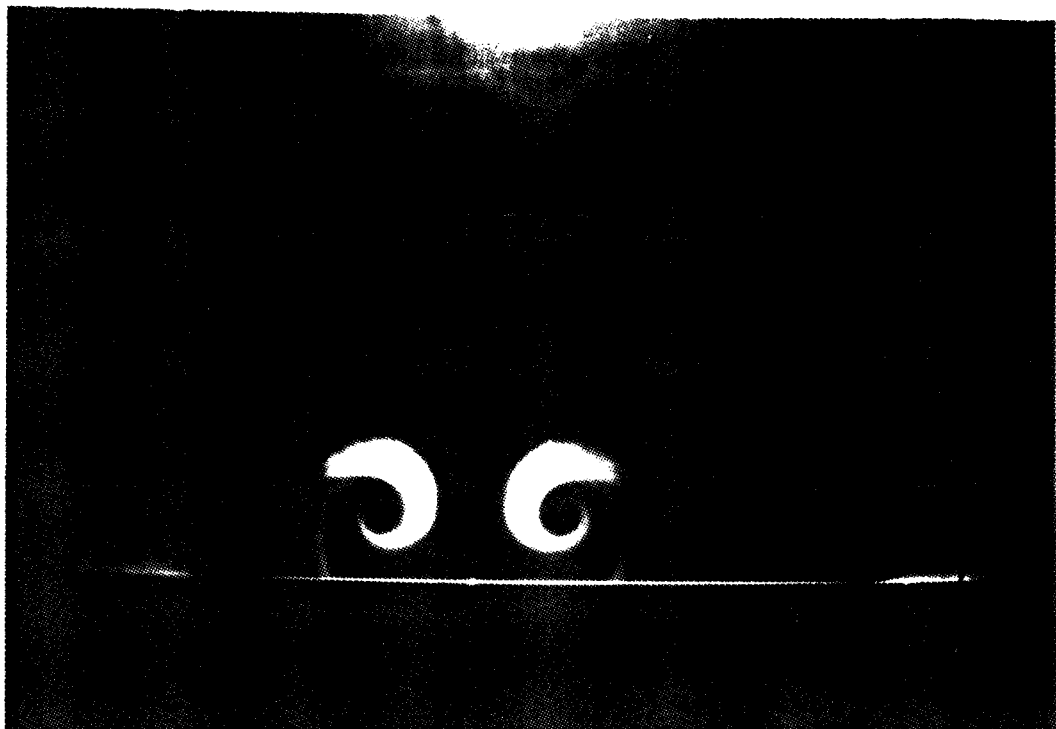


1(b) "delta-wing high" case.



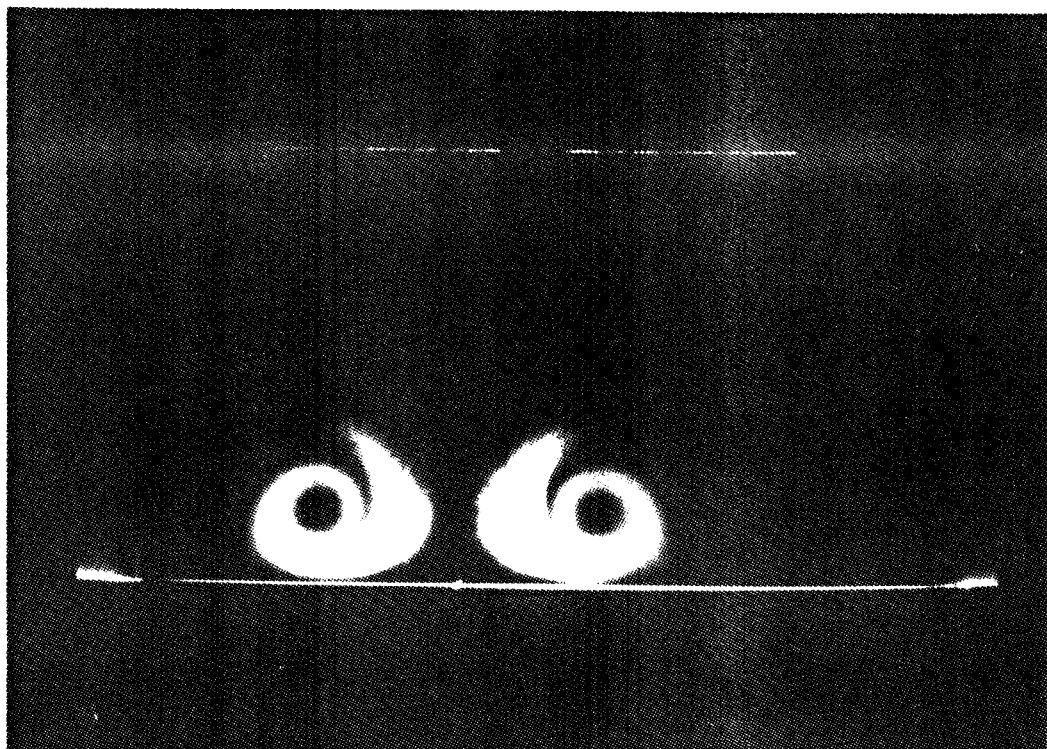
2(a)  $x/s = 0$

ORIGINAL PAGE IS  
OF POOR QUALITY



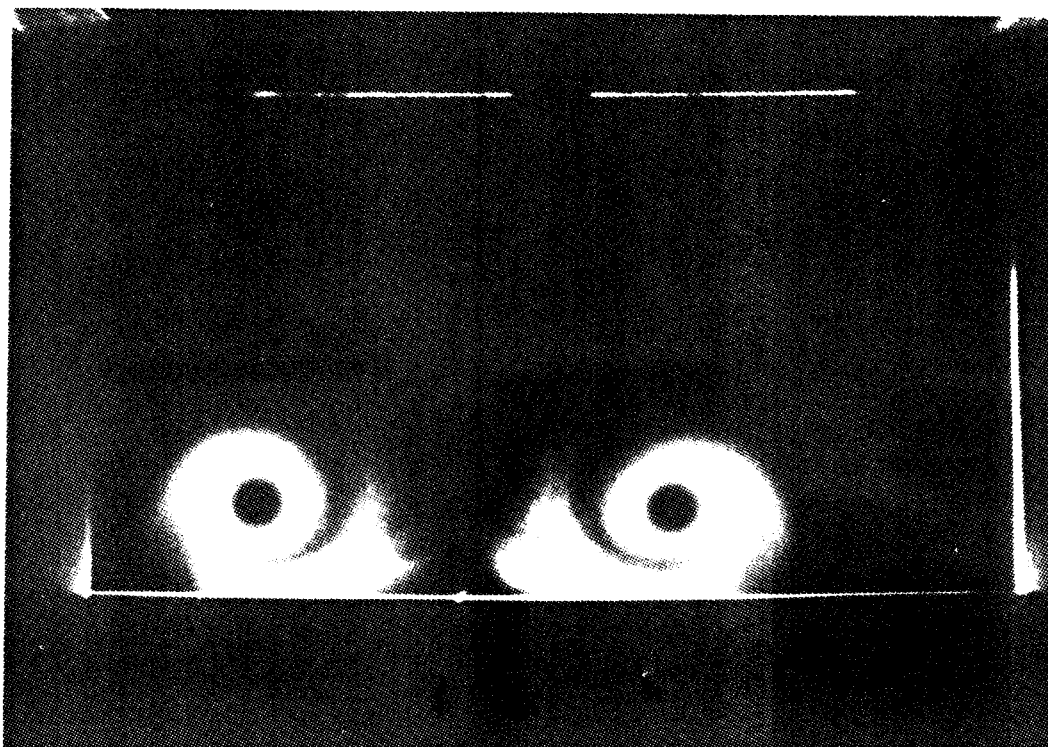
2(b)  $x/s = 0.690$

Figure 2. Smoke flow-visualization (viewed from downstream) for the "delta-wing low" case with the smoke introduced at the trailing edge of the delta-wing.

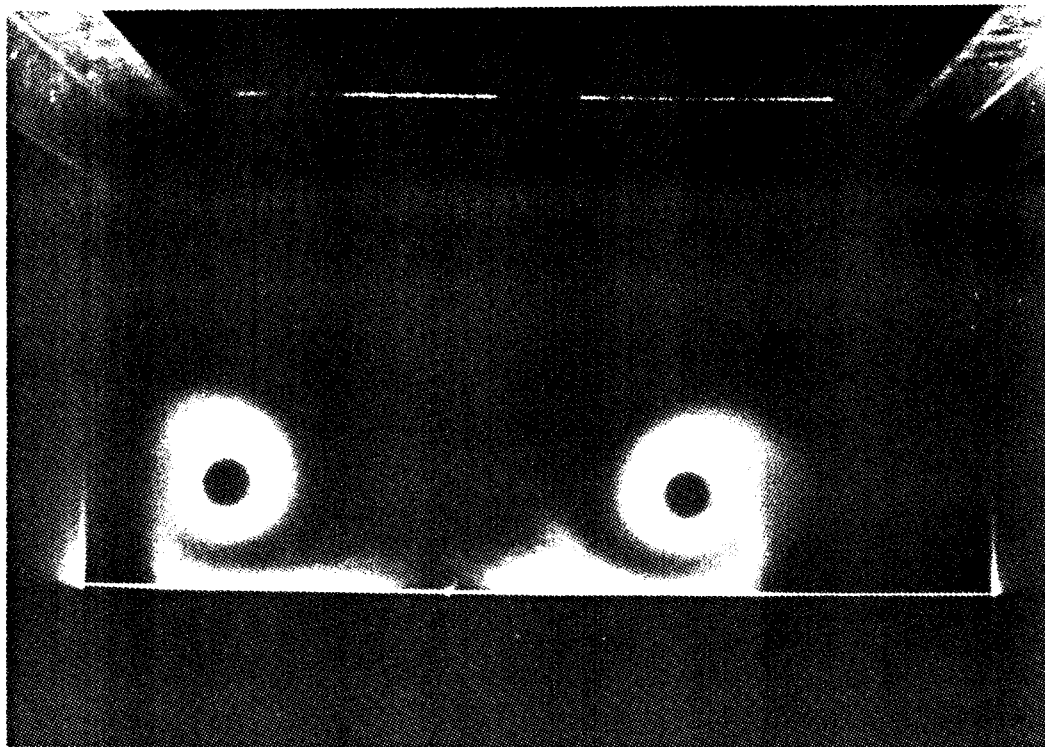


2(c)  $x/s = 1.833$

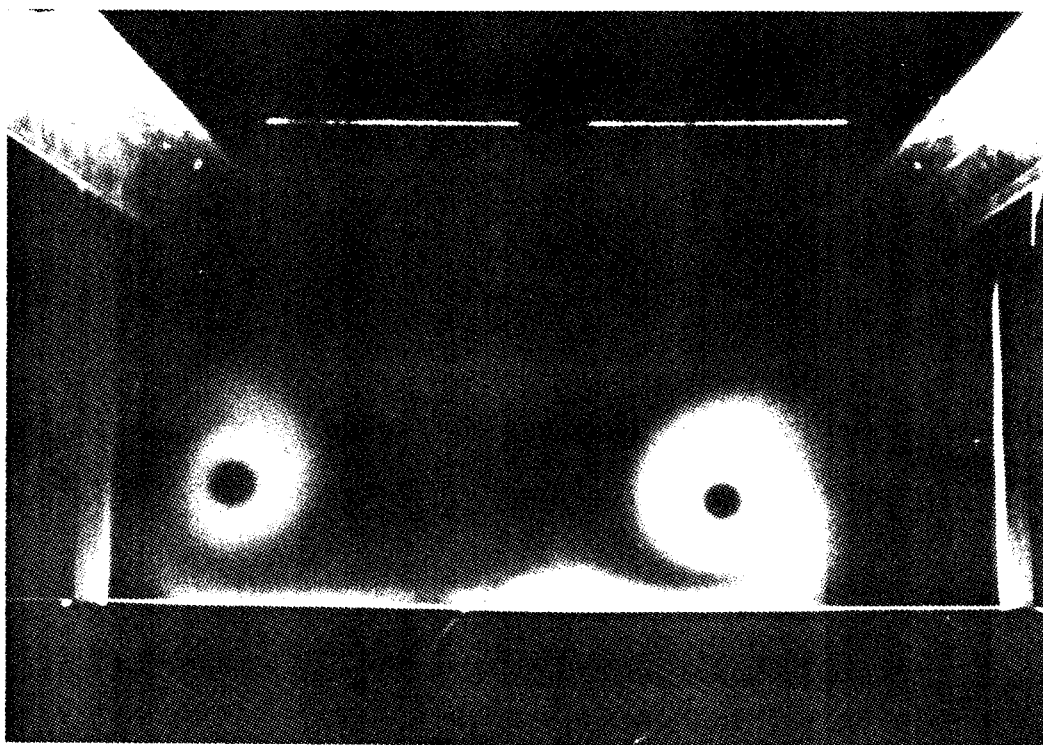
ORIGINAL PAGE IS  
OF POOR QUALITY



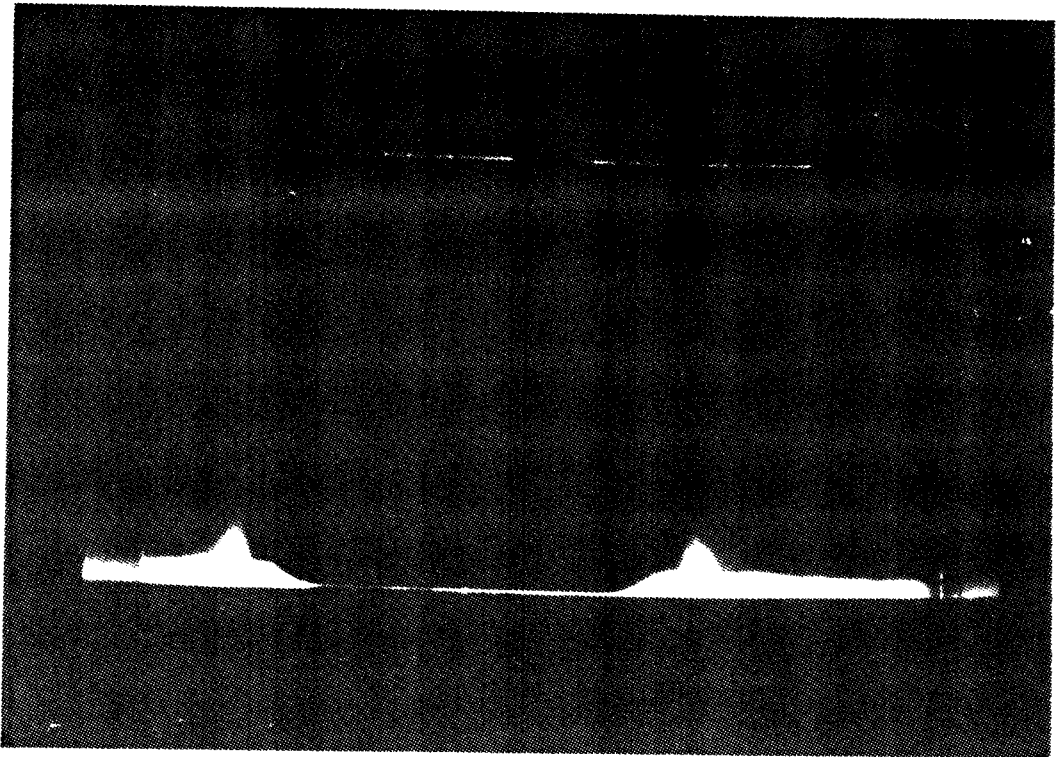
2(d)  $x/s = 2.976$



2(e)  $x/s = 4.119$  ORIGINAL PAGE IS  
OF POOR QUALITY

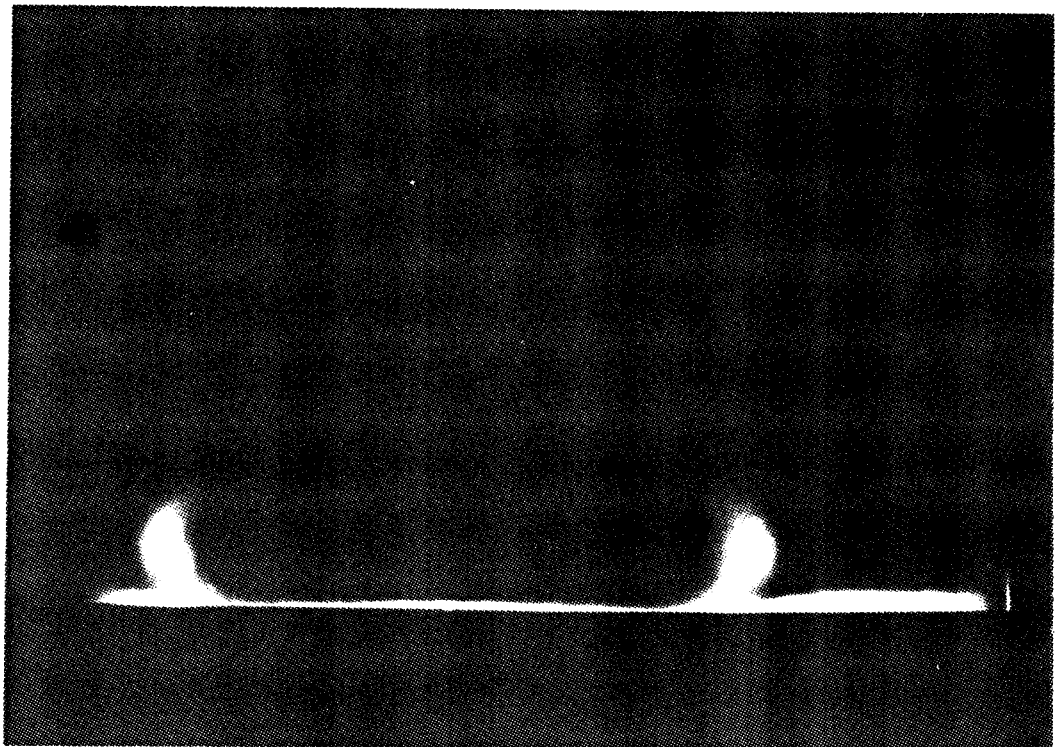


2(f)  $x/s = 5.262$



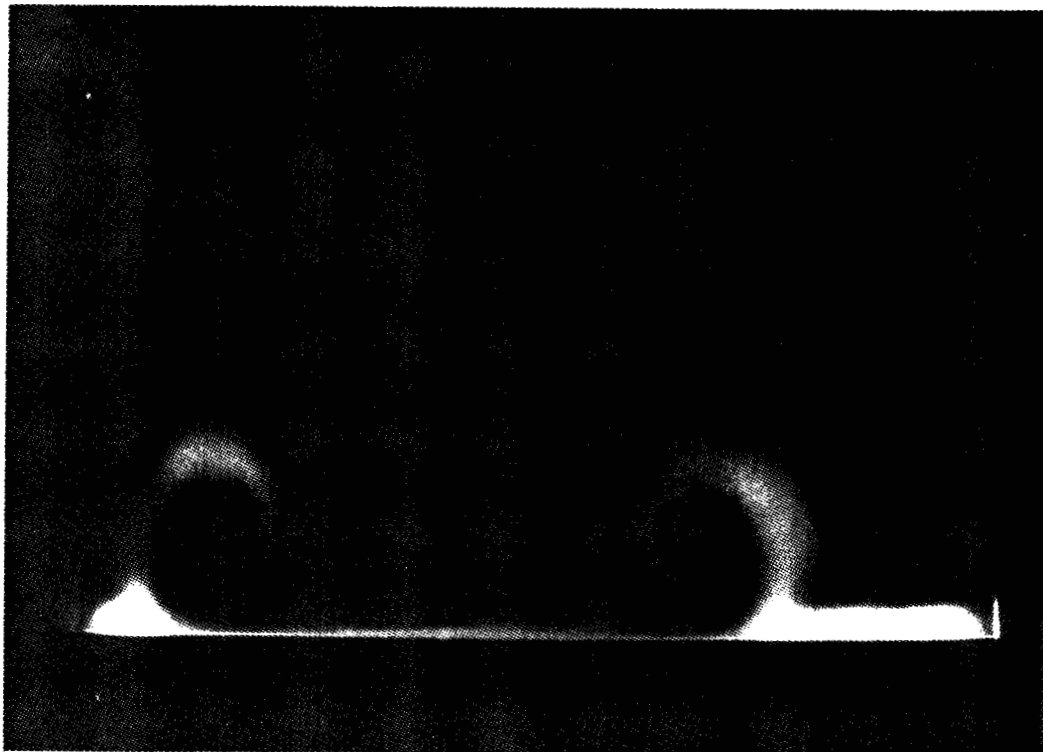
3(a)  $x/s = 1.833$

ORIGINAL PAGE IS  
OF POOR QUALITY



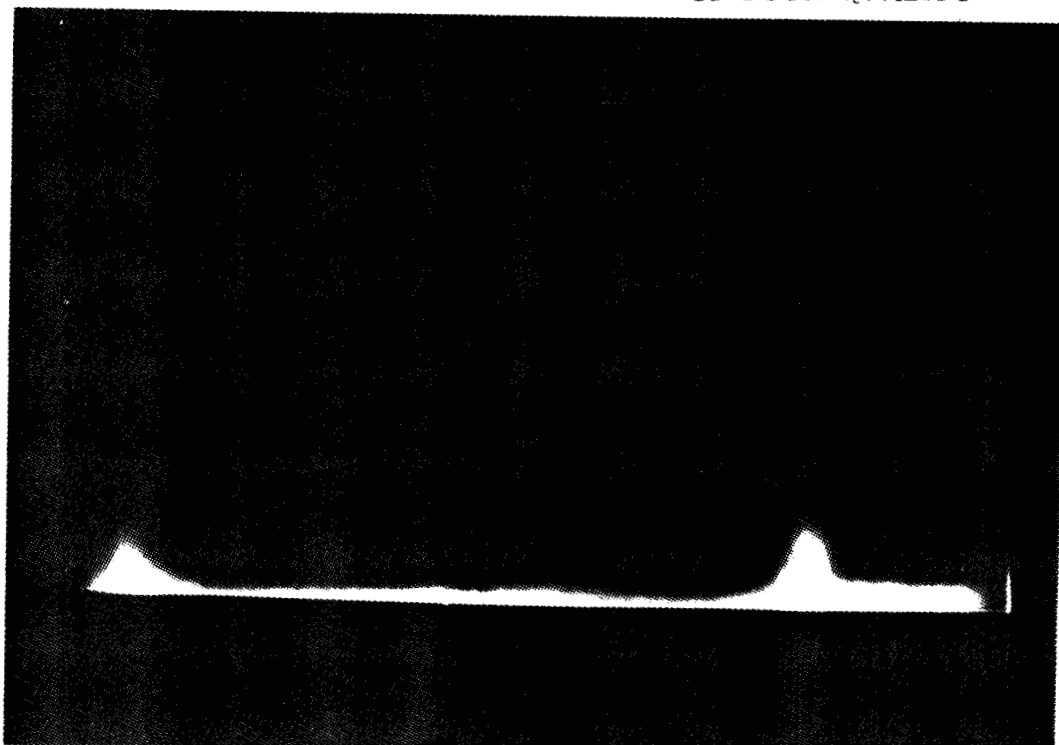
3(b)  $x/s = 2.976$

Figure 3. Smoke flow-visualization (viewed from downstream) for the "delta-wing low" case with the smoke introduced into the boundary layer.

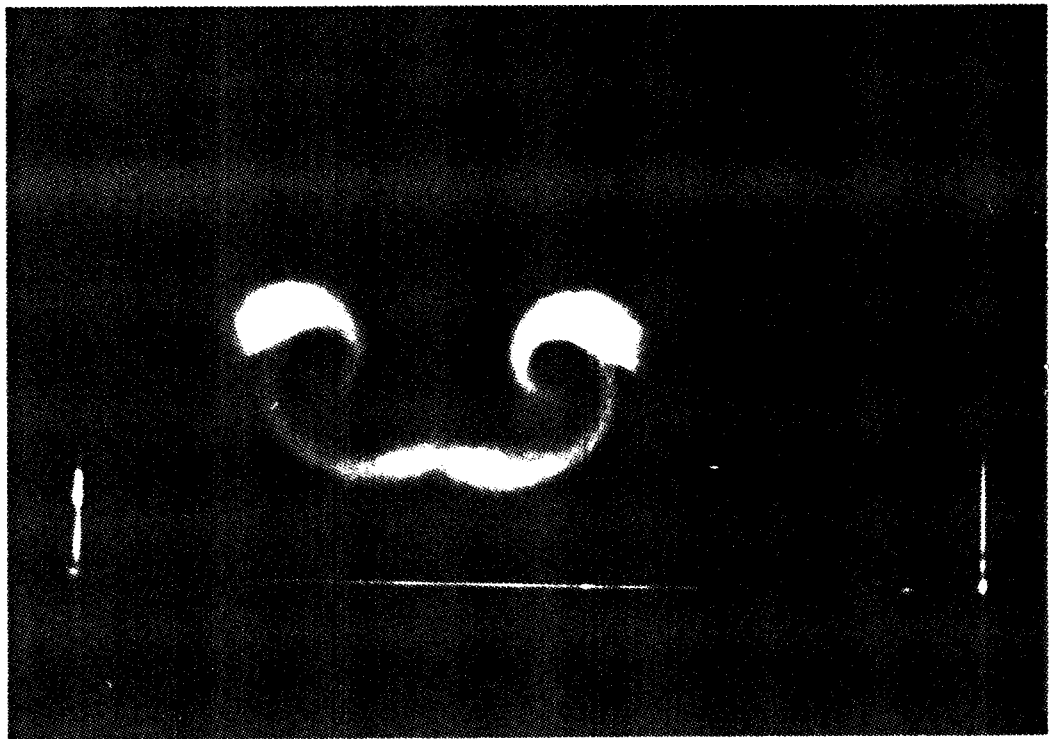


3(c)  $x/s = 4.119$

ORIGINAL PAGE IS  
OF POOR QUALITY



3(d)  $x/s = 5.262$



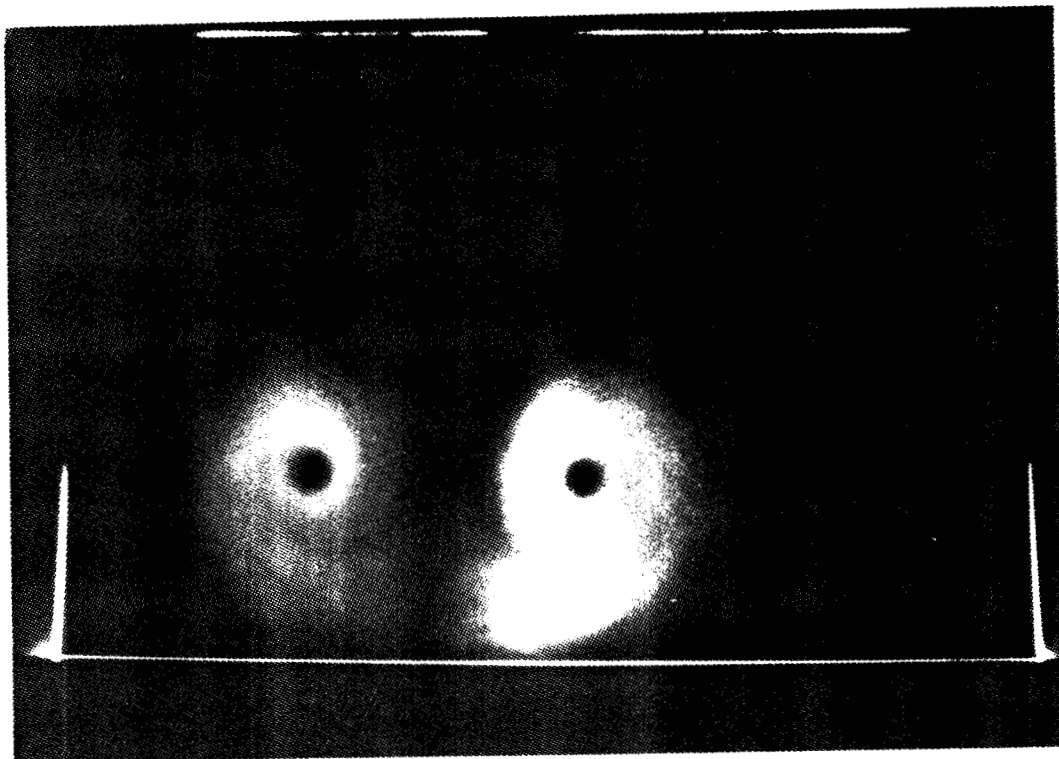
4(a)  $x/s = 0.095$

ORIGINAL PAGE IS  
OF POOR QUALITY



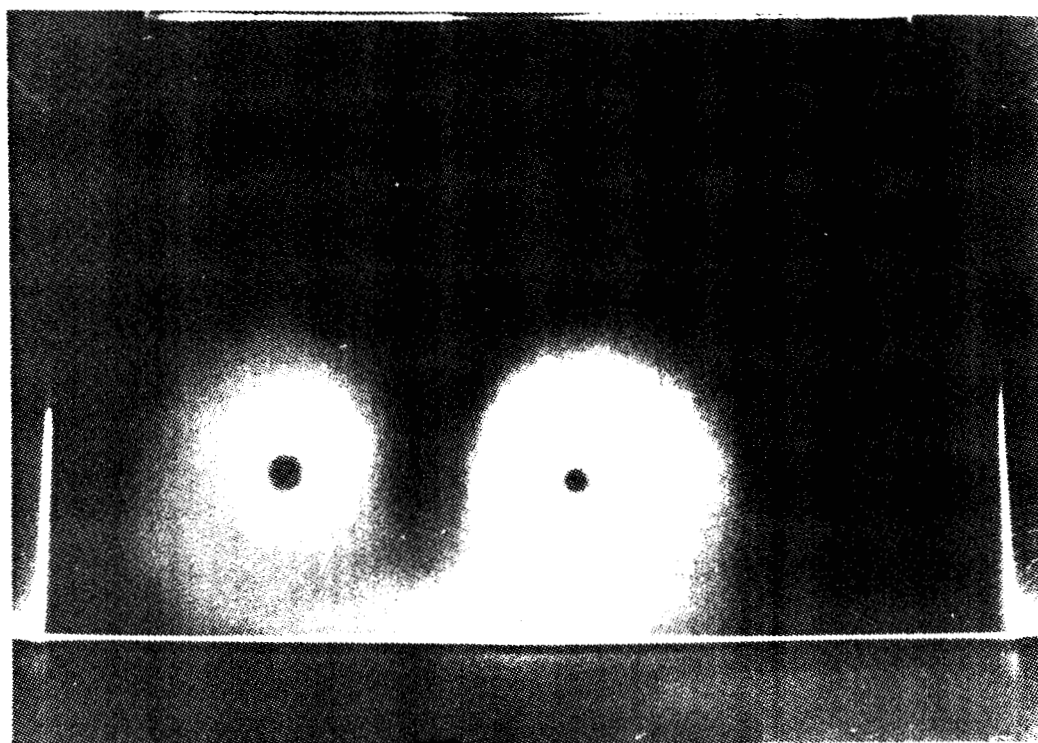
4(b)  $x/s = 1.524$

Figure 4. Smoke flow-visualization (viewed from downstream) for the "delta-wing high" case with the smoke introduced at the trailing edge of the delta-wing.



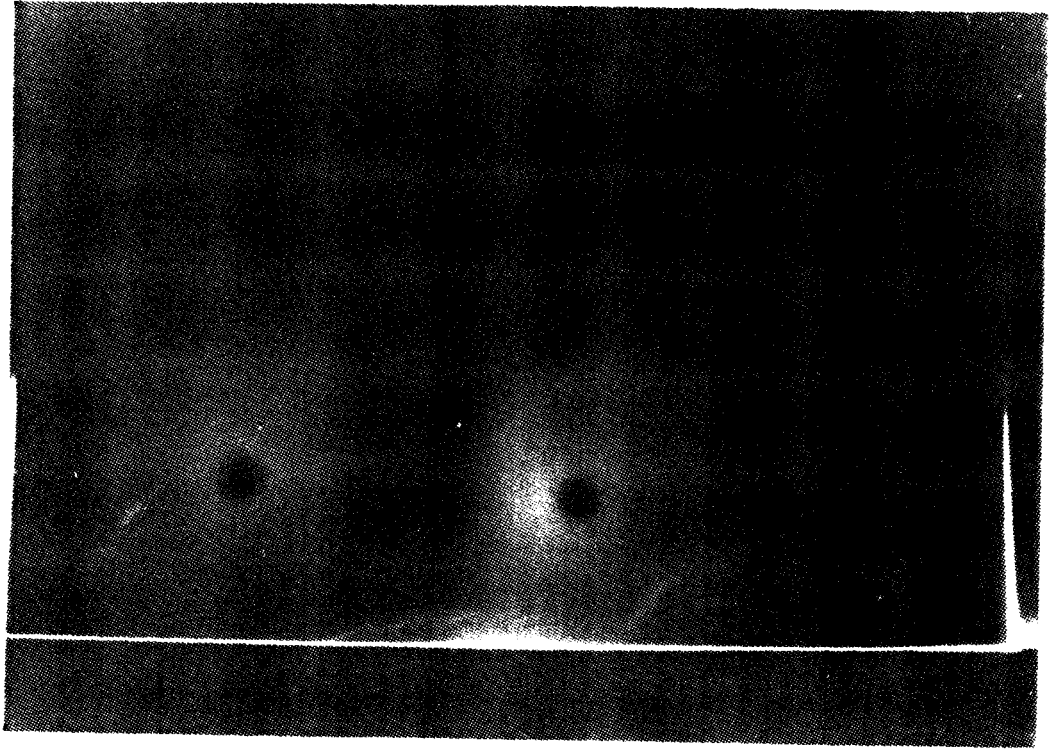
4(c)  $x/s = 3.238$

ORIGINAL PAGE IS  
OF POOR QUALITY



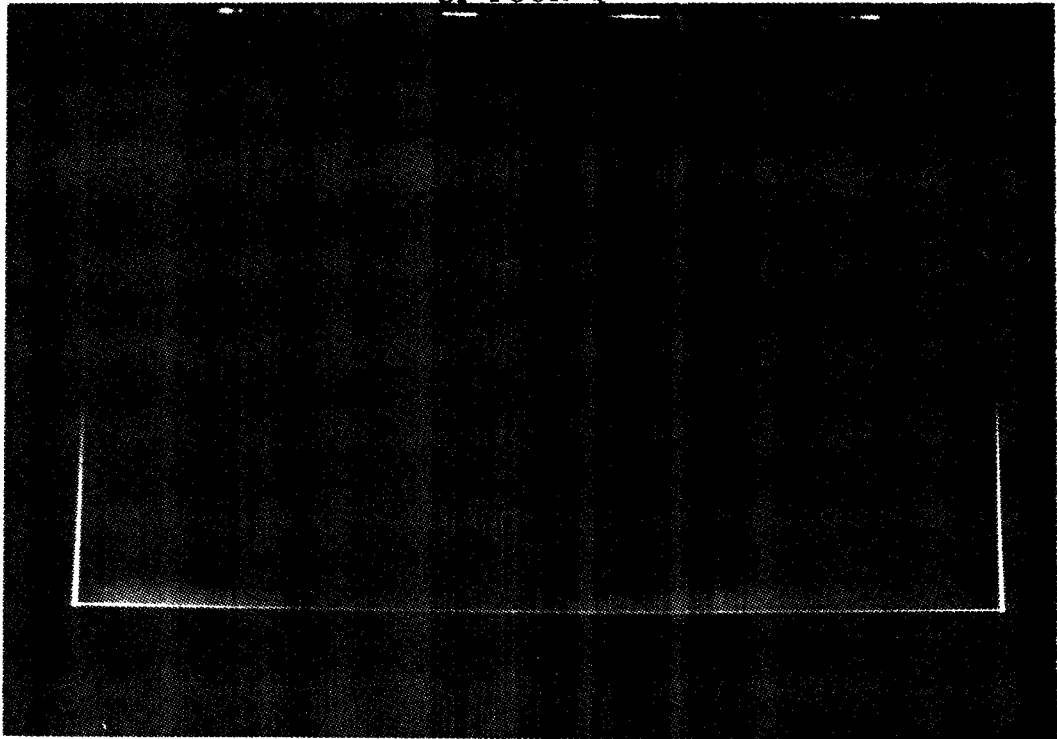
4(d)  $x/s = 4.952$

ORIGINAL PAGE IS  
OF POOR QUALITY

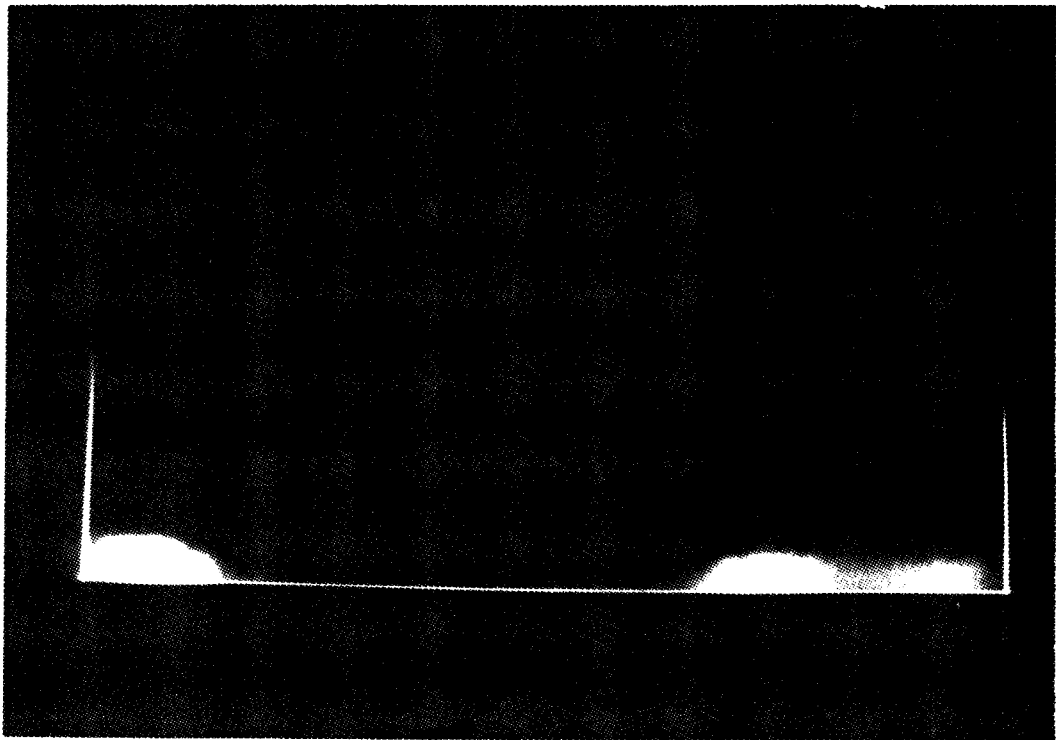


4(e)  $x/s = 6.667$

ORIGINAL PAGE IS  
OF POOR QUALITY



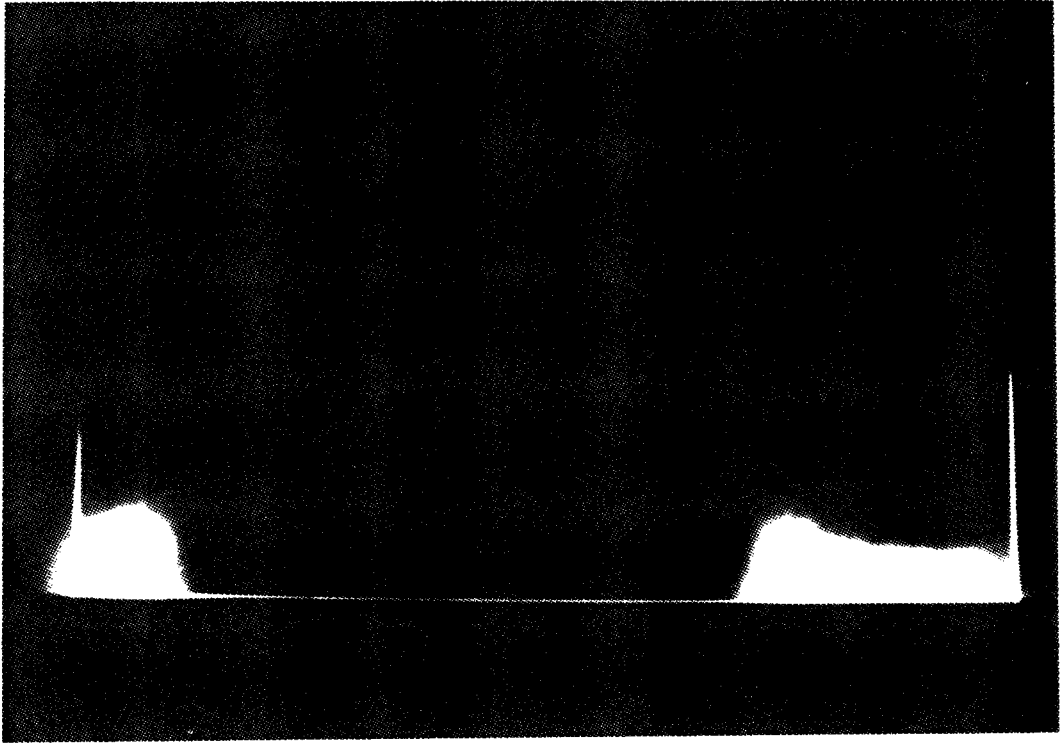
5(a)  $x/s = 3.238$



5(b)  $x/s = 4.952$

Figure 5. Smoke flow-visualization (viewed from downstream) for the "delta-wing high" case with the smoke introduced in the boundary layer.

ORIGINAL PAGE IS  
OF POOR QUALITY



5(c) x/s = 6.667

ORIGINAL PAGE IS  
OF POOR QUALITY



Figure 6. Surface-oil flow visualization on the test plate:  
"delta-wing low" case

\*\*\*Figures 7-12;  $U_i$  and  $\overline{u_i u_j}$  , "delta wing low" \*\*\*

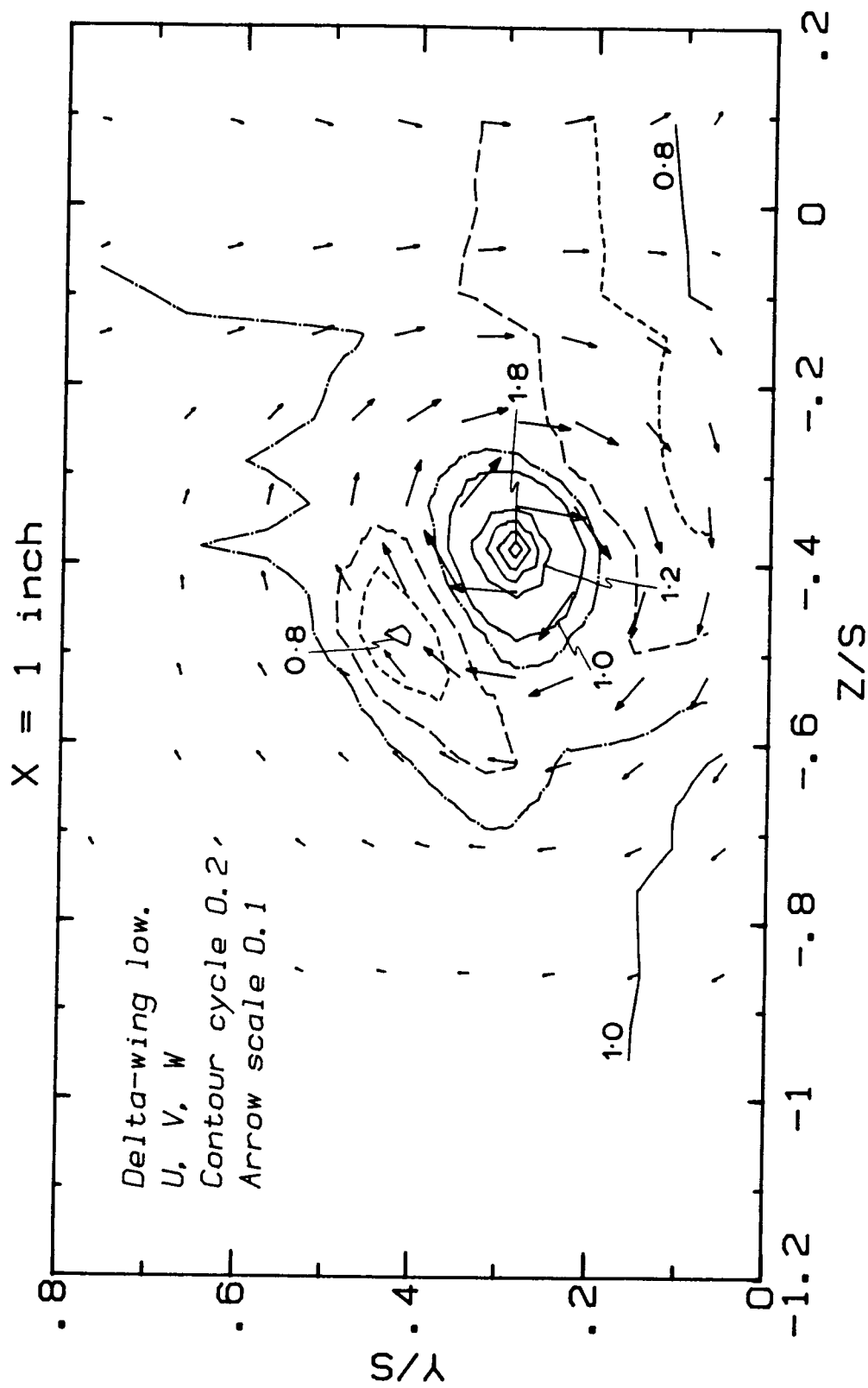
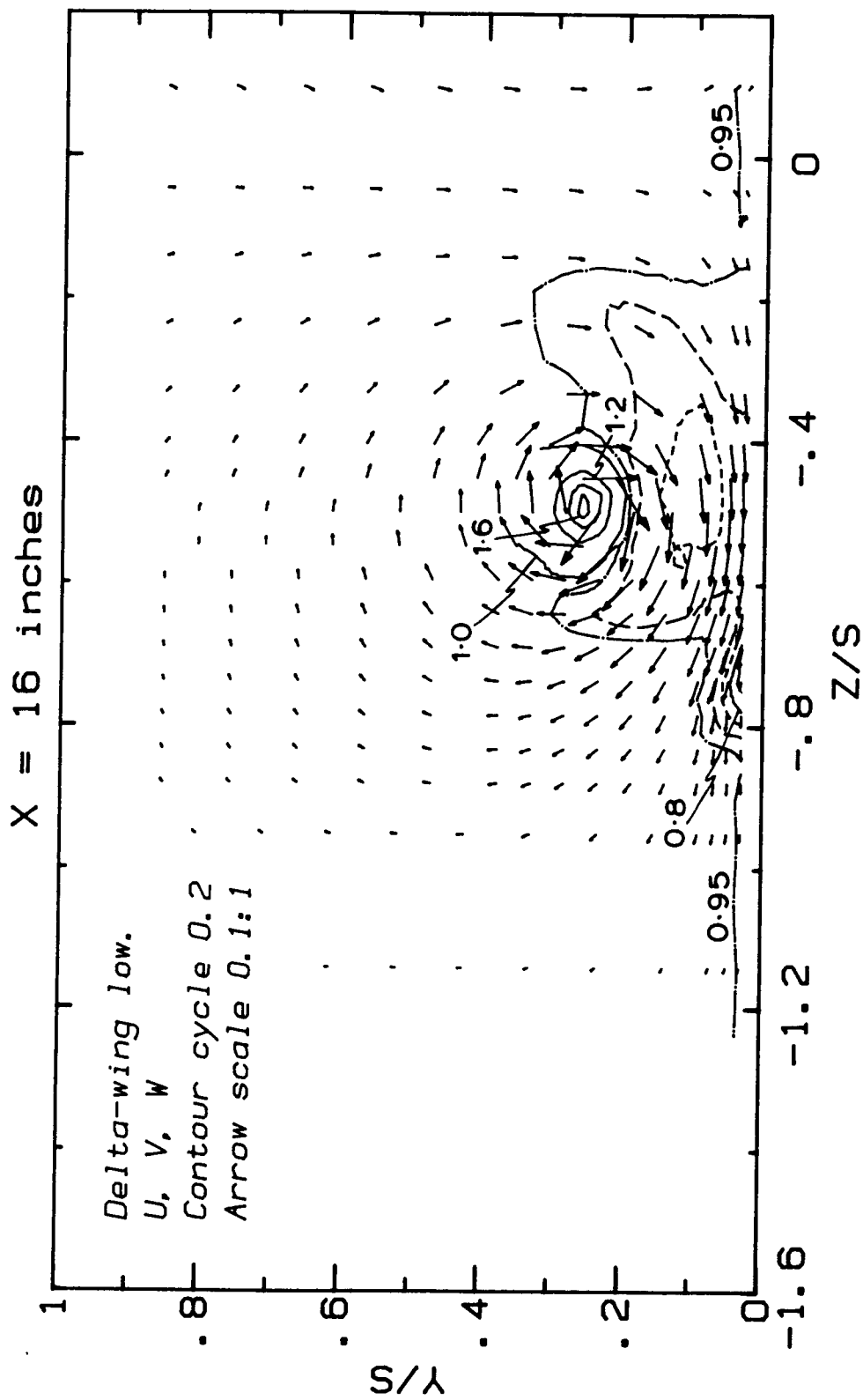
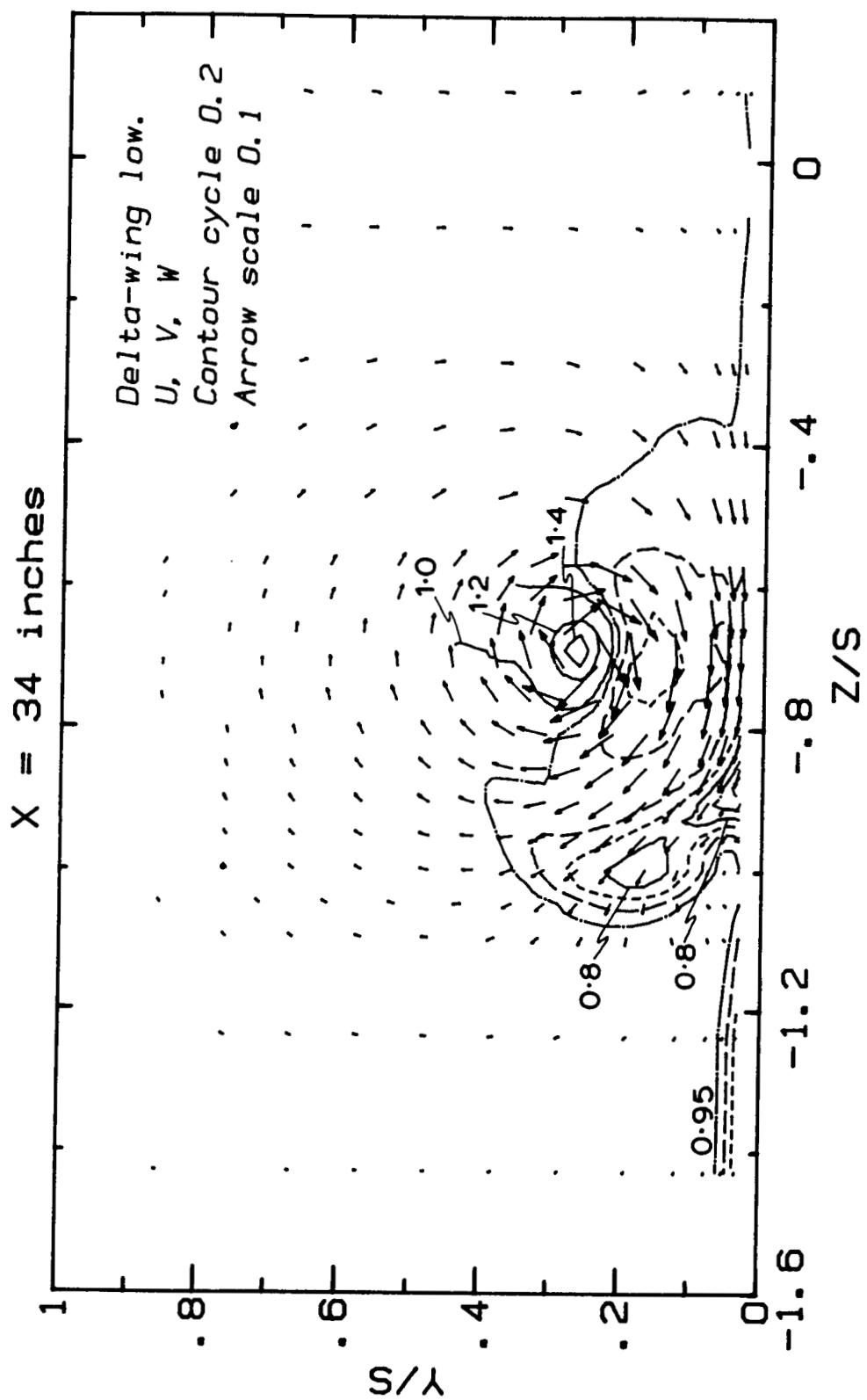


Figure 7. Contours of mean U component velocity and vectors of mean secondary-flow velocity components (V,W) for the "delta-wing low" case:

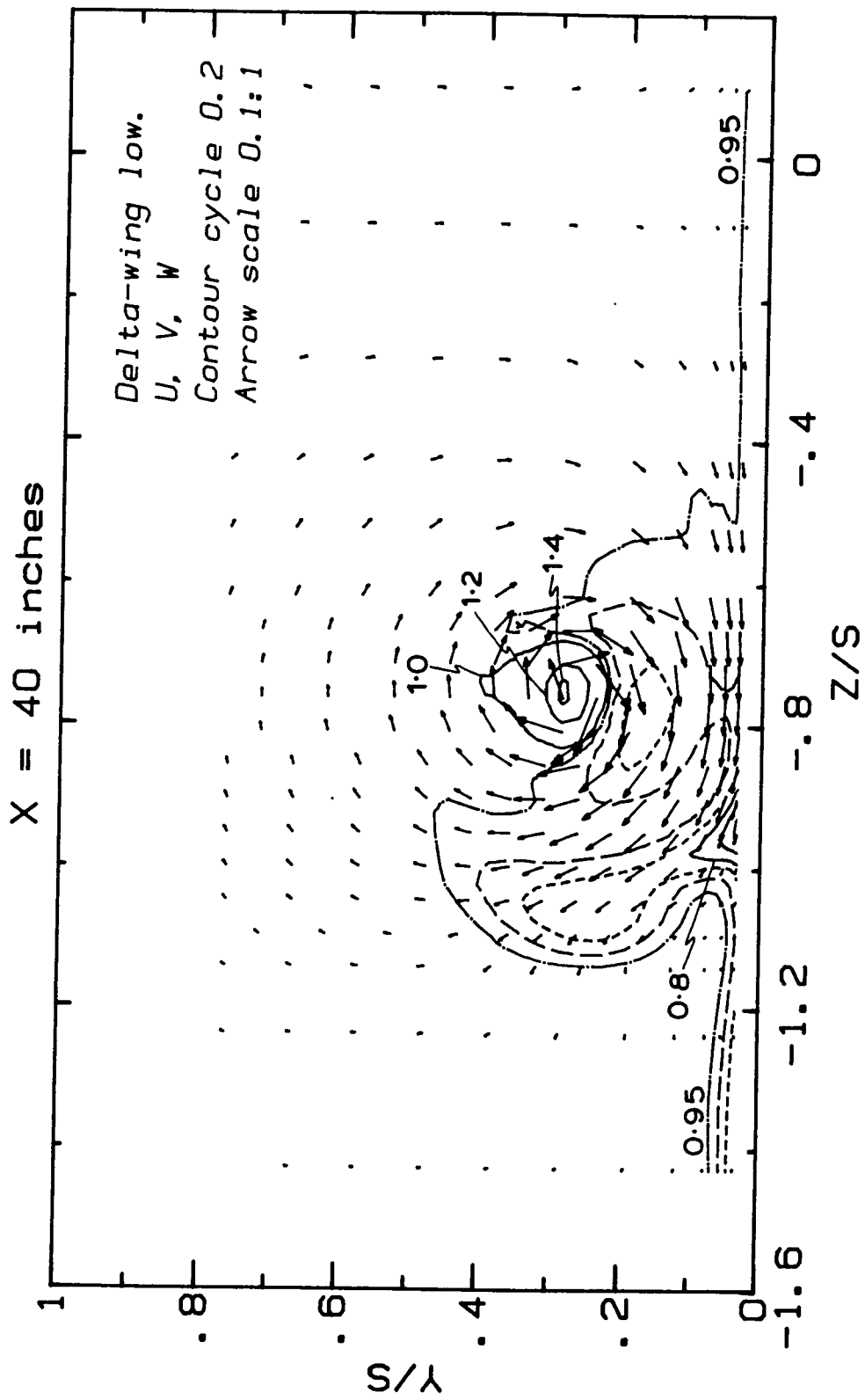
7(a)  $x/s = 0.095$



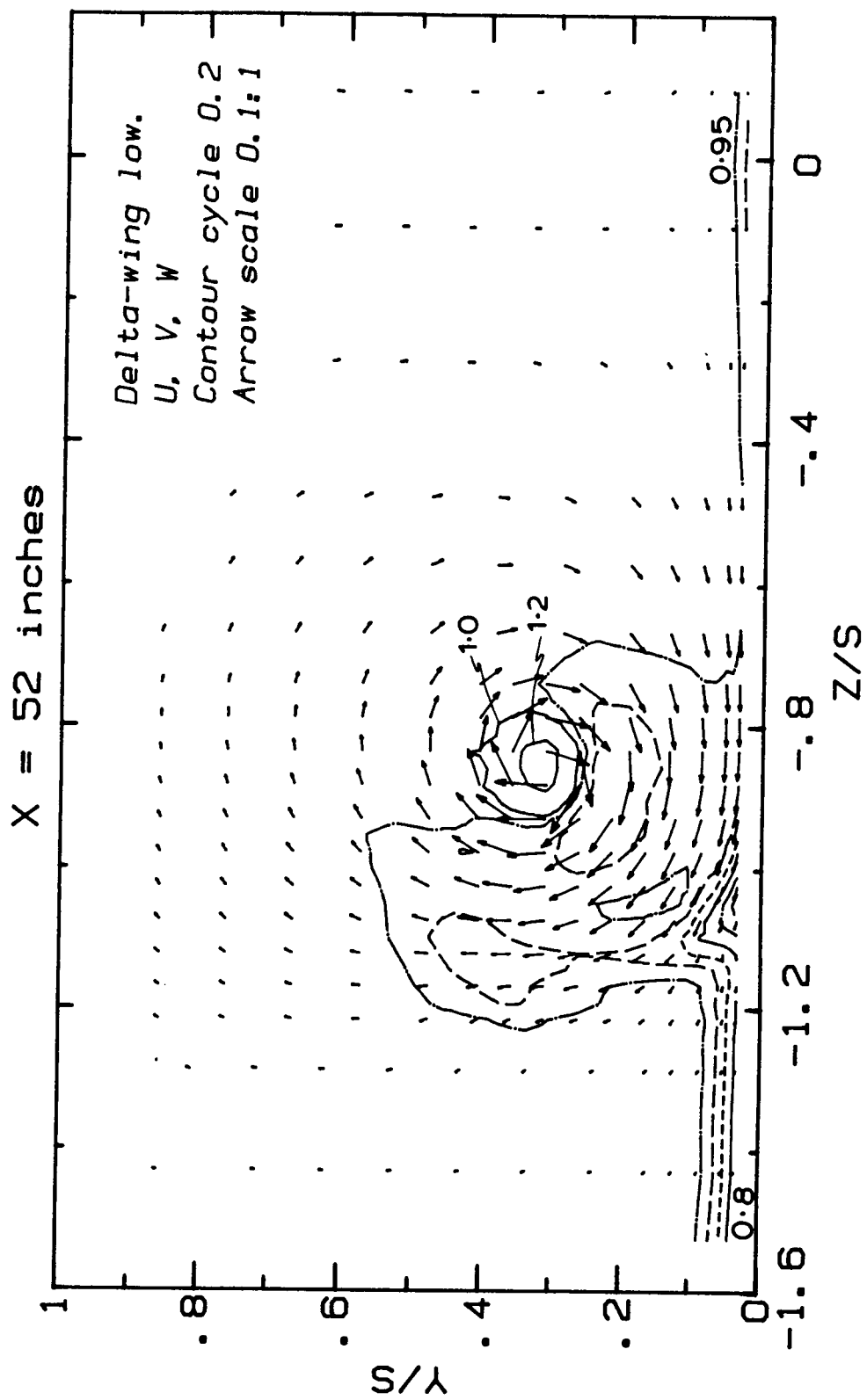
7(b)  $x/s = 1.524$



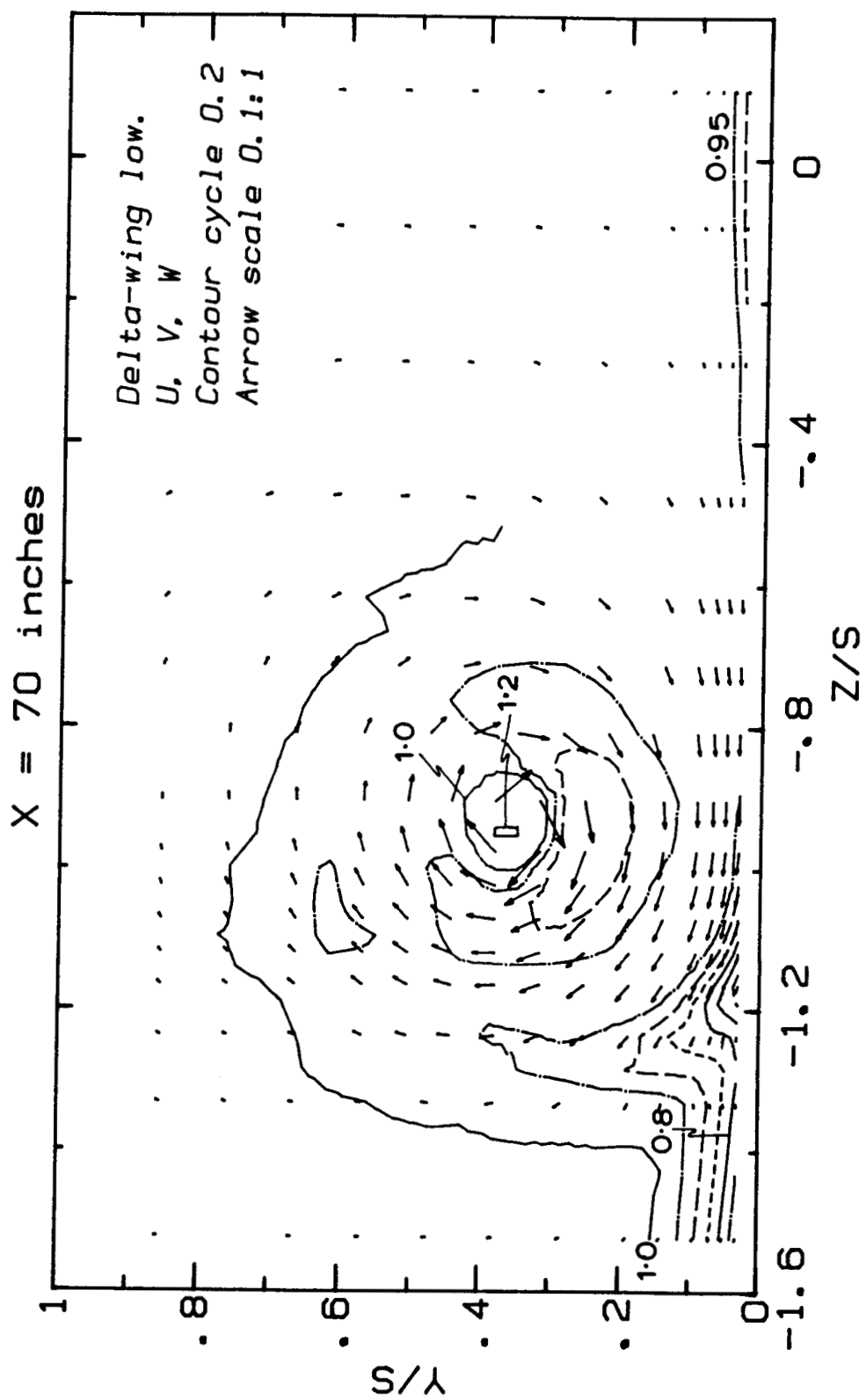
$\gamma(c) \quad x/s = 3.238$



7(d)  $x/s = 3.810$



7(e)  $x/s = 4.952$



$$\gamma(f) \ x/s = 6.667$$

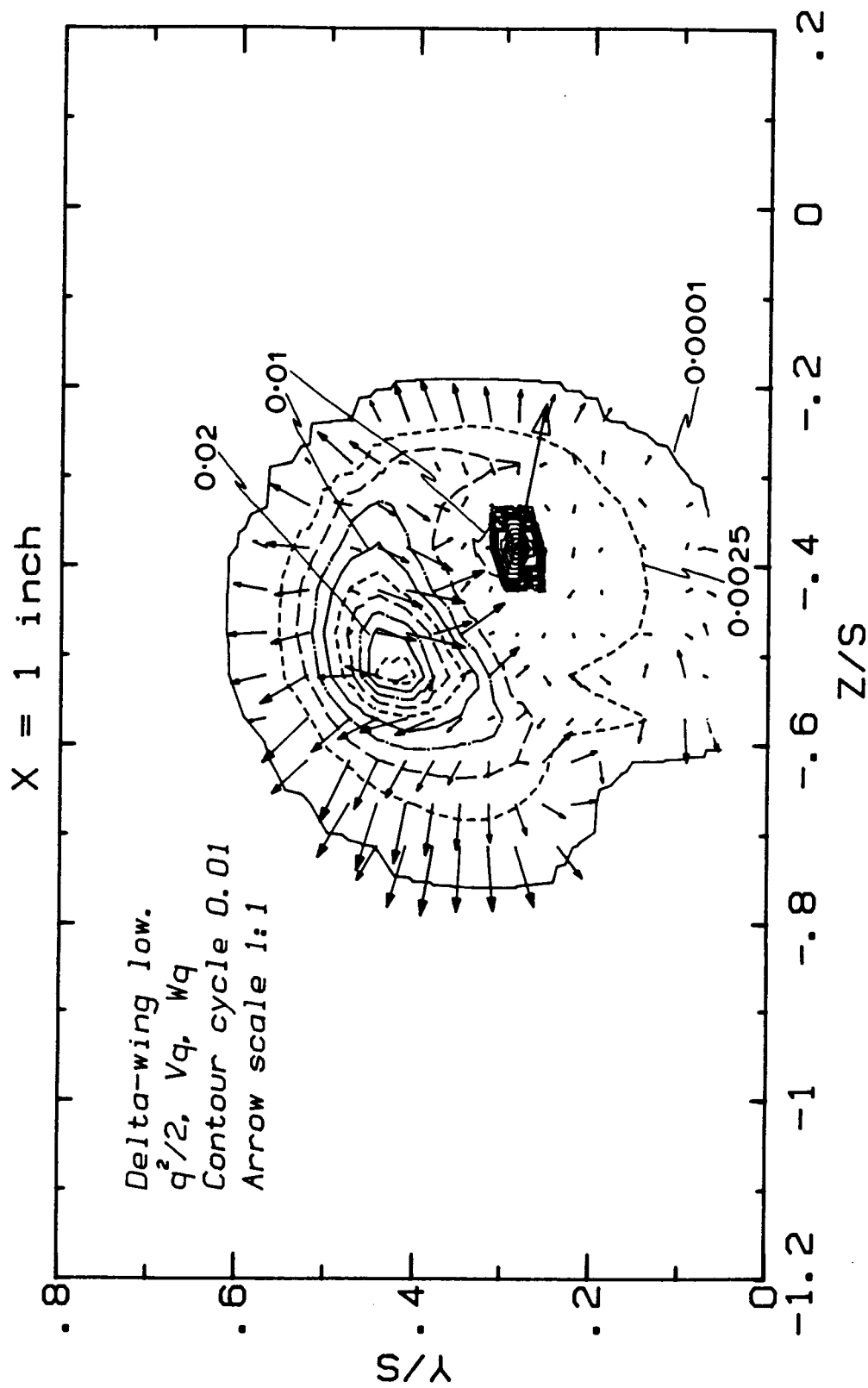
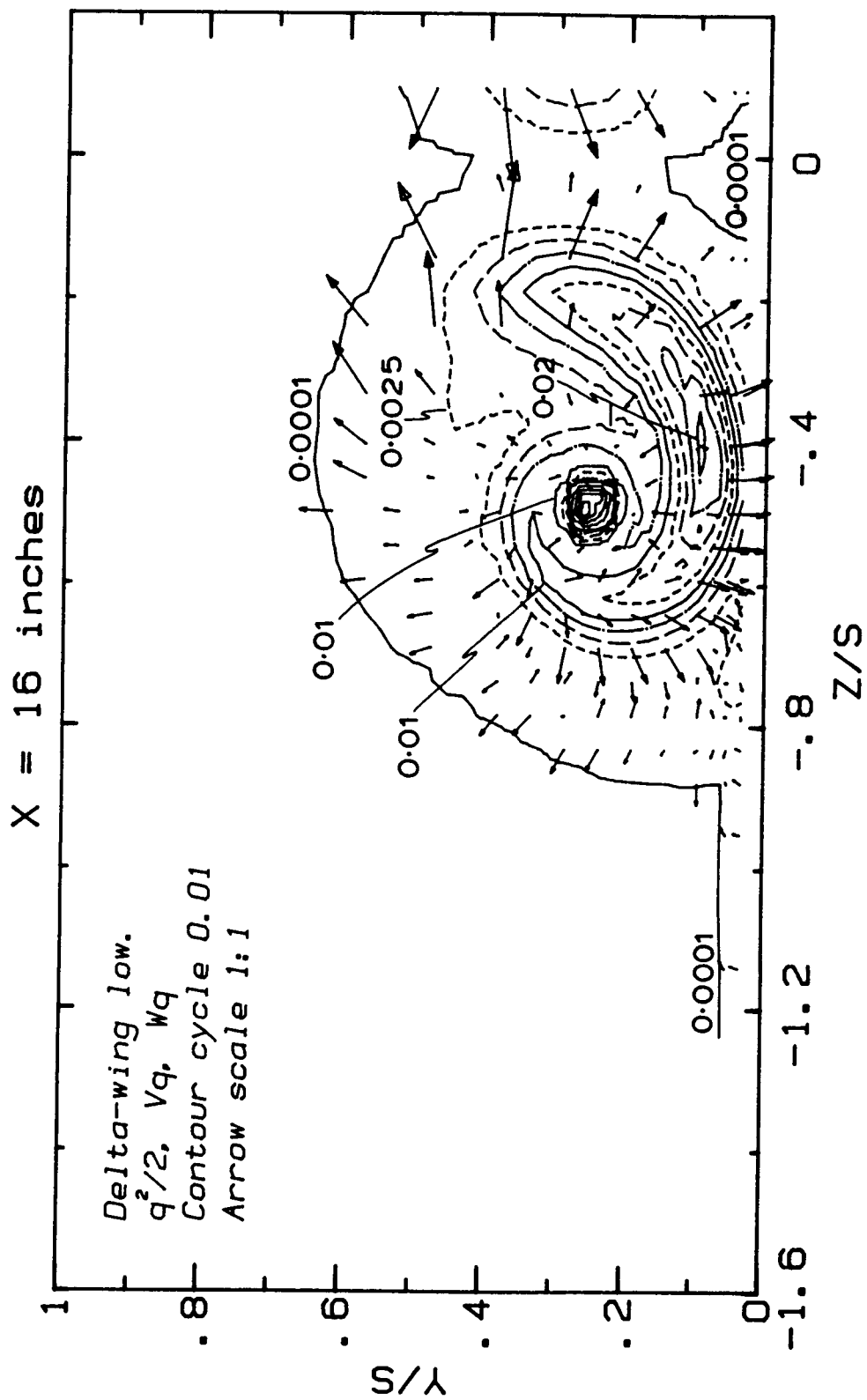
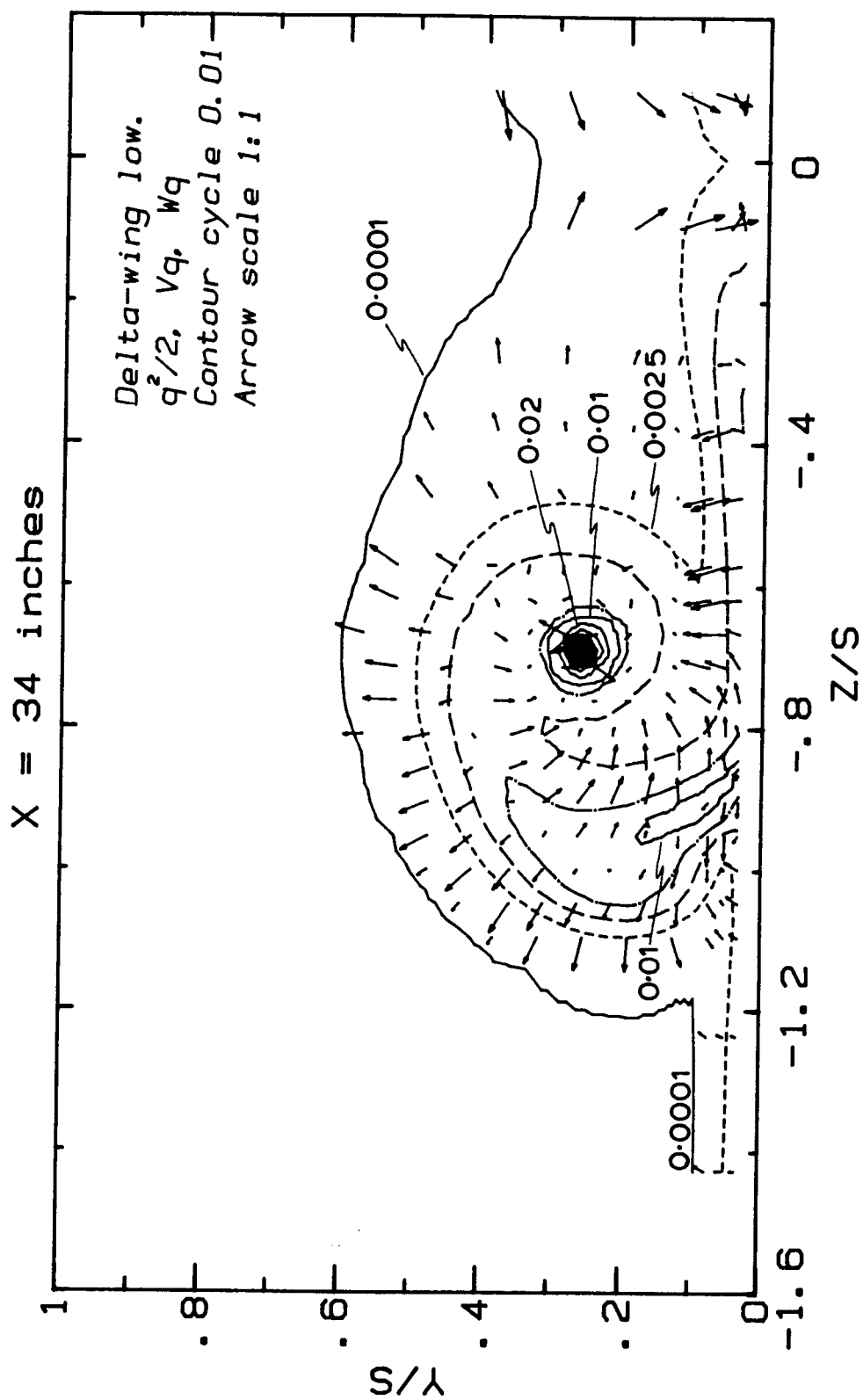


Figure 8. Contours of turbulent kinetic energy ( $q^2/2 = (\bar{u}^2 + \bar{v}^2 + \bar{w}^2)/2$ ), and vectors of turbulent diffusion velocity ( $Vq = \bar{q}^2 v / \bar{q}^2$ ,  $Wq = \bar{q}^2 w / \bar{q}^2$ ) for the "delta-wing low" case:

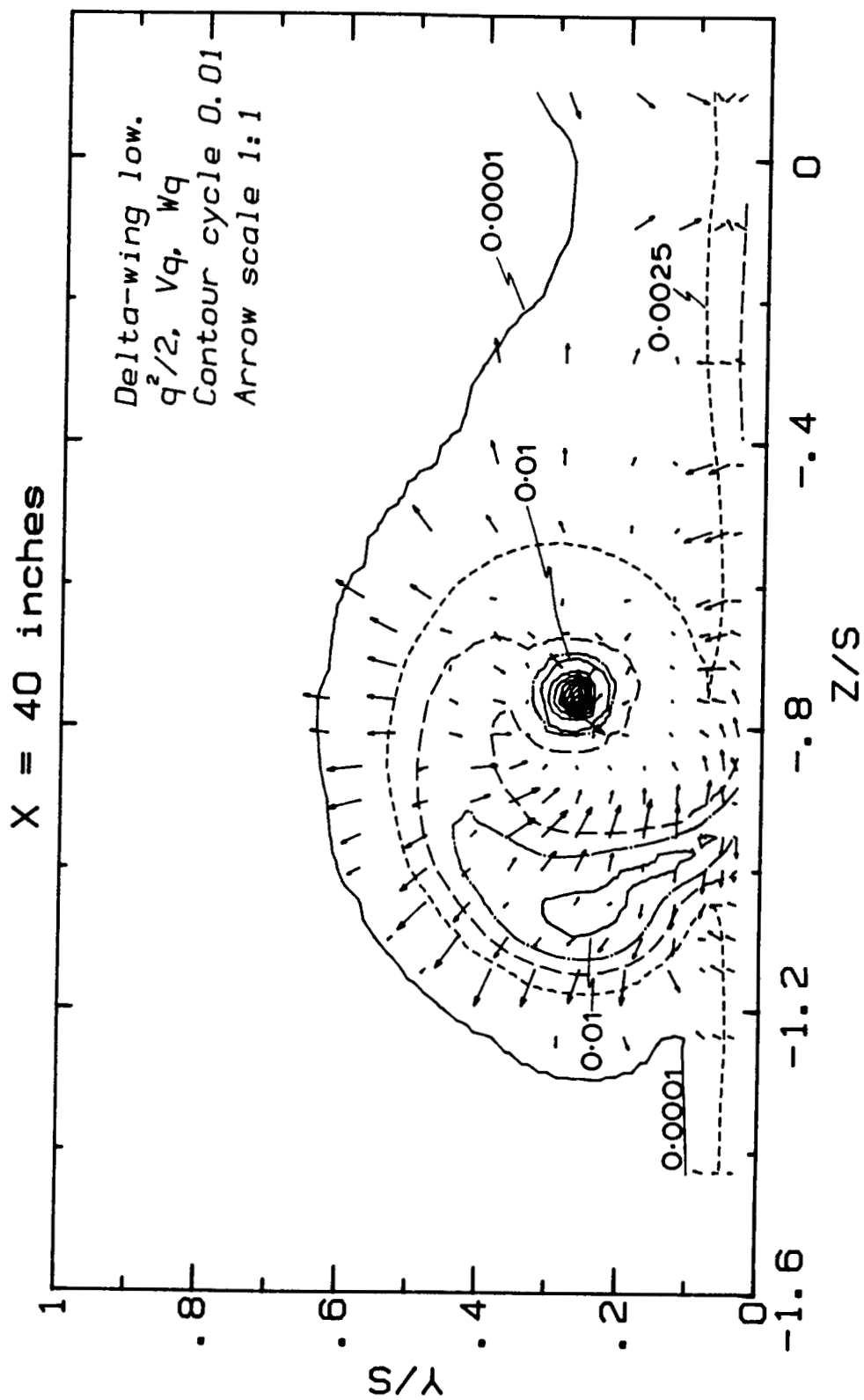
8(a)  $x/s = 0.095$



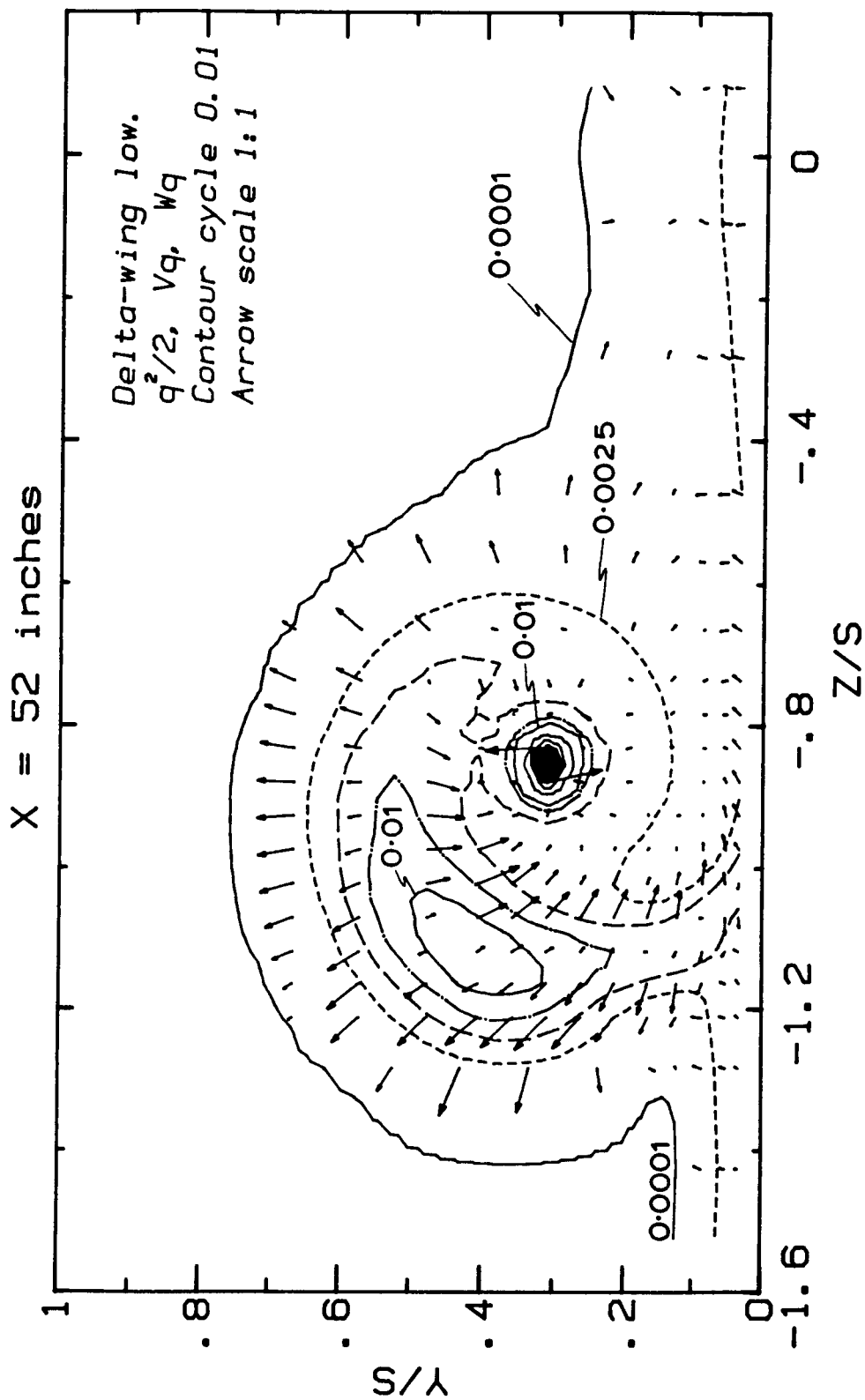
8(b)  $x/s = 1.524$



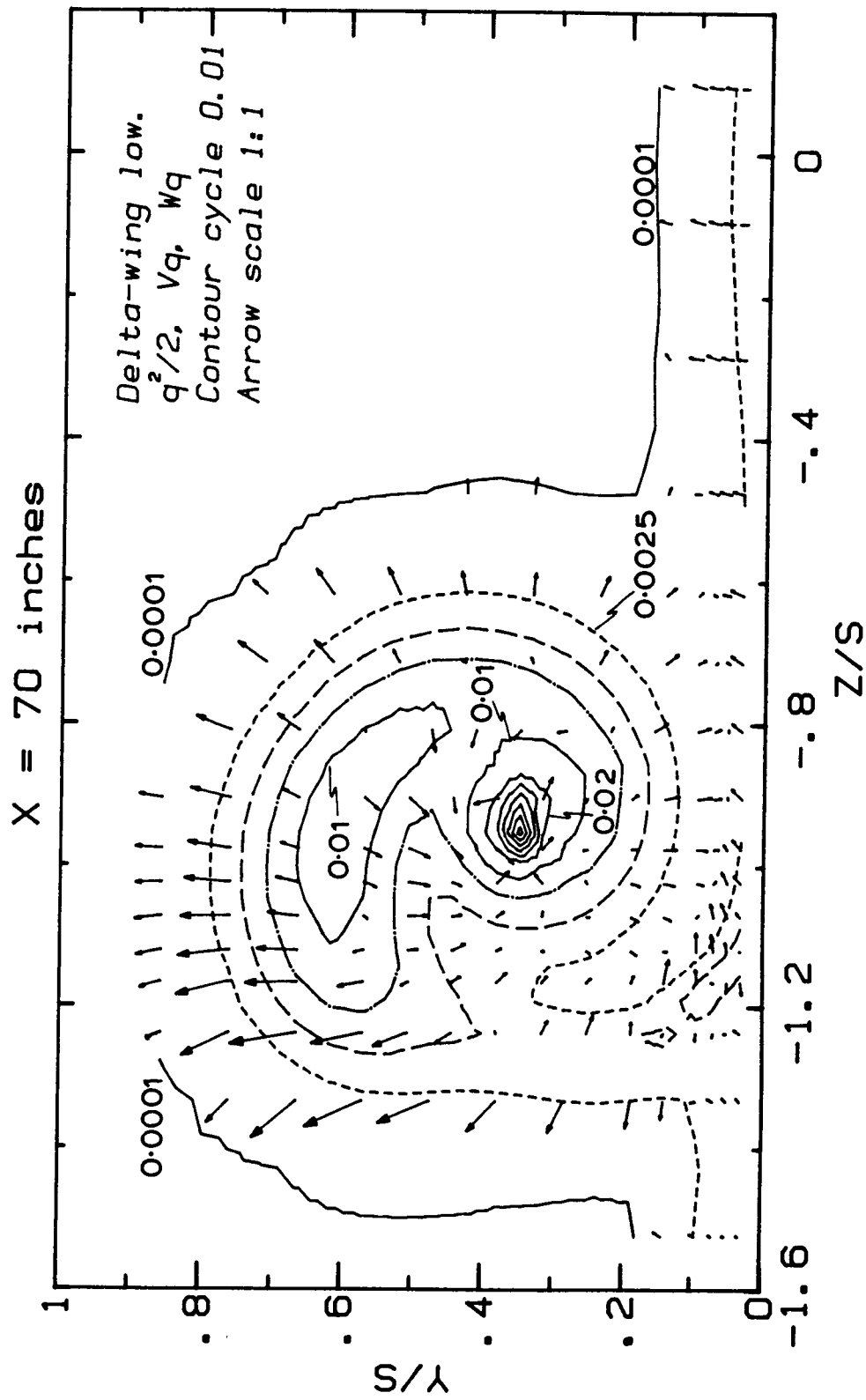
8(c)  $x/s = 3.238$



8(d)  $x/s = 3.810$



8(e)  $x/s = 4.952$



$$8(f) \times / s = 6.667$$

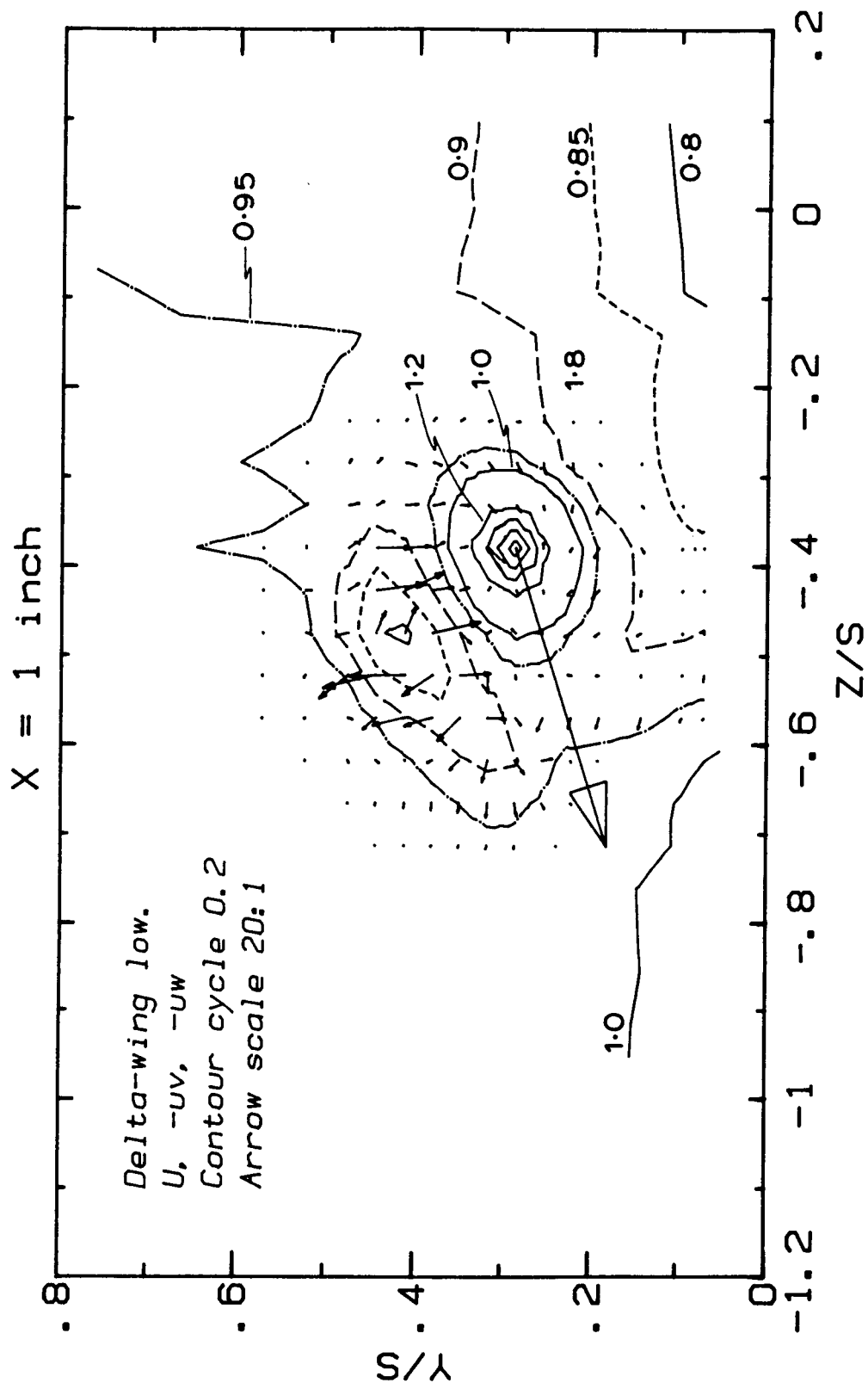
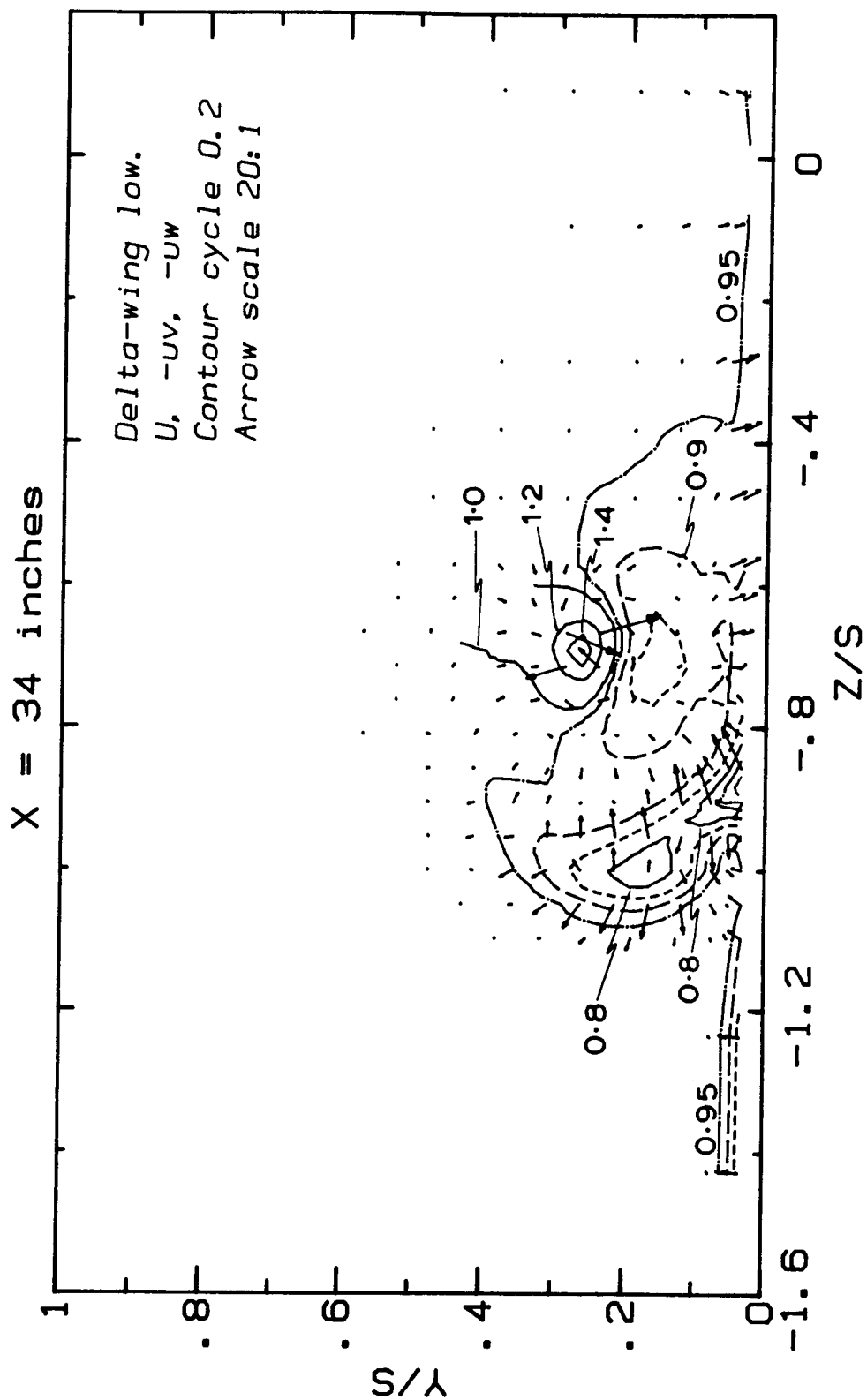
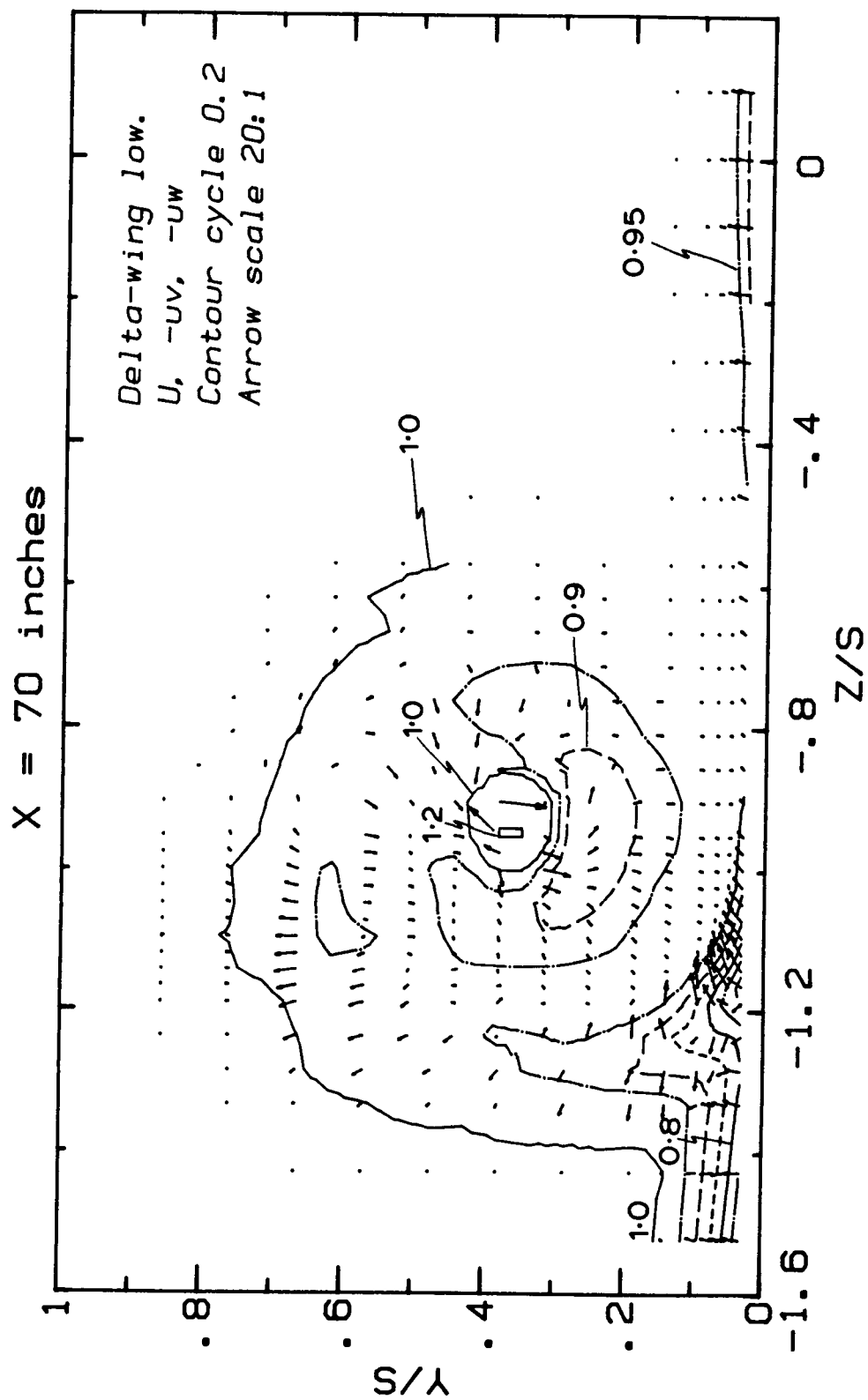


Figure 9. Contours of mean  $U$  component velocity and shear-stress vector components ( $-\overline{uv}$ ,  $-\overline{uw}$ ) for the "delta-wing low" case:

9(a)  $x/s = 0.095$



9(b)  $x/s = 3.238$



9(c)  $x/s = 6.667$

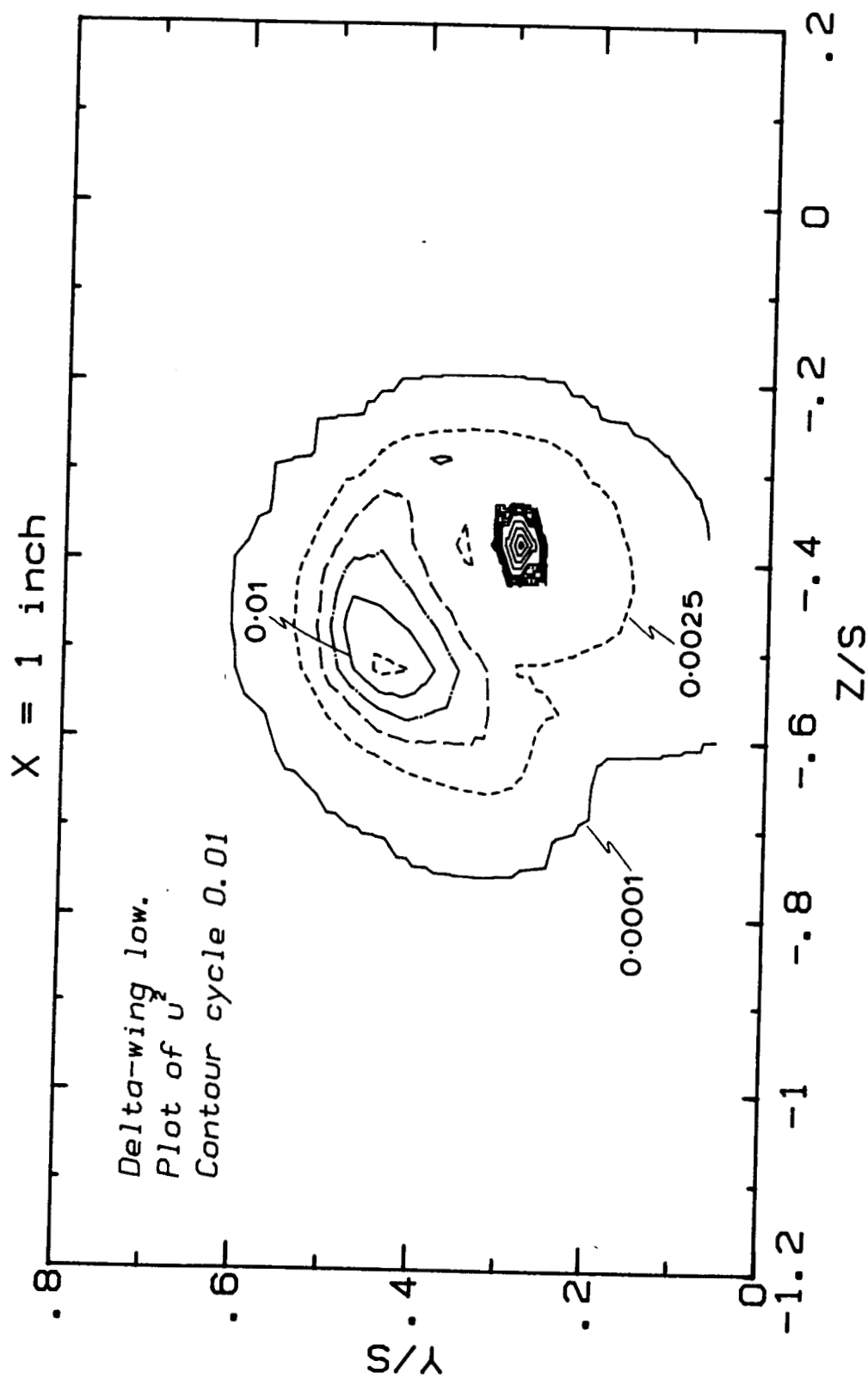
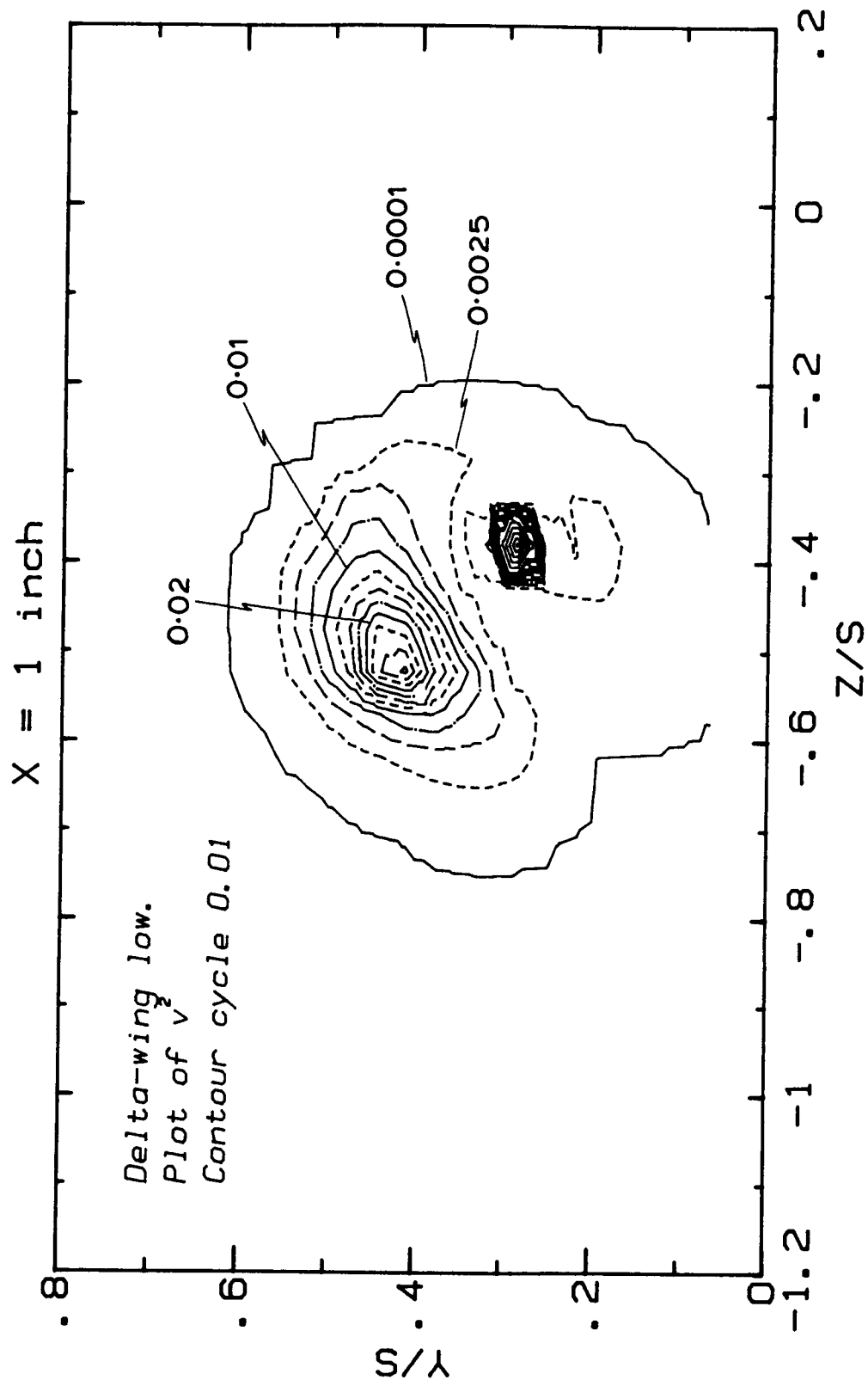
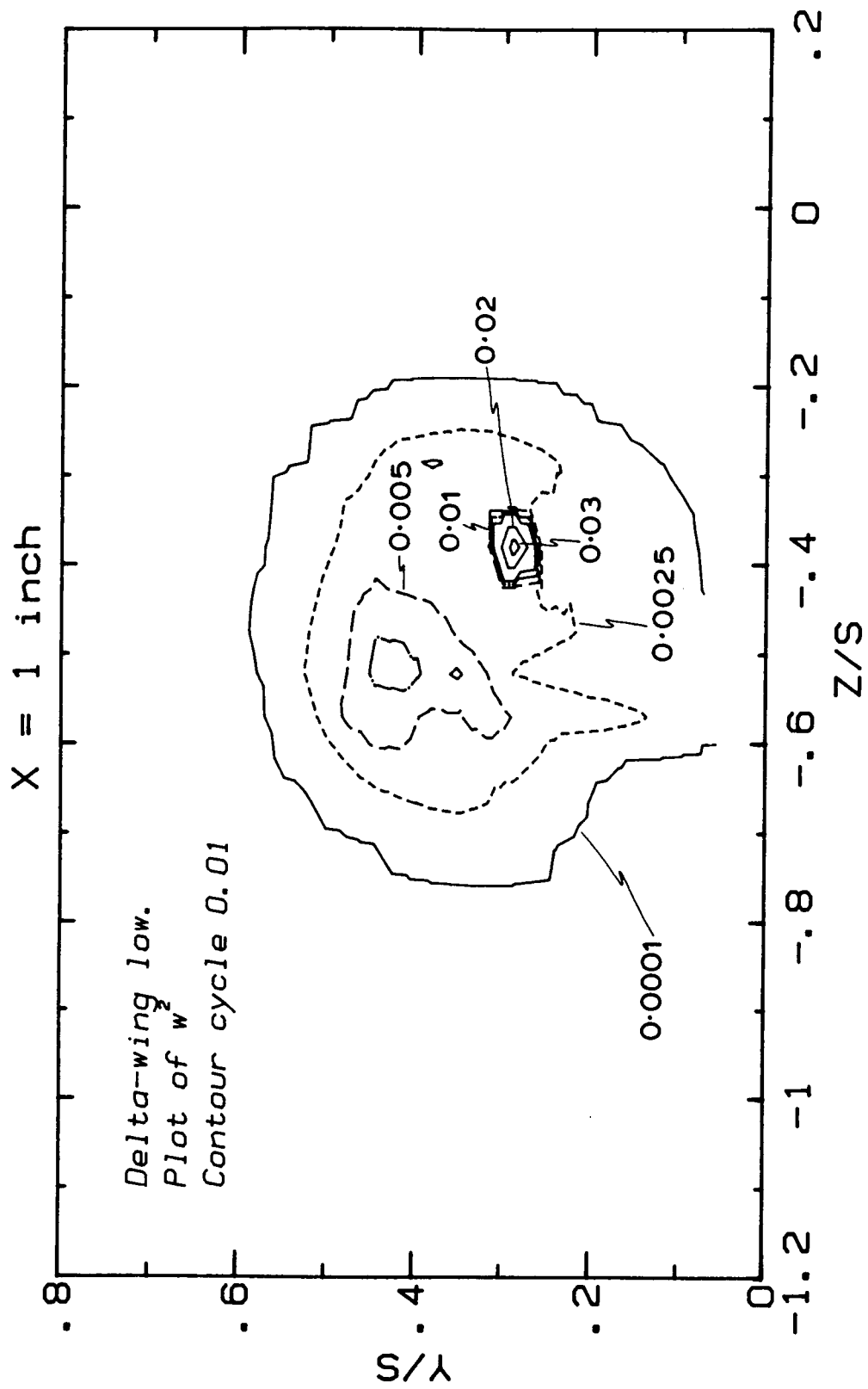


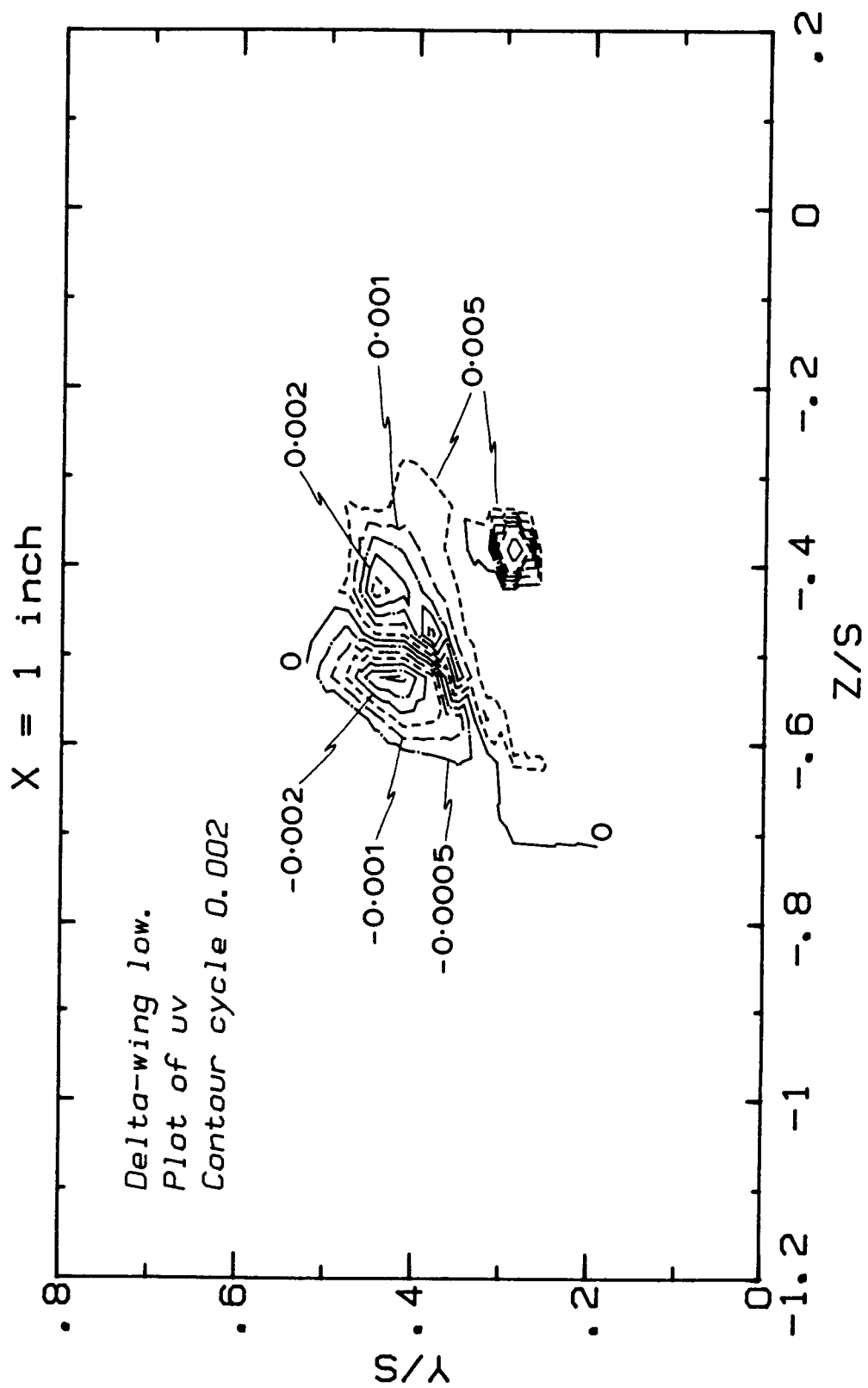
Figure 10. Contours of the Reynolds stresses at  $x/s = 0.095$  for the "delta-wing low" case:

10(a)  $\overline{u'v'}$

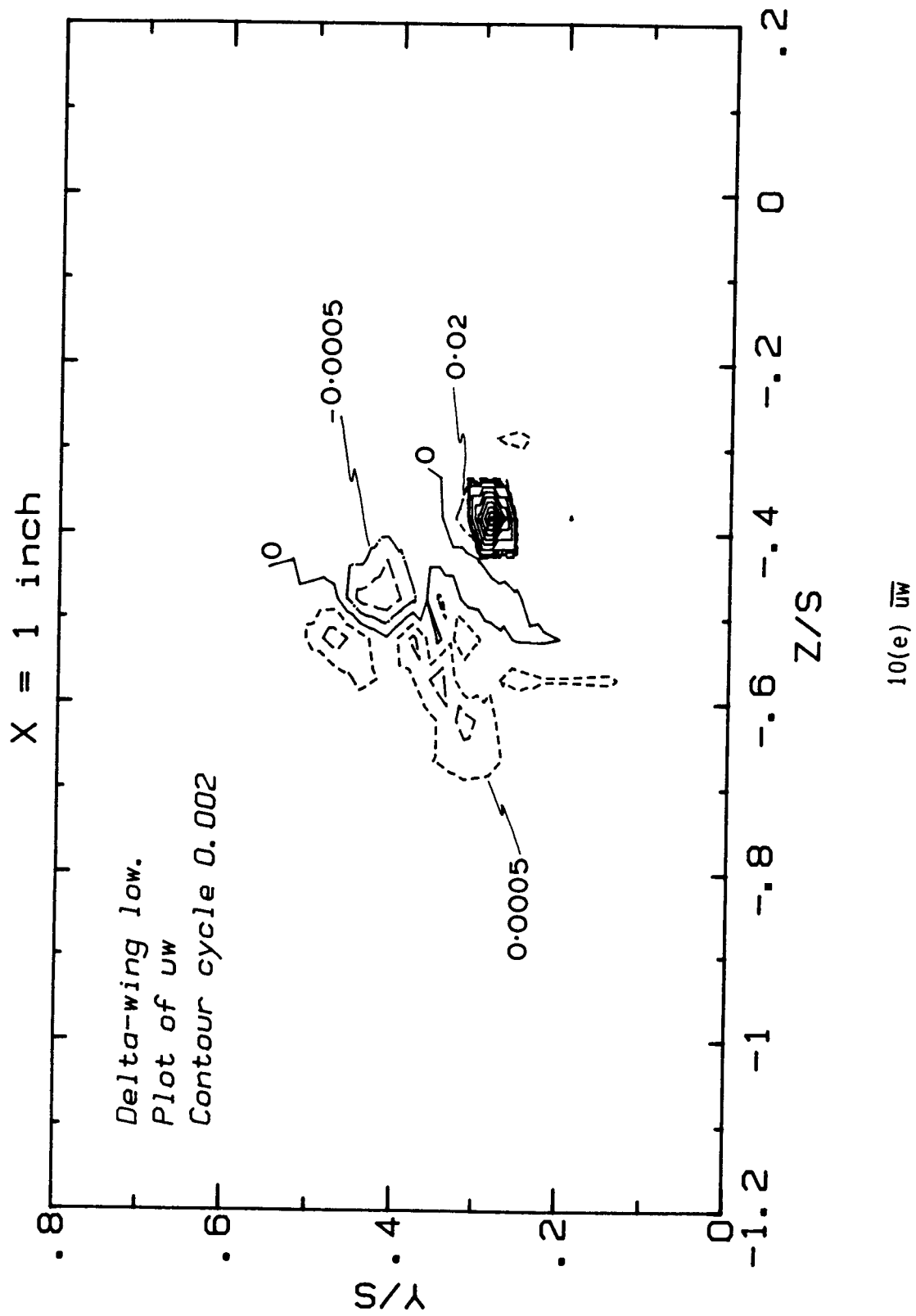


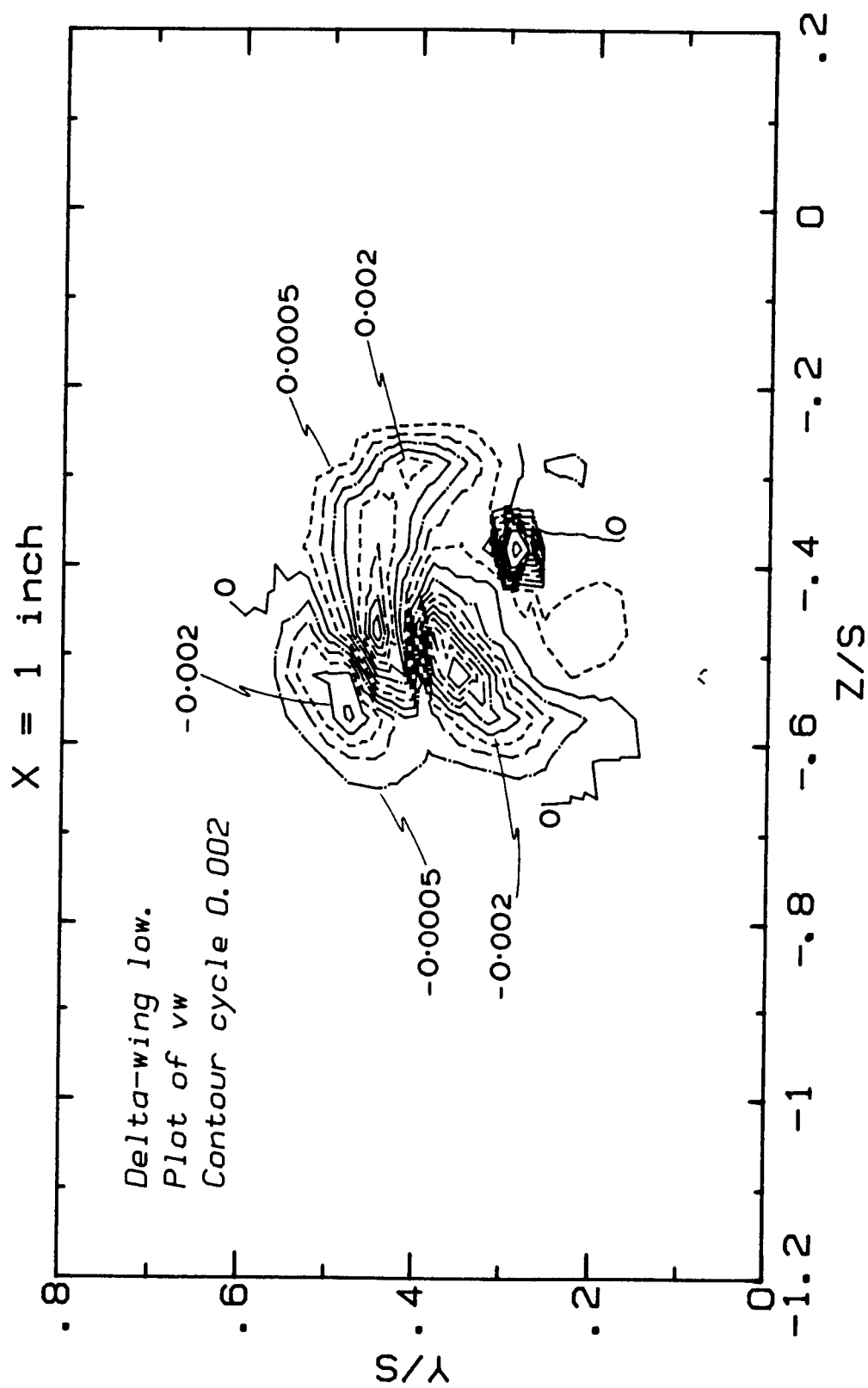
10(b)  $\bar{v}_z$





$10(d) \overline{uv}$





$10(f) \bar{v}_w$

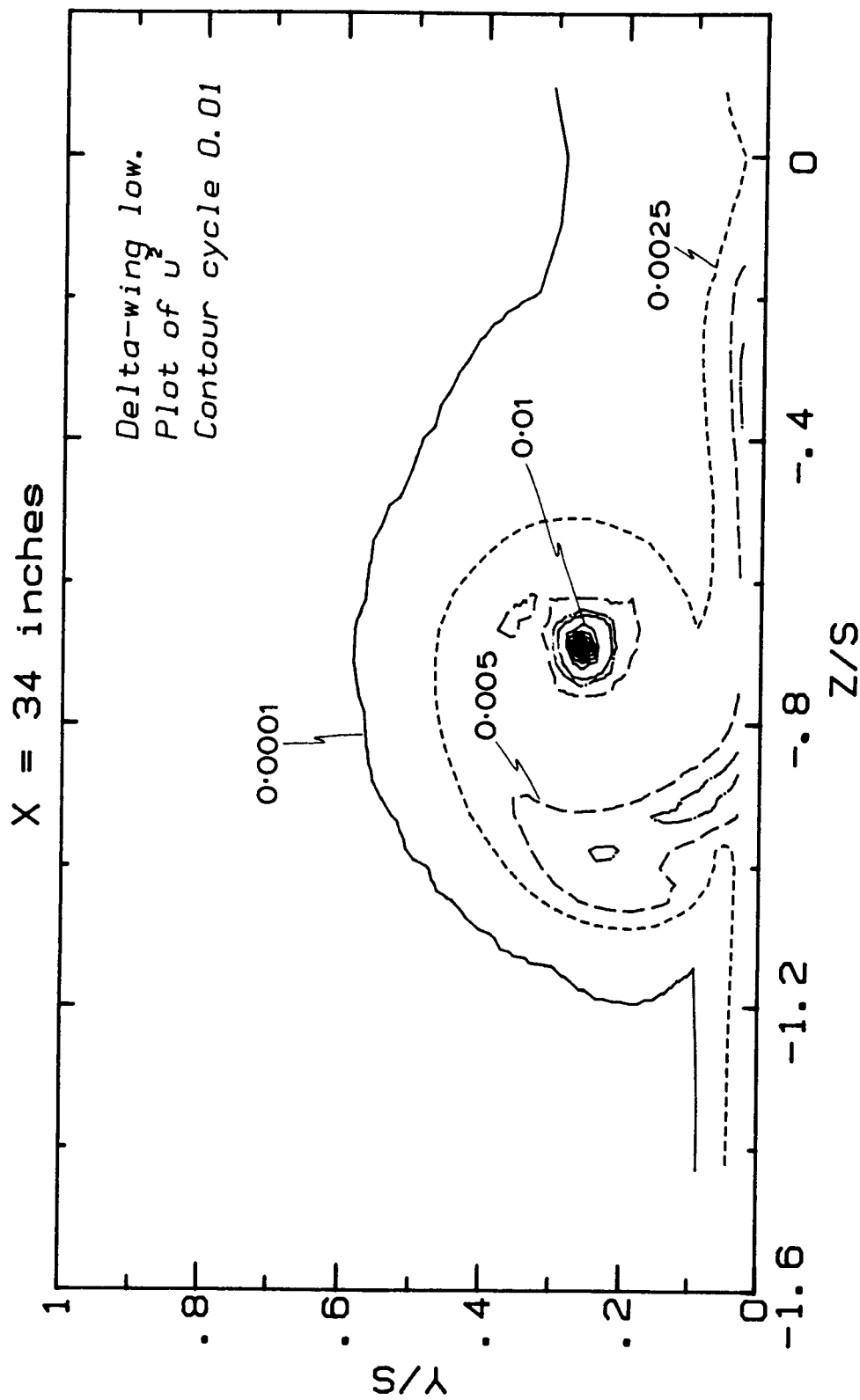
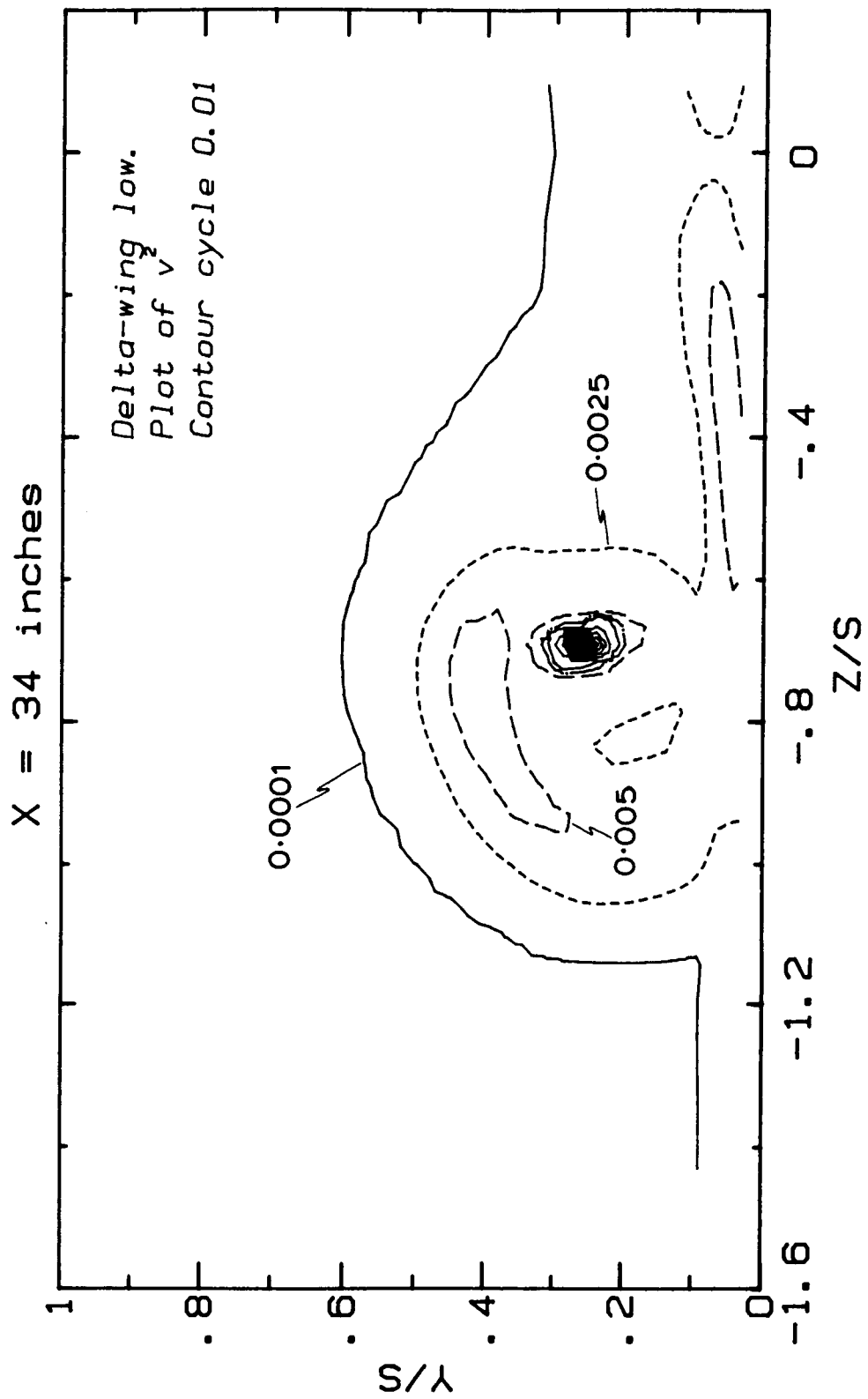
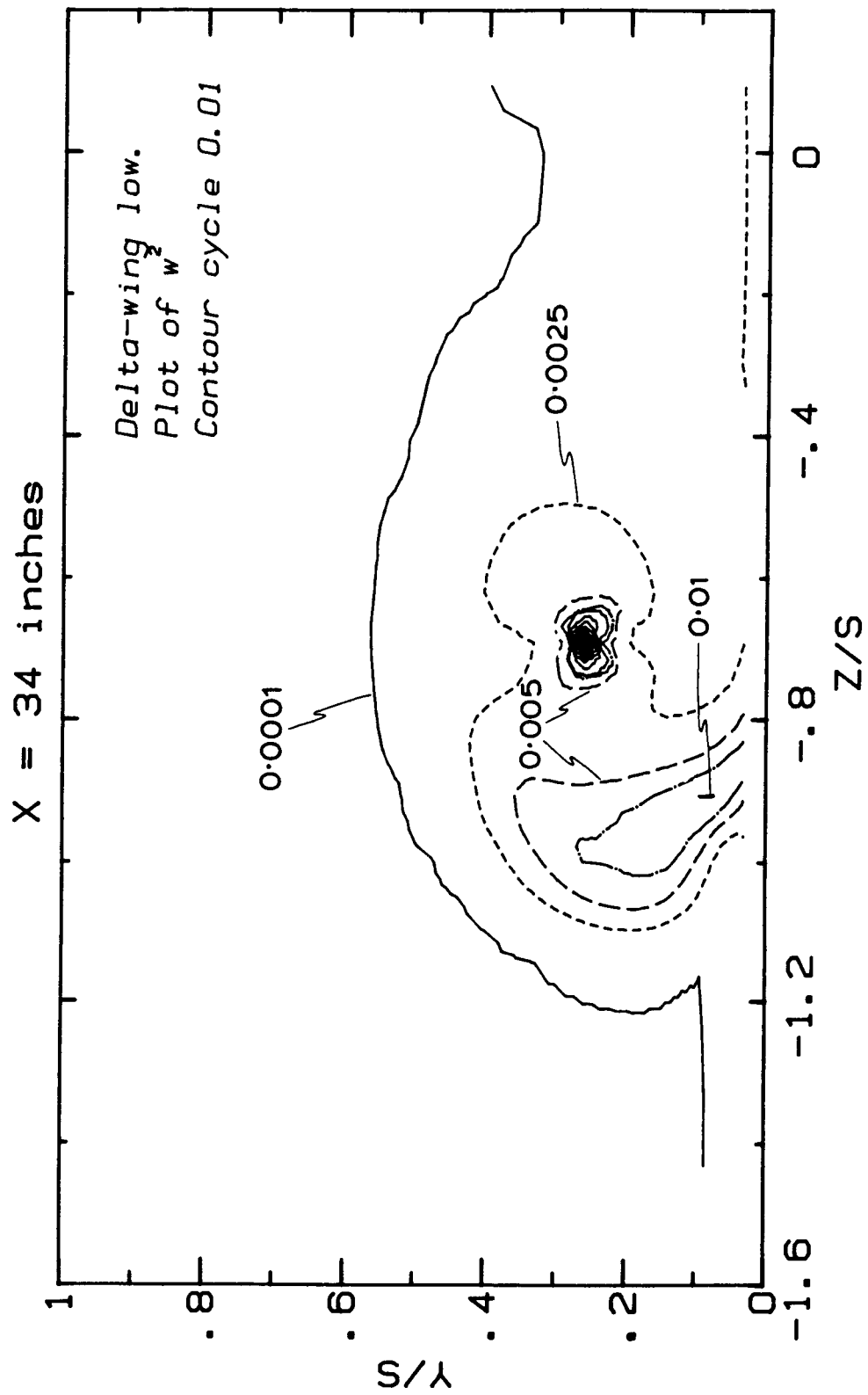


Figure 11. Contours of the Reynolds stresses at  $x/s = 3.238$  for the "delta-wing low" case:

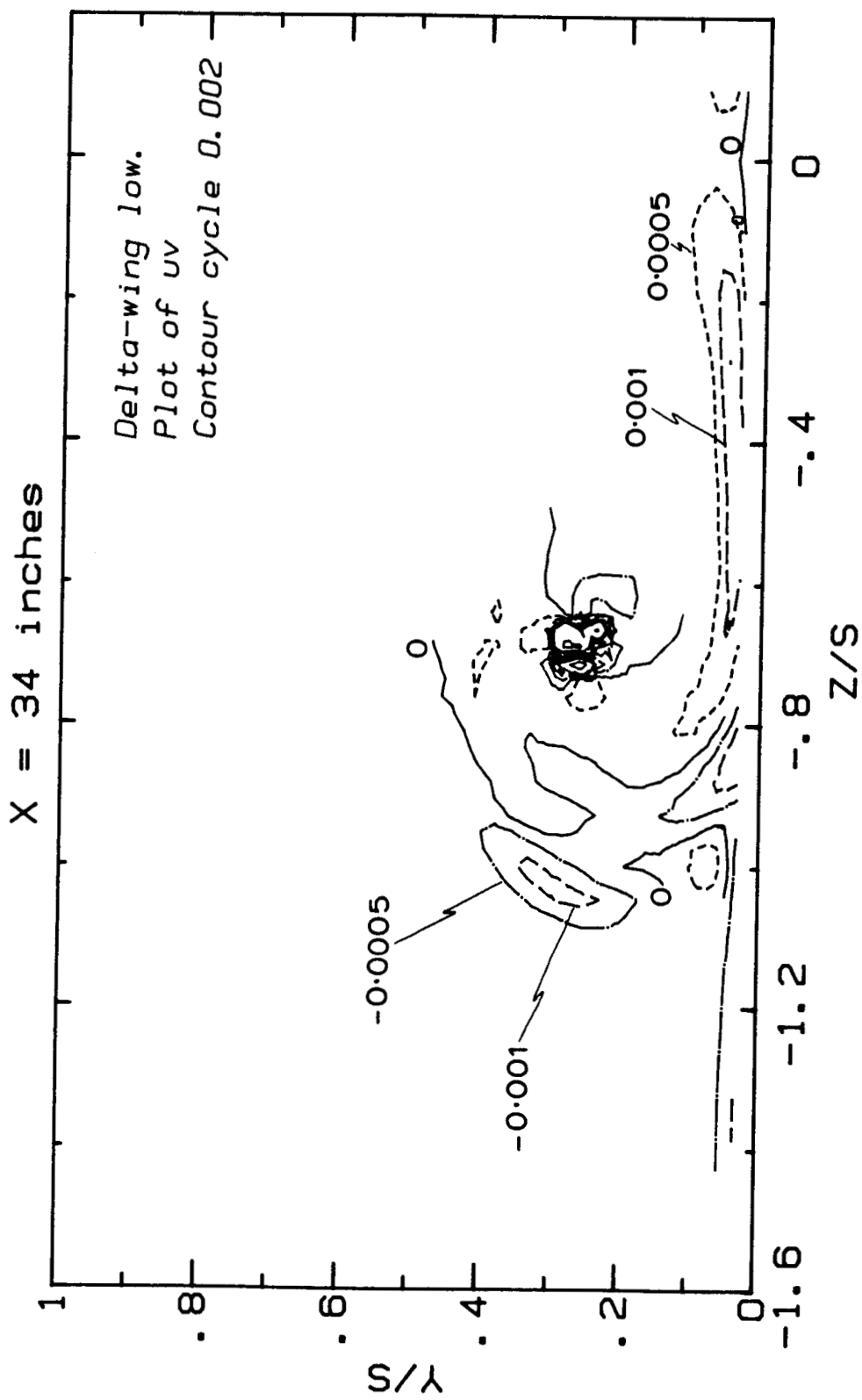
11(a)  $\overline{u'^2}$



11(b)  $\bar{v}^2$

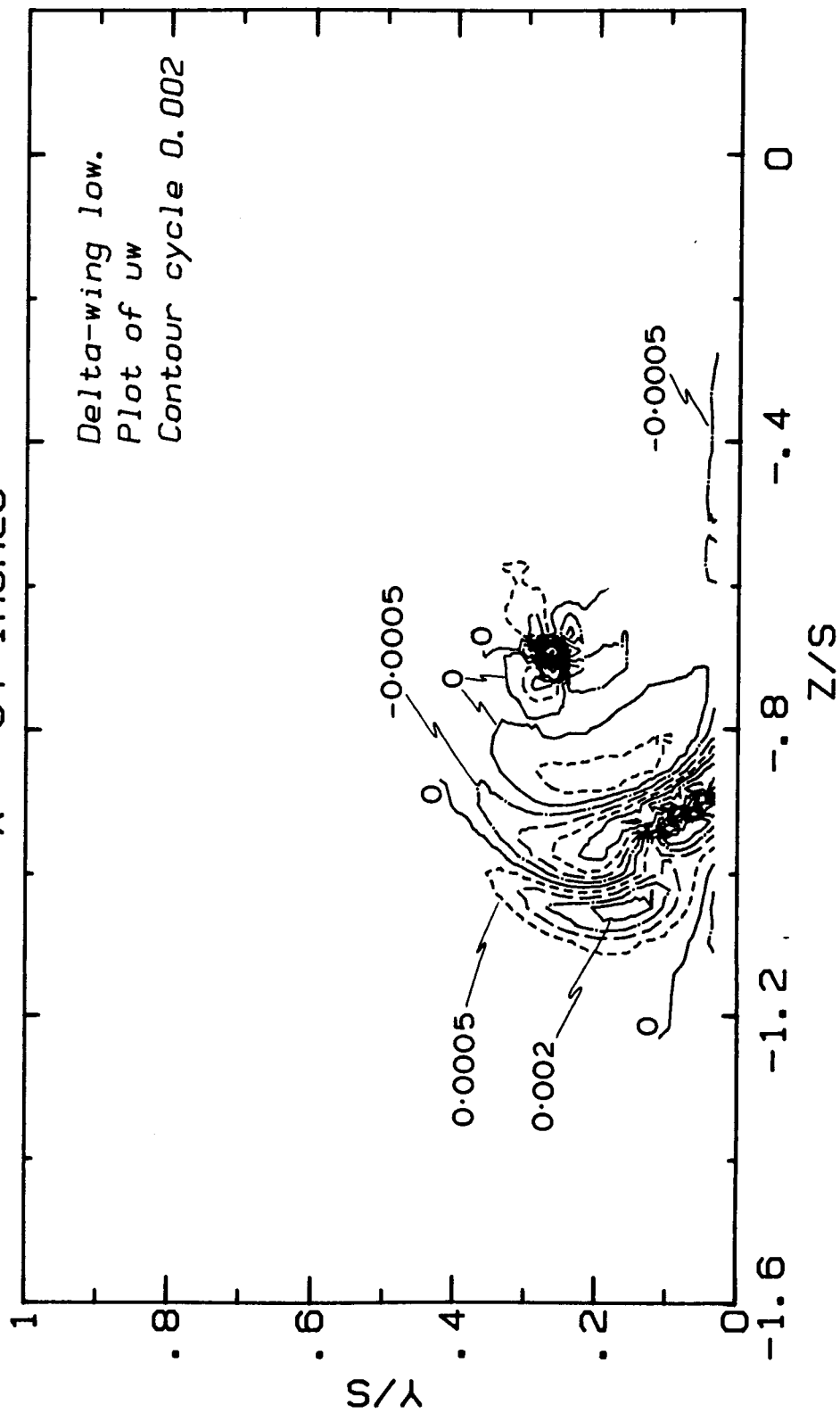


11(c)  $\overline{w^2}$

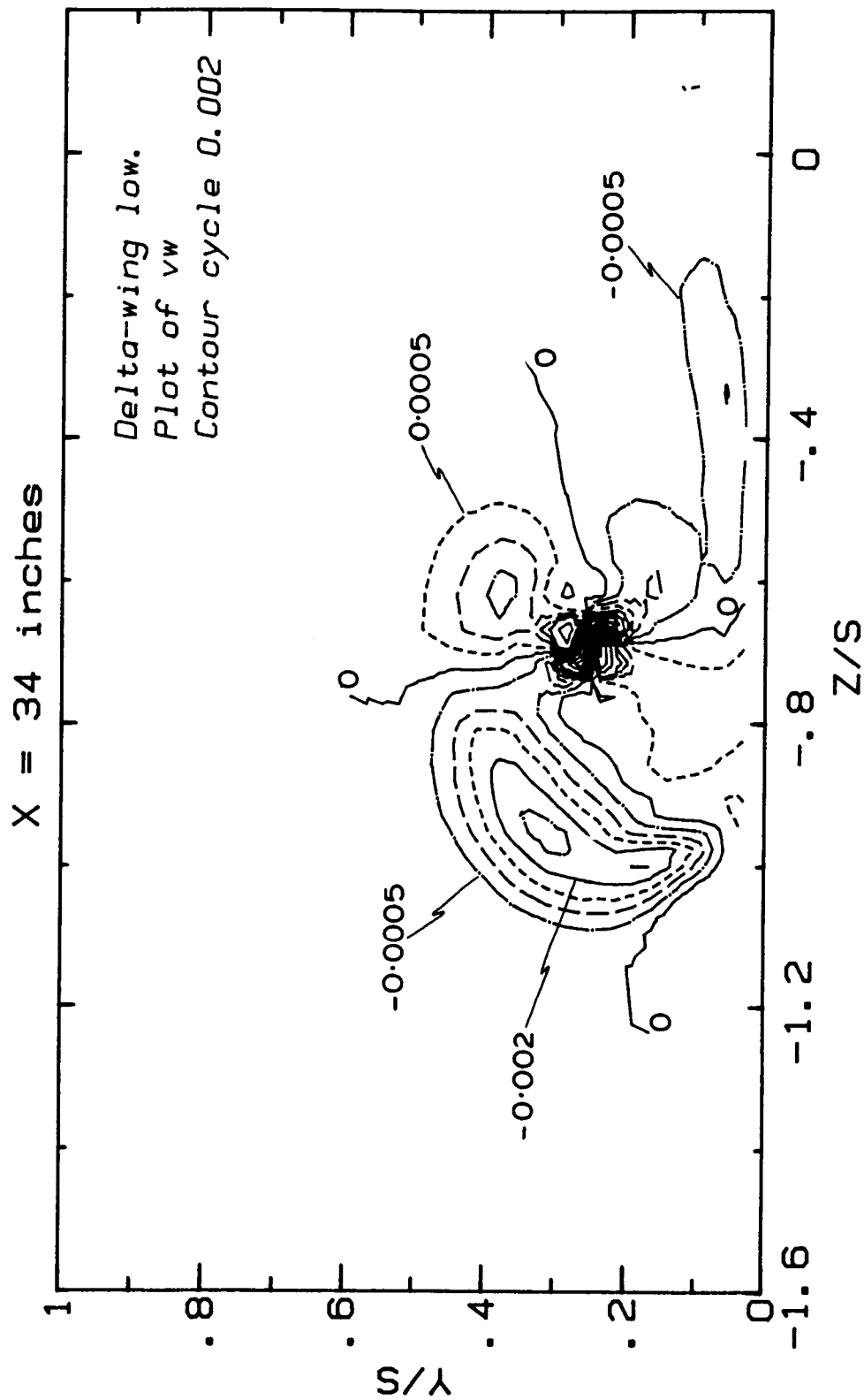


11(d)  $\overline{uv}$

X = 34 inches



11(e)  $\overline{u-w}$



11(f)  $\bar{v}_w$

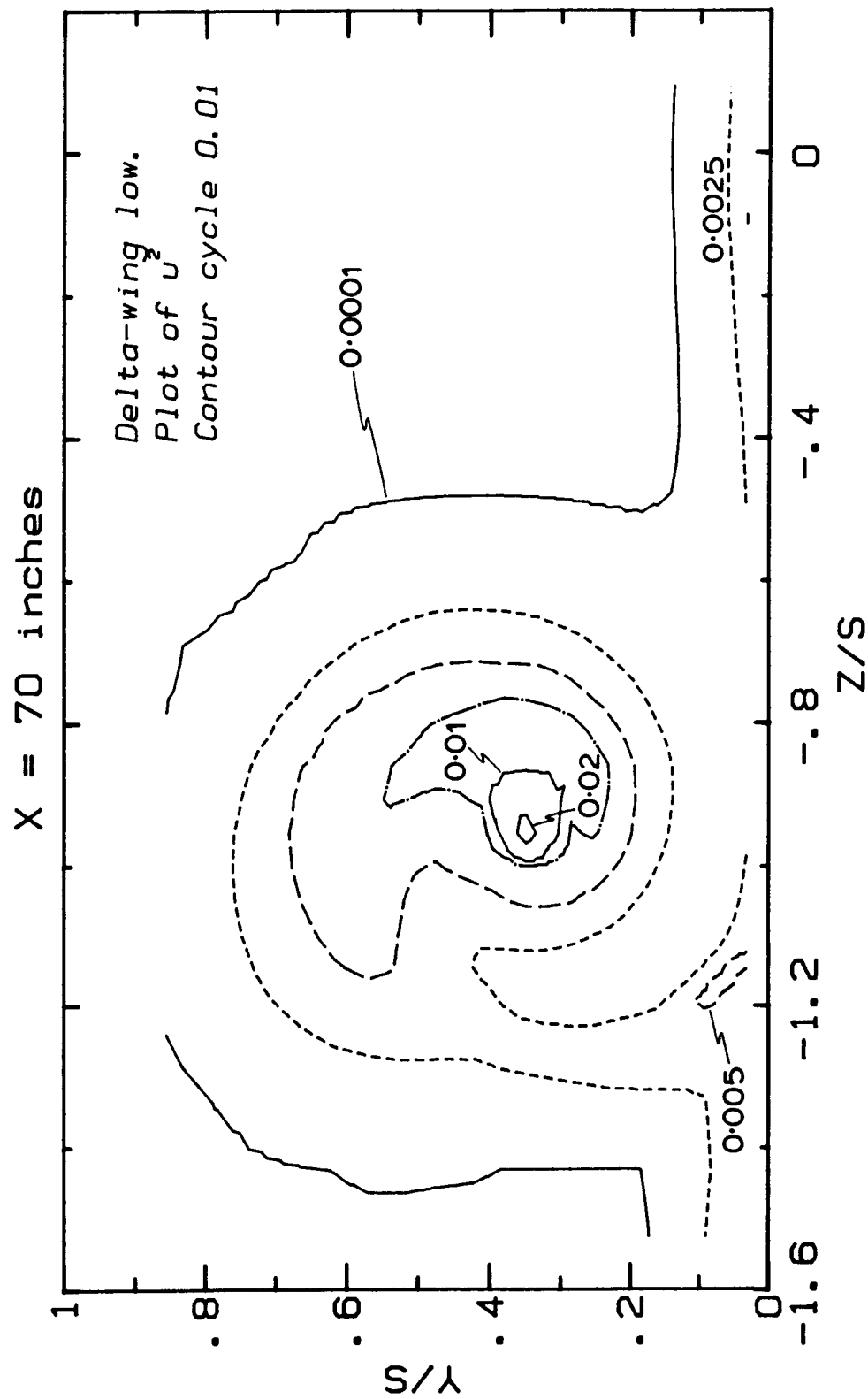
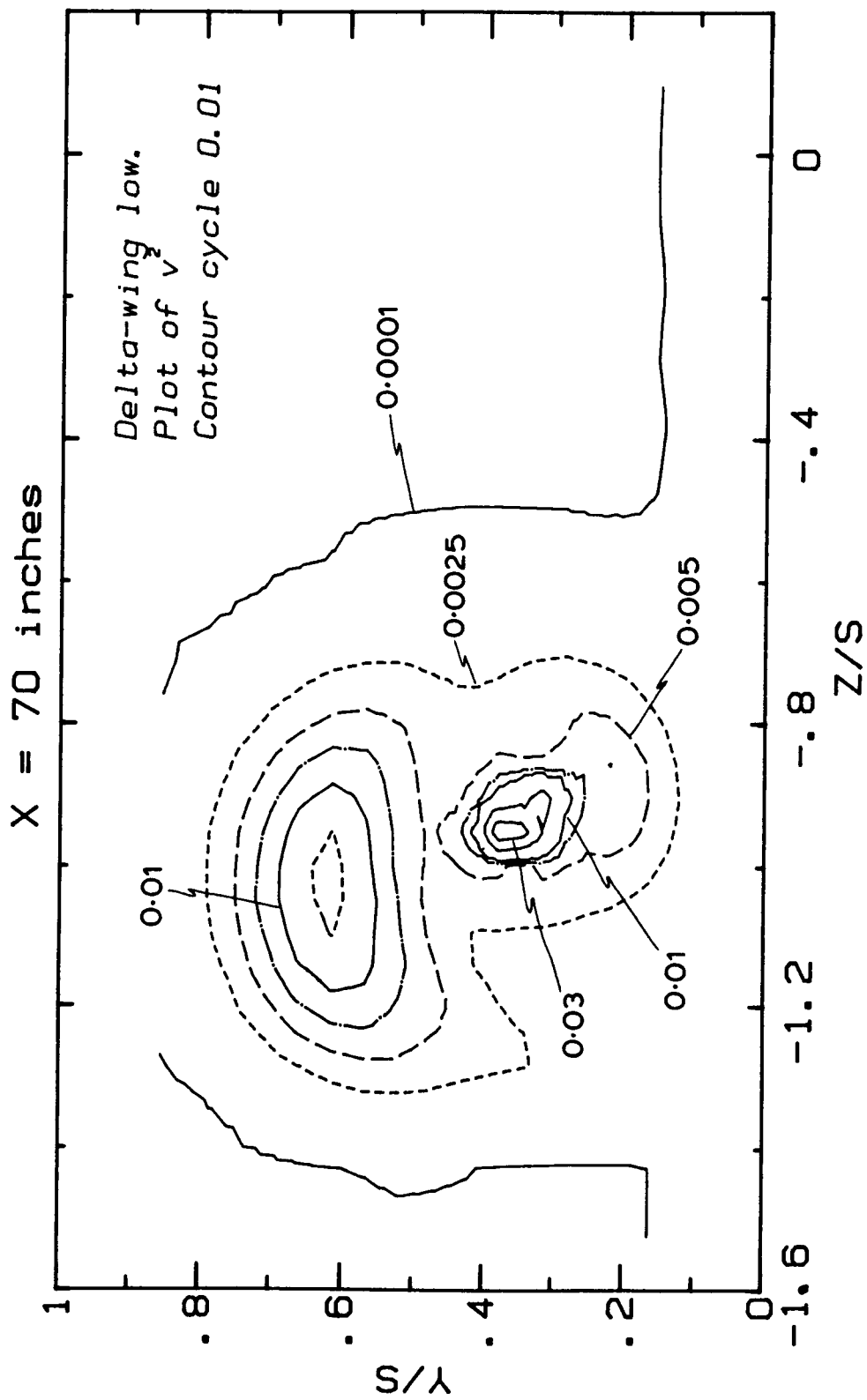
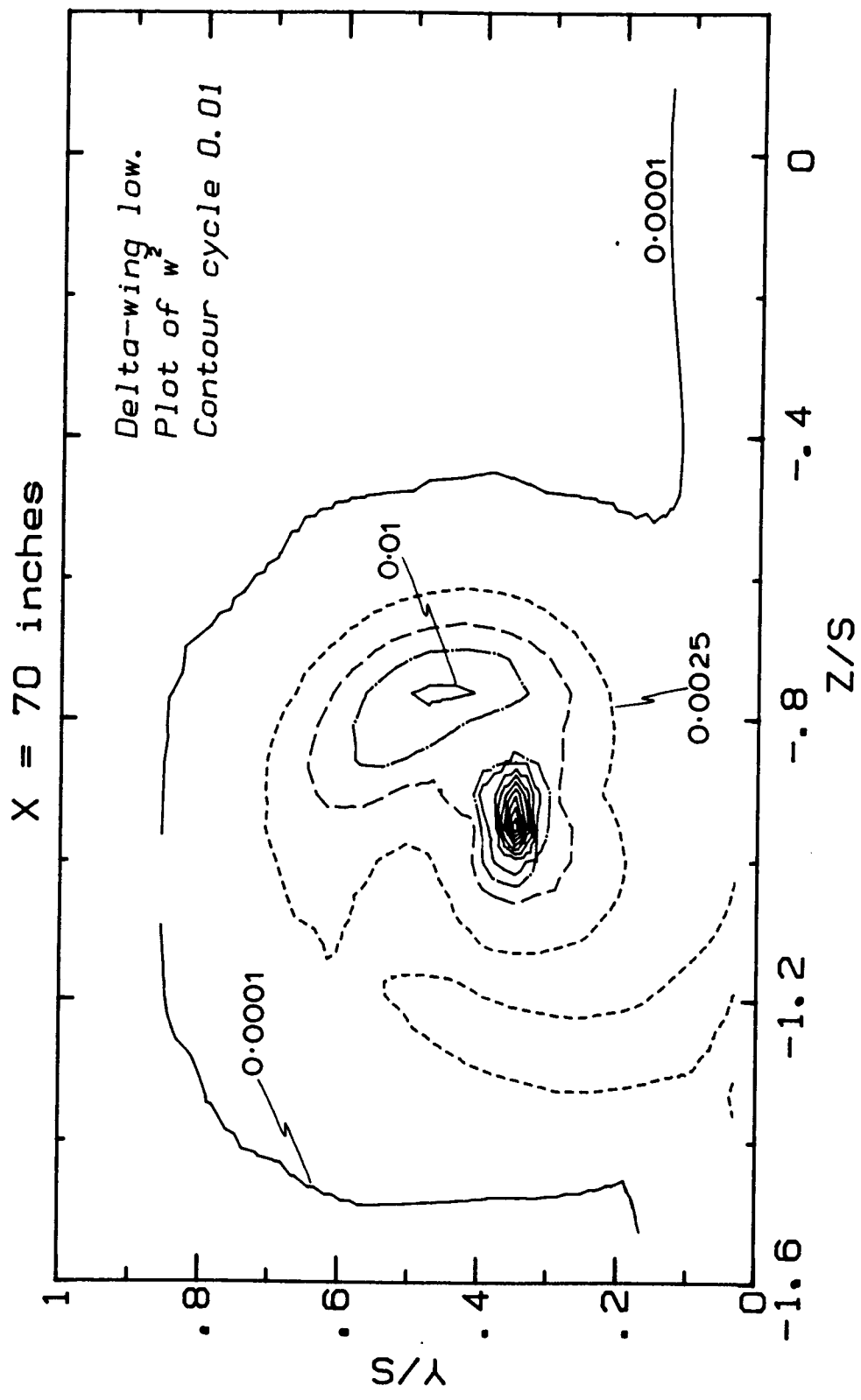


Figure 12. Contours of the Reynolds stresses at  $x/s = 6.667$  for the "delta-wing low" case:

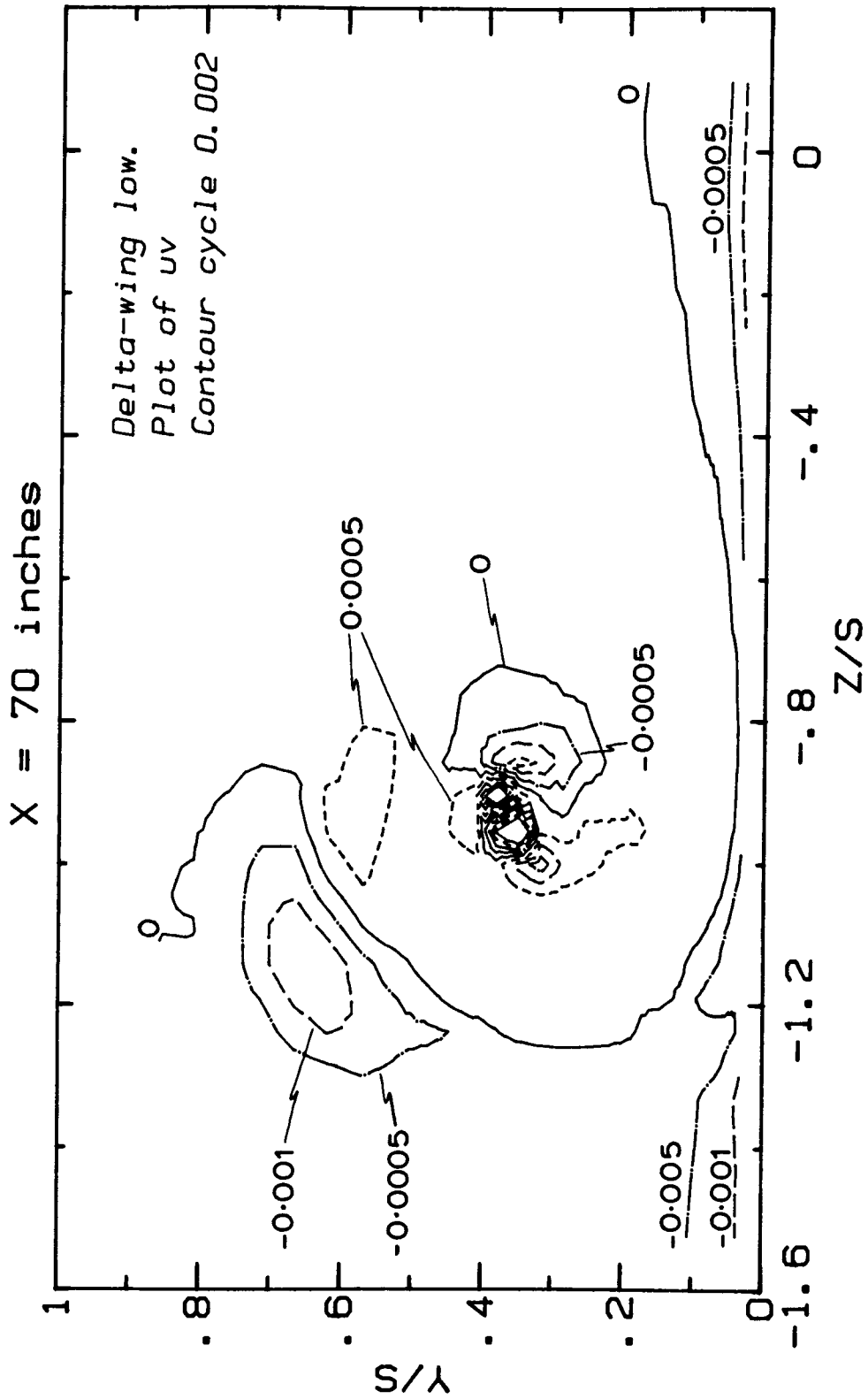
12(a)  $\overline{u^2}$



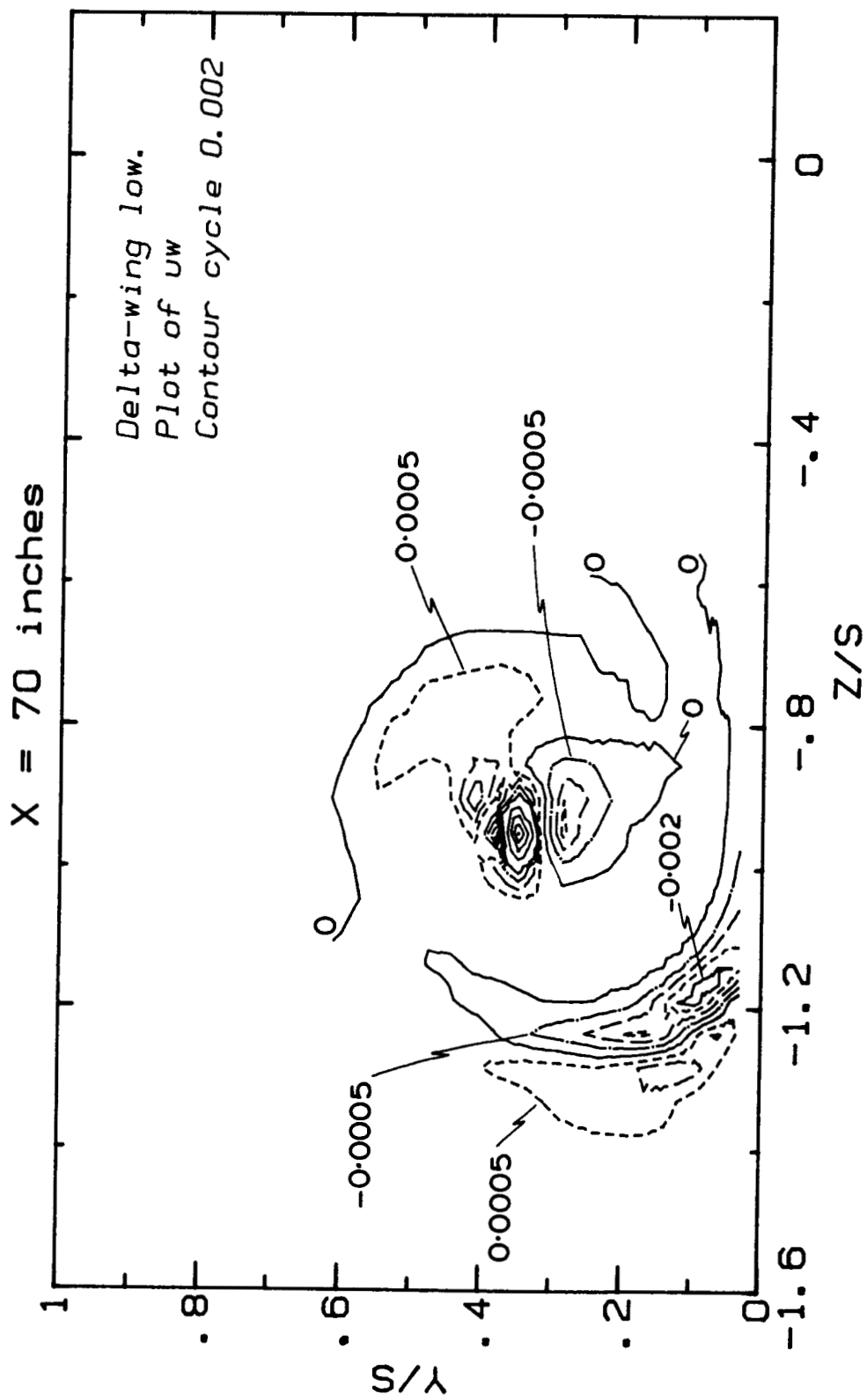
12(b)  $\overline{v^2}$



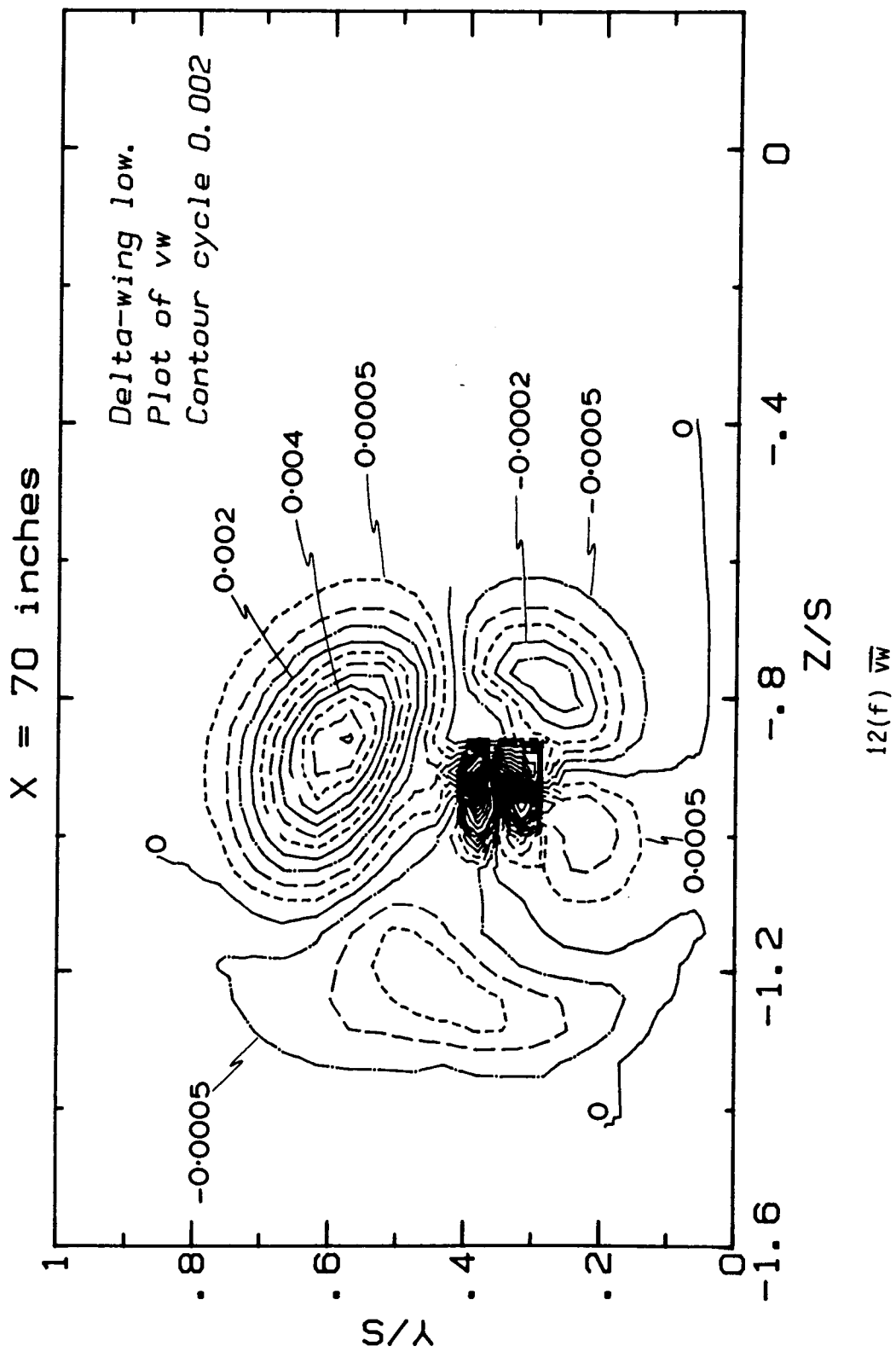
12(c)  $\overline{w^2}$



12(d)  $\overline{uv}$



12(e)  $u_w$



\*\*\*Figures 13-17:  $U_i$  and  $\overline{u_i u_j}$ , "delta wing high"\*\*\*

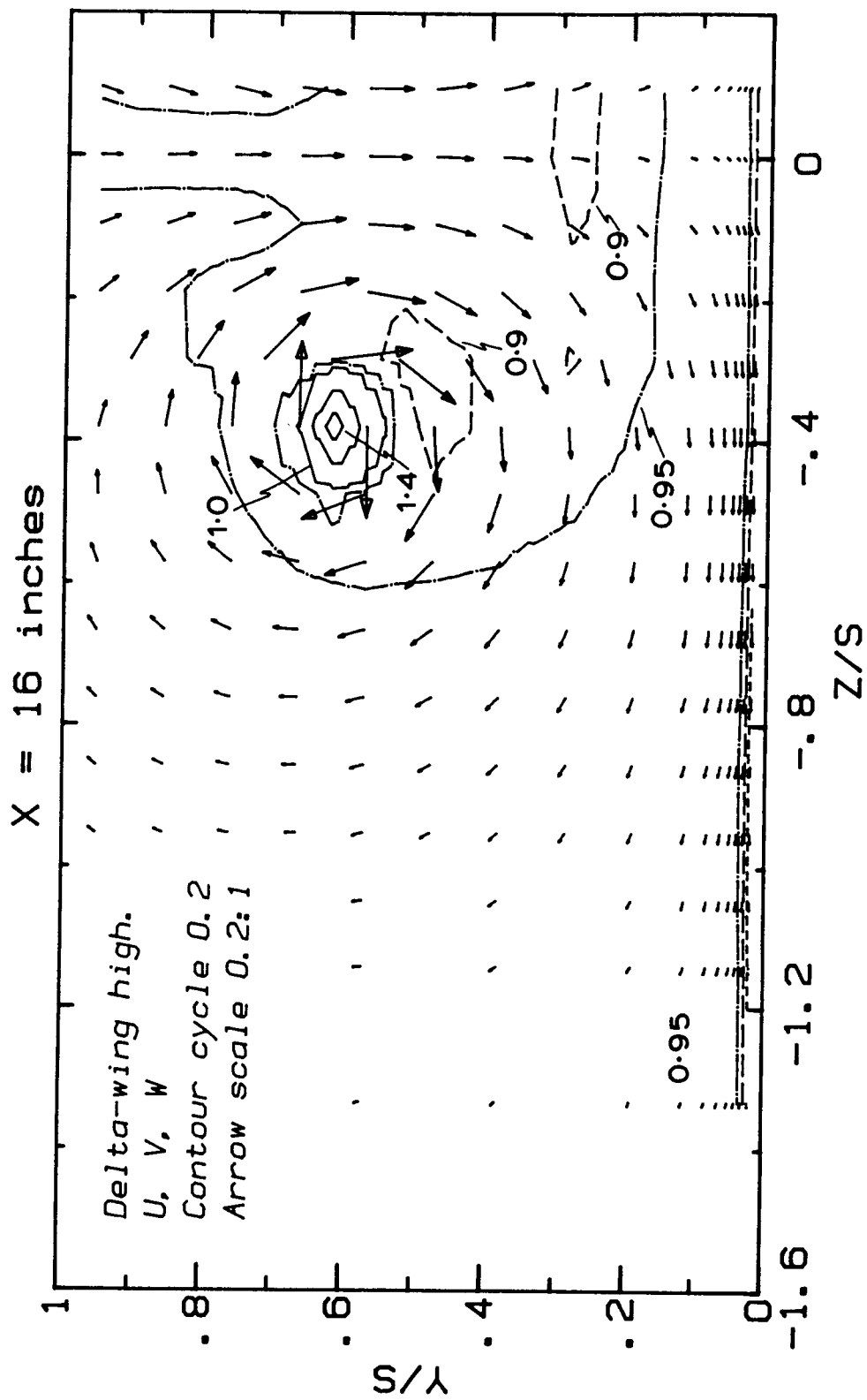
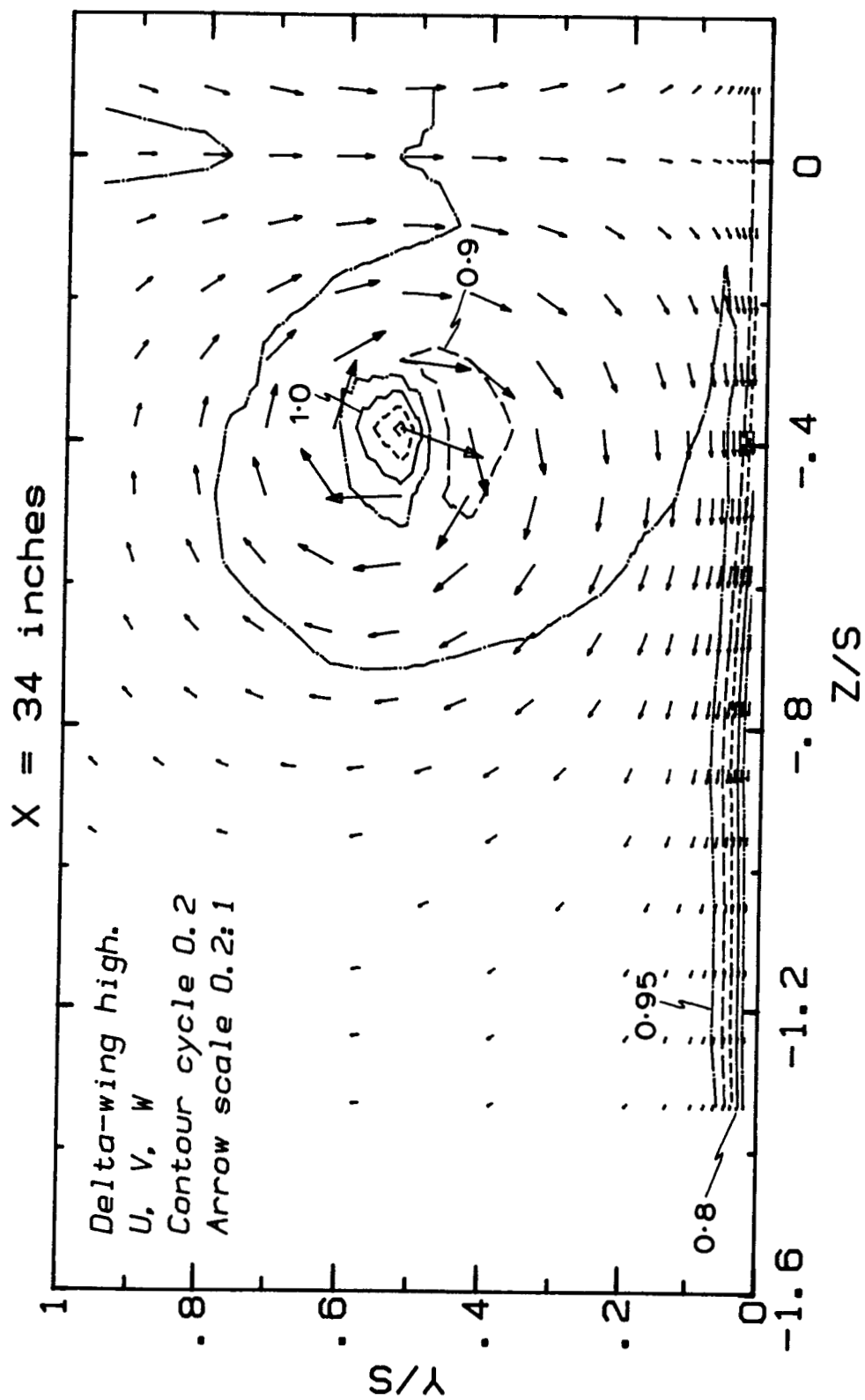
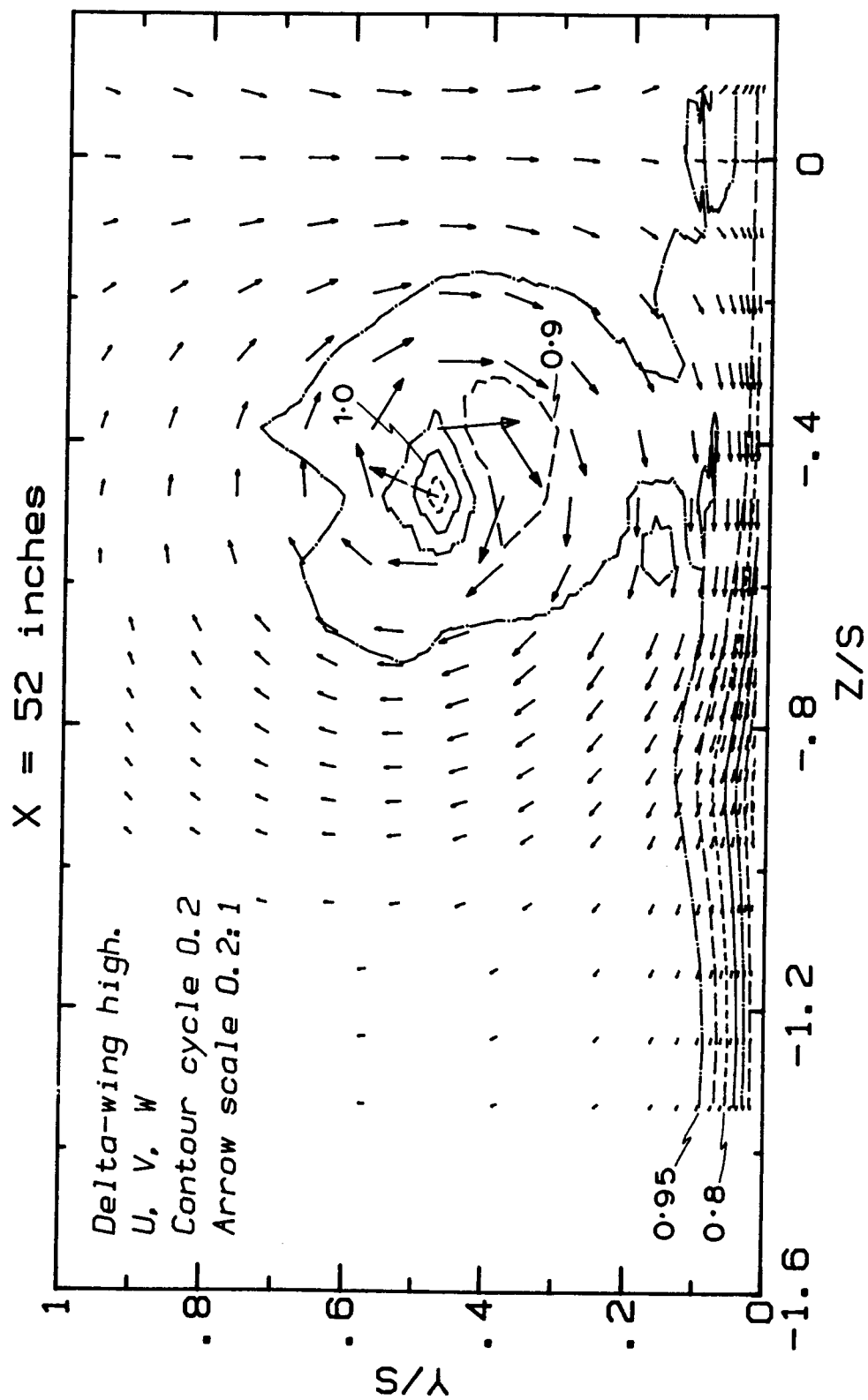


Figure 13. Contours of mean U-component velocity and vectors of mean secondary-flow velocity components V, W for the "delta-wing high" case:

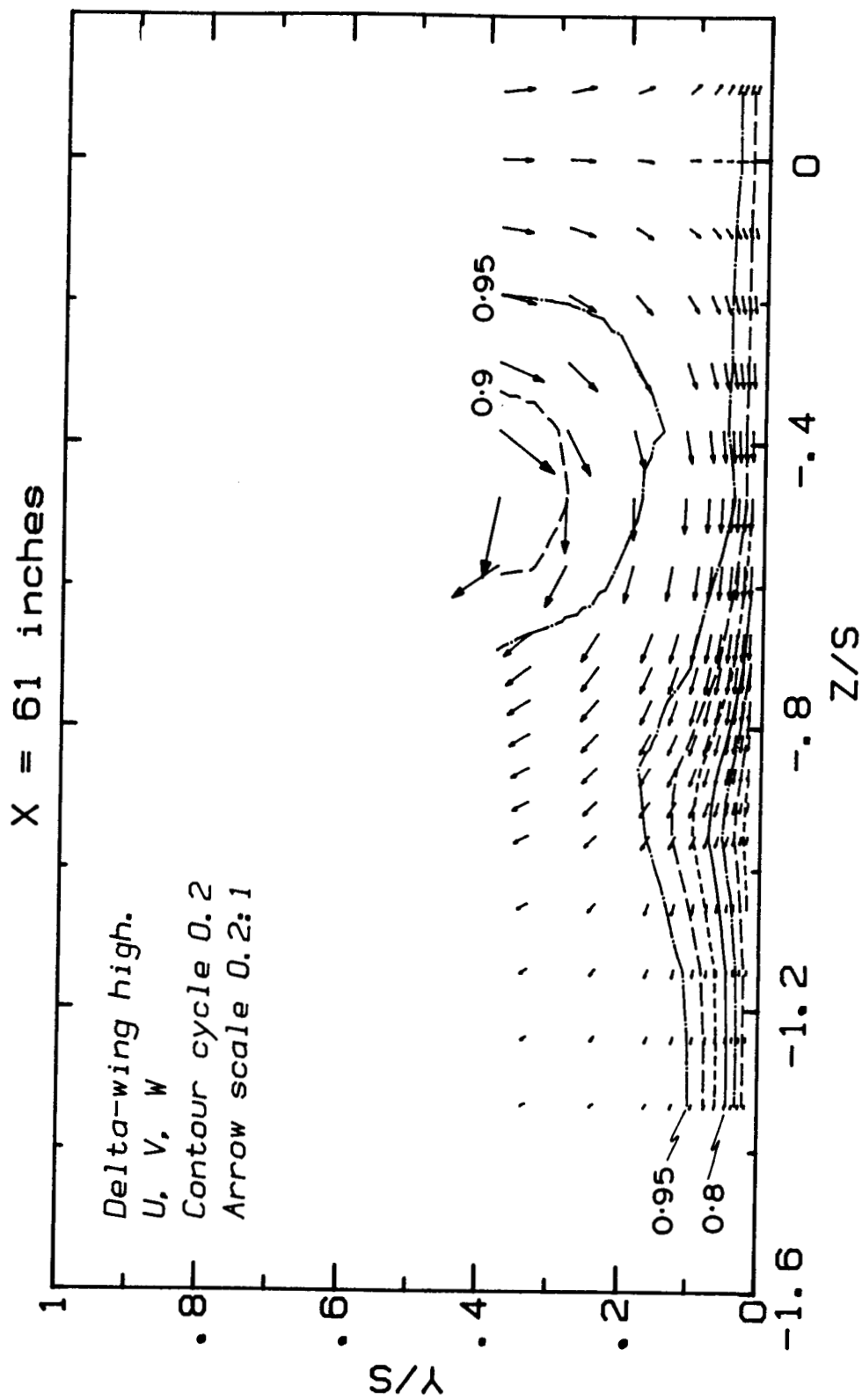
13(a)  $x/s = 1.524$



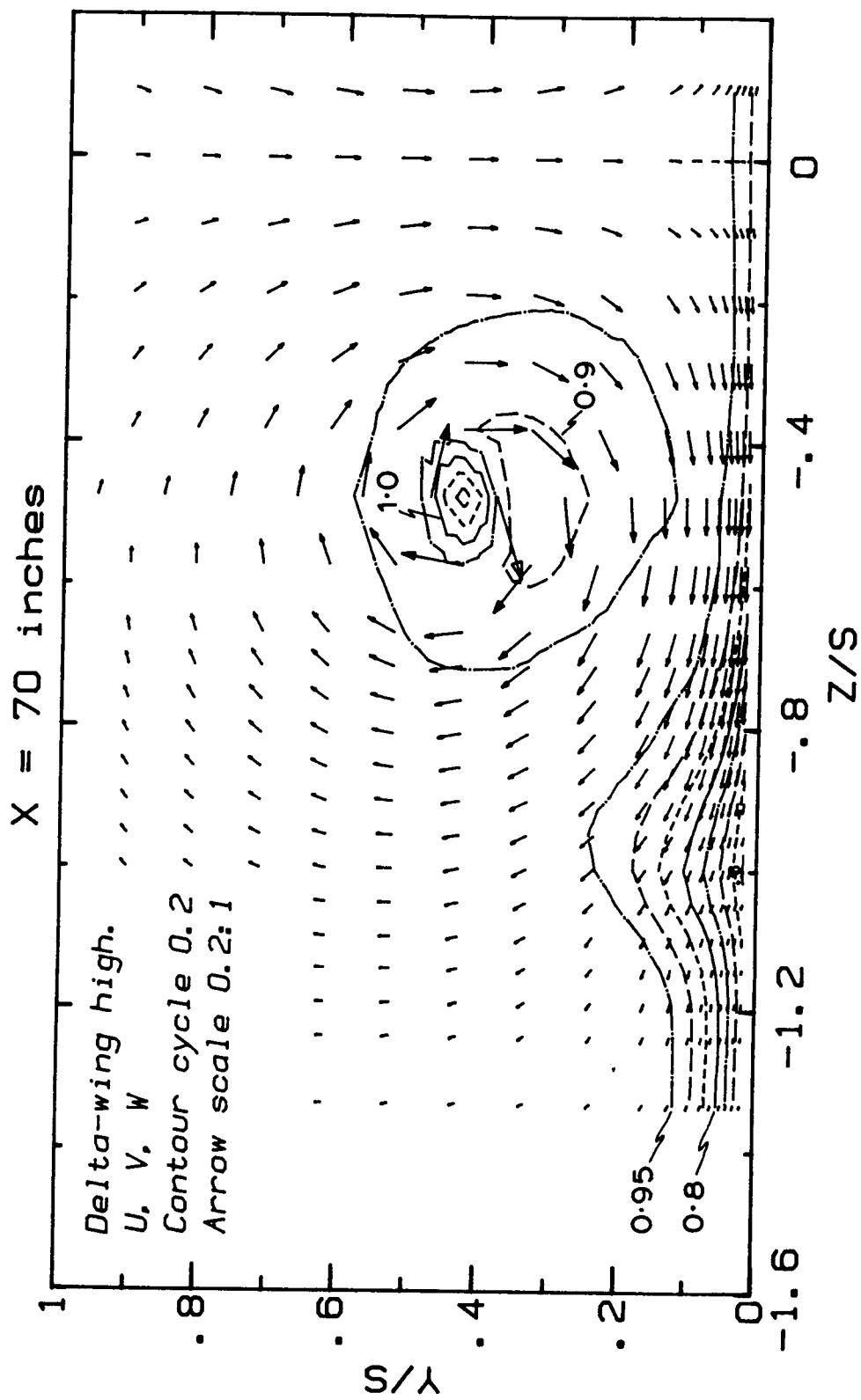
13(b)  $x/s = 3.238$



13(c)  $x/s = 4.952$



13(d)  $x/s = 5.810$



13(e)  $x/s = 6.667$

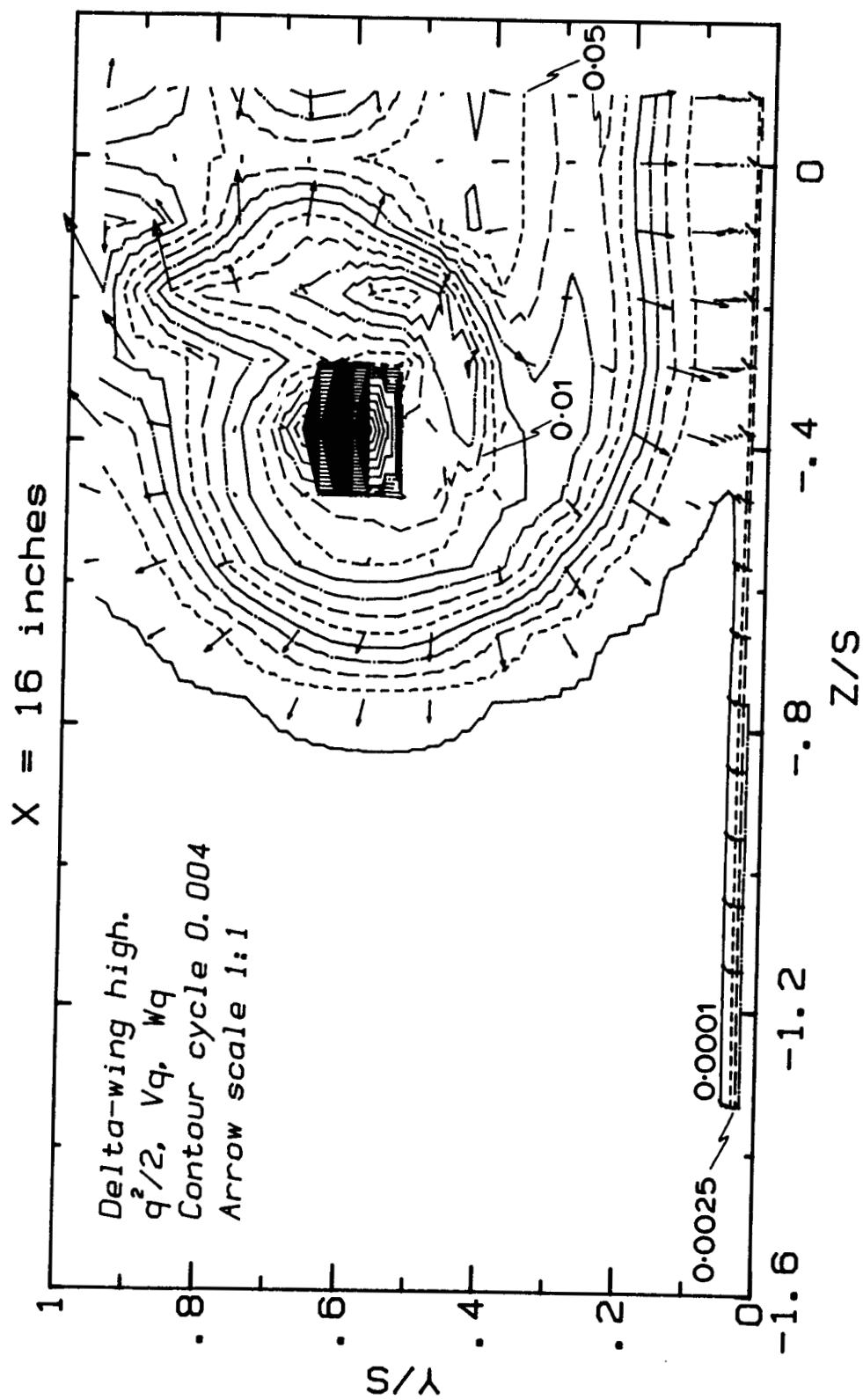
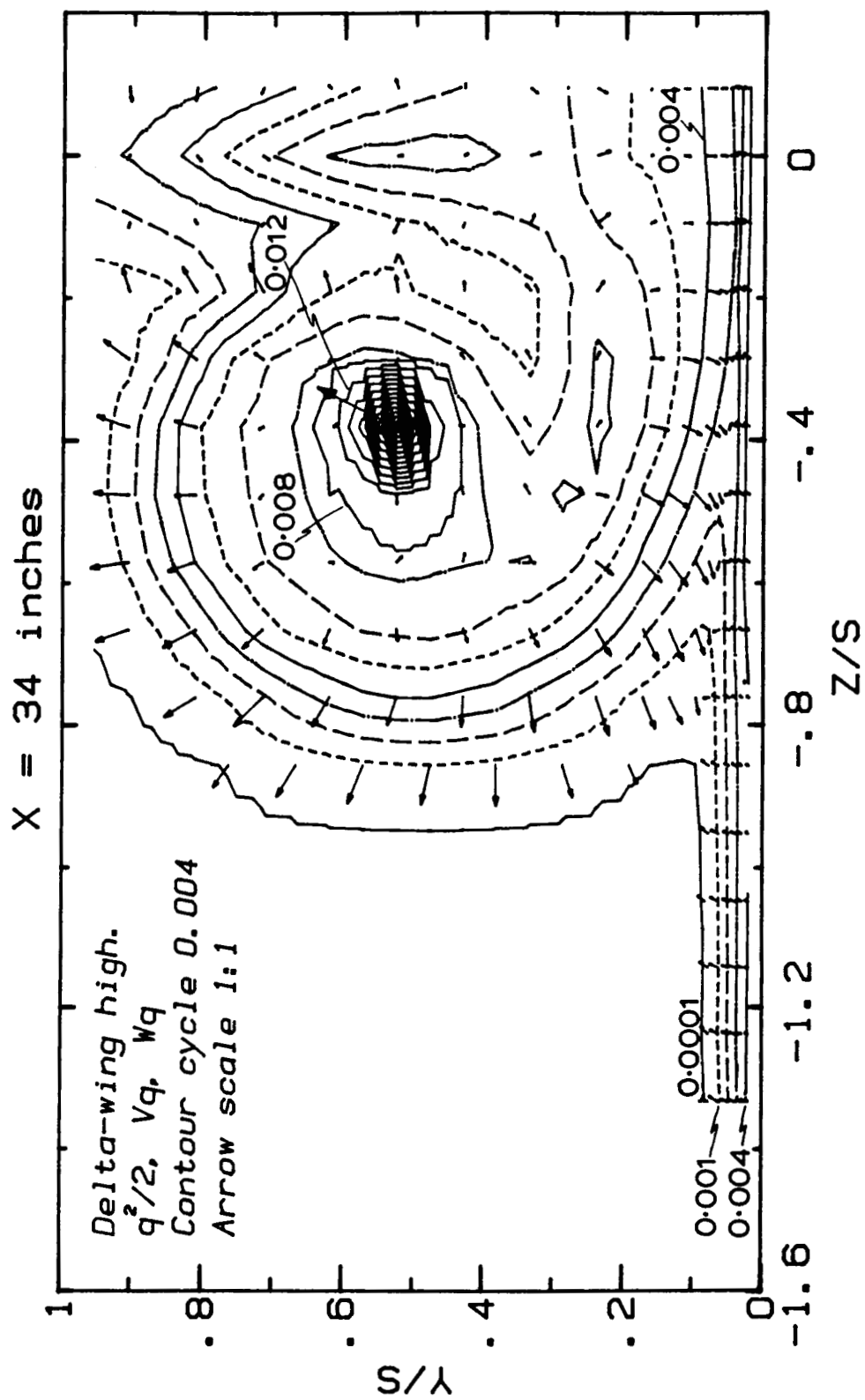
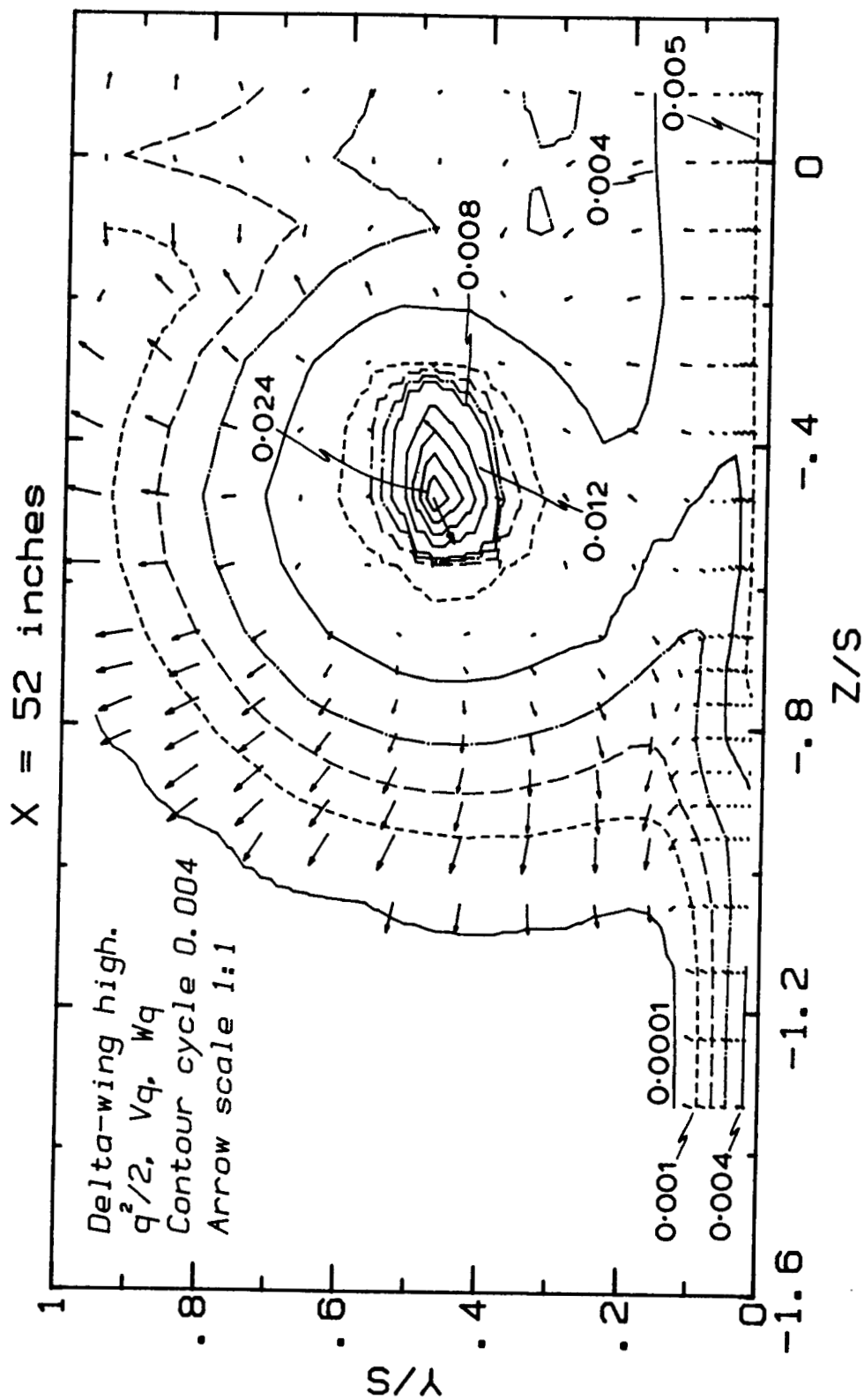


Figure 14. Contours of turbulent kinetic energy  $(\overline{q^2}/2 = (\overline{u^2} + \overline{v^2} + \overline{w^2})/2)$  and vectors of turbulent diffusion velocity ( $Vq = \overline{q^2}v/\overline{q^2}$ ,  $Wq = \overline{q^2}w/\overline{q^2}$ ) for the "delta-wing high" case:

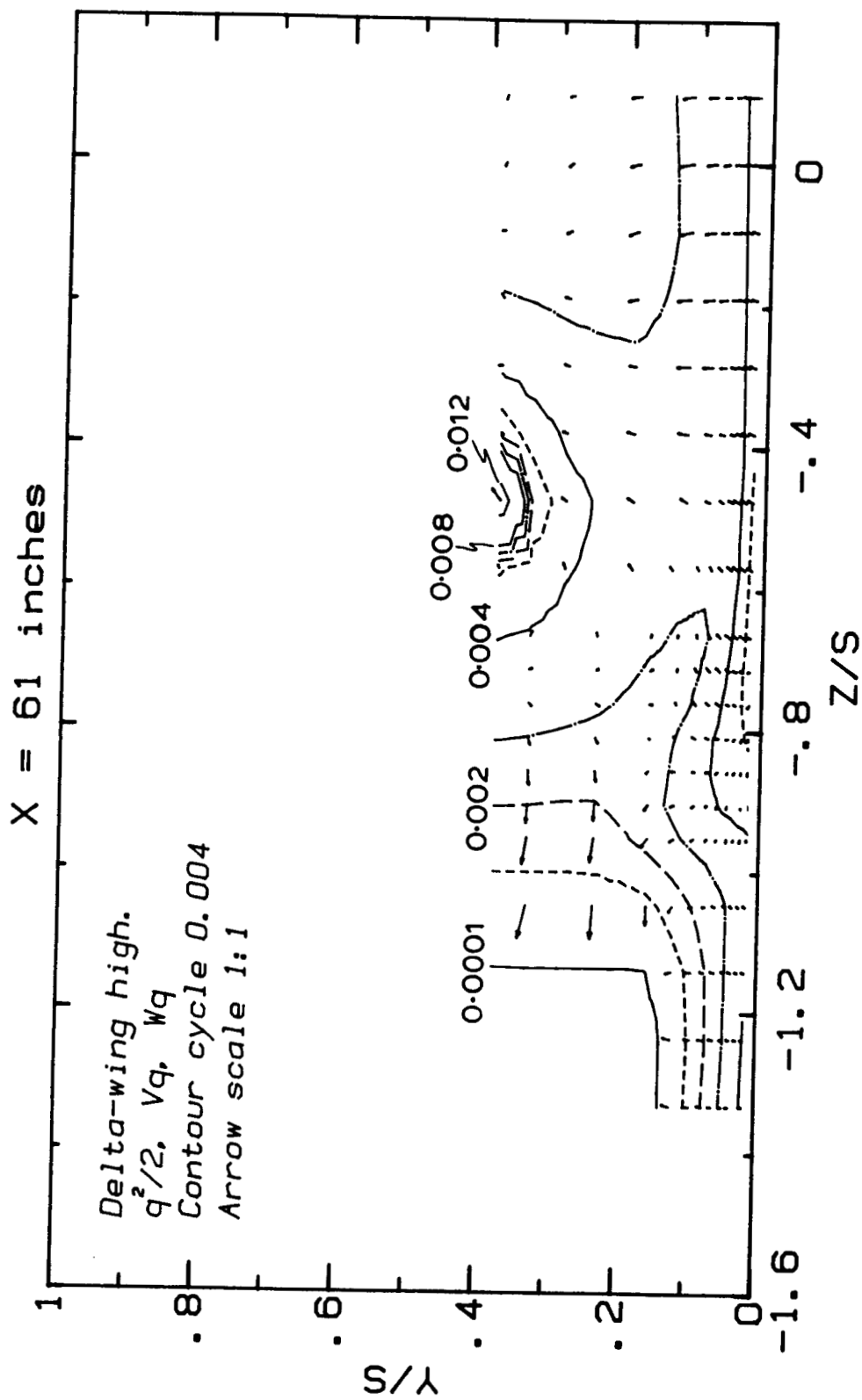
14(a)  $x/s = 1.524$



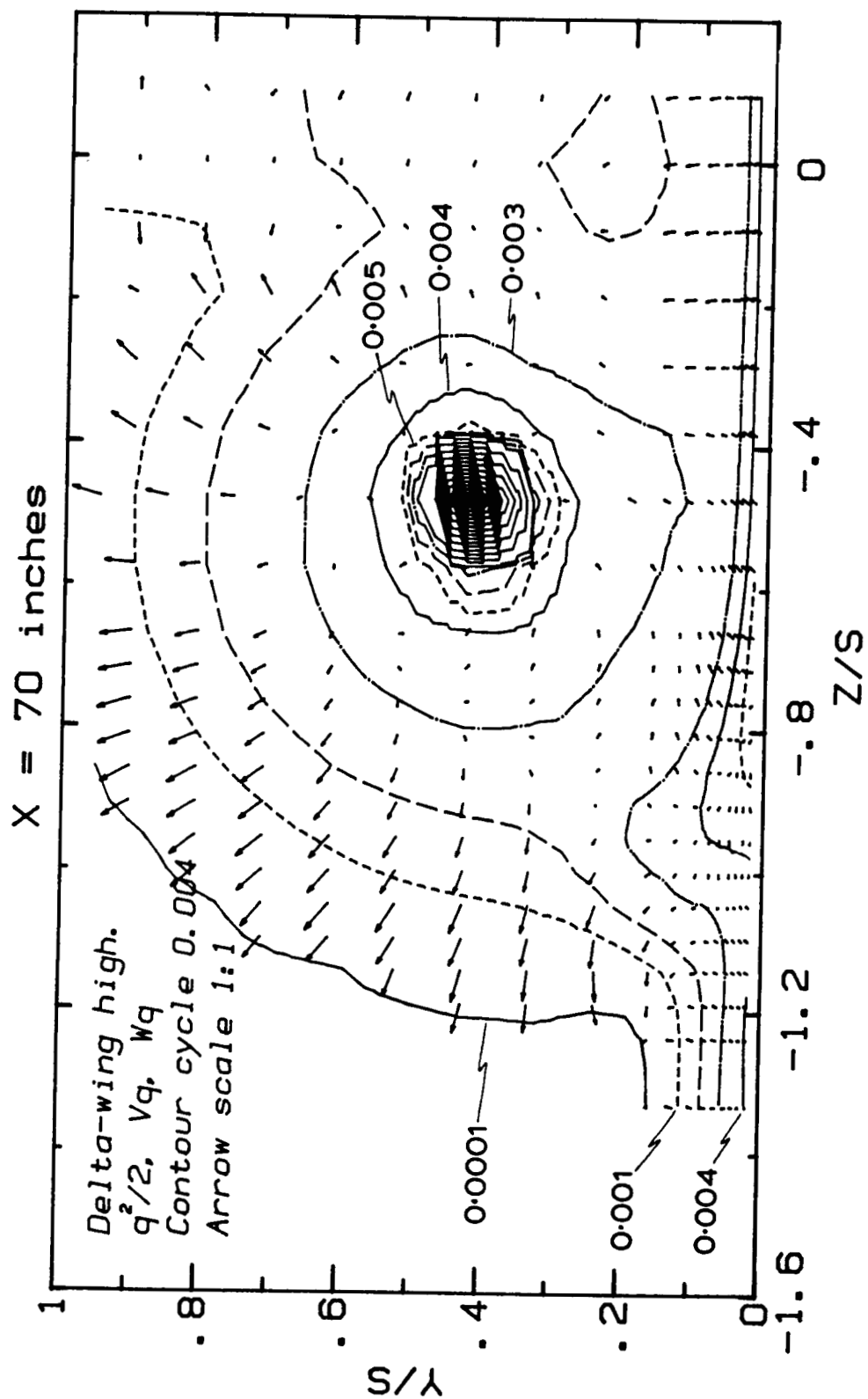
14(b)  $x/s = 3.238$



14(c)  $x/s = 4.952$



14(d)  $x/s = 5.810$



14(e)  $x/s = 6.667$

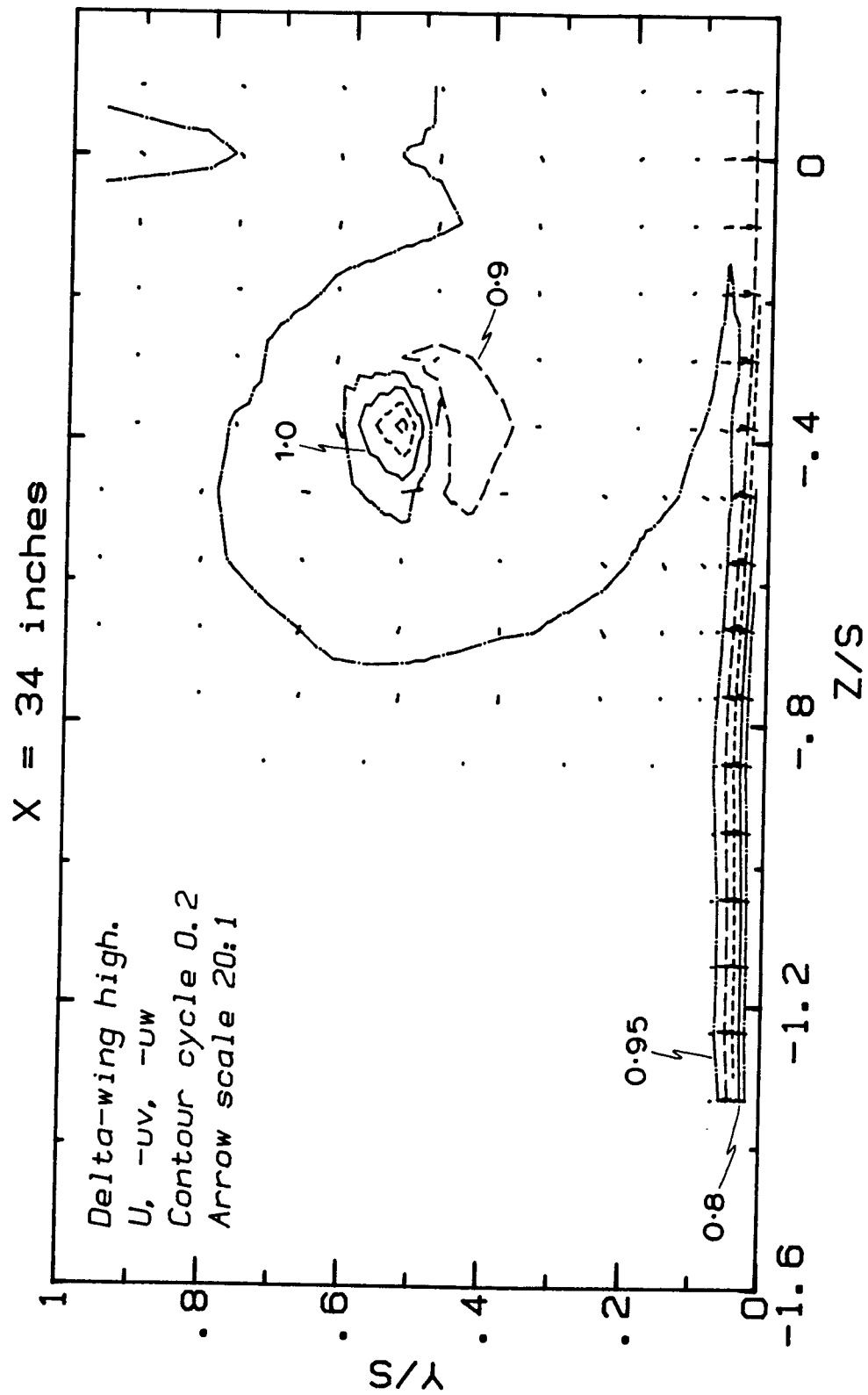
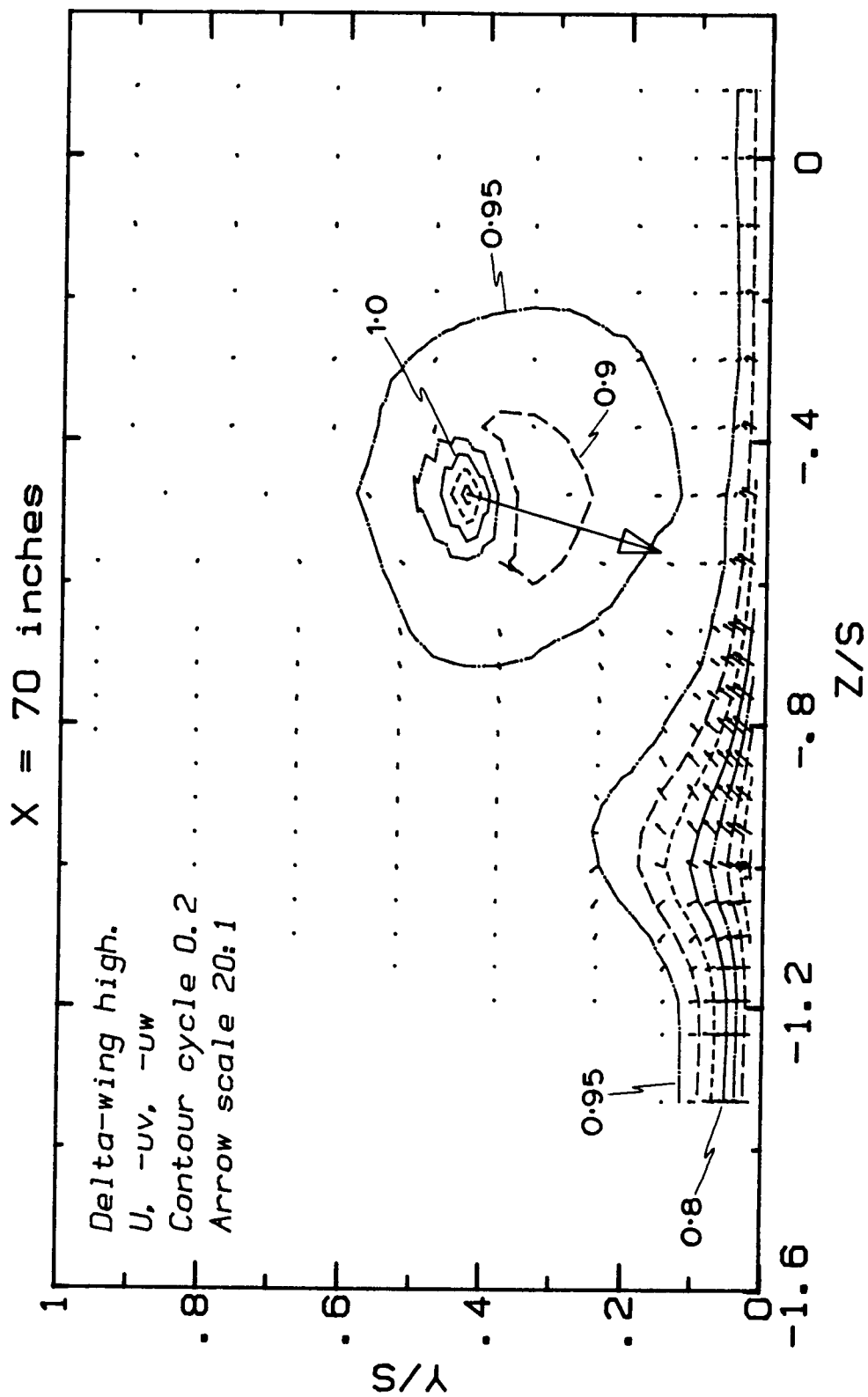


Figure 15. Contours of mean  $U$  component velocity and shear-stress vectors ( $-\overline{uv}$ ,  $-\overline{uw}$ ) for the "delta-wing high" case:

15(a)  $x/s = 3.238$



15(b)  $x/s = 6.667$

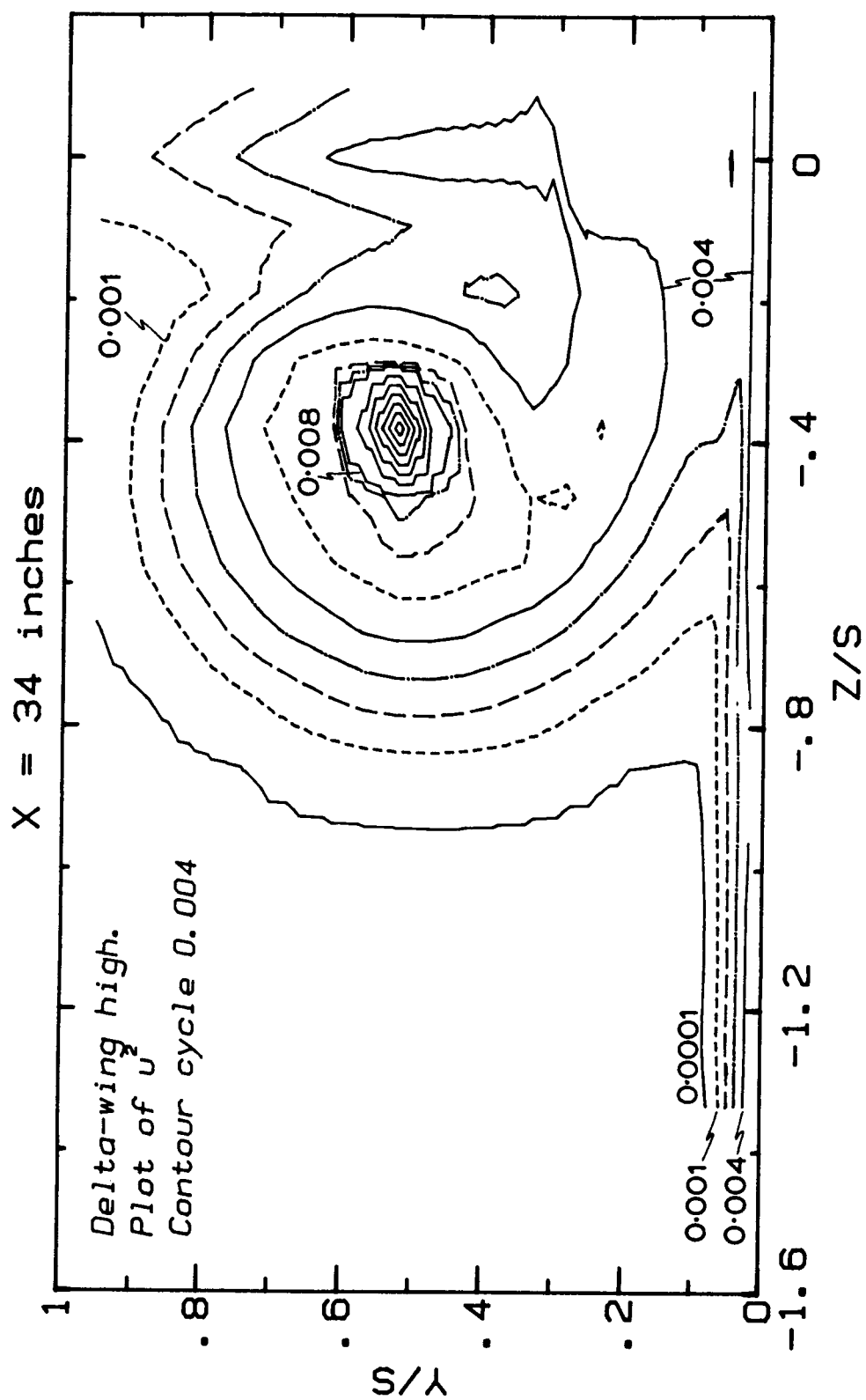
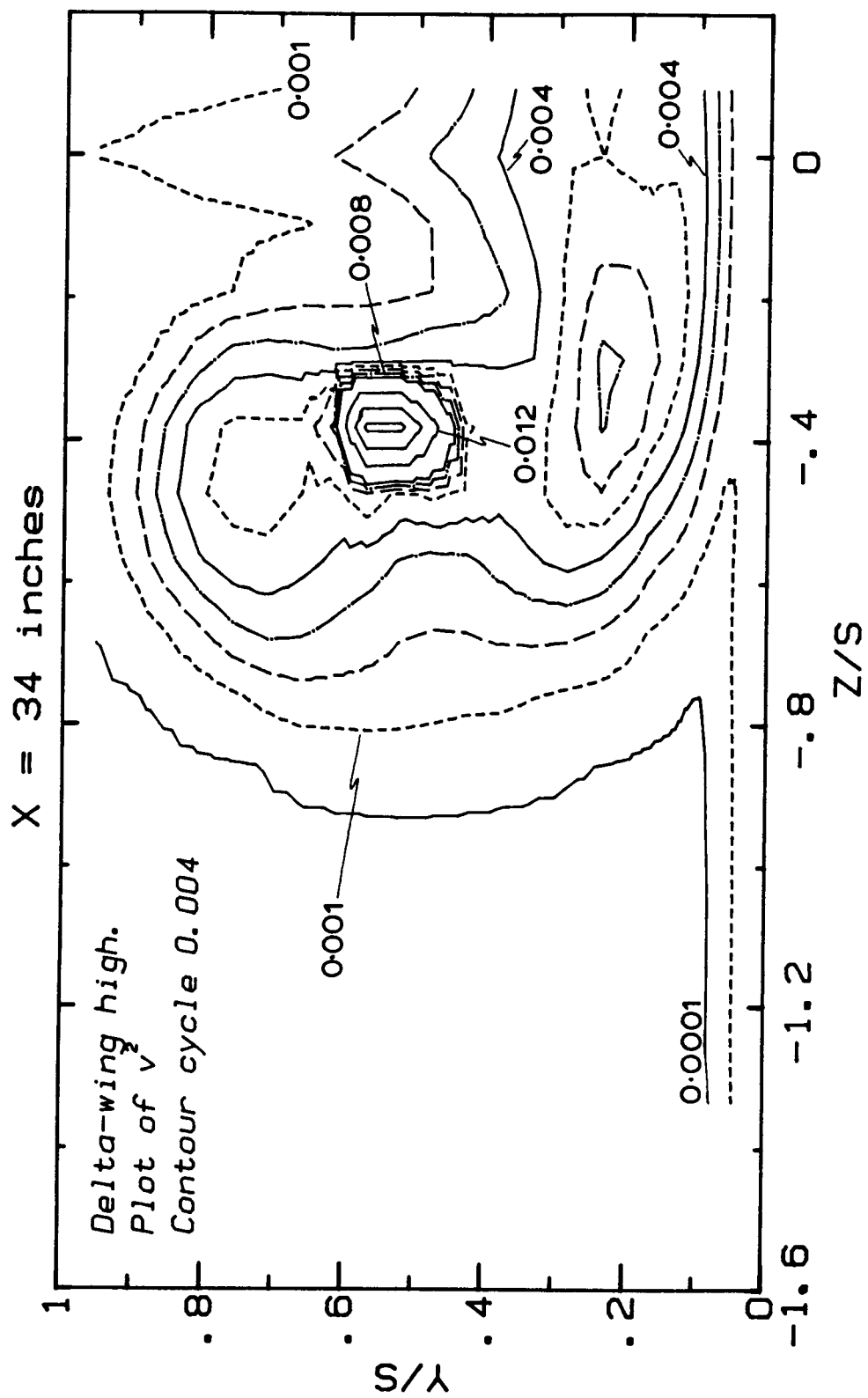
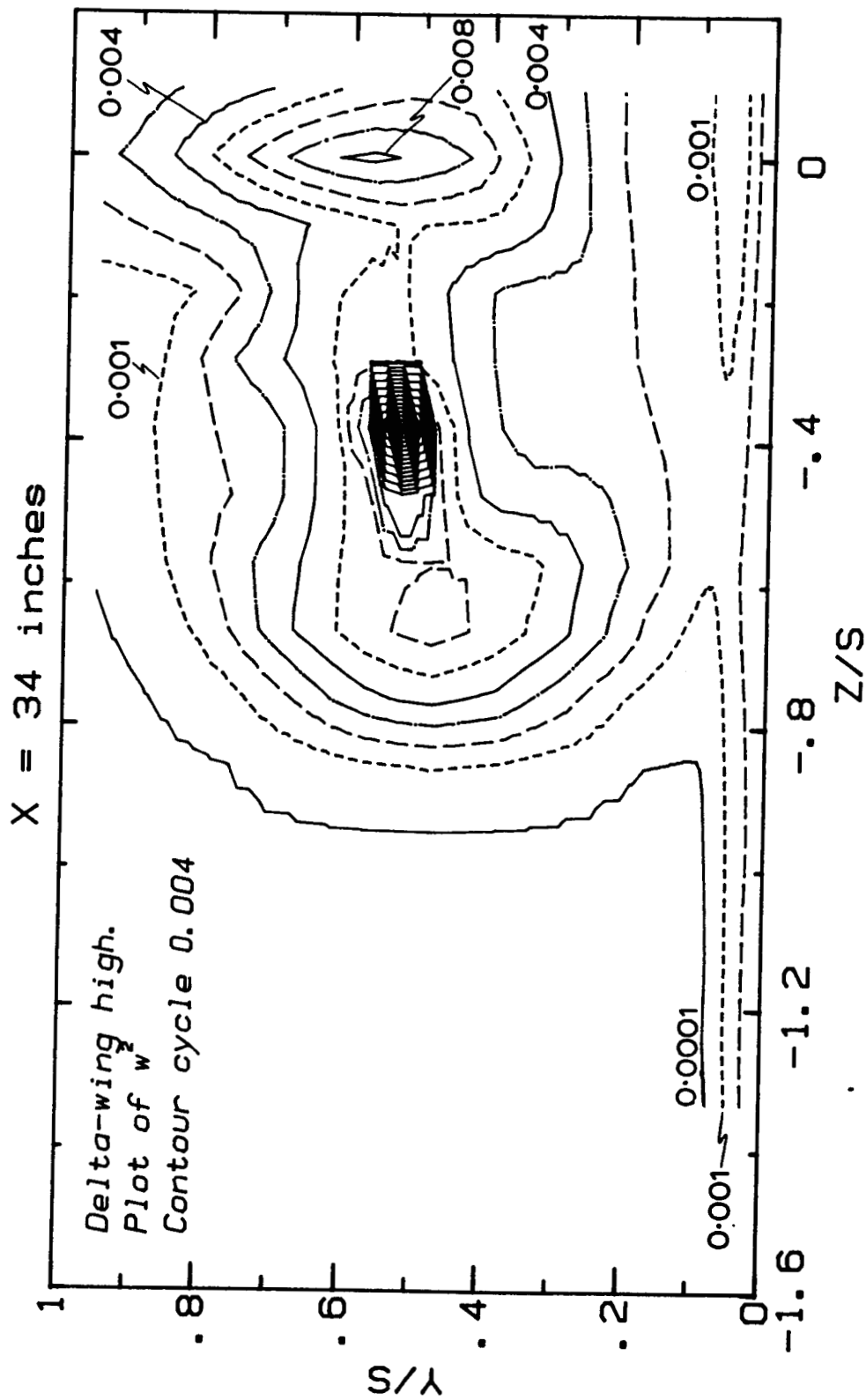


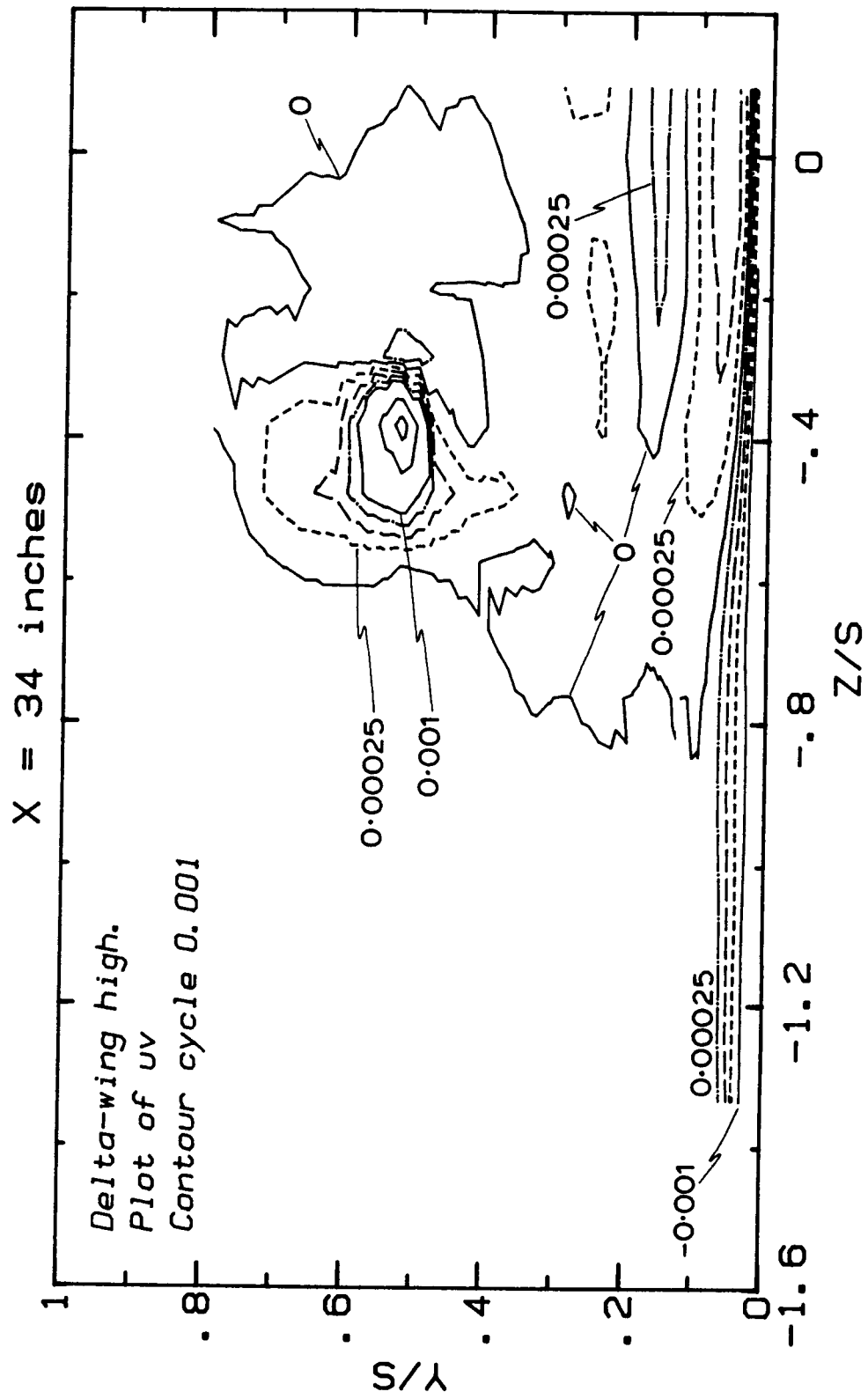
Figure 16. Contours of the Reynolds stresses at  $x/s = 3.238$  for the "delta-wing high" case:

$$16(a) \overline{u^2}$$

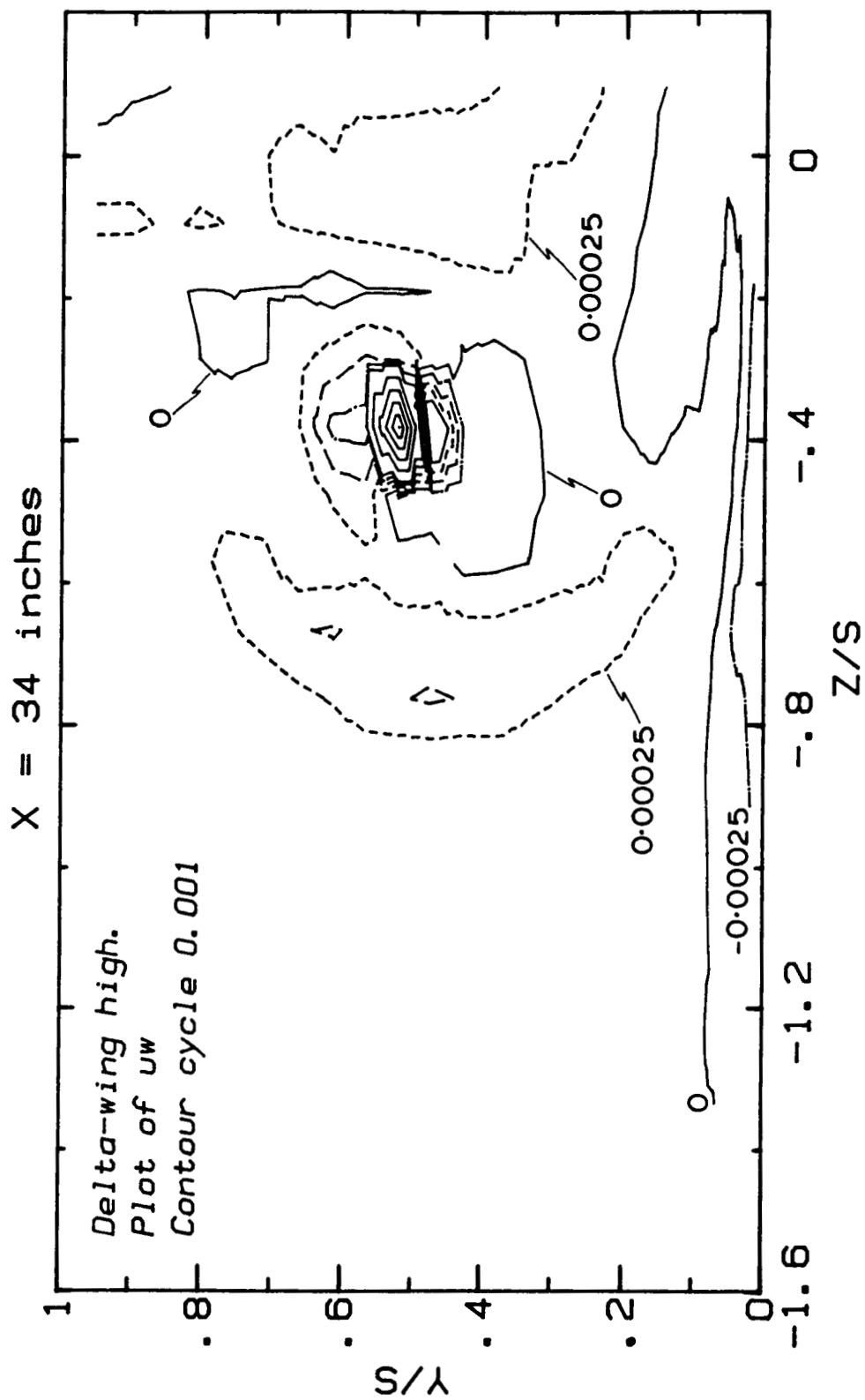


16(b)  $\overline{v_z^2}$

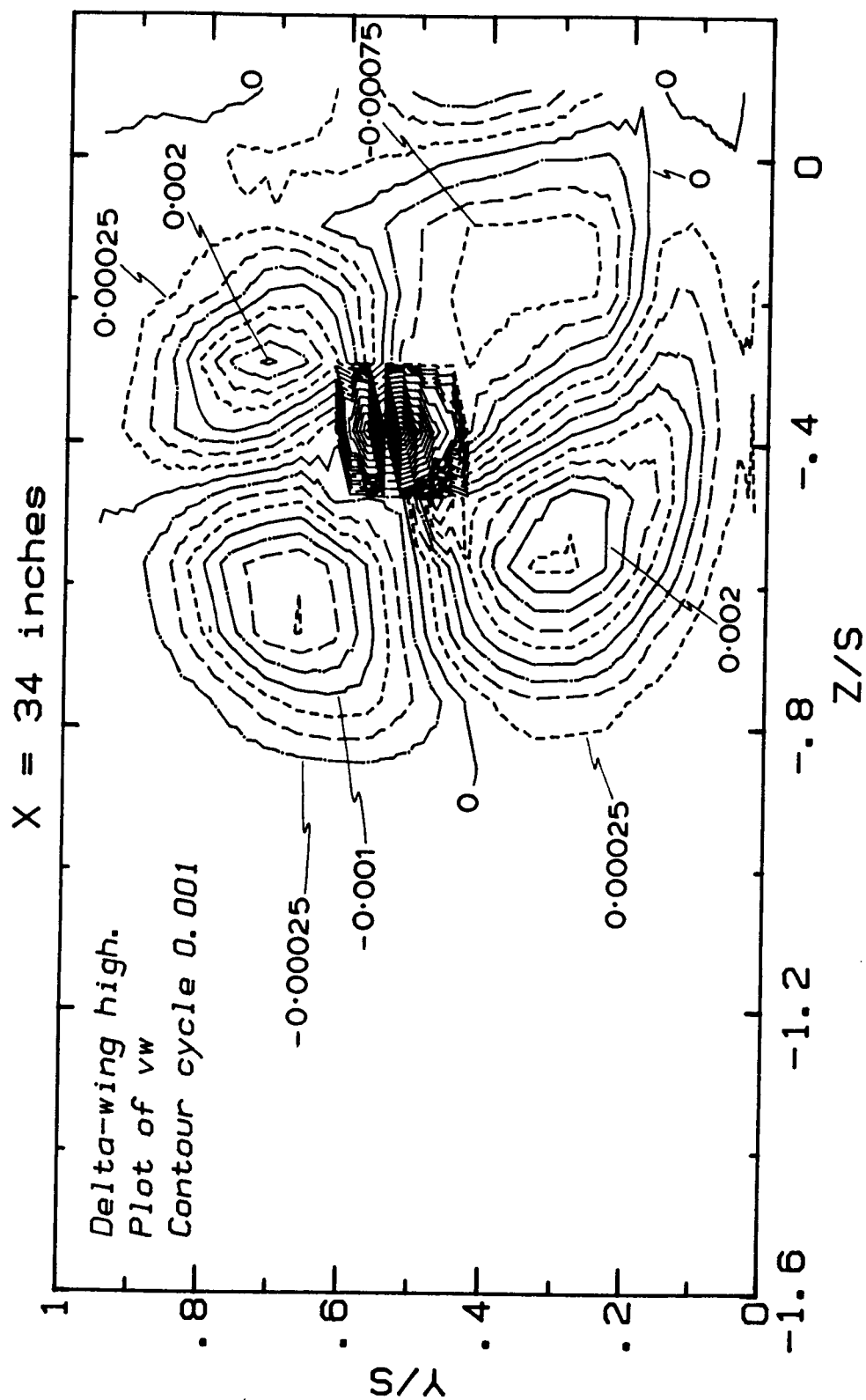




16(d)  $\overline{uv}$



16(e)  $\overline{uw}$



16(f)  $\overline{v_w}$

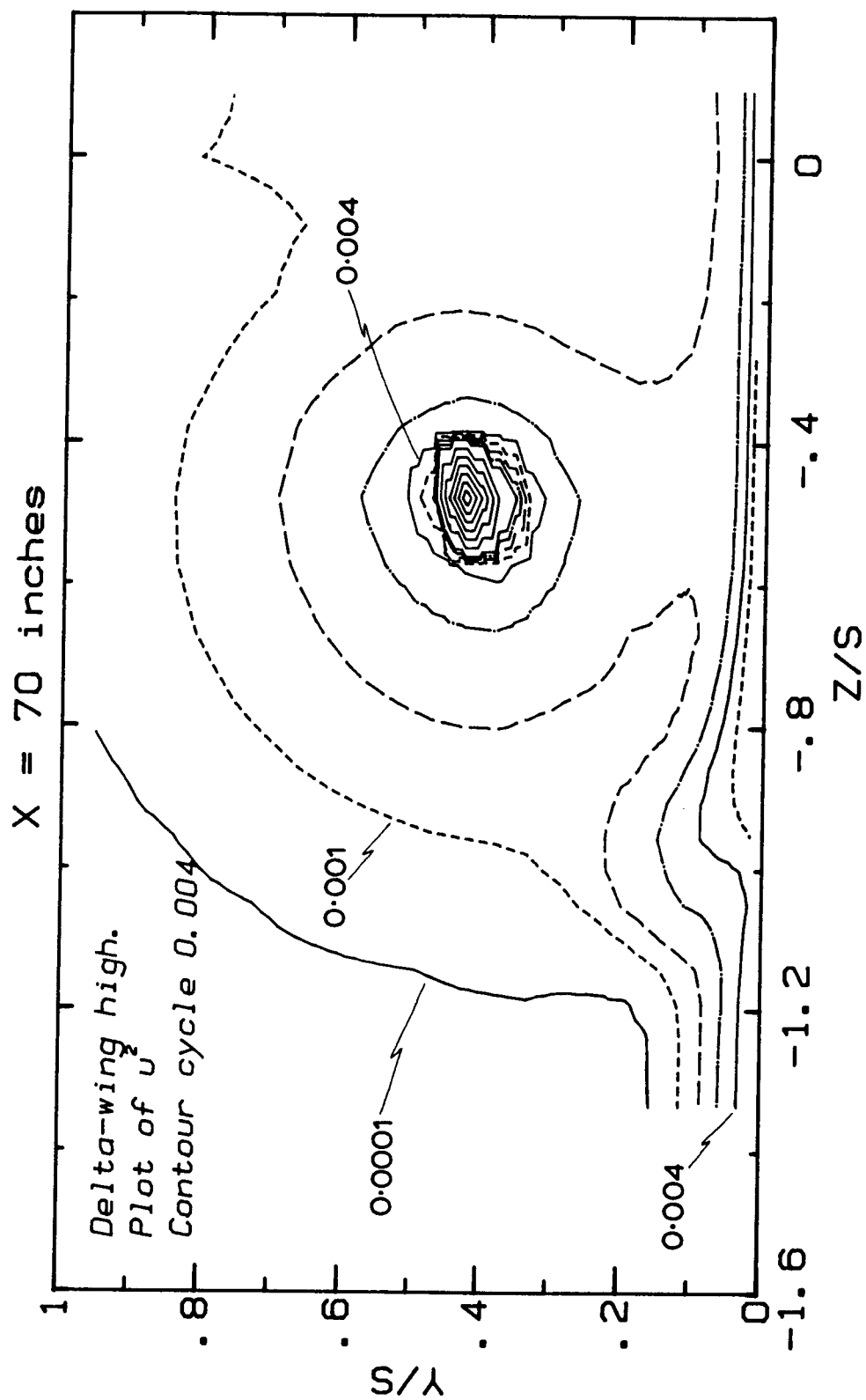
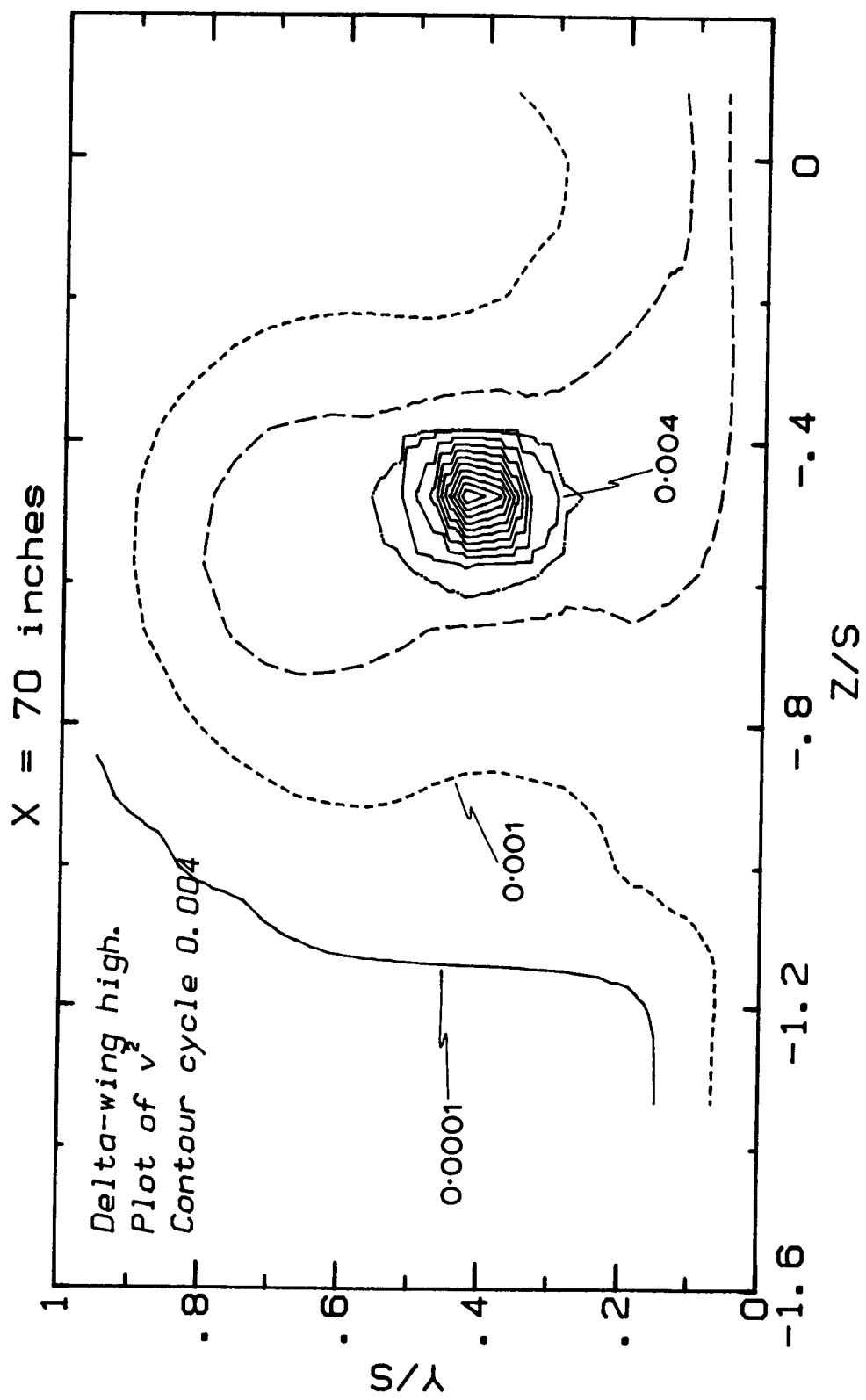
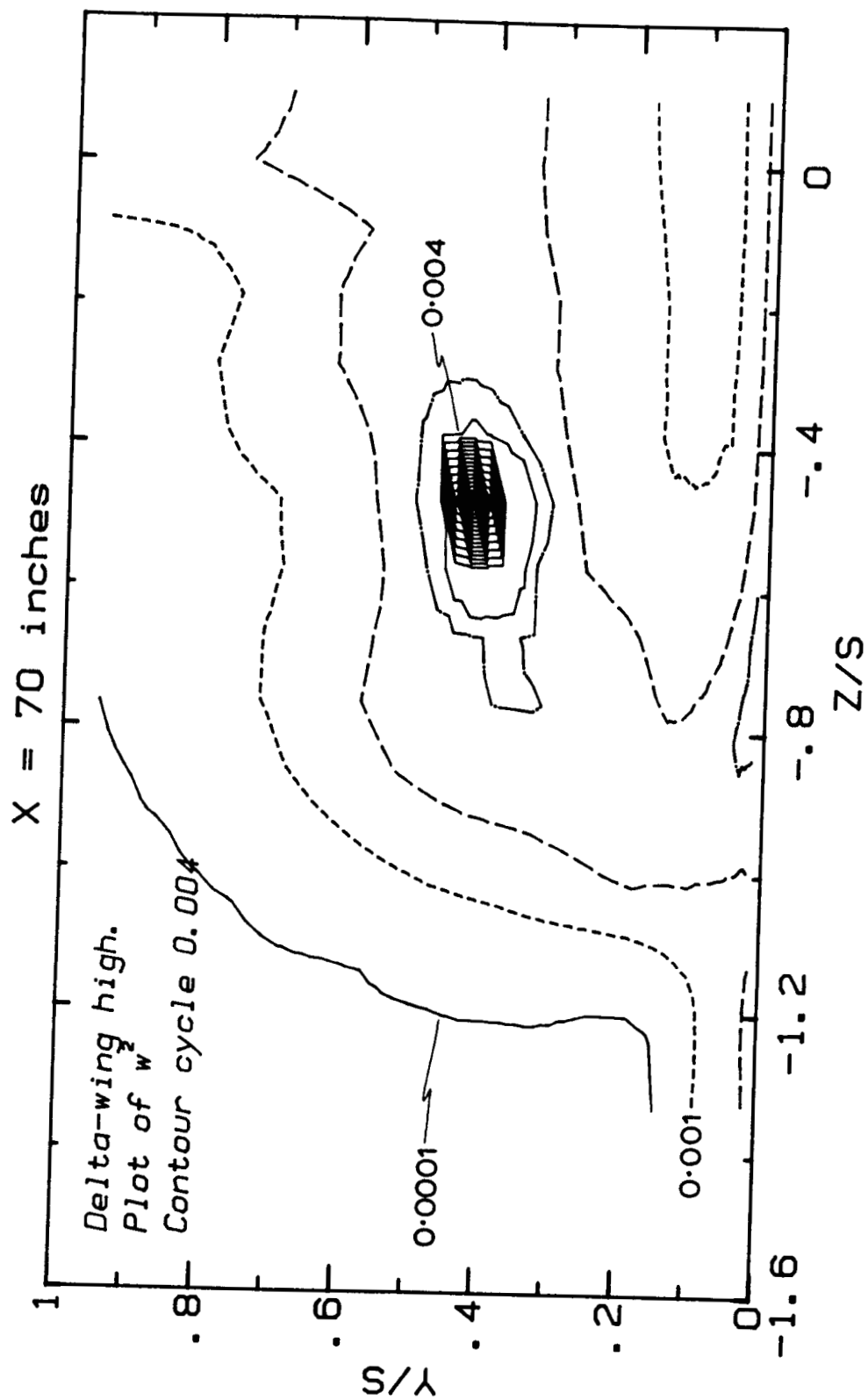
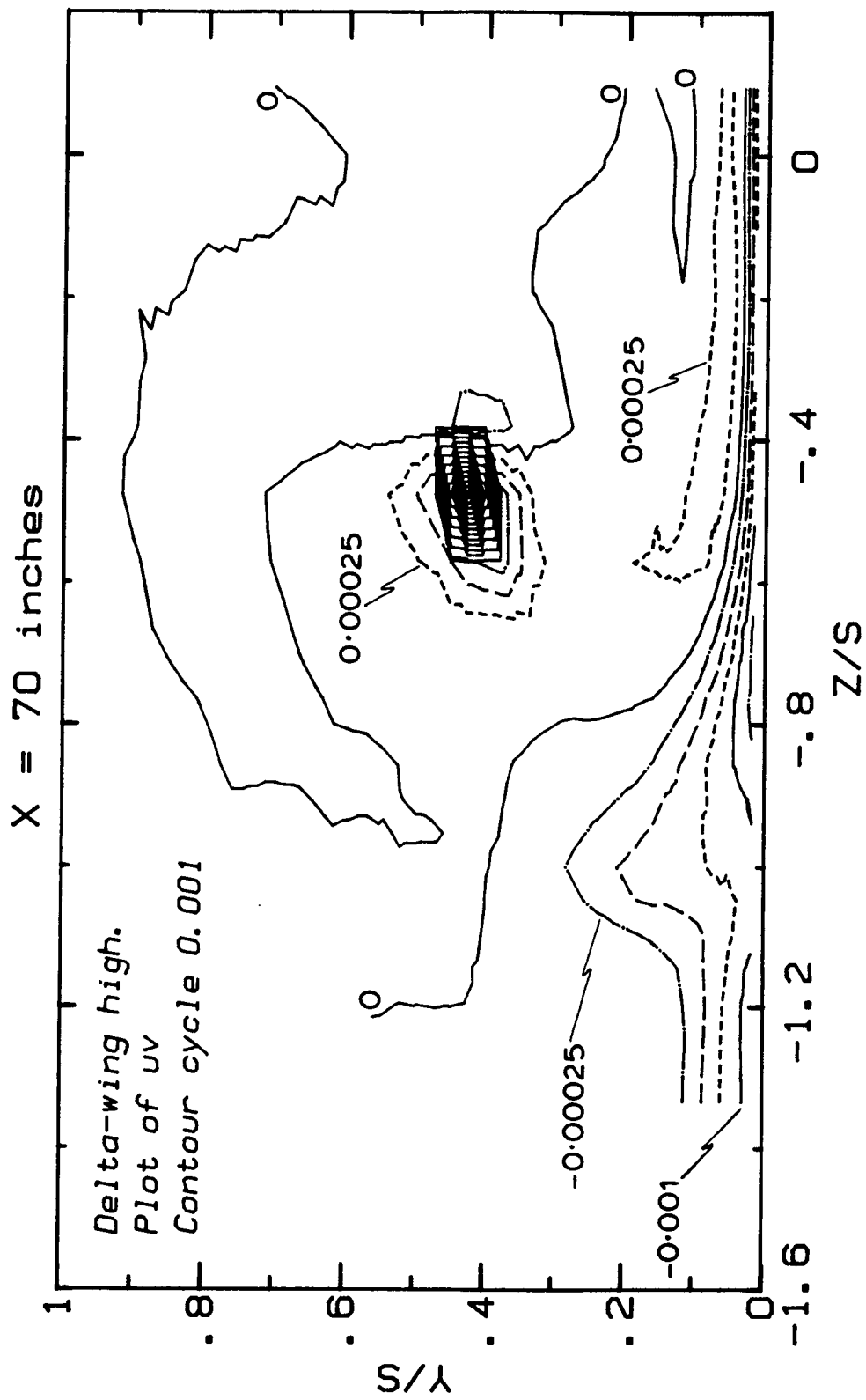


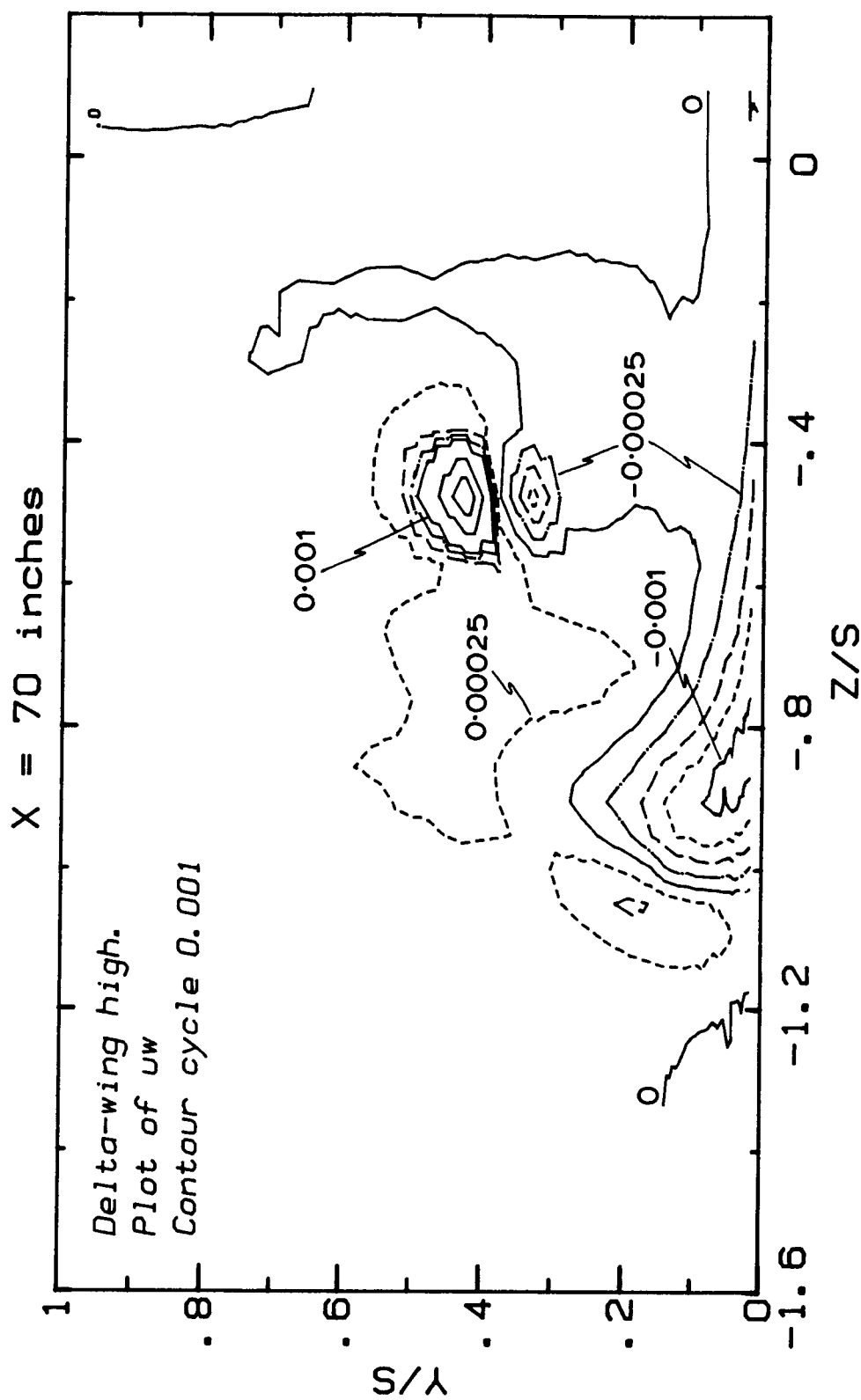
Figure 17. Contours of the Reynolds stresses at  $x/s = 6.667$  for the "delta-wing high" case:

17(a)  $\overline{u'v'}$

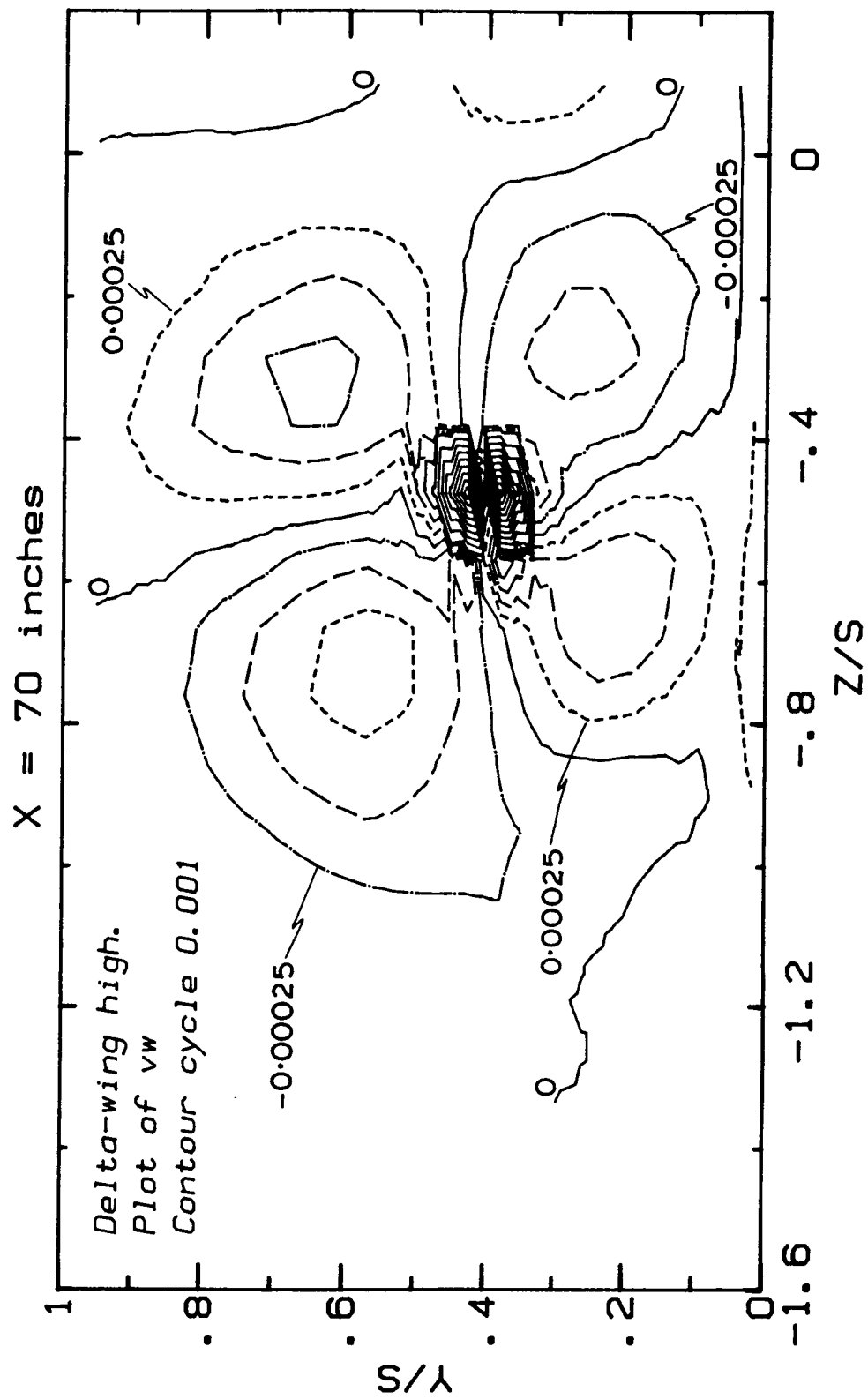








17(e)  $\overline{uw}$



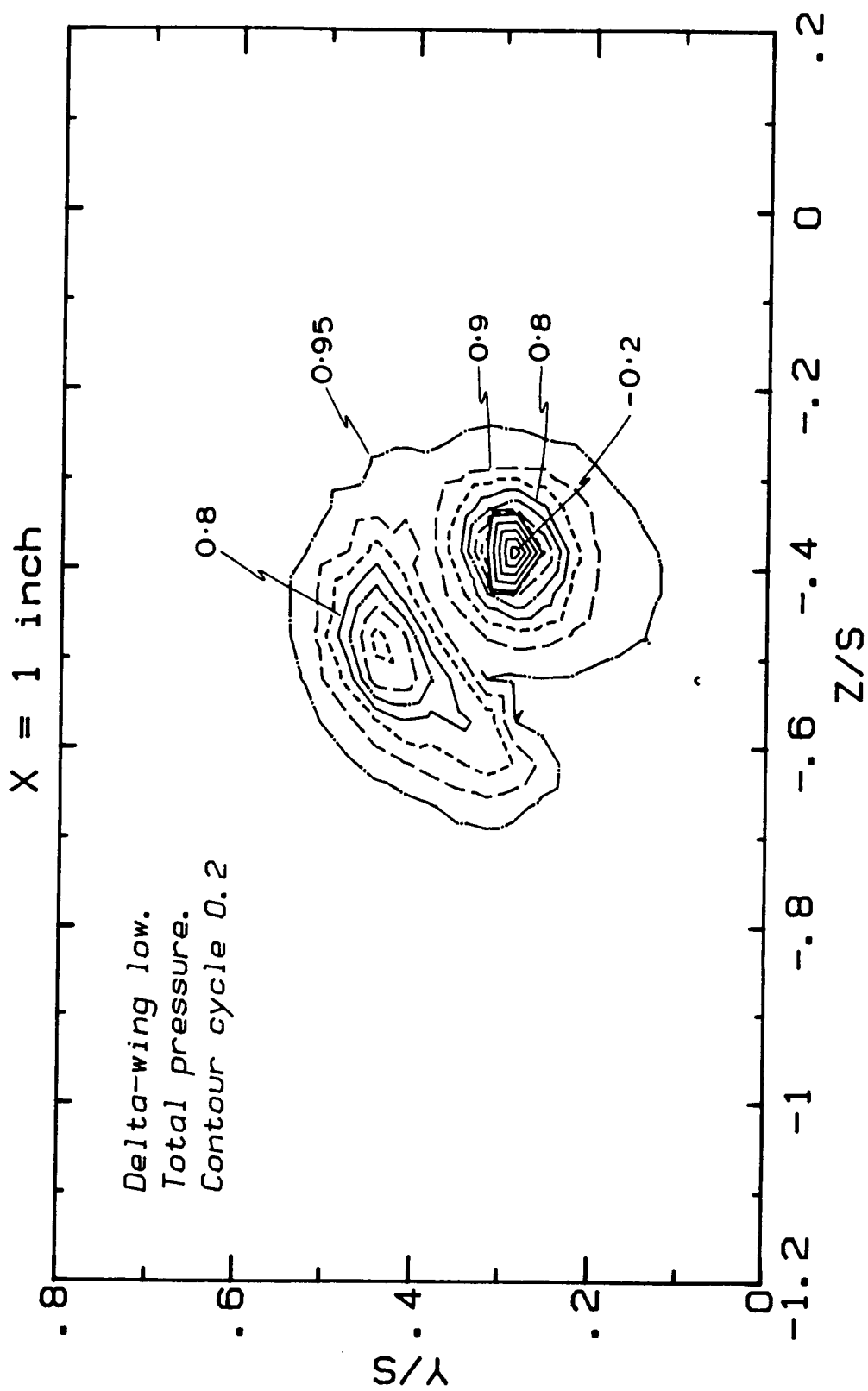
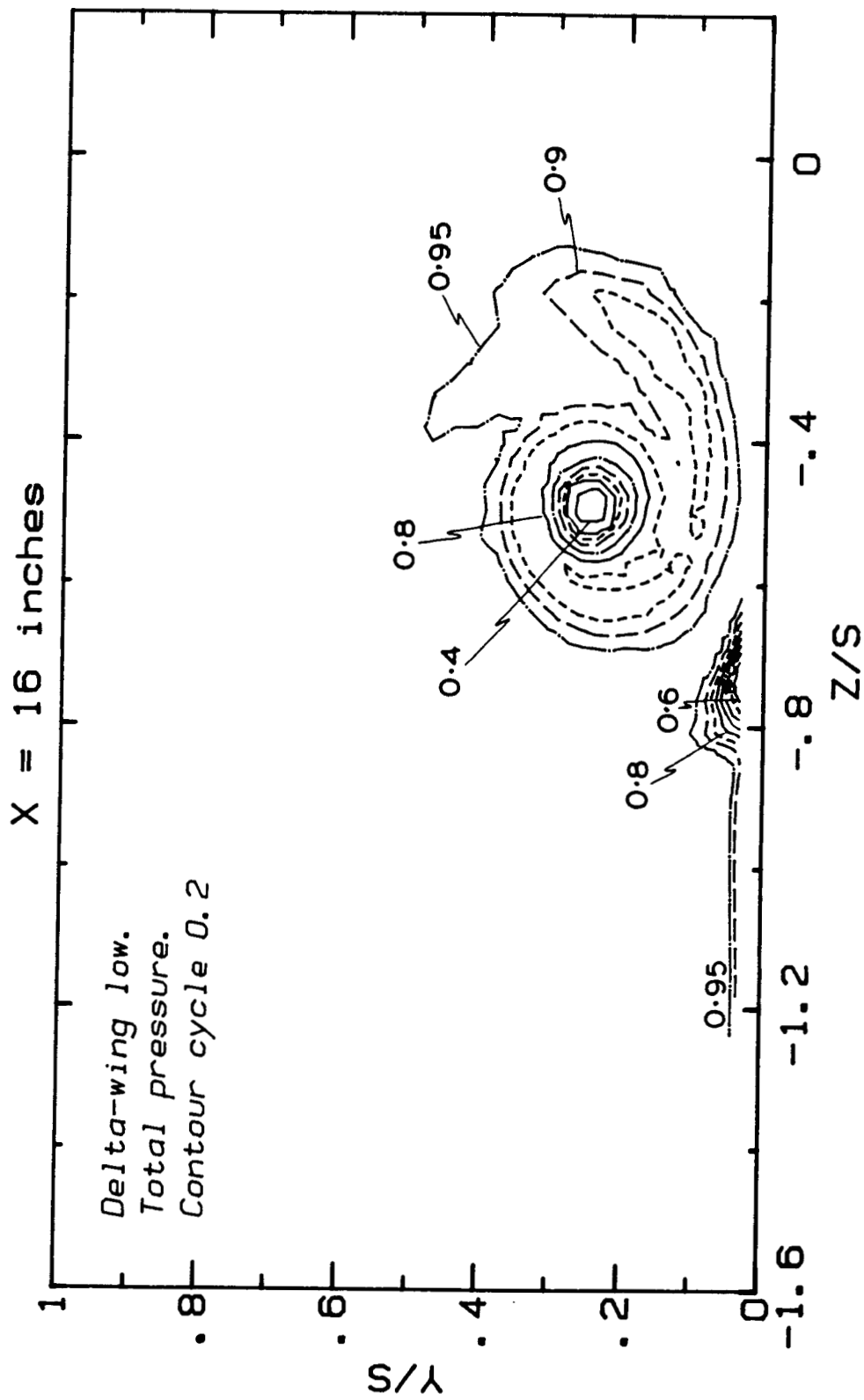
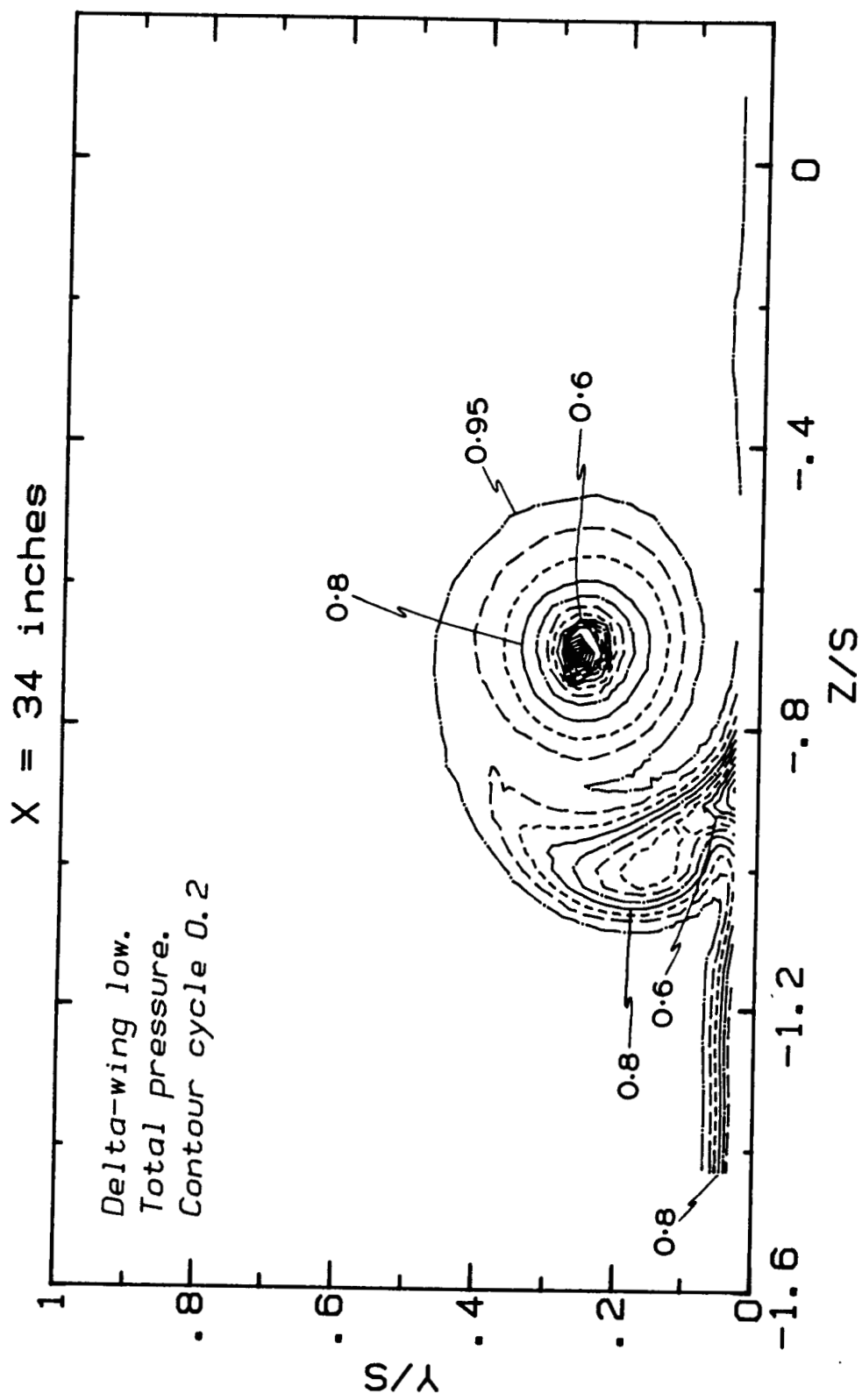


Figure 18. Contours of the total pressure coefficient  $(P - P_{\text{Pref}}) / (P_{\text{Pref}} - P_{\text{Pref}})$  for the "delta-wing low" case:

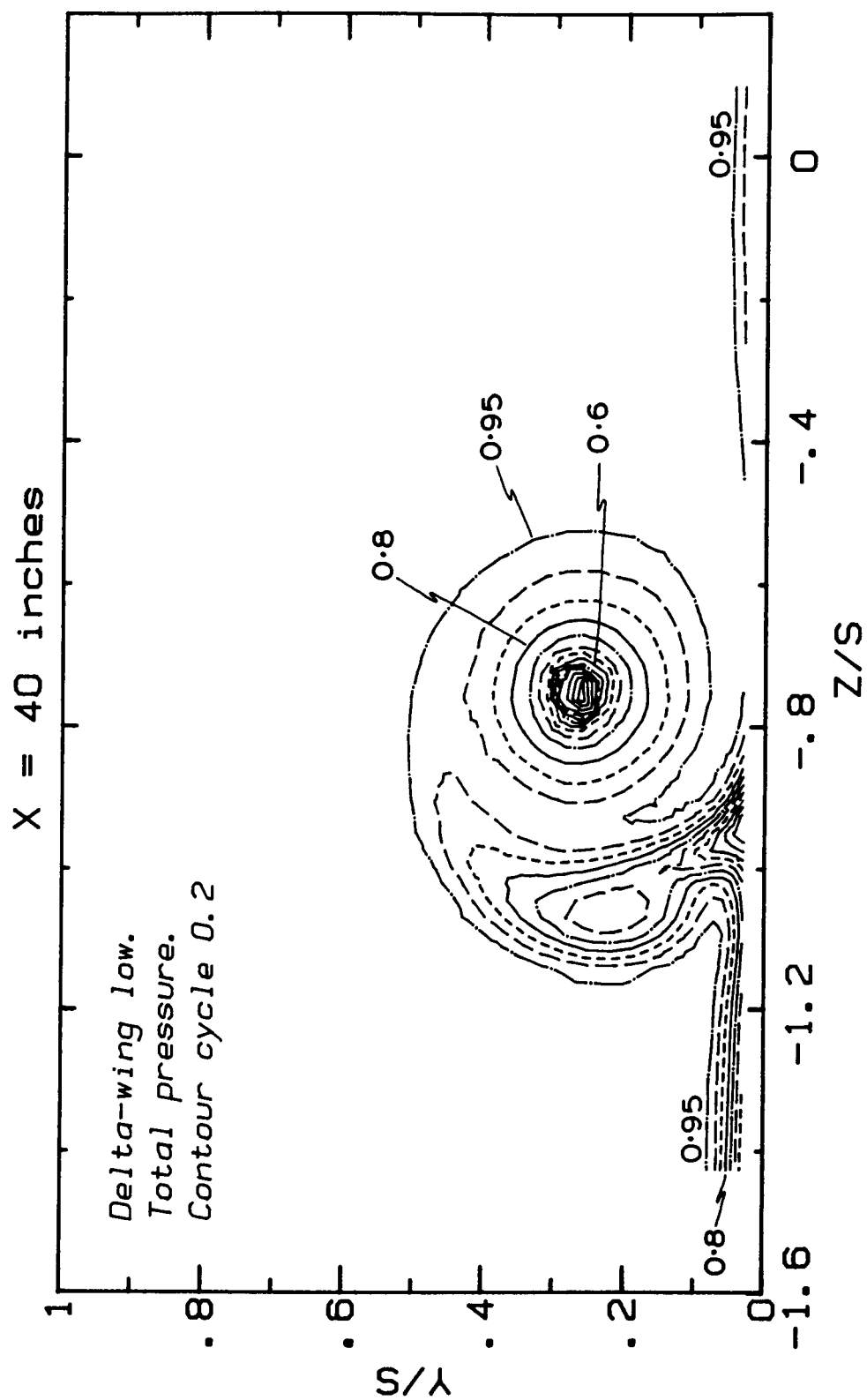
18(a)  $x/s = 0.095$



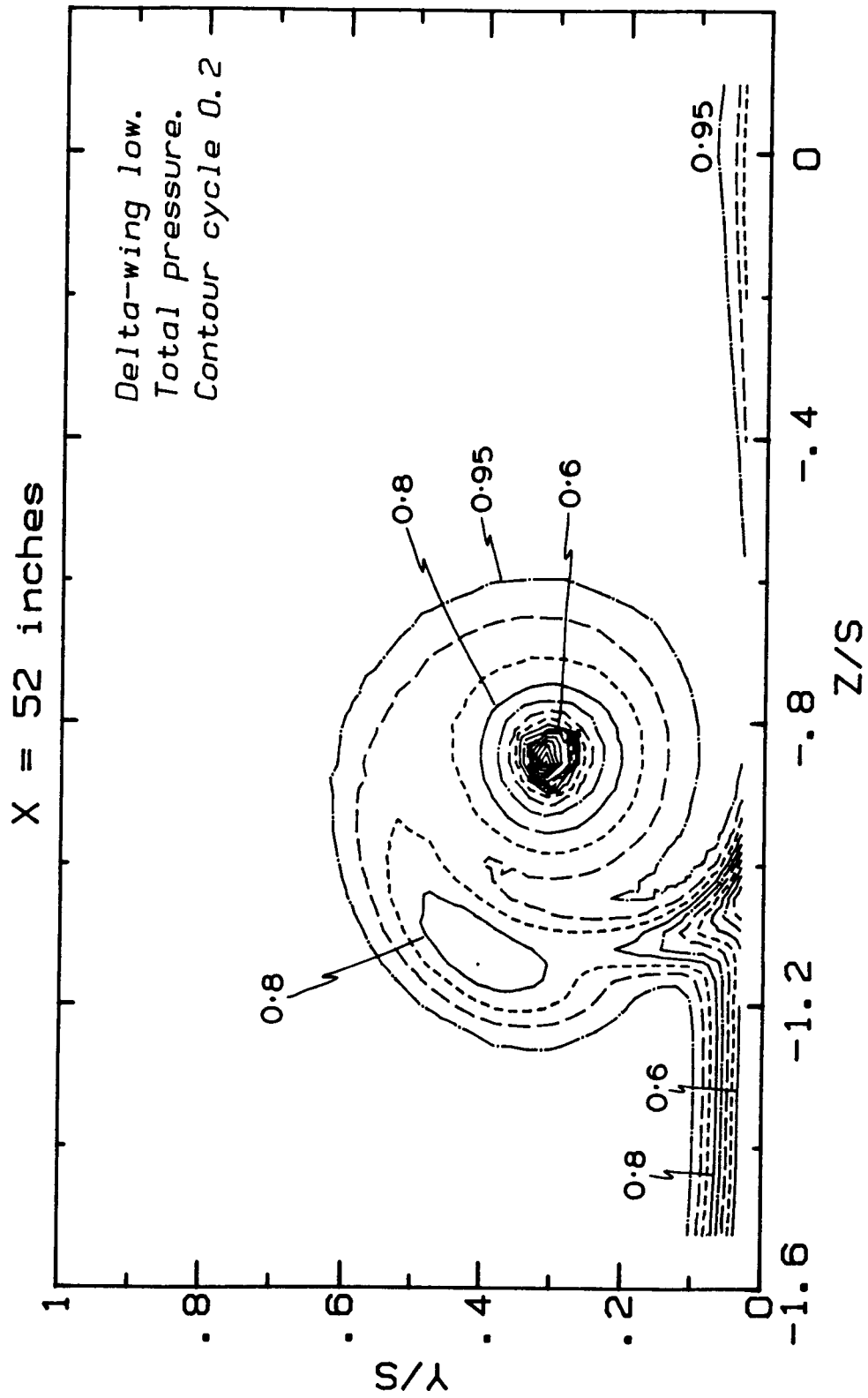
18(b)  $x/s = 1.524$



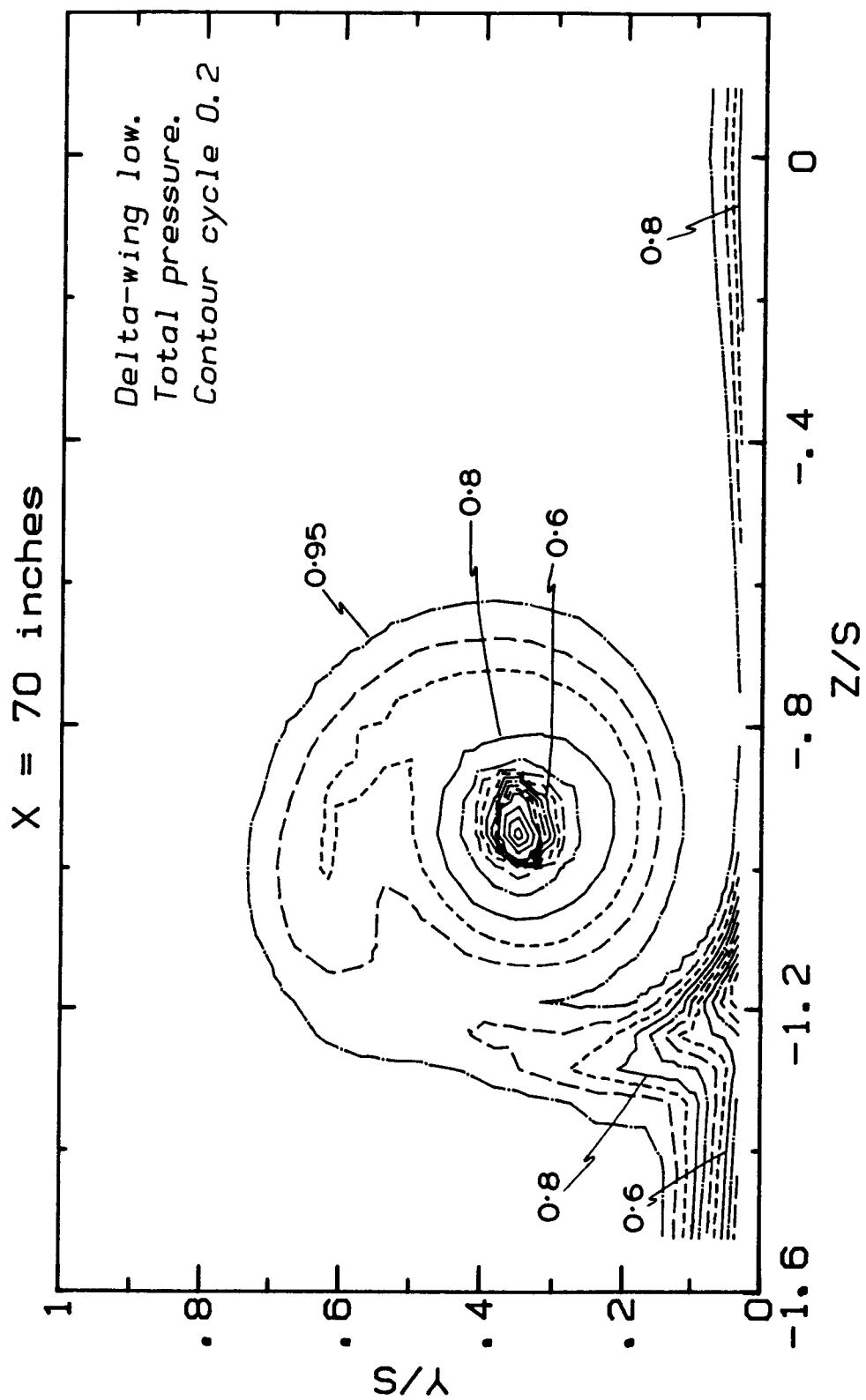
18(c)  $x/s = 3.238$



18(d)  $x/s = 3.810$

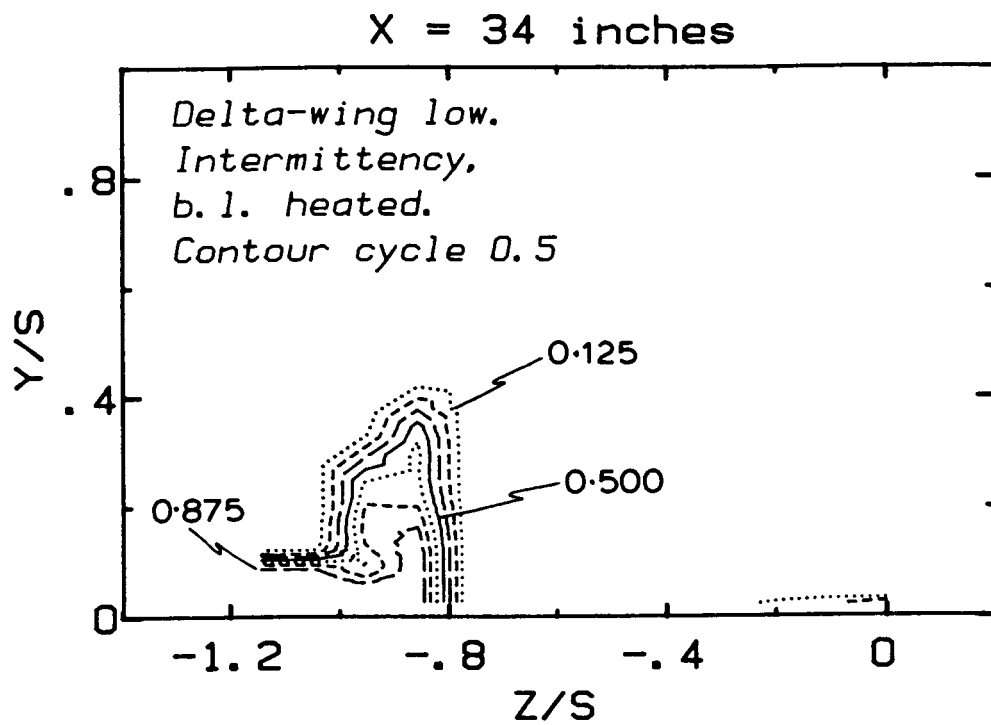


18(e)  $x/s = 4.952$

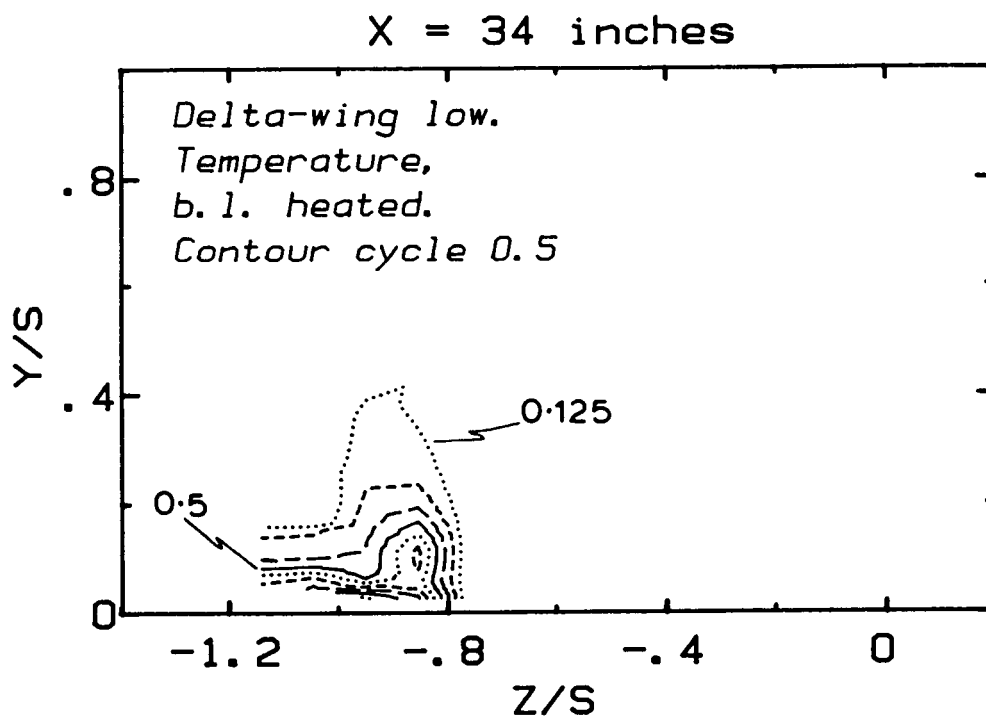


18(f)  $x/s = 6.667$

\*\*\*Figures 19-21: intermittency, etc. "delta wing low"\*\*\*

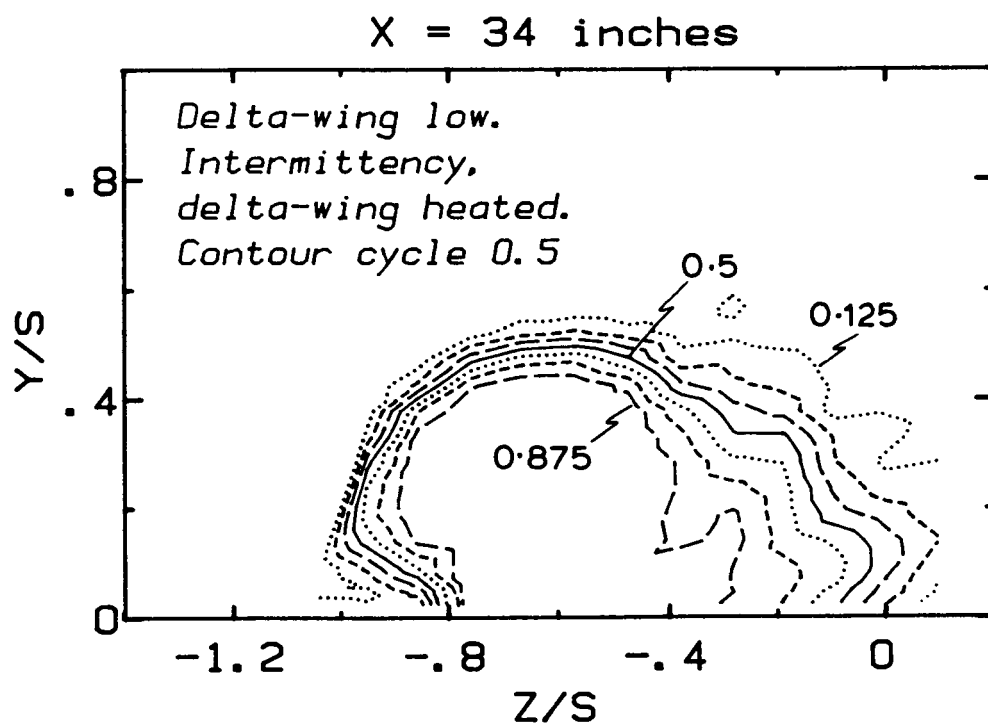


(a) intermittency I

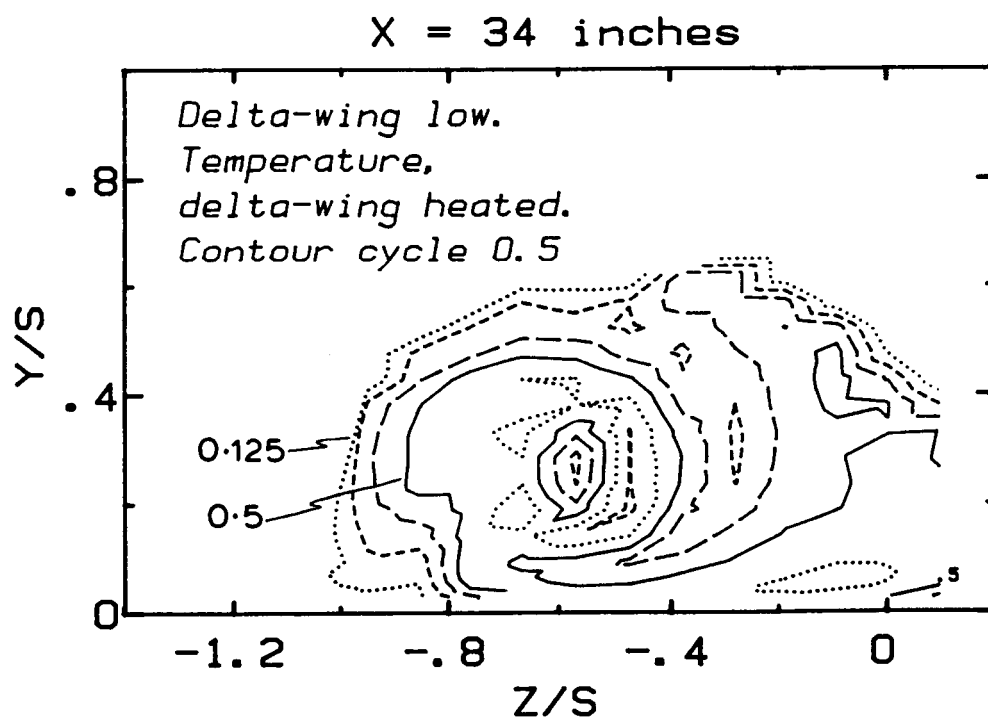


(b) temperature  $(T_h - T_c)/T_{ref}$  with the boundary layer heated at  $x/s = 3.238$  for the "delta-wing low" case.

Figure 19. Contours

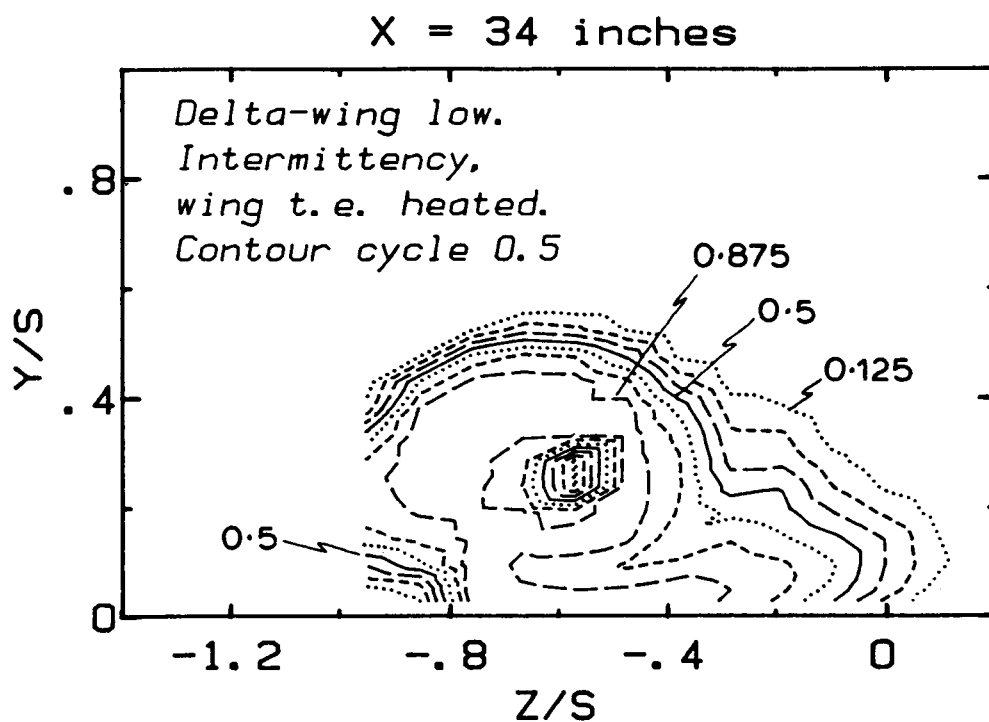


(a) intermittency I

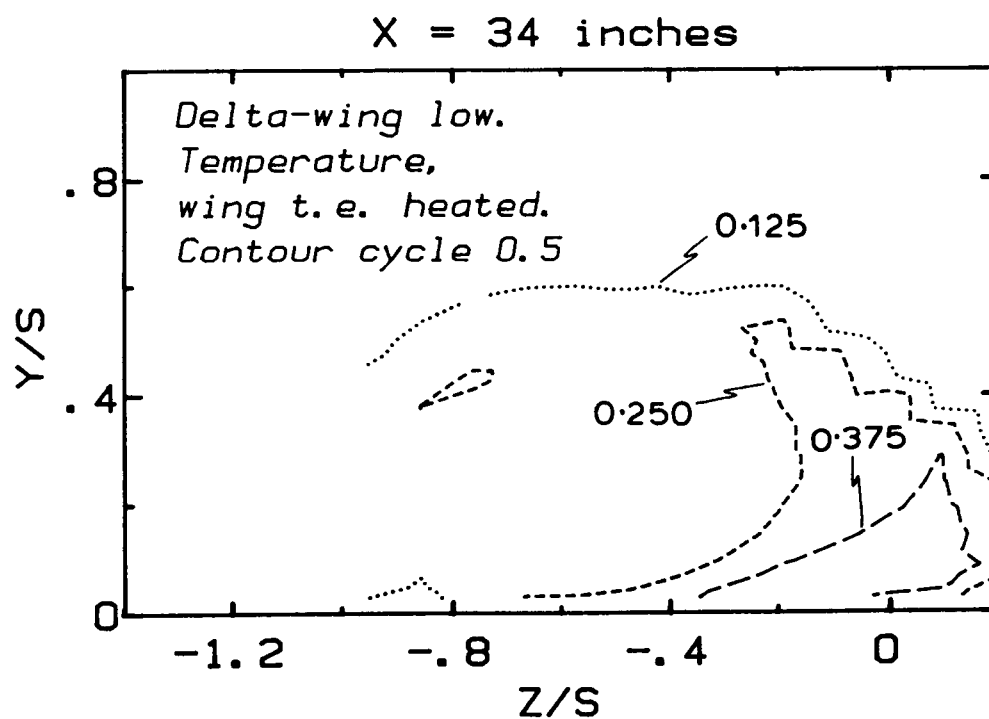


(b) temperature  $(T_h - T_c)/T_{ref}$  with the delta-wing heated at  $x/s = 3.238$  for the "delta-wing low" case.

Figure 20. Contours



(a) intermittency I



(b) temperature  $(T_h - T_c)/T_{ref}$  with the fluid heated at the trailing edge of the delta wing at  $x/s = 3.238$  for the "delta-wing low" case.

Figure 21. Contours

\*\*\*Figures 22-32: derived results, both cases.\*\*\*

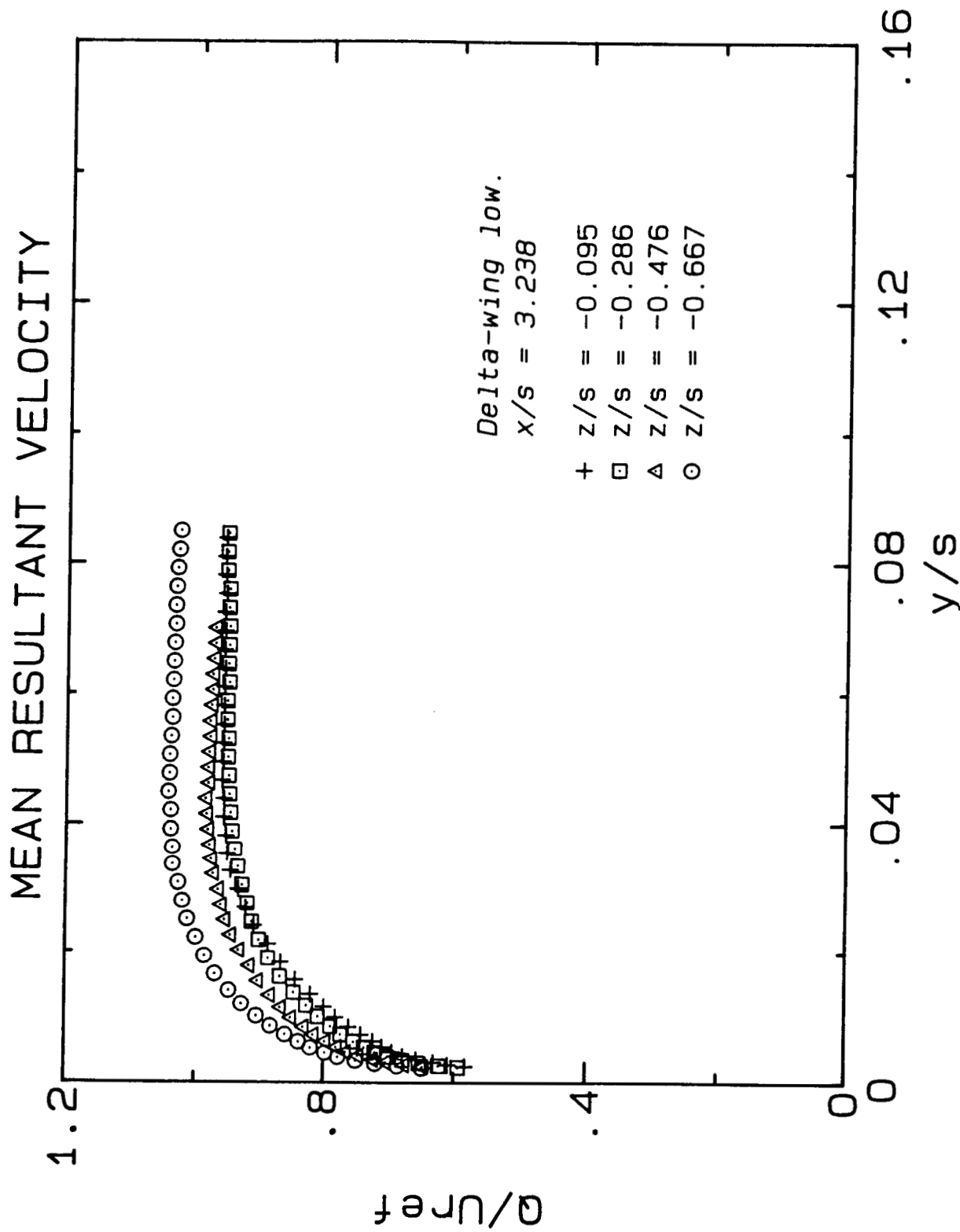
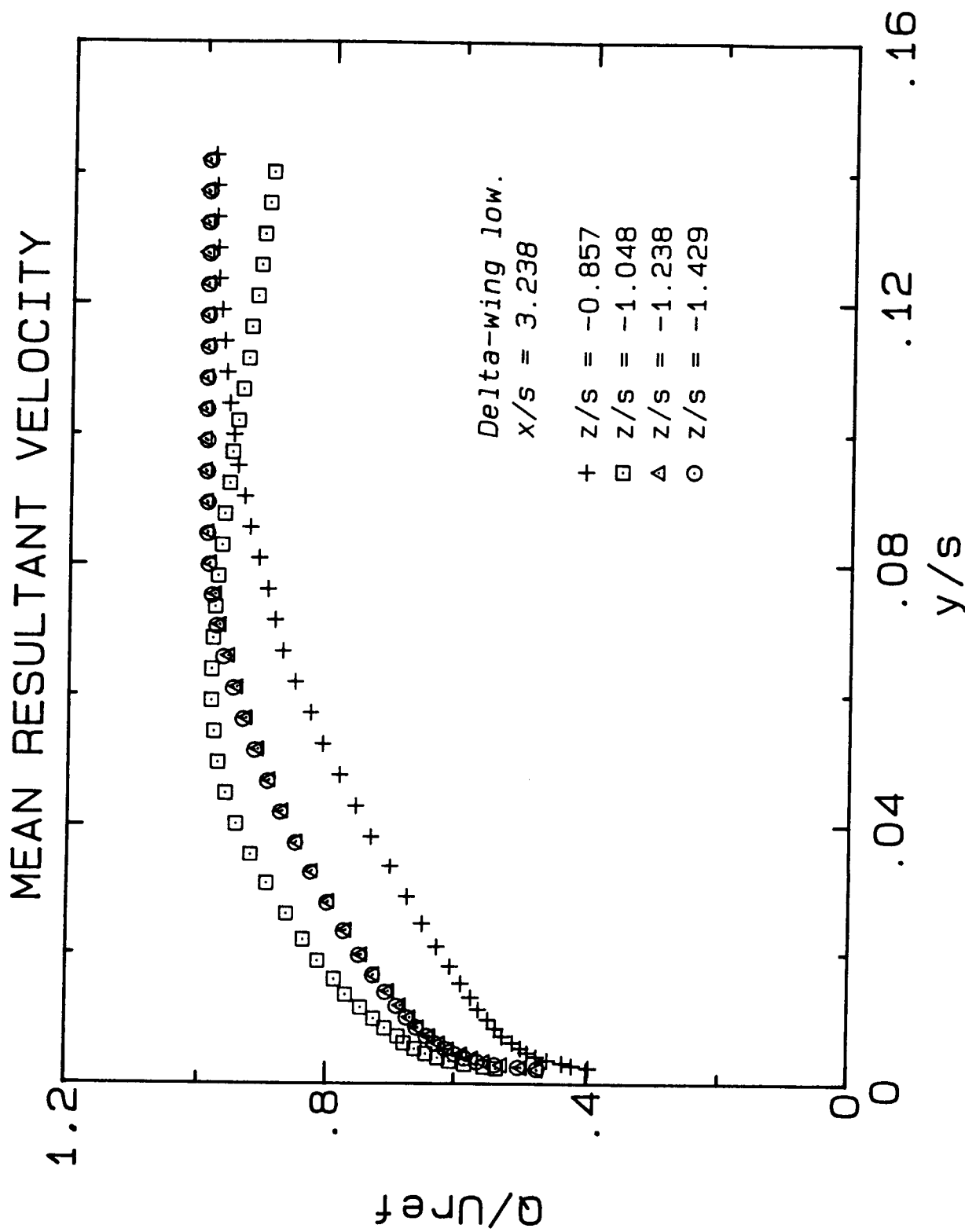


Figure 22. Profiles of mean resultant velocity measured with a three-tube pitot probe:

22(a) "delta-wing" low case at  $x/s = 3.238$

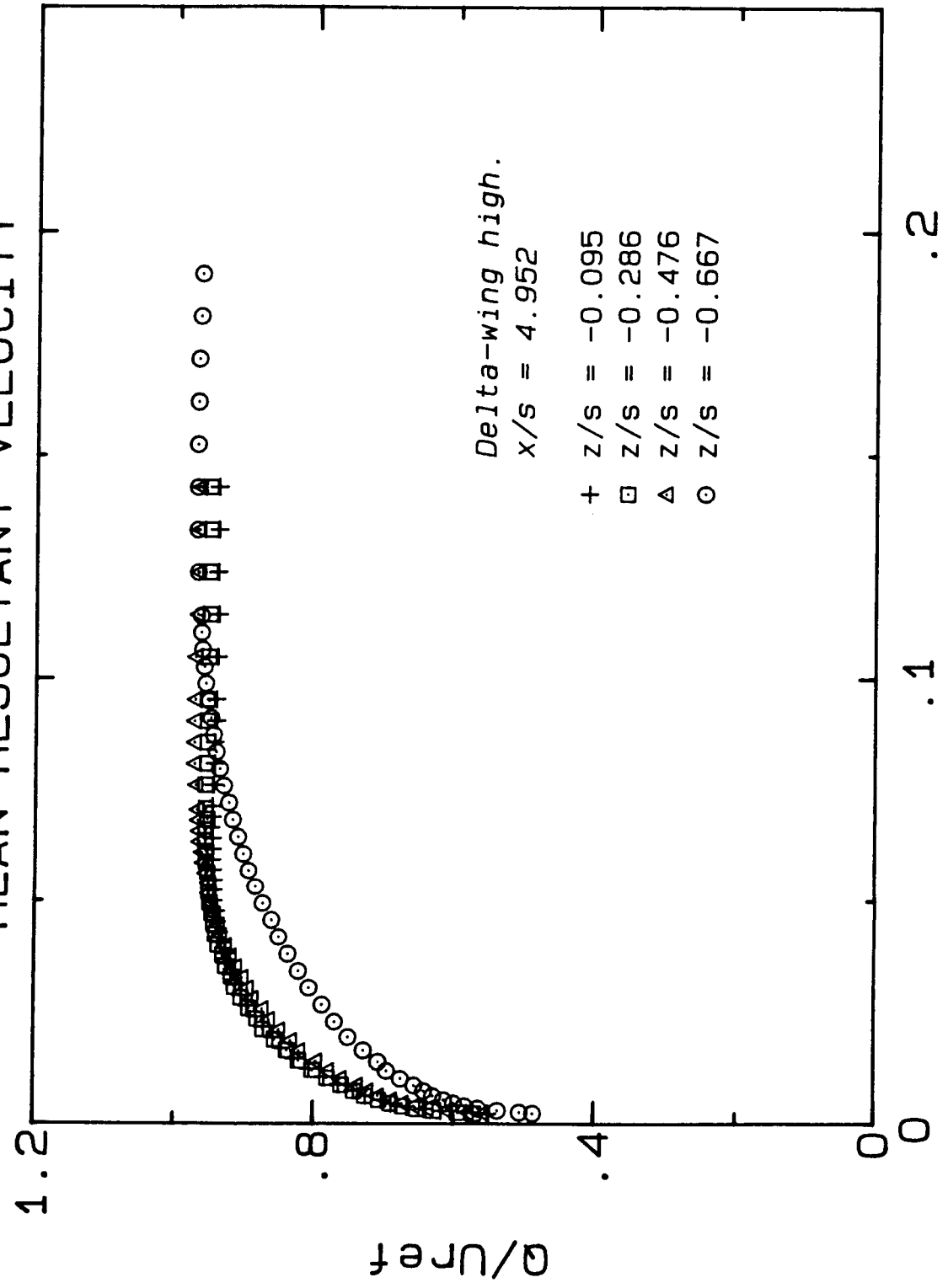
cyb 100 21/1/71



22(b) "delta-wing low" case at  $x/s = 3.238$  (continued)

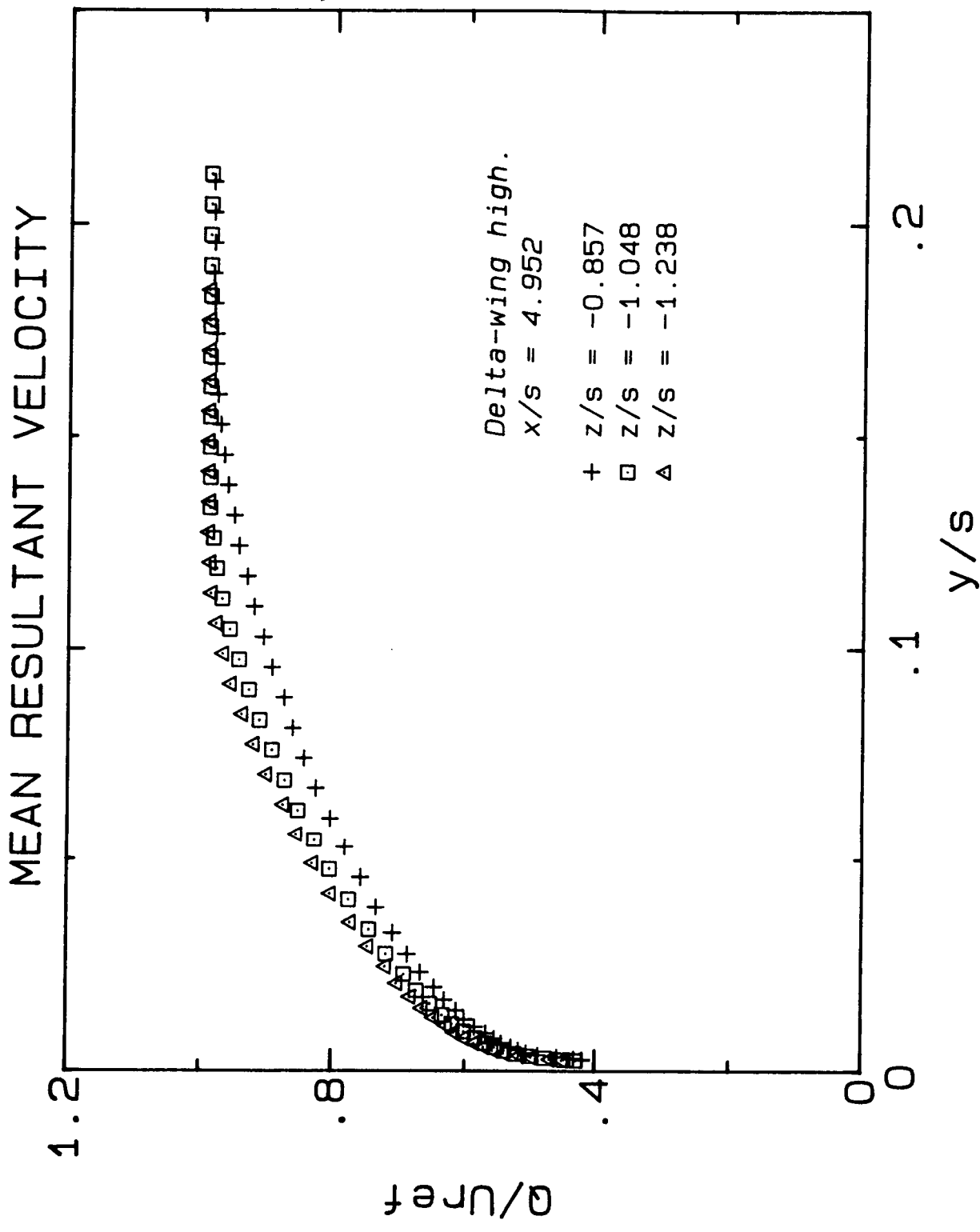
11.1

# MEAN RESULTANT VELOCITY



22(c) "delta-wing high" case at x/s = 4.952

Page 6



22(d) "delta-wing high" case at x/s = 4.952 (continued)

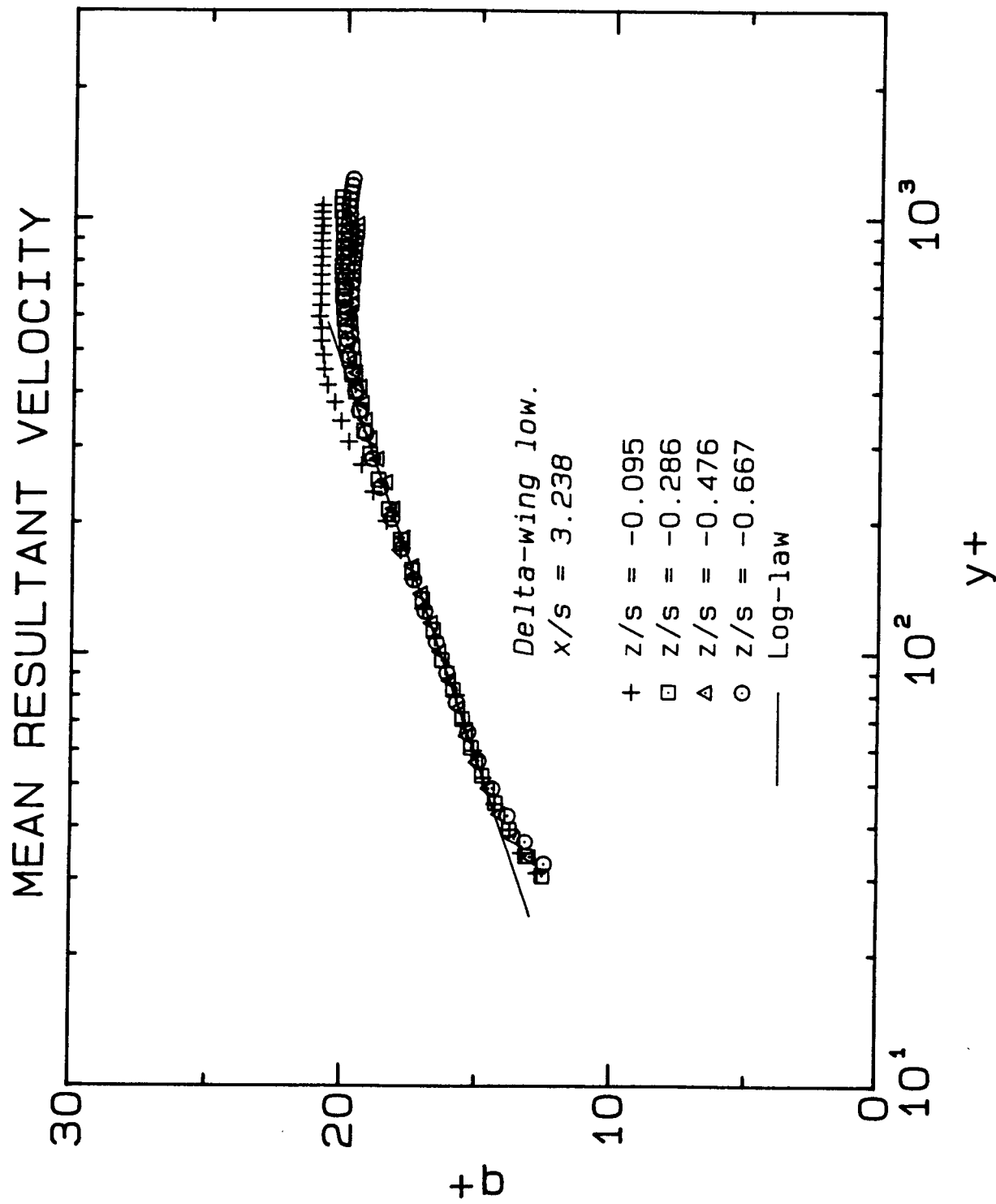
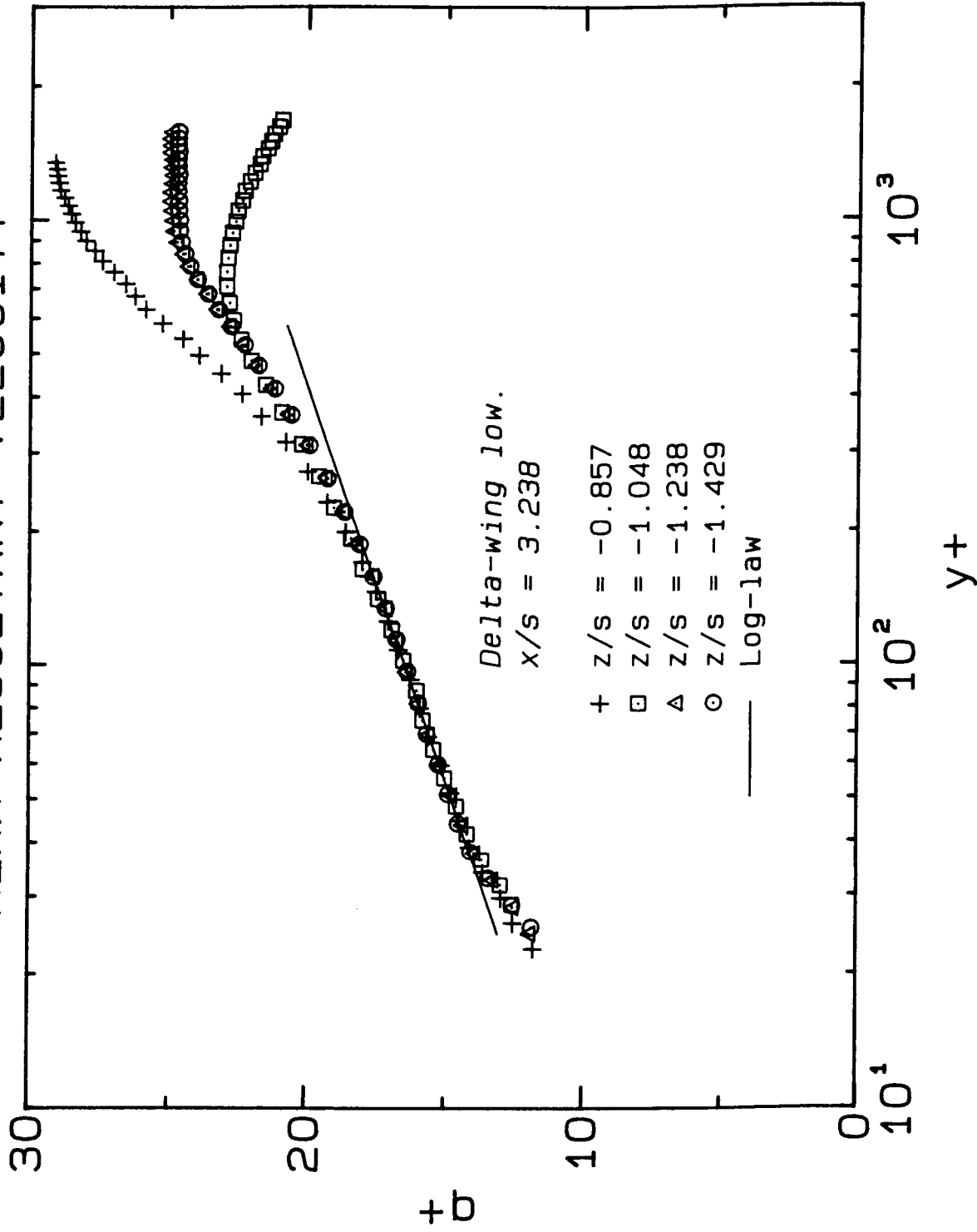
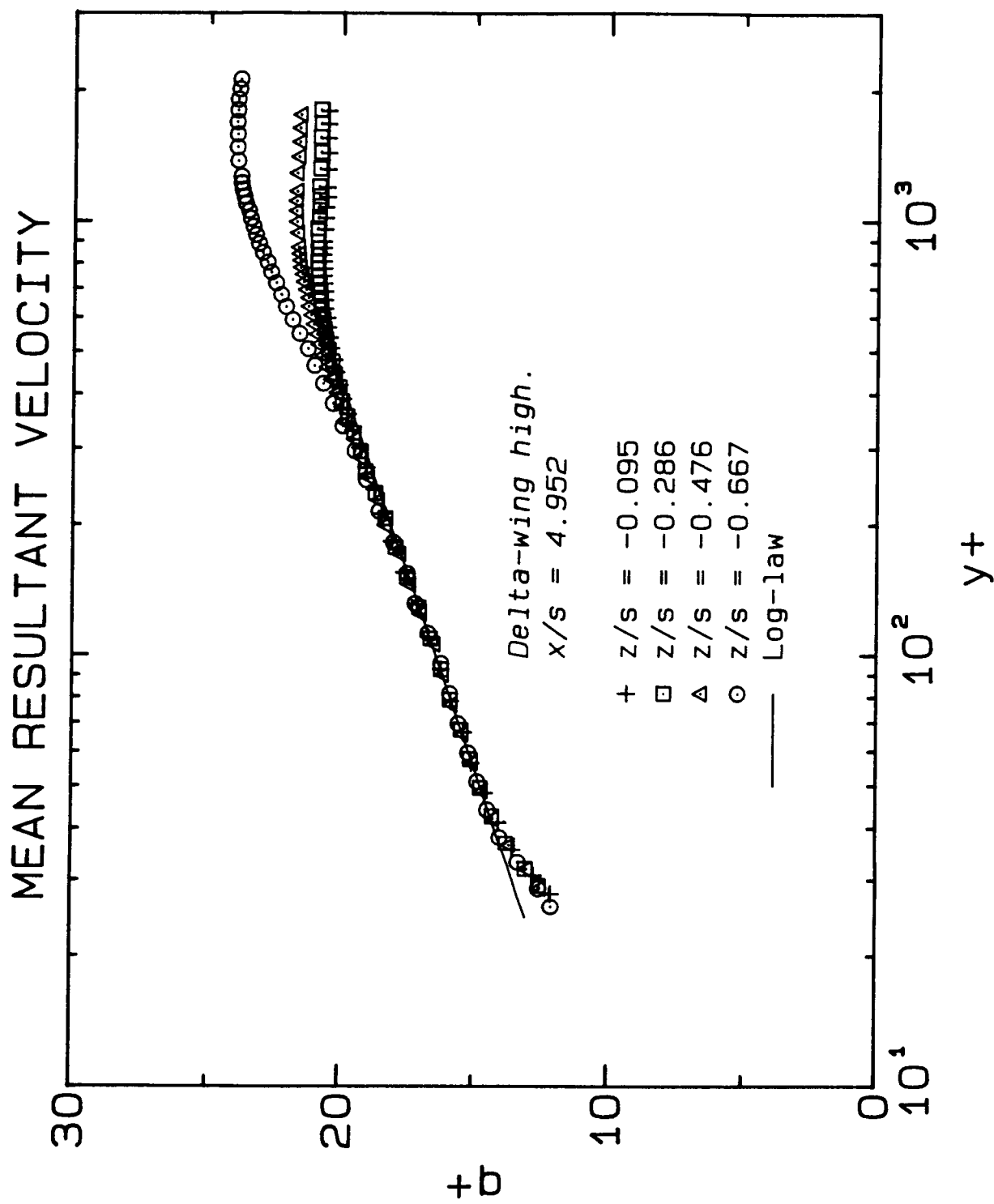


Figure 23. Profiles of mean resultant velocity in wall coordinates:  
 23(a) "delta-wing low" case at  $x/s = 3.238$

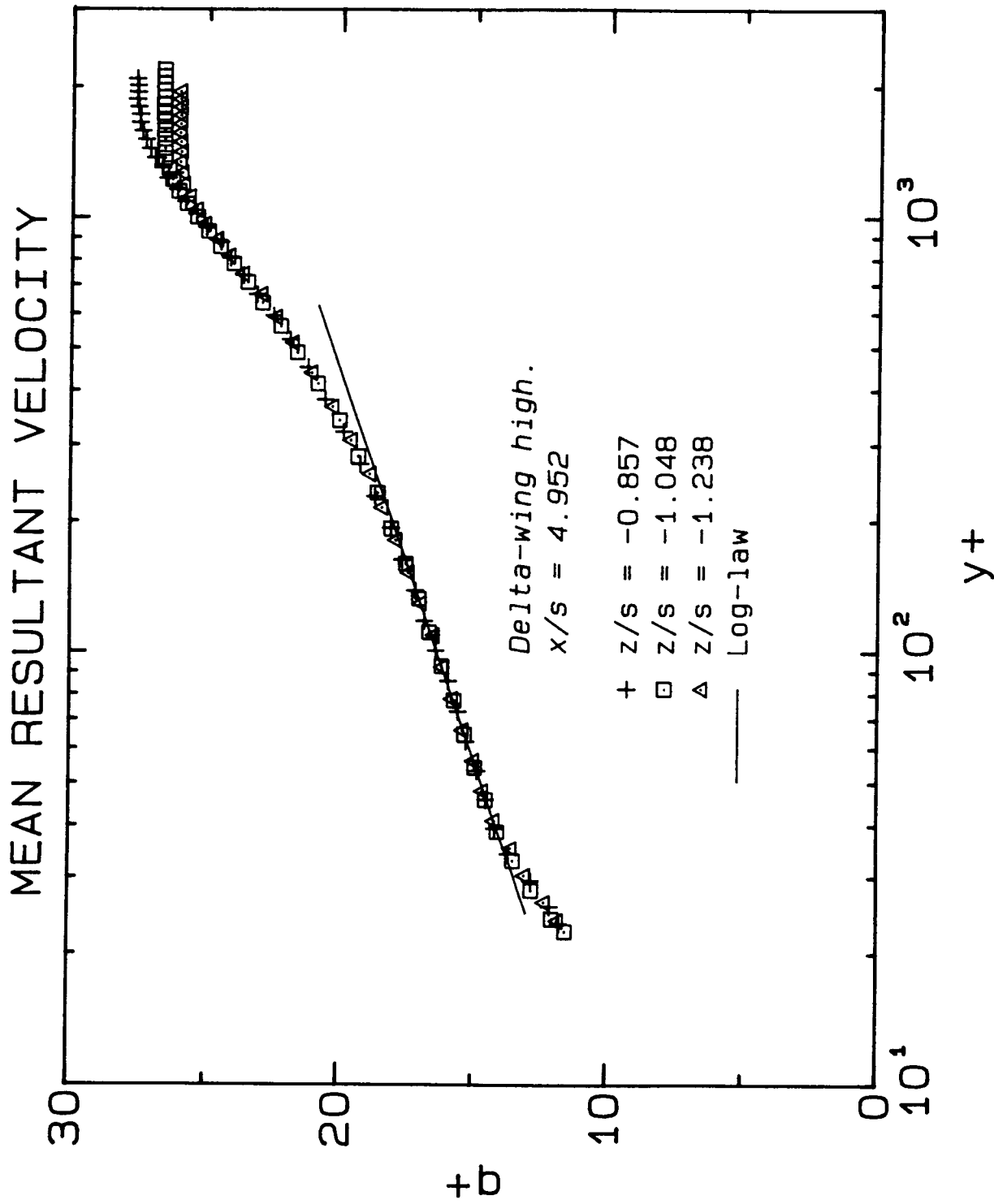
# MEAN RESULTANT VELOCITY



23(b) "delta-wing low" case at  $x/s = 3.238$  (continued)



23(c) "delta-wing high" case at  $x/s = 4.952$



23(d) "delta-wing high" case at  $x/s = 4.952$  (continued)

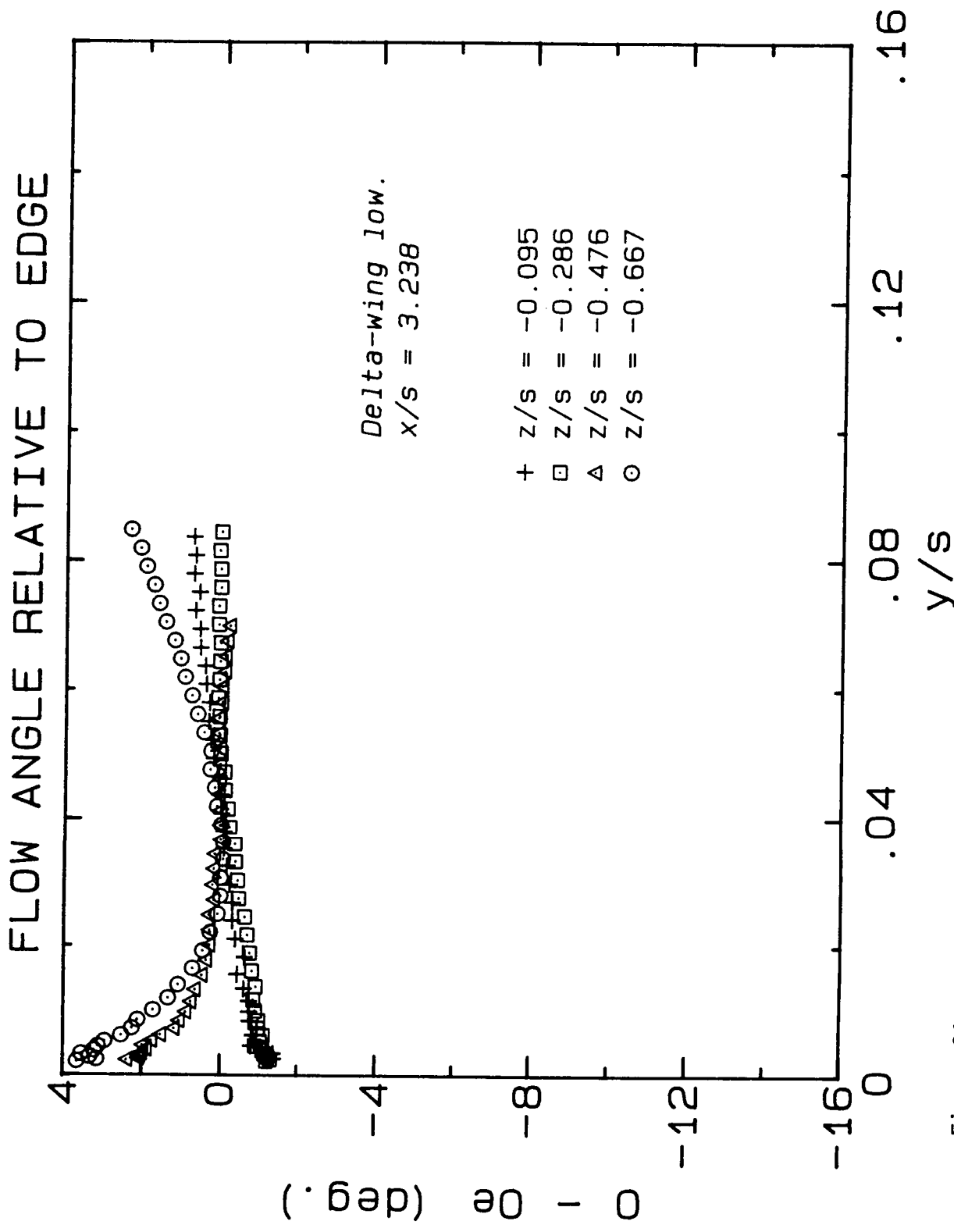
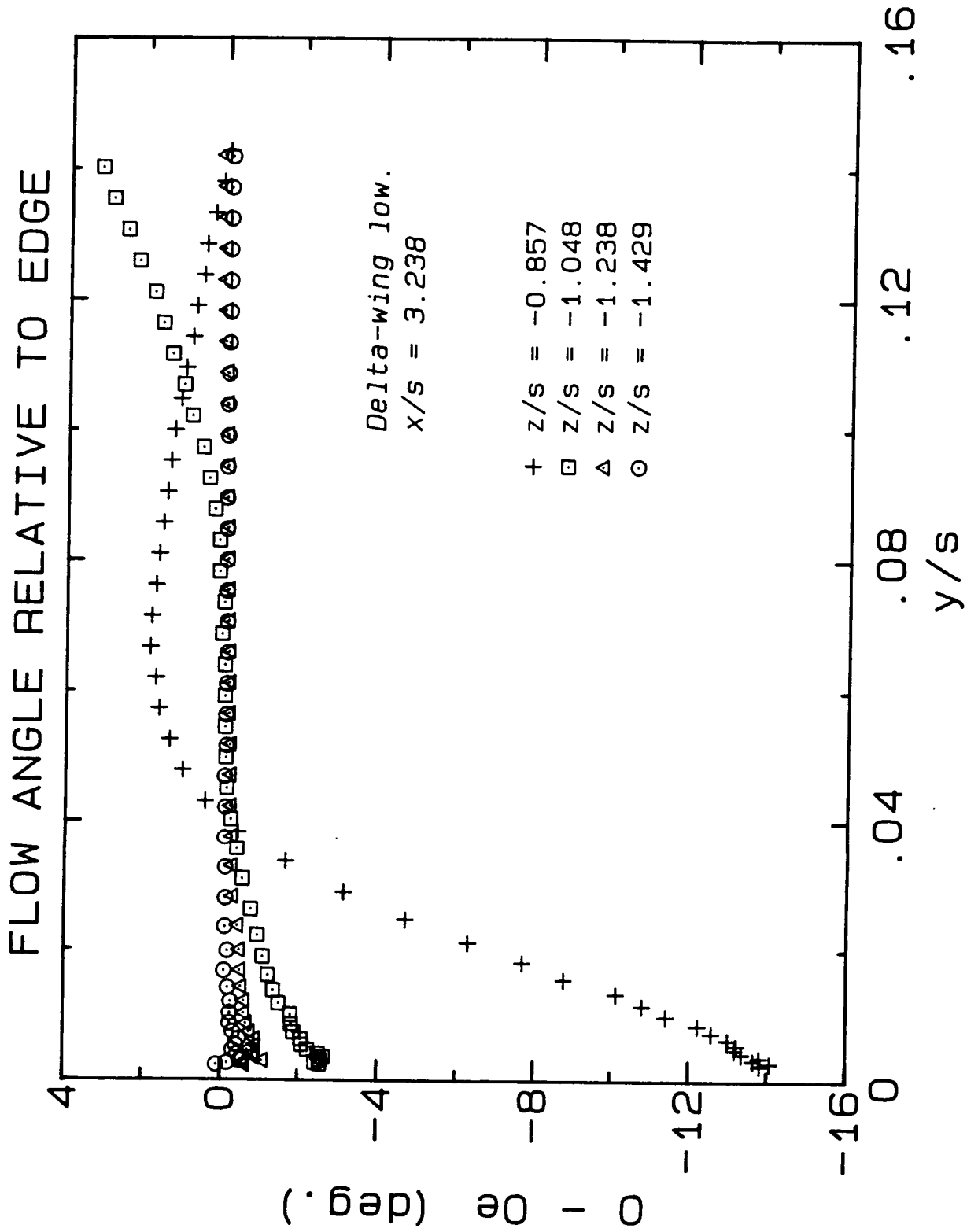


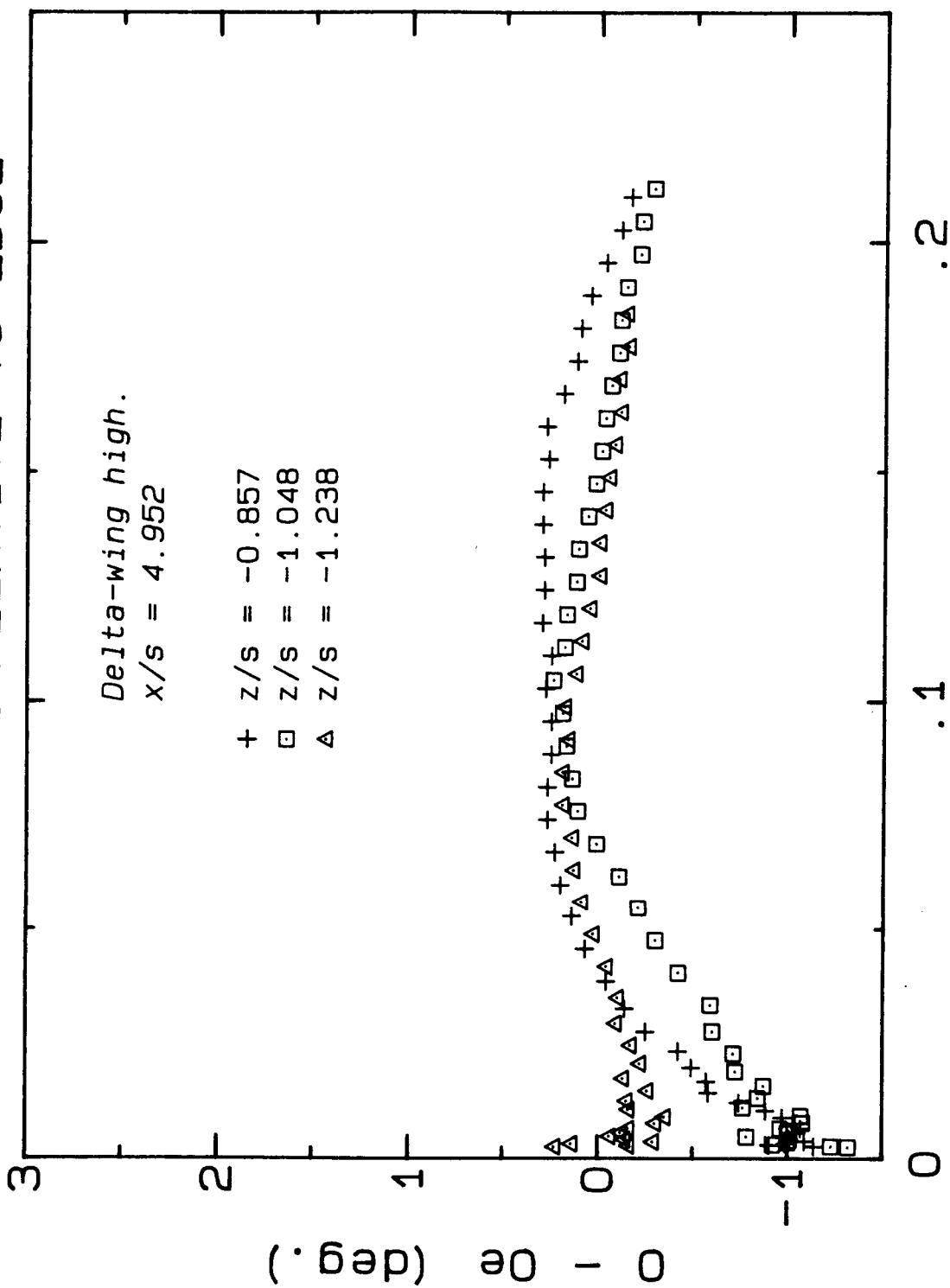
Figure 24. Profiles of crossflow angle relative to the crossflow angle at the edge of the boundary layer:

24(a) "delta-wing low" case at x/s = 3.238



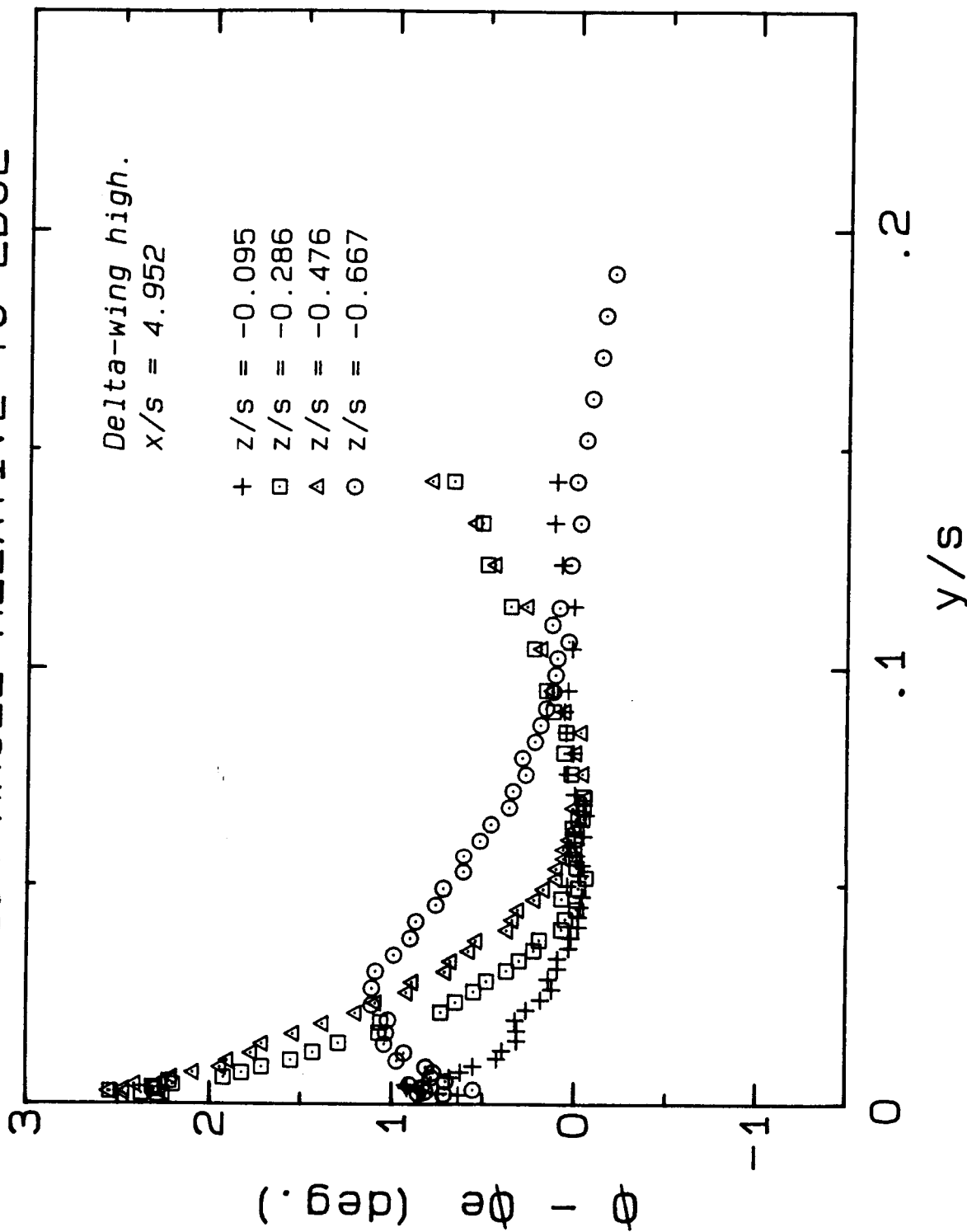
24(b) "delta-wing low" case at  $x/s = 3.238$  (continued)

# FLOW ANGLE RELATIVE TO EDGE



24(c) "delta-wing high" case at  $x/s = 4.952$

# FLOW ANGLE RELATIVE TO EDGE



24(d) "delta-wing high" case at  $x/s = 4.952$  (continued)

# SKIN FRICTION COEFFICIENT

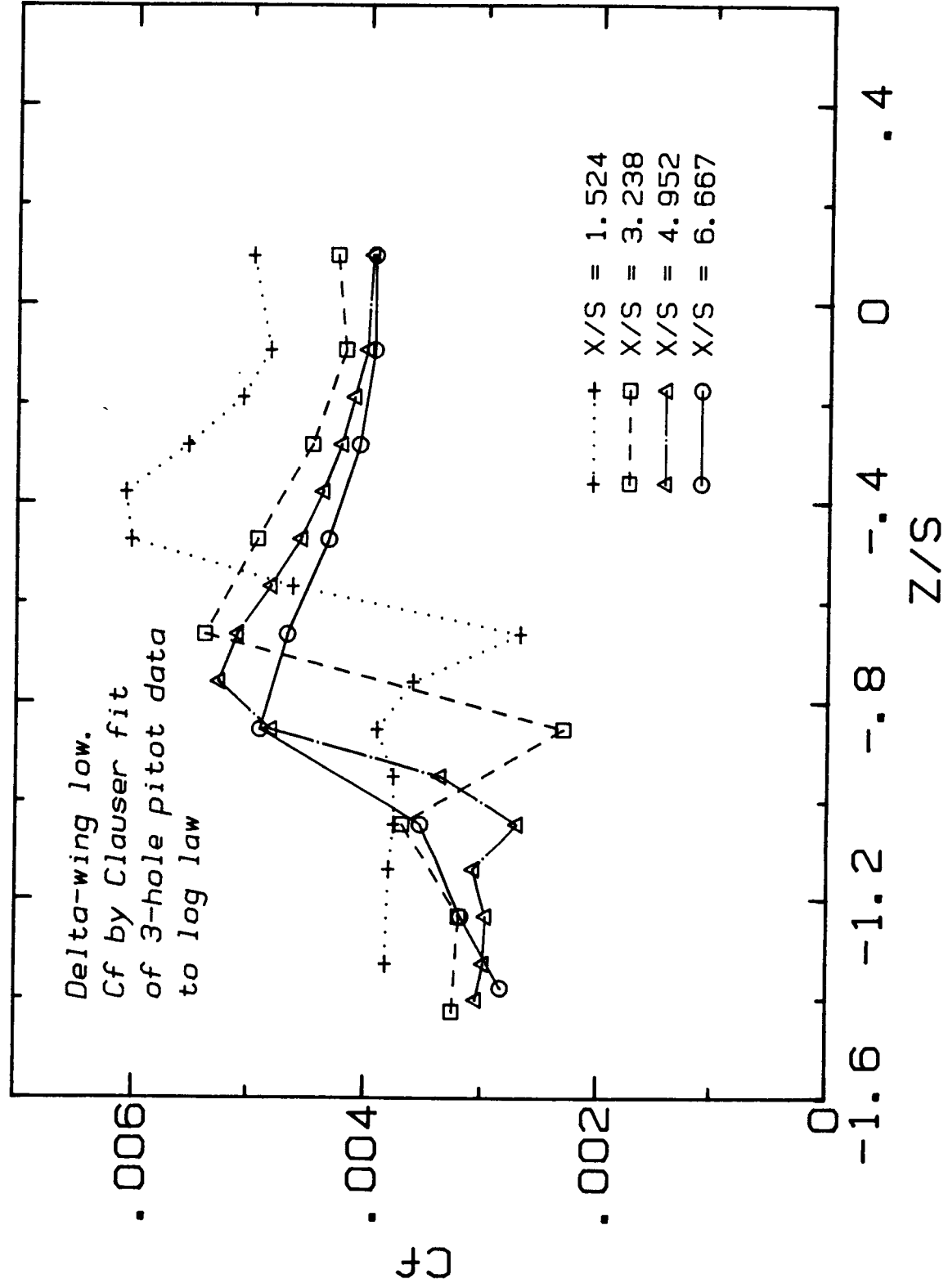
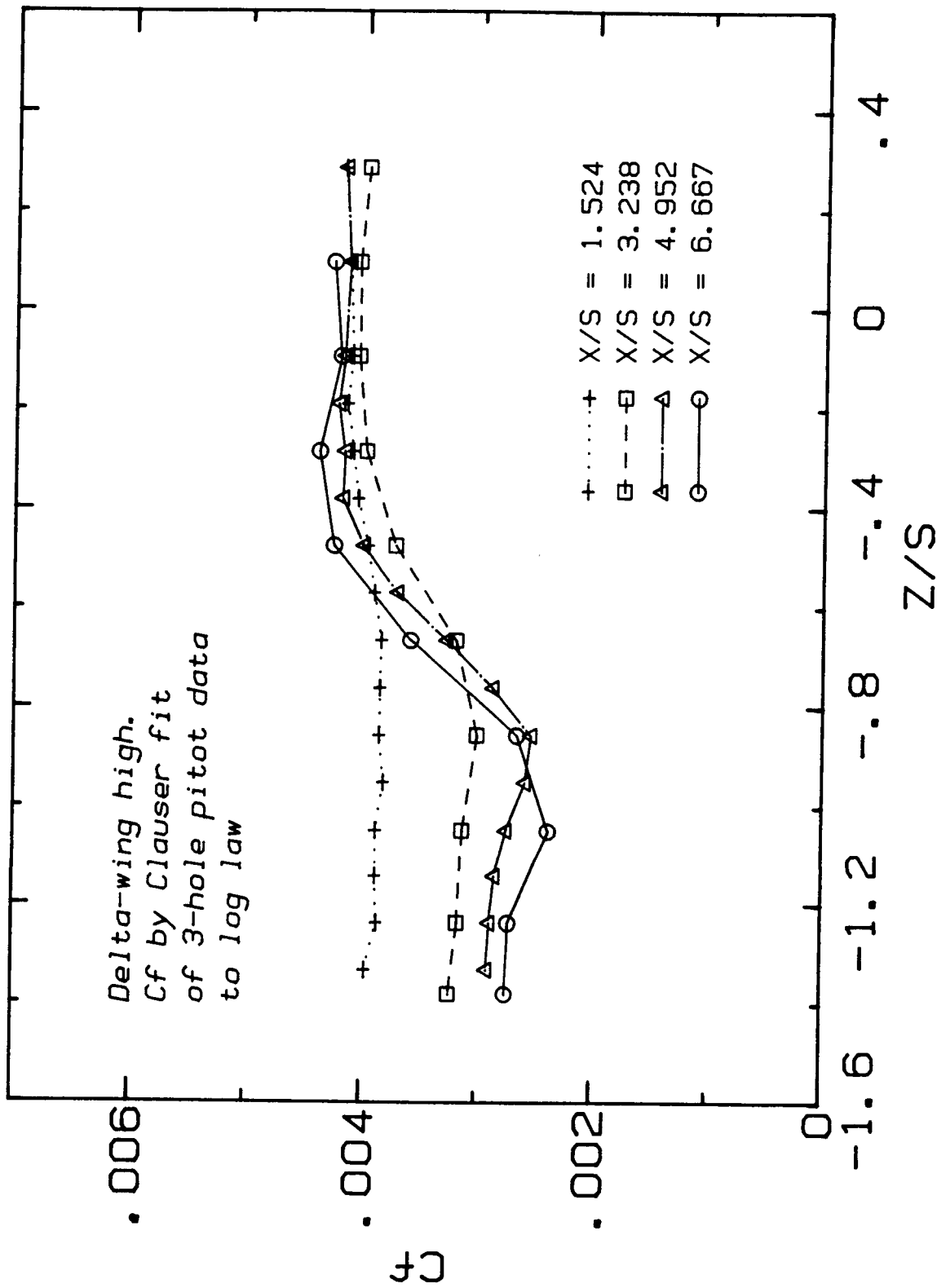


Figure 25. Profiles of skin friction coefficient given by  $C_f = \tau_w / (\frac{1}{2} \rho U_{ref}^2)$ :  
25(a) "delta-wing low" case

# SKIN FRICTION COEFFICIENT



25(b) "delta-wing high" case

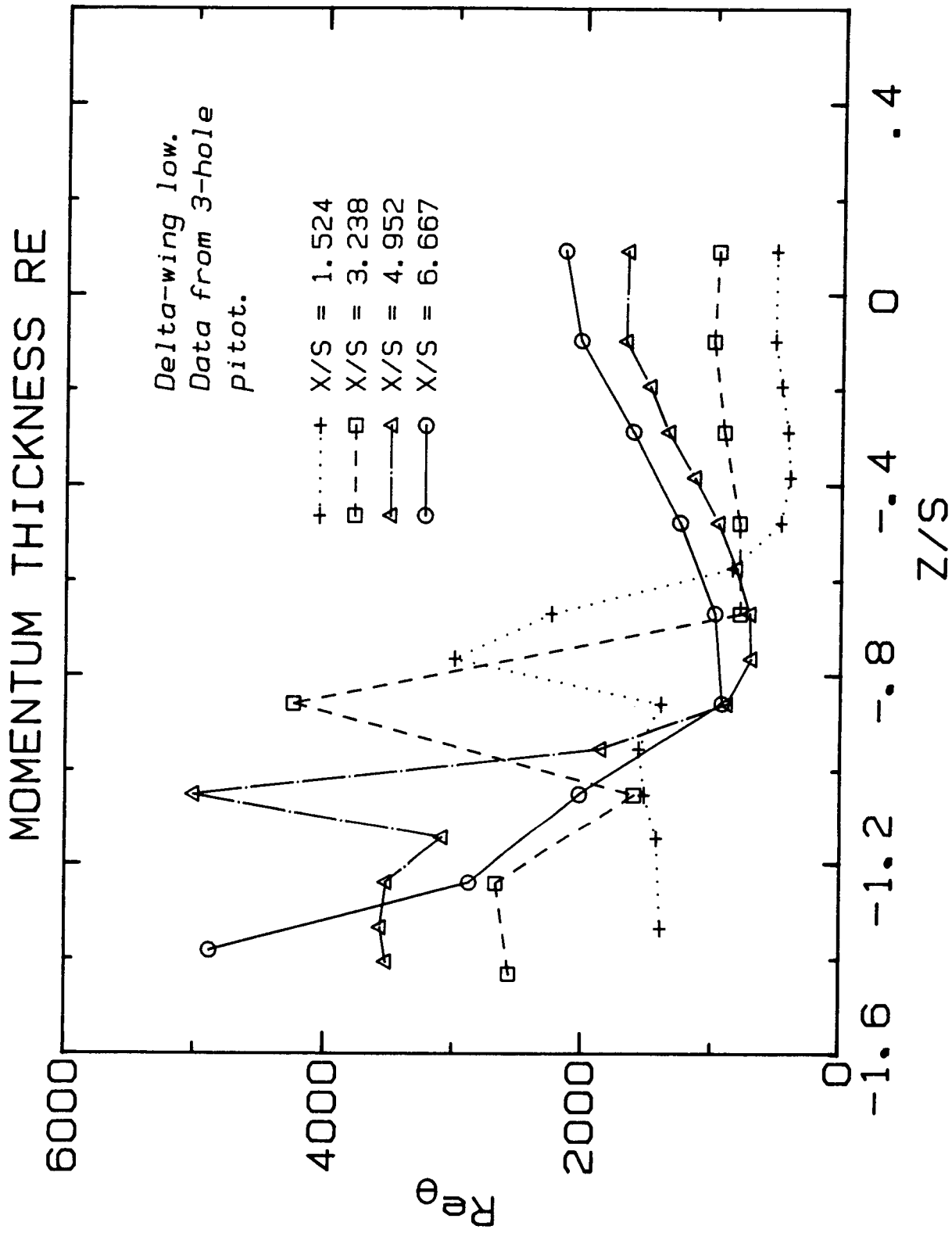
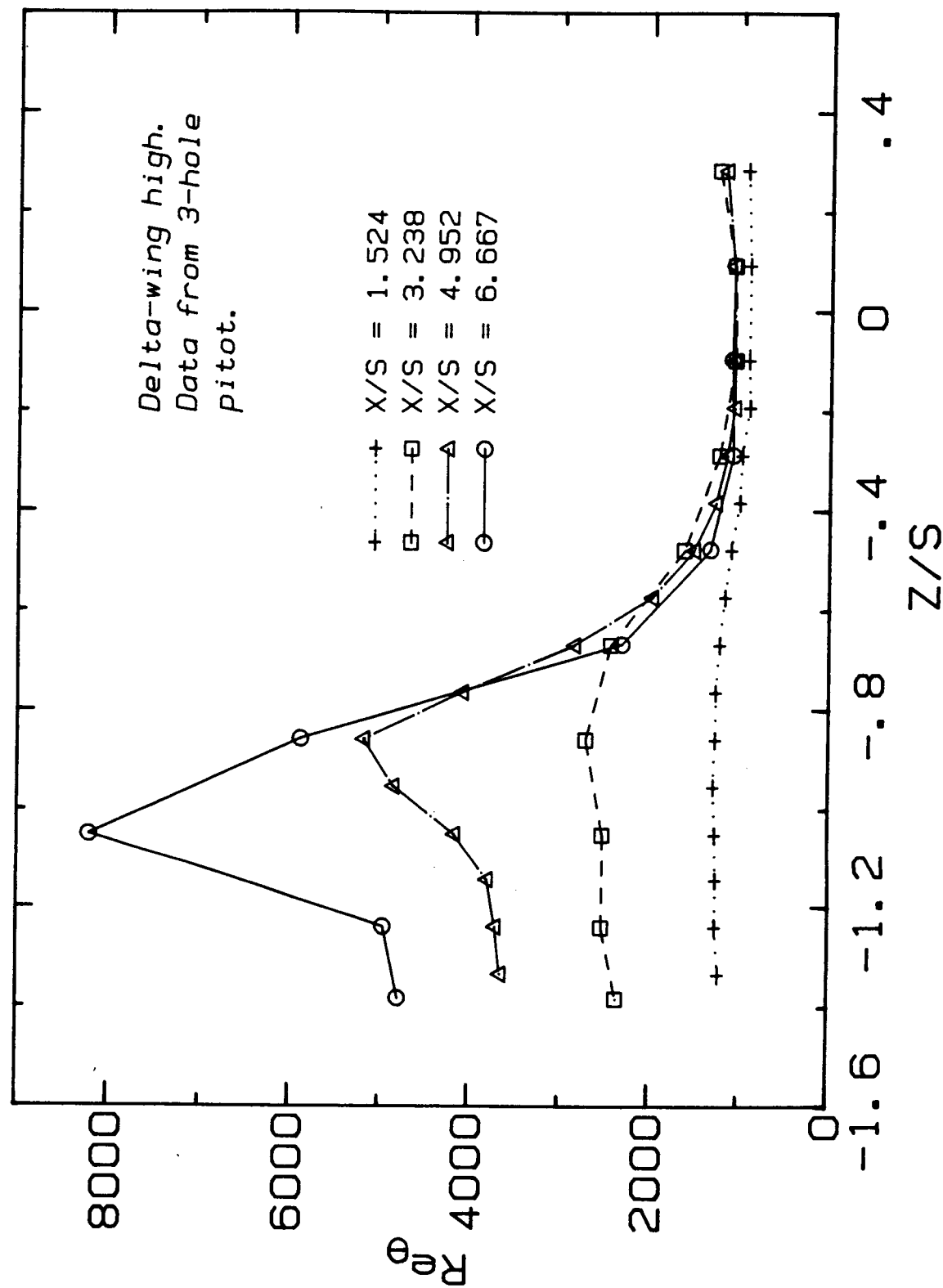


Figure 26. Profiles of momentum thickness Reynolds number  
given by  $Re_{\theta} = U_{ref} \theta_{11} / \nu$ :  
26(a) "delta-wing low" case

# MOMENTUM THICKNESS RE



26(b) "delta-wing high" case.

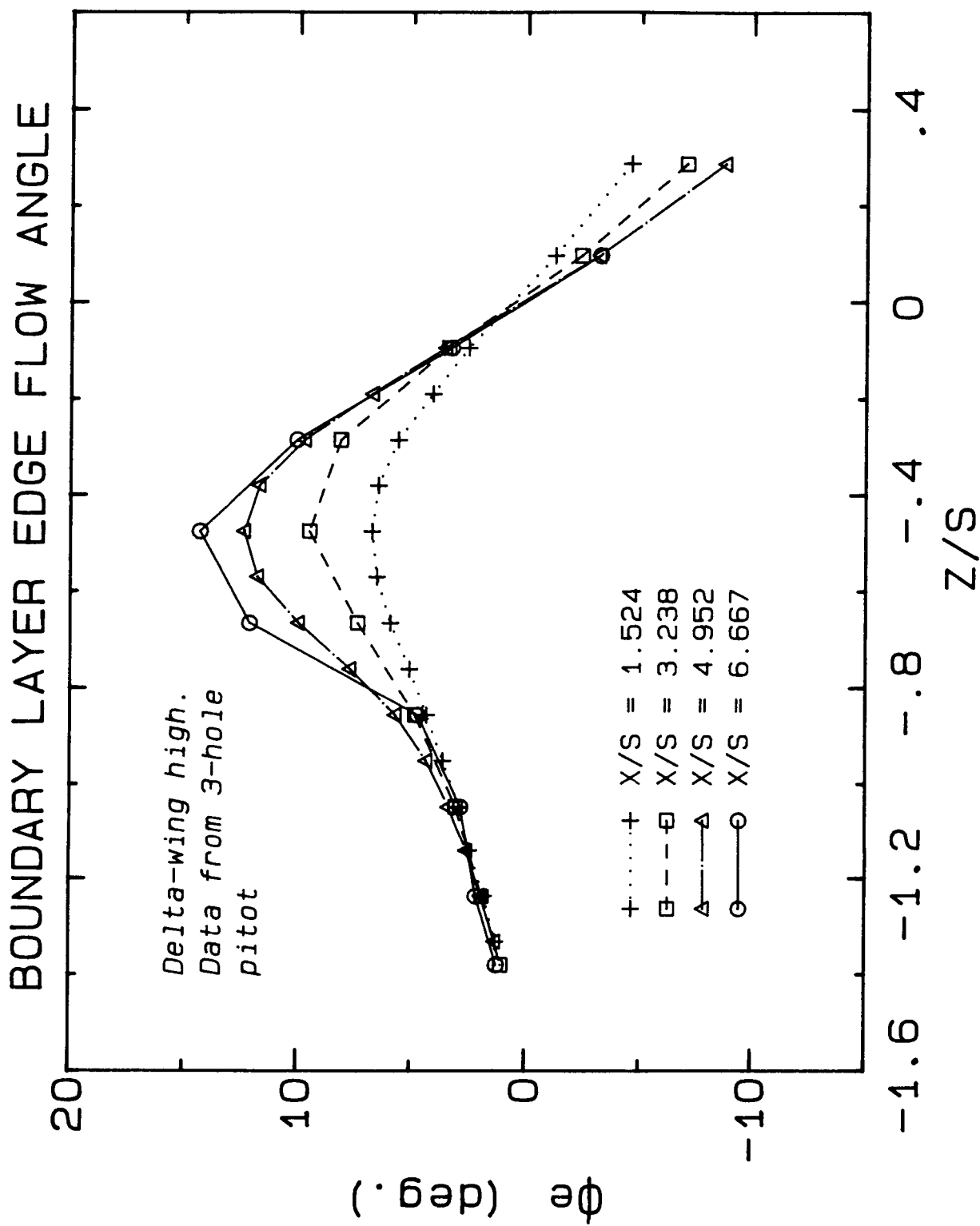
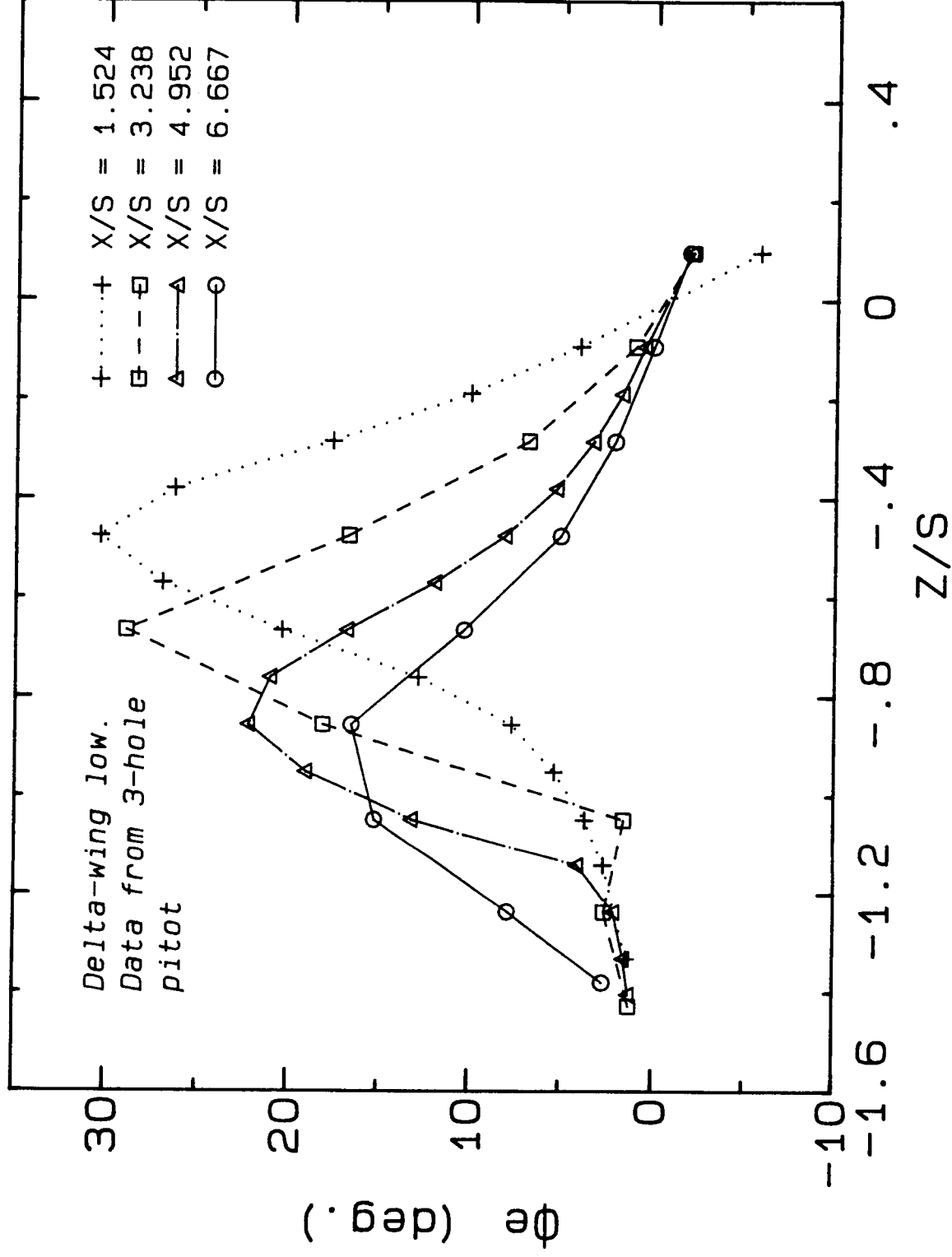


Figure 27. Profiles of boundary-layer edge flow angle  $\phi_e$ :  
27(a) "delta-wing low" case

# BOUNDARY LAYER EDGE FLOW ANGLE



27(b) "delta-wing high" case

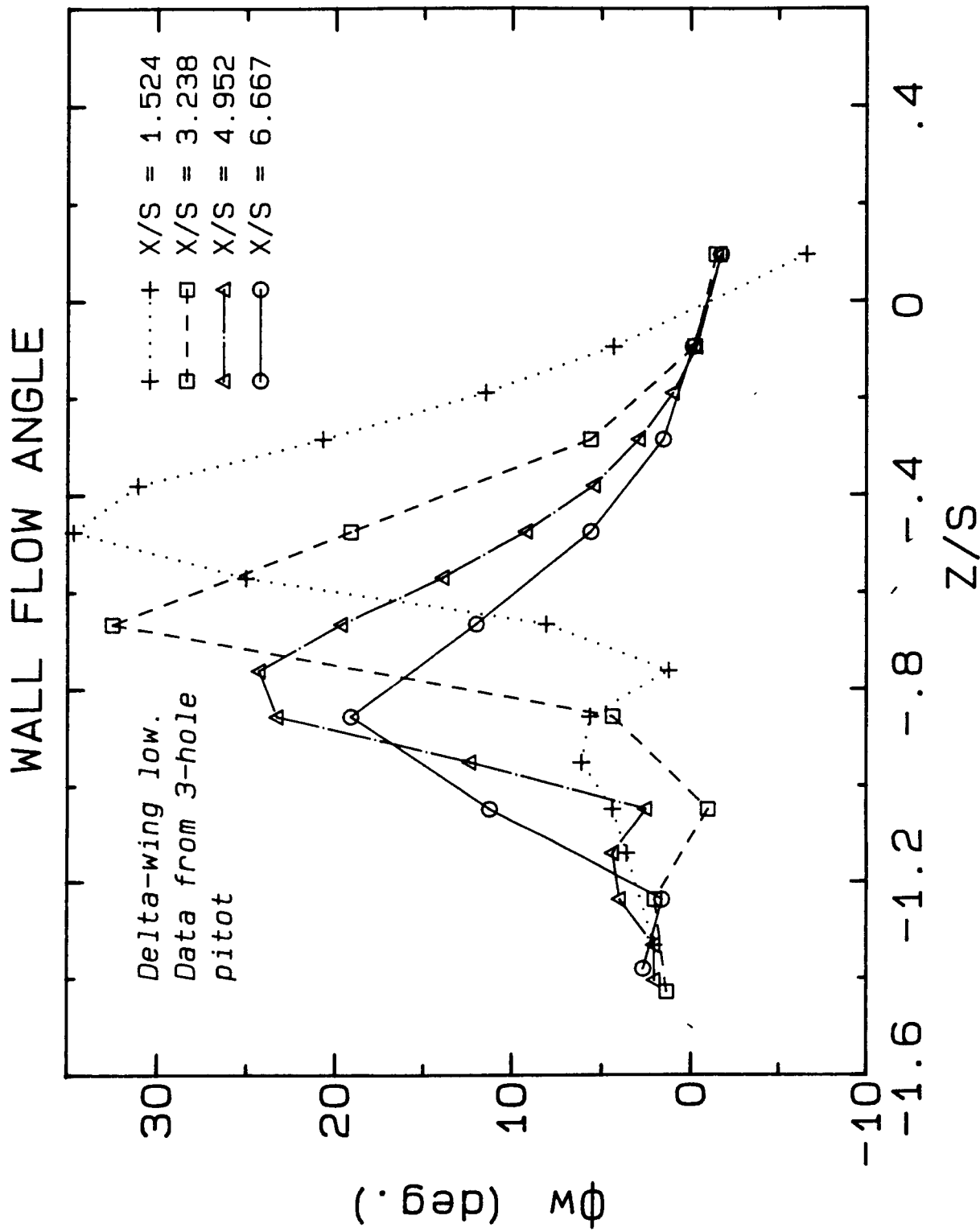
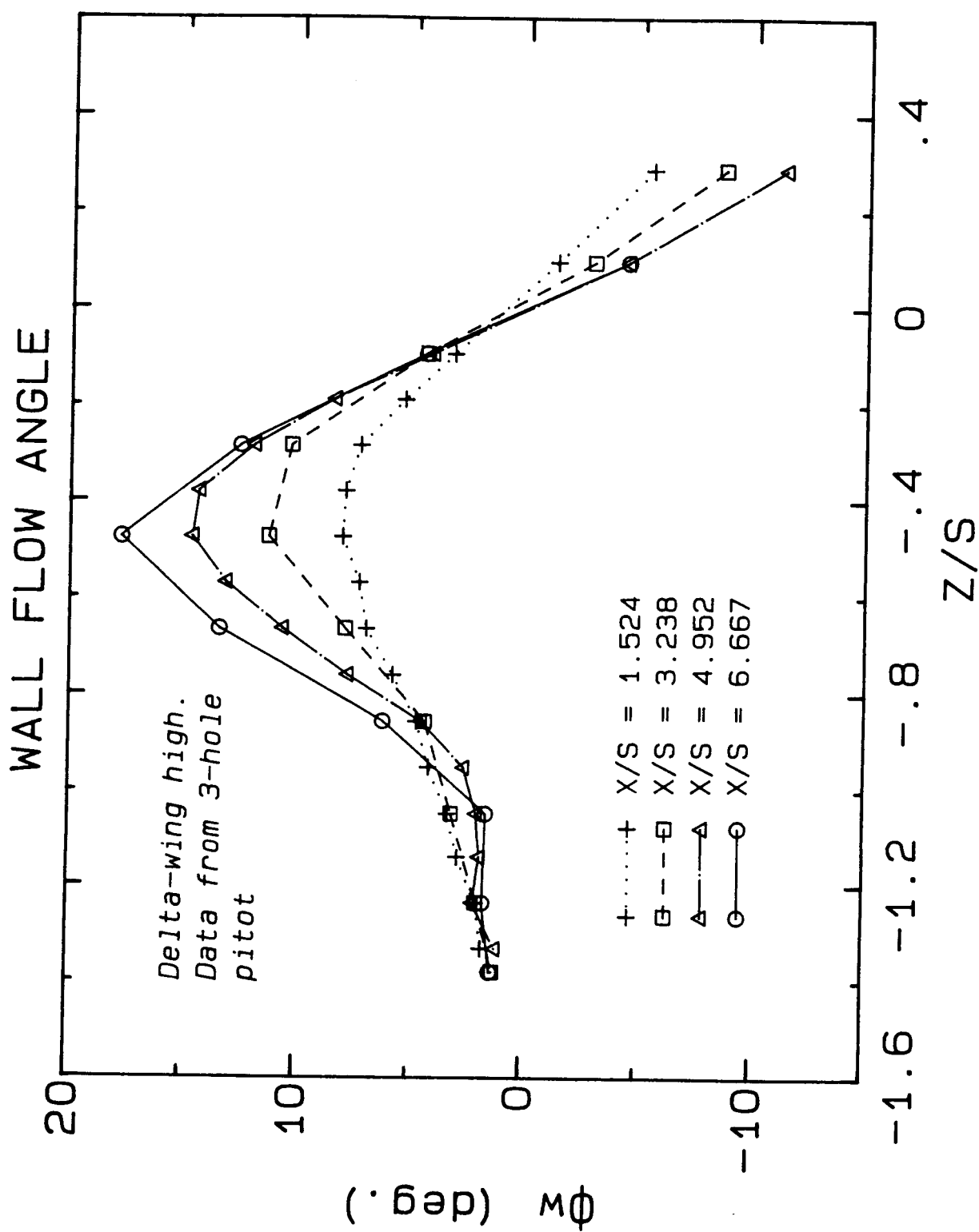


Figure 28. Profiles of wall flow angle  $\phi_w$ :  
28(a) "delta-wing low" case



28(b) "delta-wing high" case

# SKIN FRICTION VS. REO

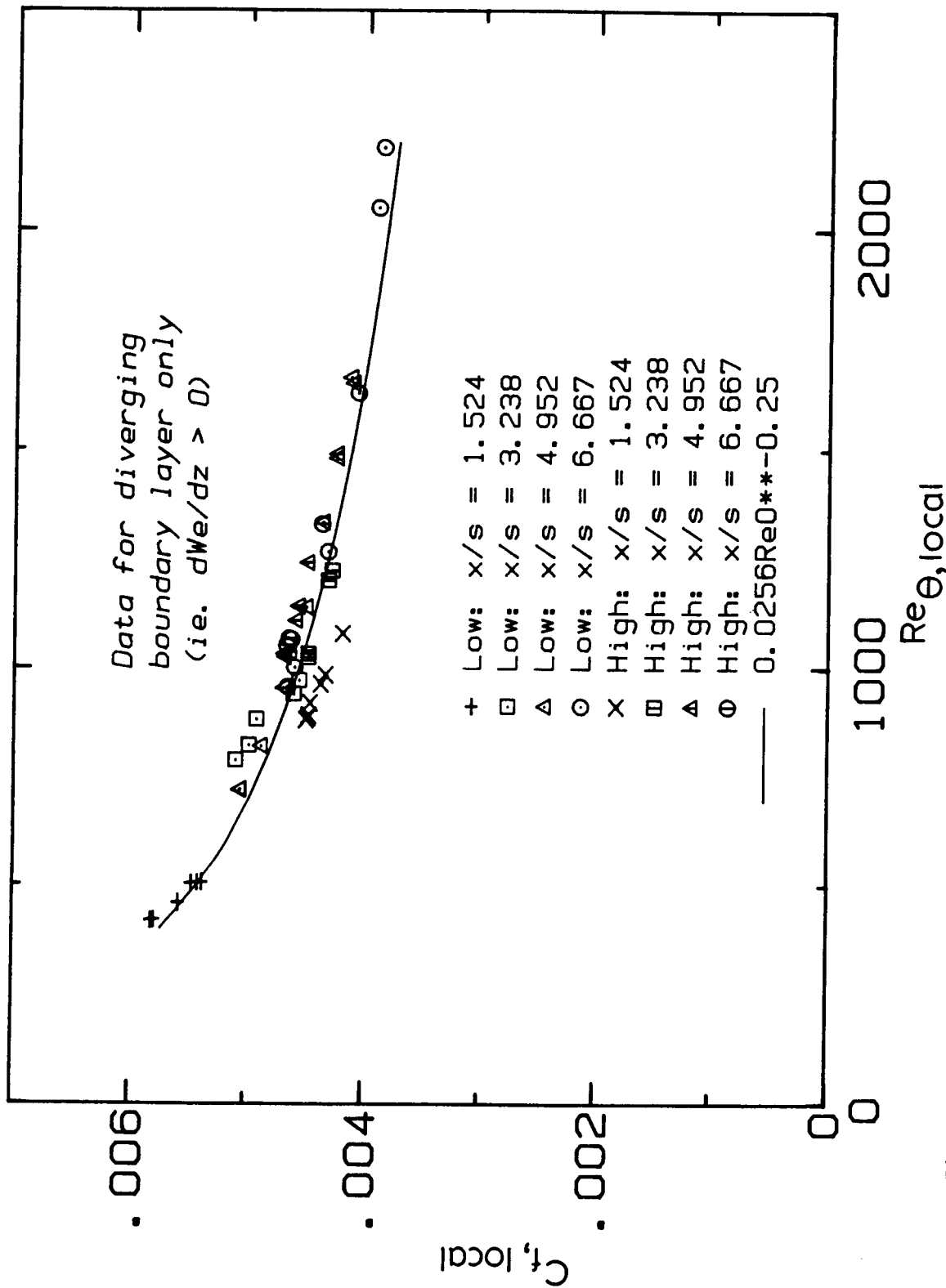


Figure 29. Plot of the local skin friction coefficient ( $C_{f, local} = \tau_w / (\frac{1}{2} \rho Q_e^2)$ ) as a function of ( $Re_{\theta, local} = Q_e \theta_{1/2} / \nu$ ) for all diverging boundary layer profiles ("delta-wing low" and "delta-wing high" cases).

# SHAPE FACTOR H VS. $Re_{\theta}$

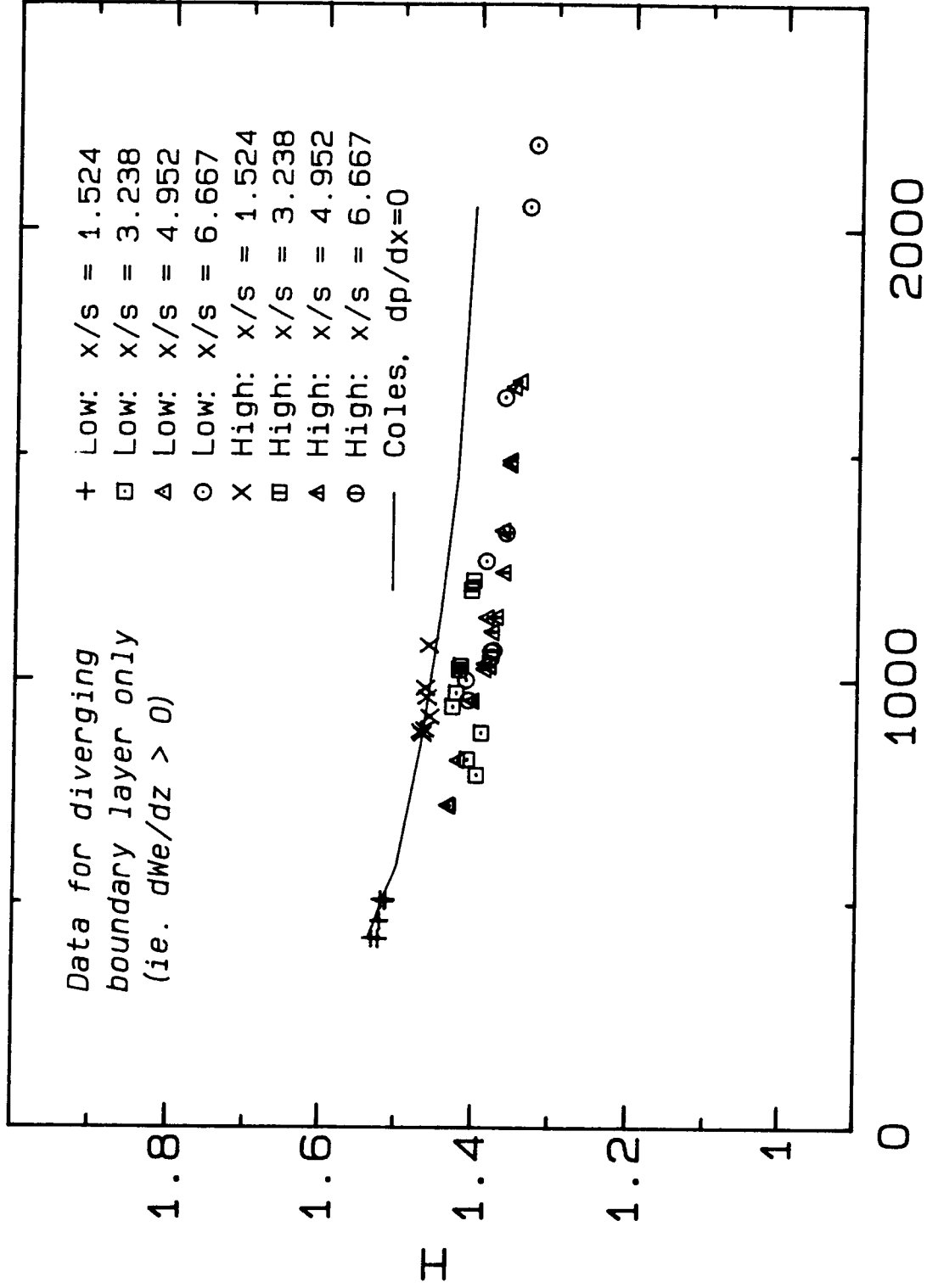


Figure 30. Plot of shape factor ( $H=\delta_1^*/\theta_{11}$ ) as a function of ( $Re_{\theta, local}$ ). Also plotted are results due to Coles (1962) for a zero pressure gradient boundary layer.

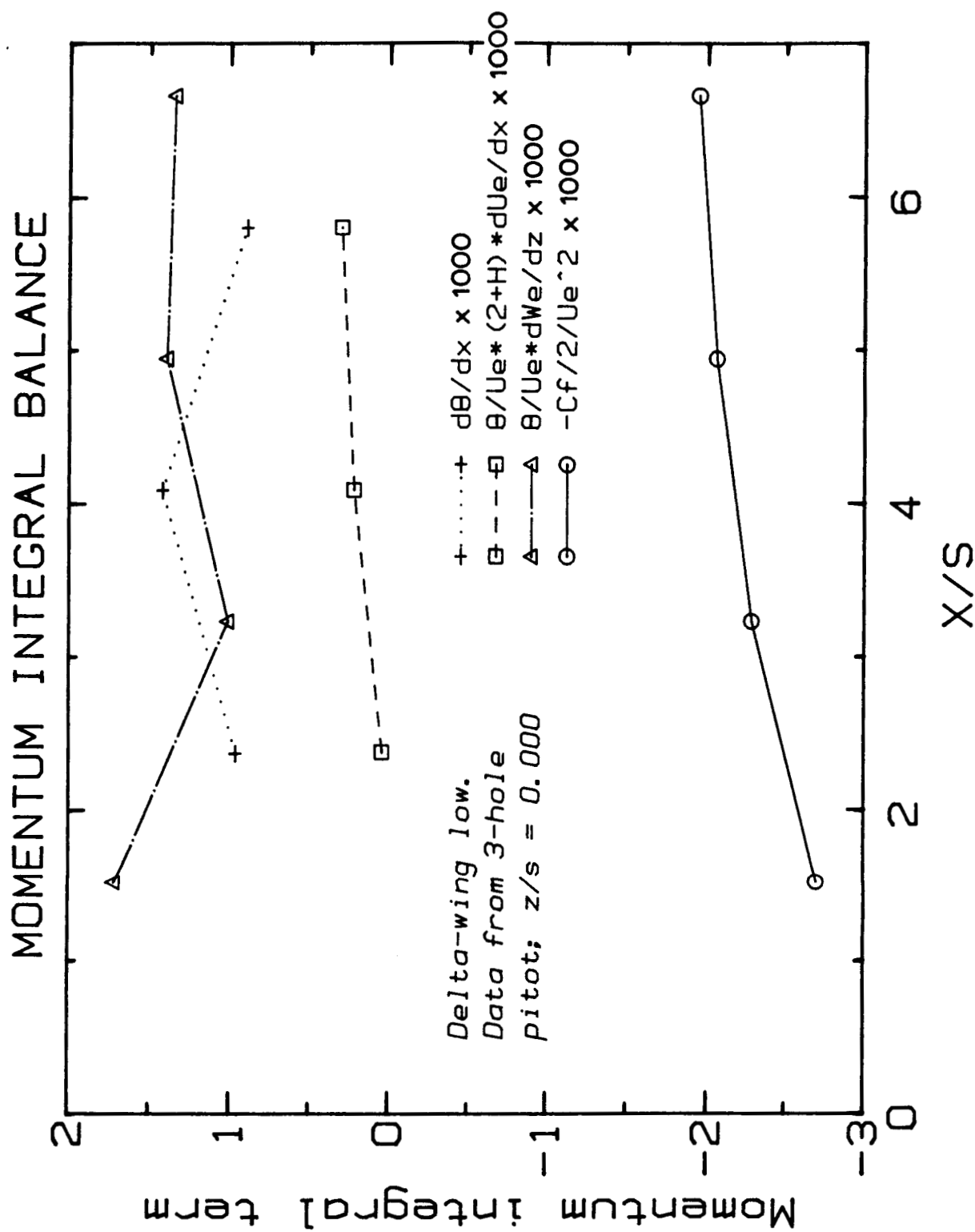
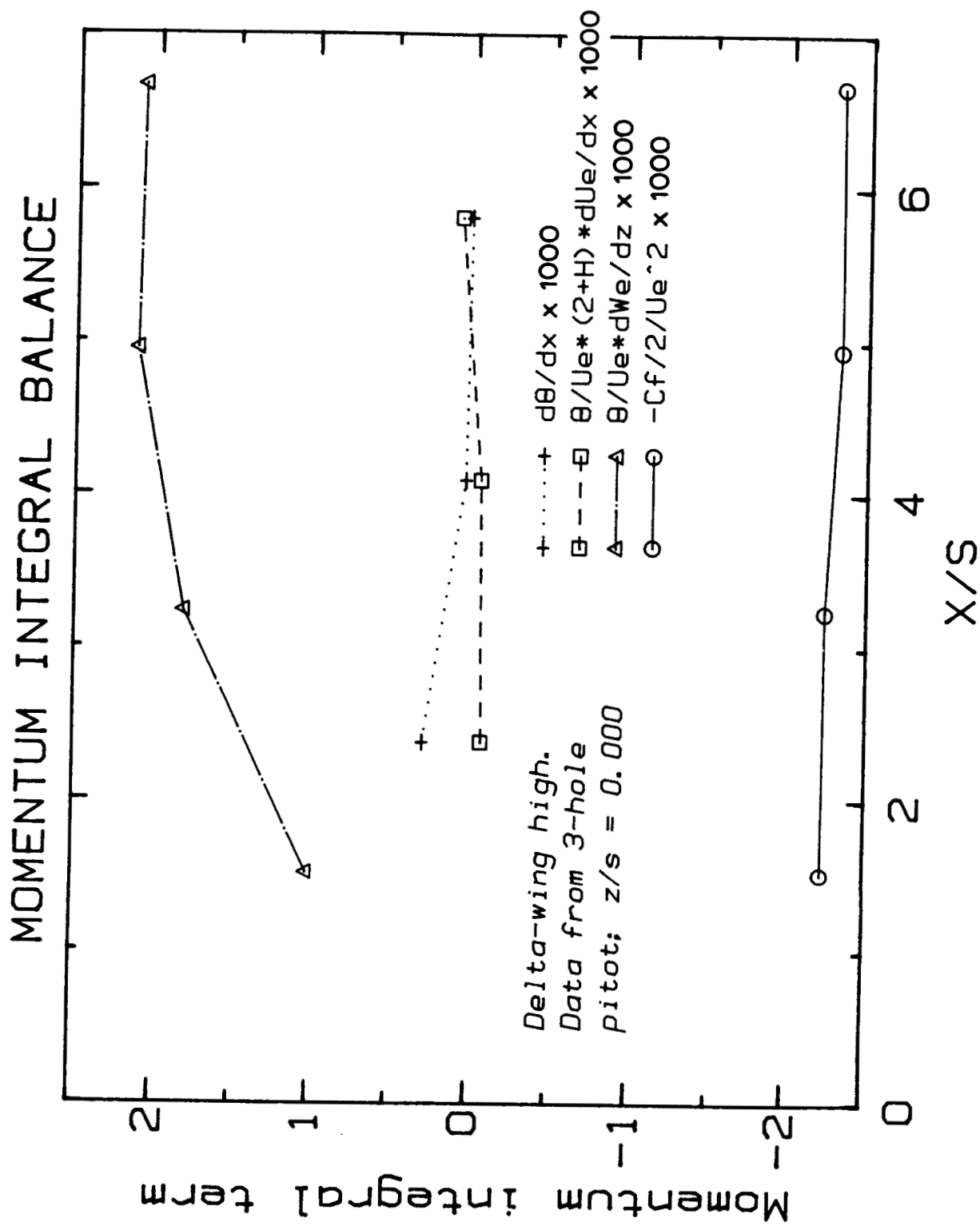


Figure 31. Plot of terms of the momentum integral equation (assuming three-dimensional collateral flow):

31(a) "delta-wing low" case



31(b) "delta-wing high" case

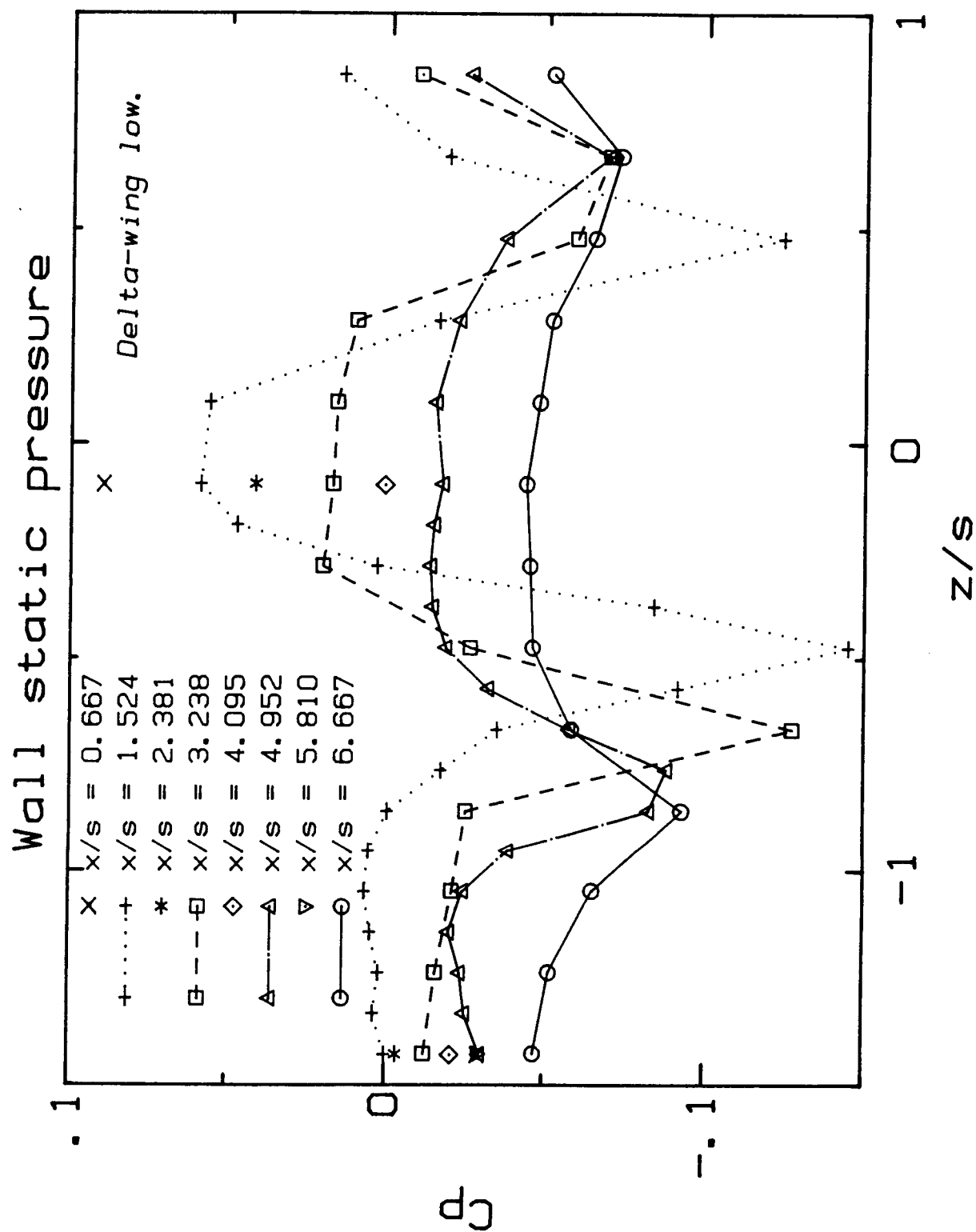
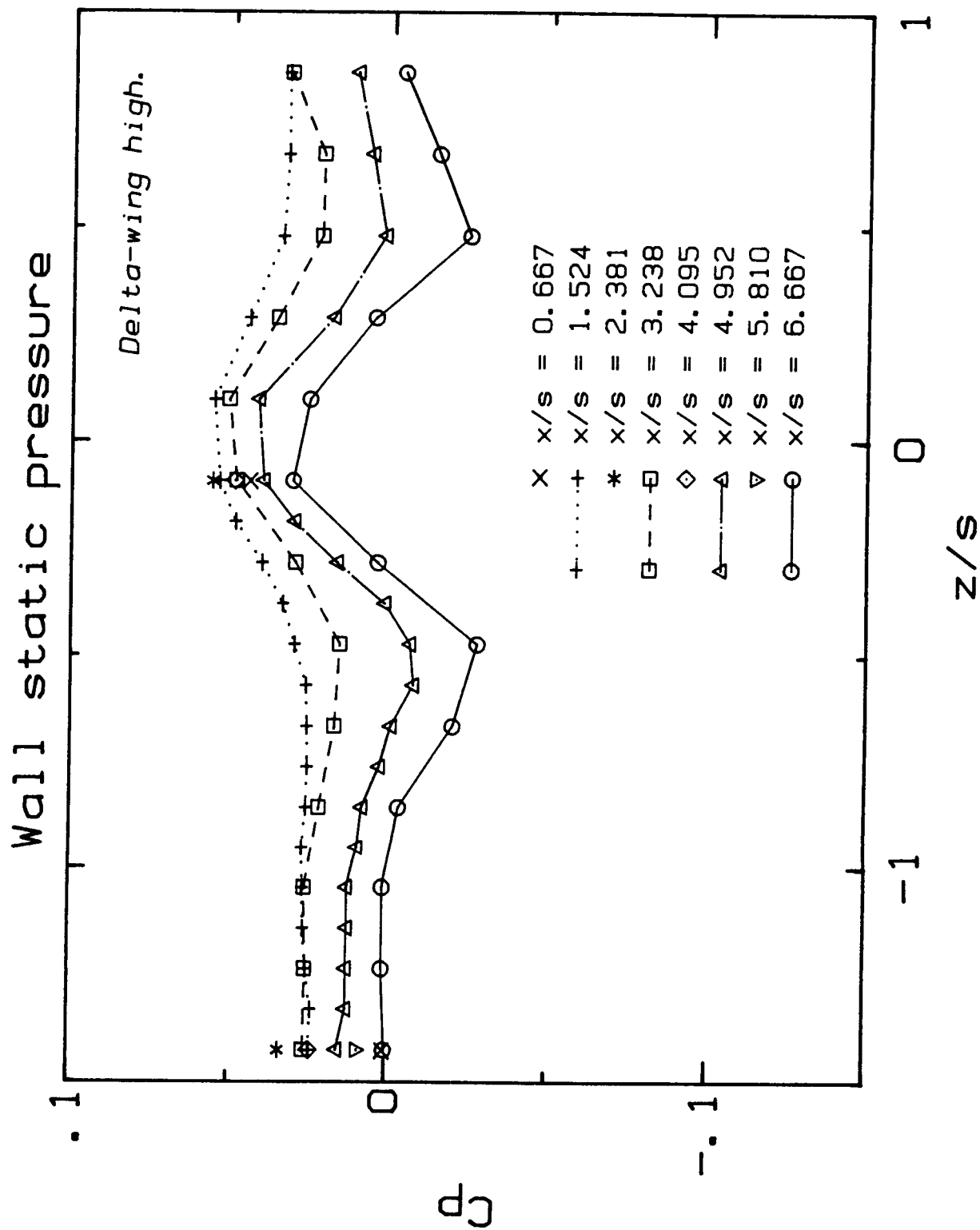


Figure 32. Profiles of wall static pressure coefficient ( $C_p = (p - p_{ref}) / (P_{ref} - p_{ref})$ )

32(a) "delta-wing low" case



32(b) "delta-wing high" case

\*\*\*Figures 33-38: vortex region\*\*\*

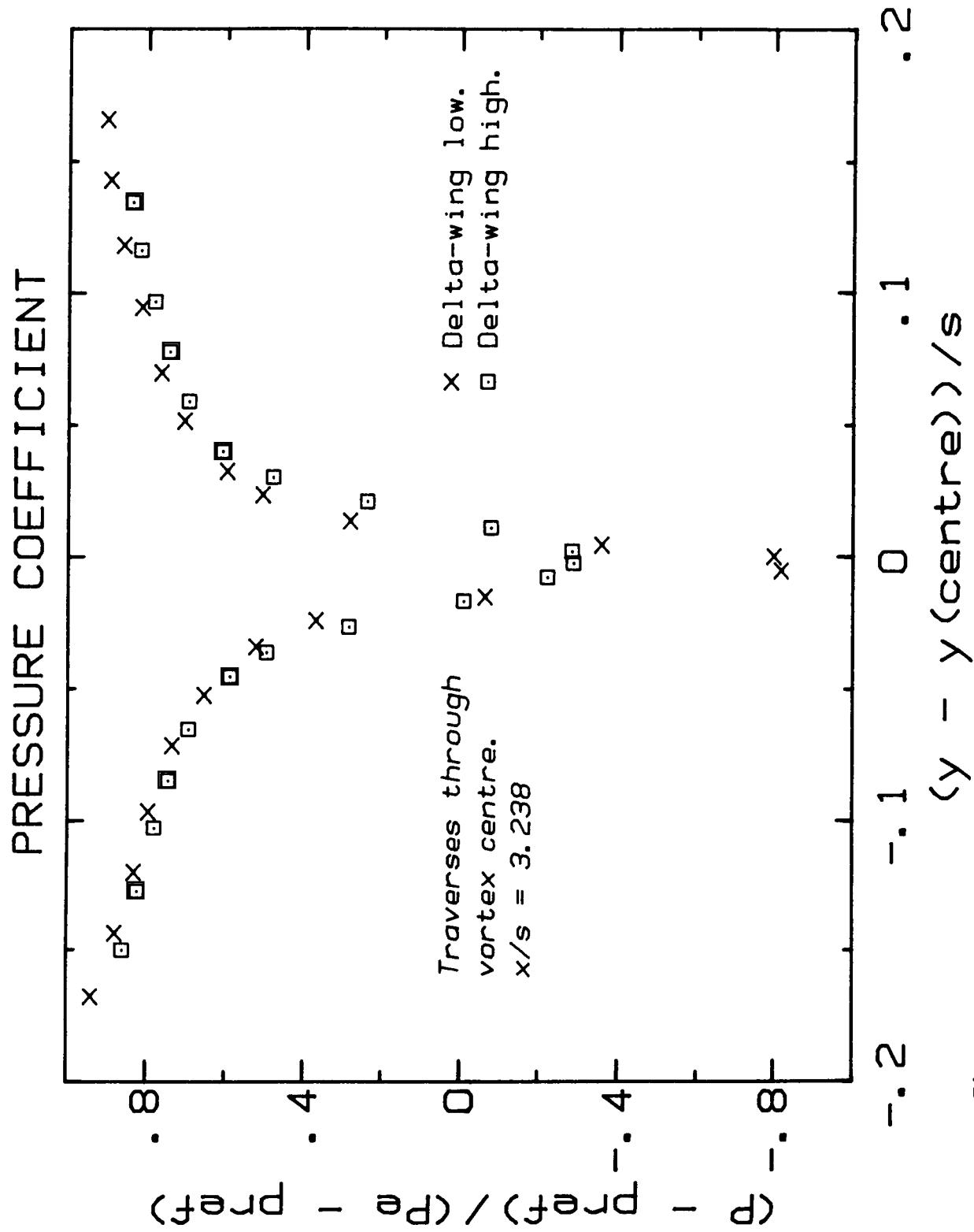


Figure 33. Profiles of total pressure coefficient  $(P - P_{ref}) / (P_e - P_{ref})$  through the vortex centre for both cases at  $x/s = 3.238$ .

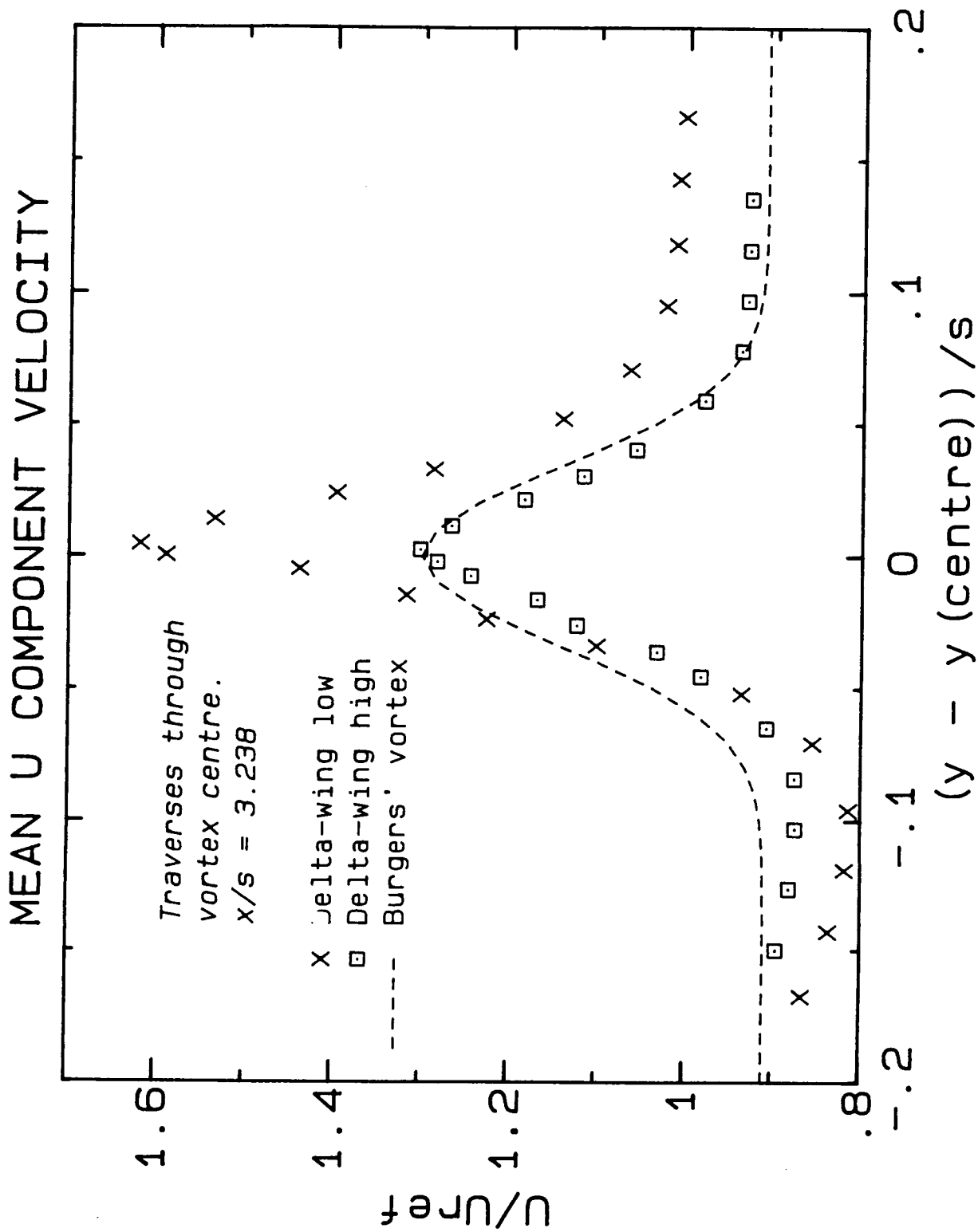


Figure 34. Profiles of mean U component velocity through the vortex centre. Also, a fit to Burger's solution for the "delta-wing high" case.

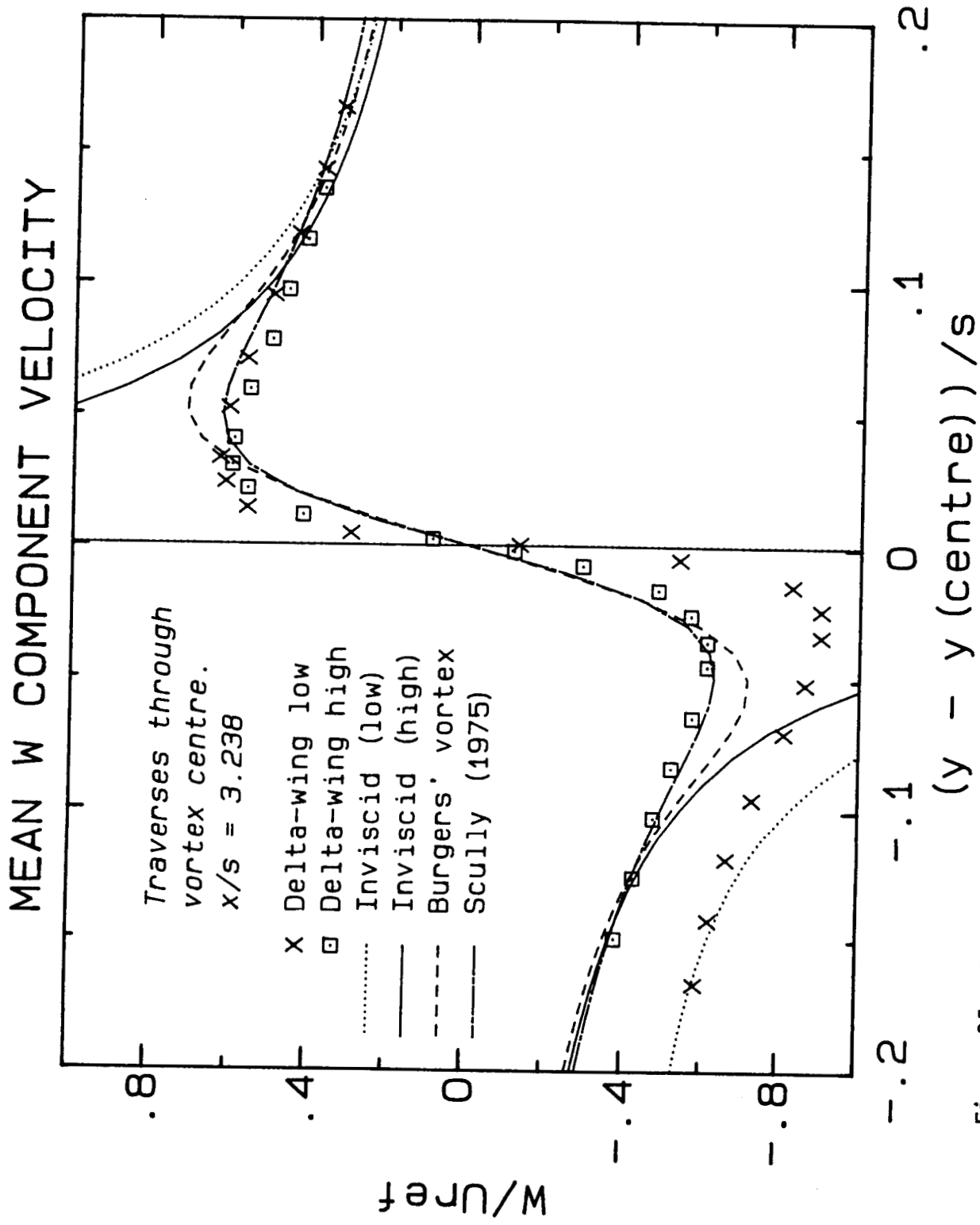


Figure 35. Profiles of mean  $W$  component velocity through the vortex centre. Also, fits to the inviscid solution and a fit to Burger's solution for the "delta-wing high" case.

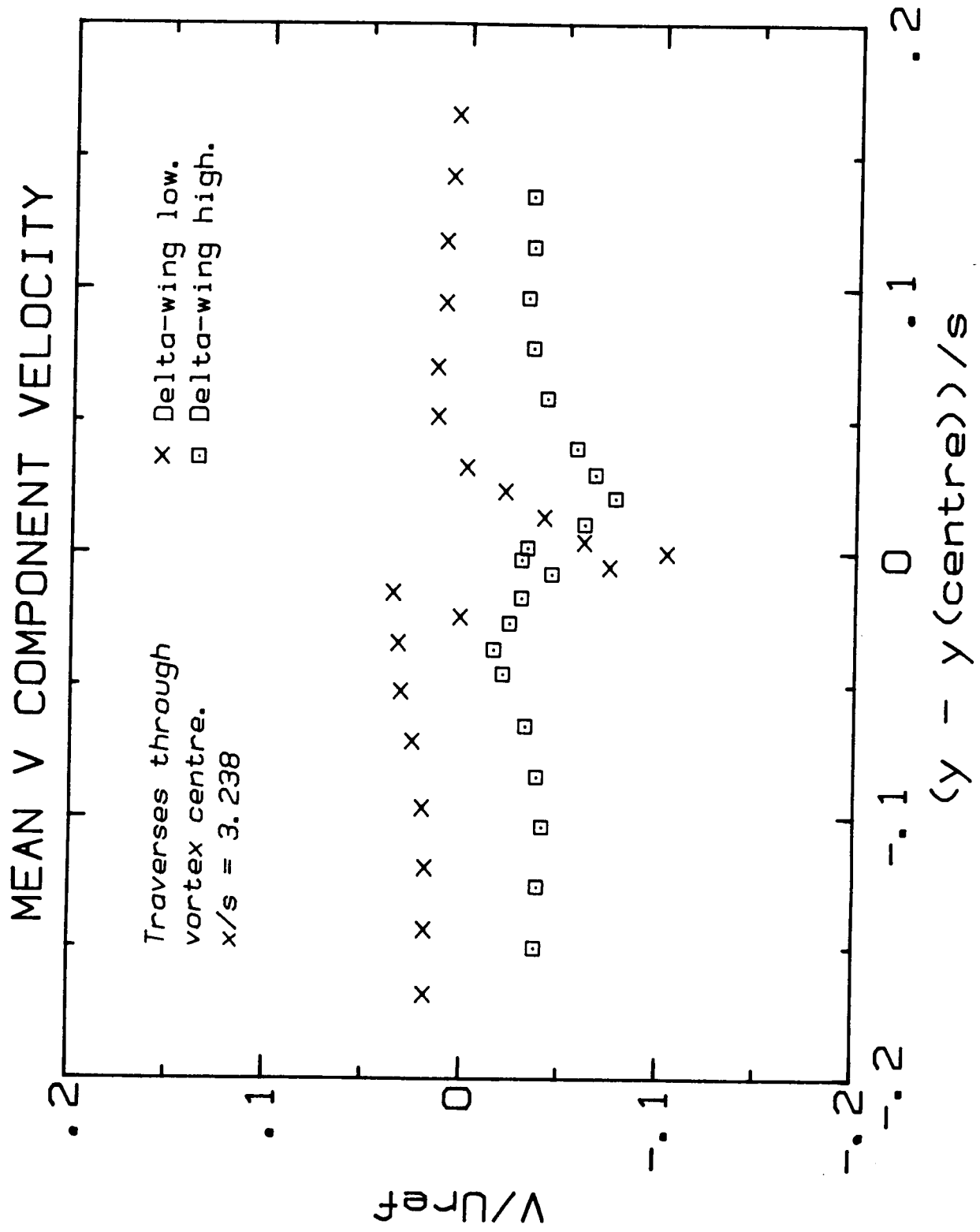


Figure 36. Profiles of mean V component velocity through the vortex centre.

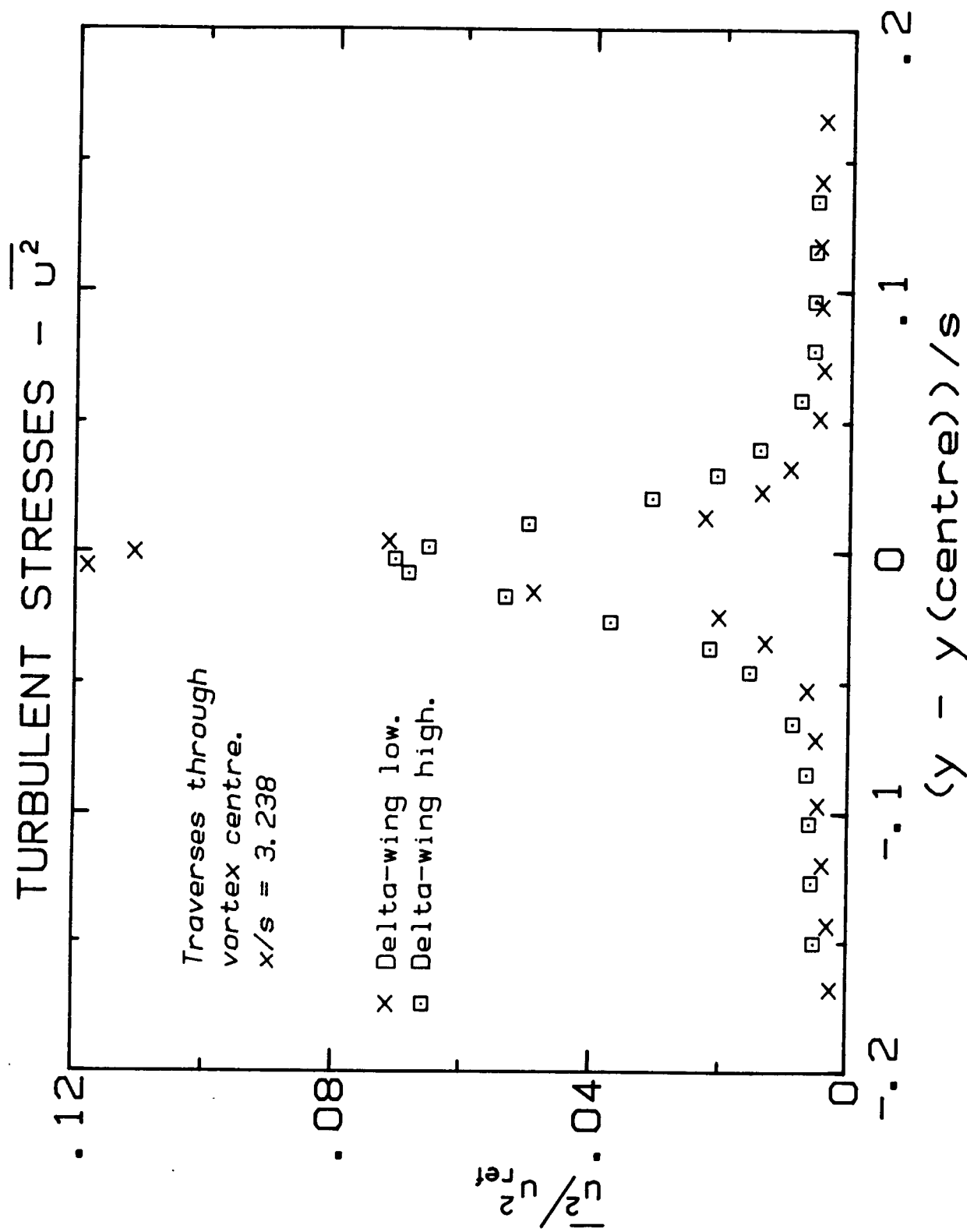
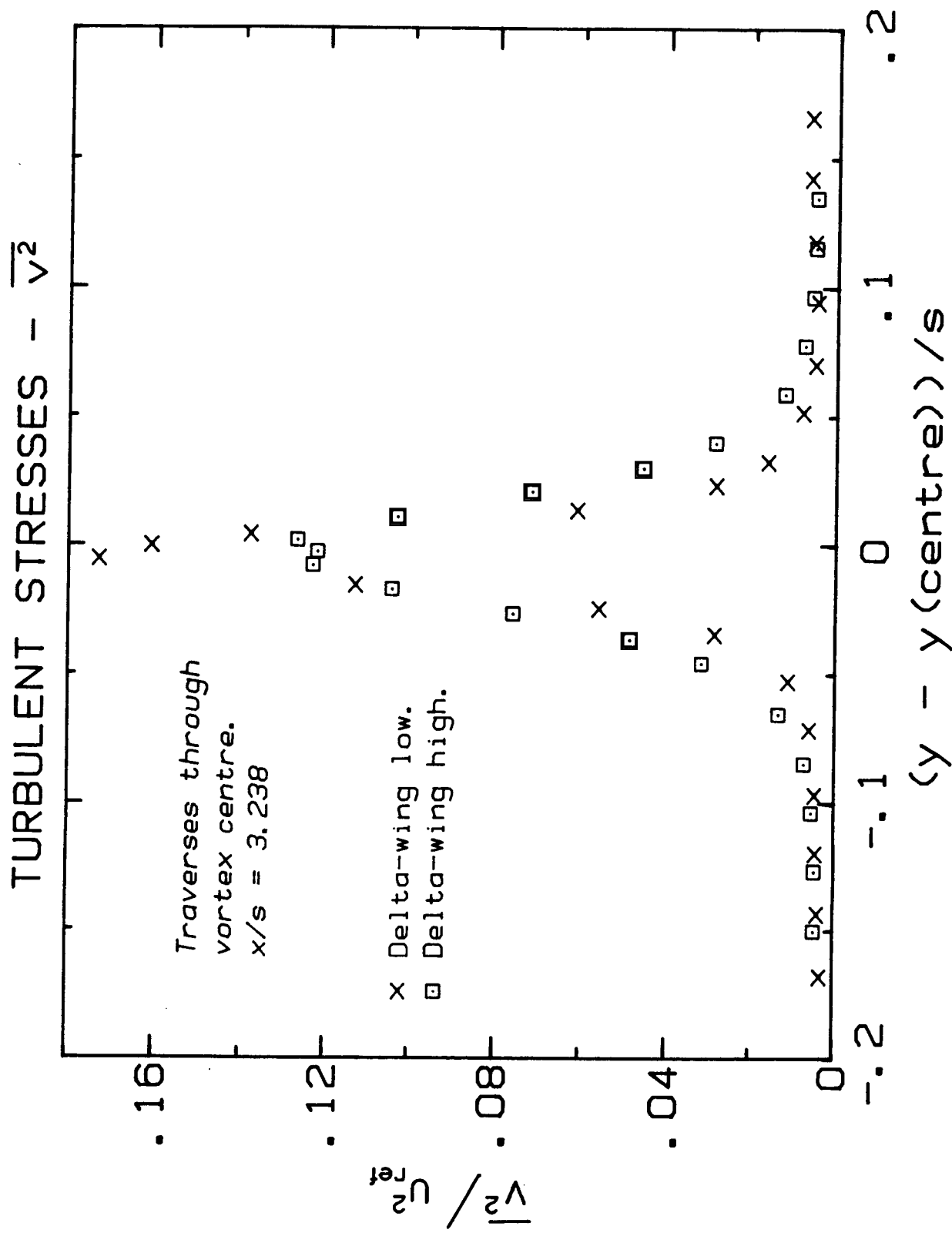
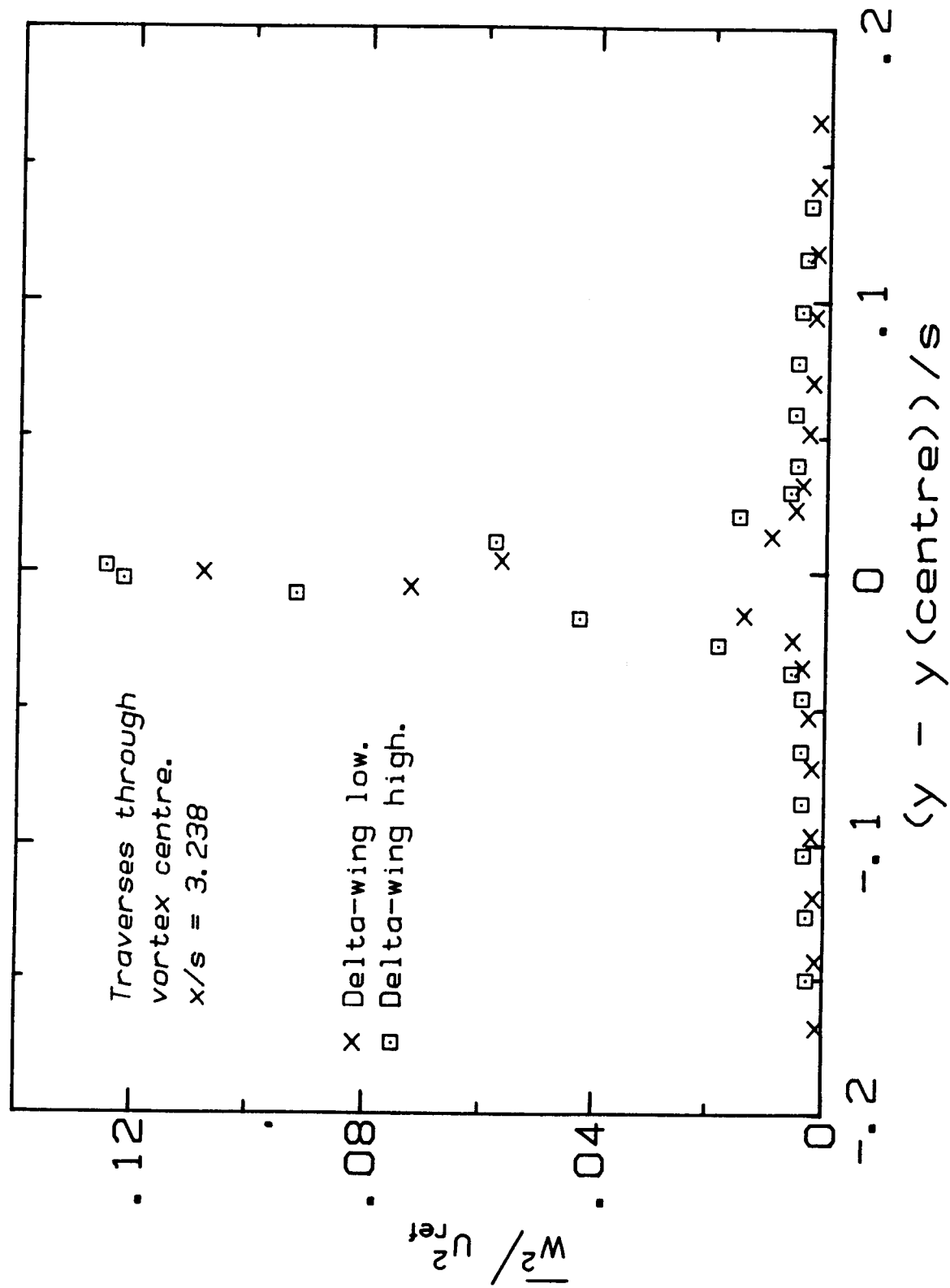
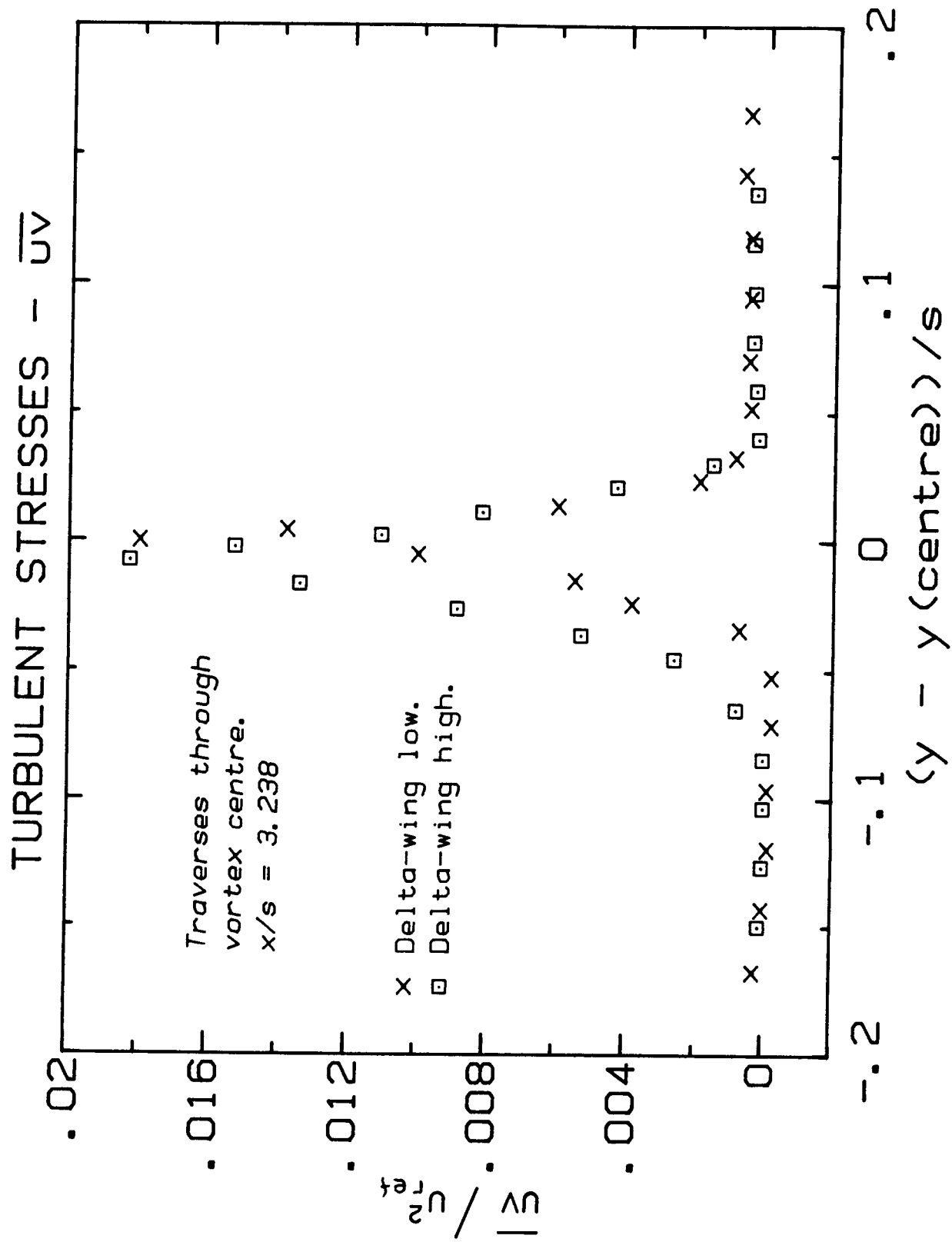


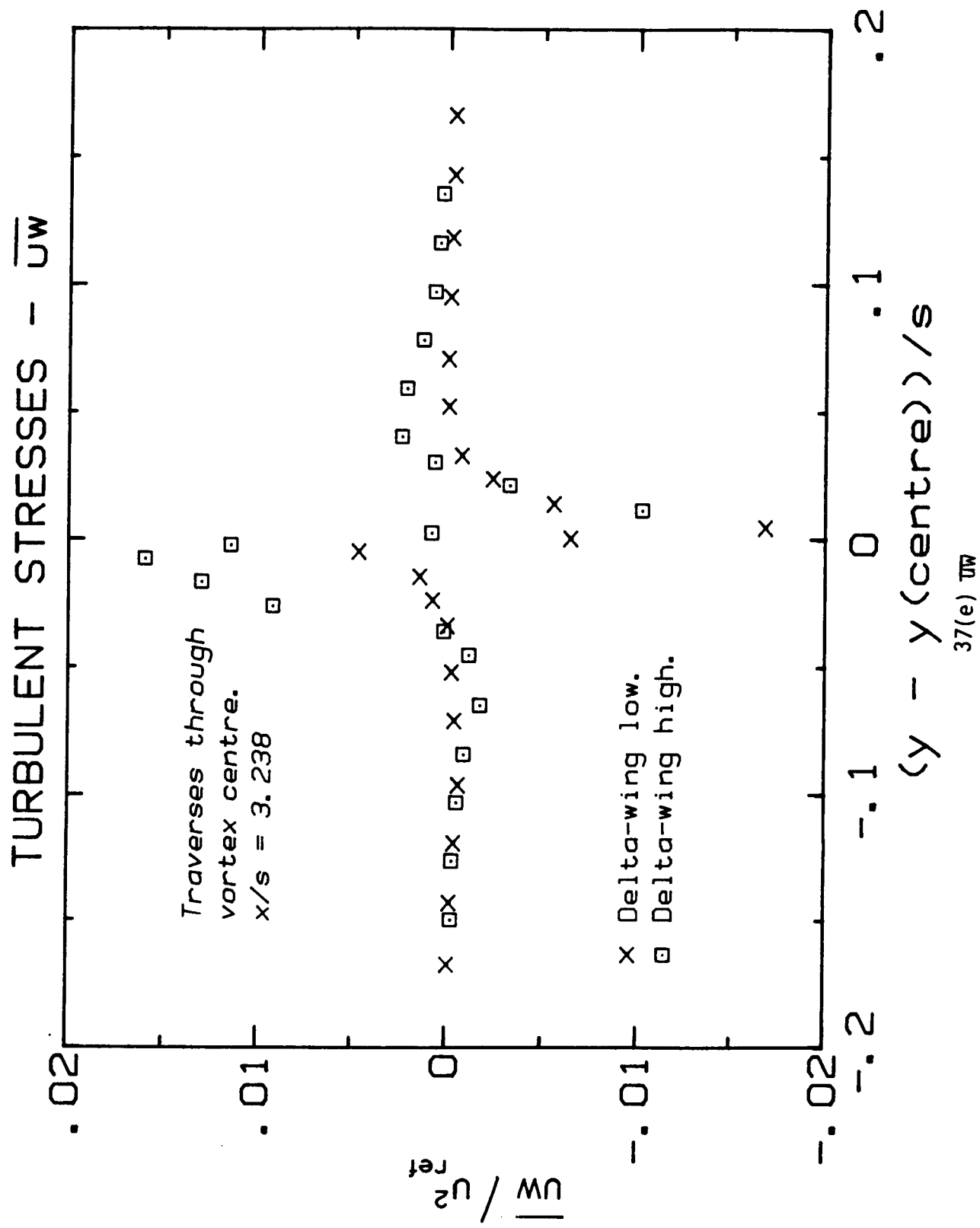
Figure 37. Profiles of the Reynolds stresses through the vortex centre:  
37(a)  $\overline{u^2}$

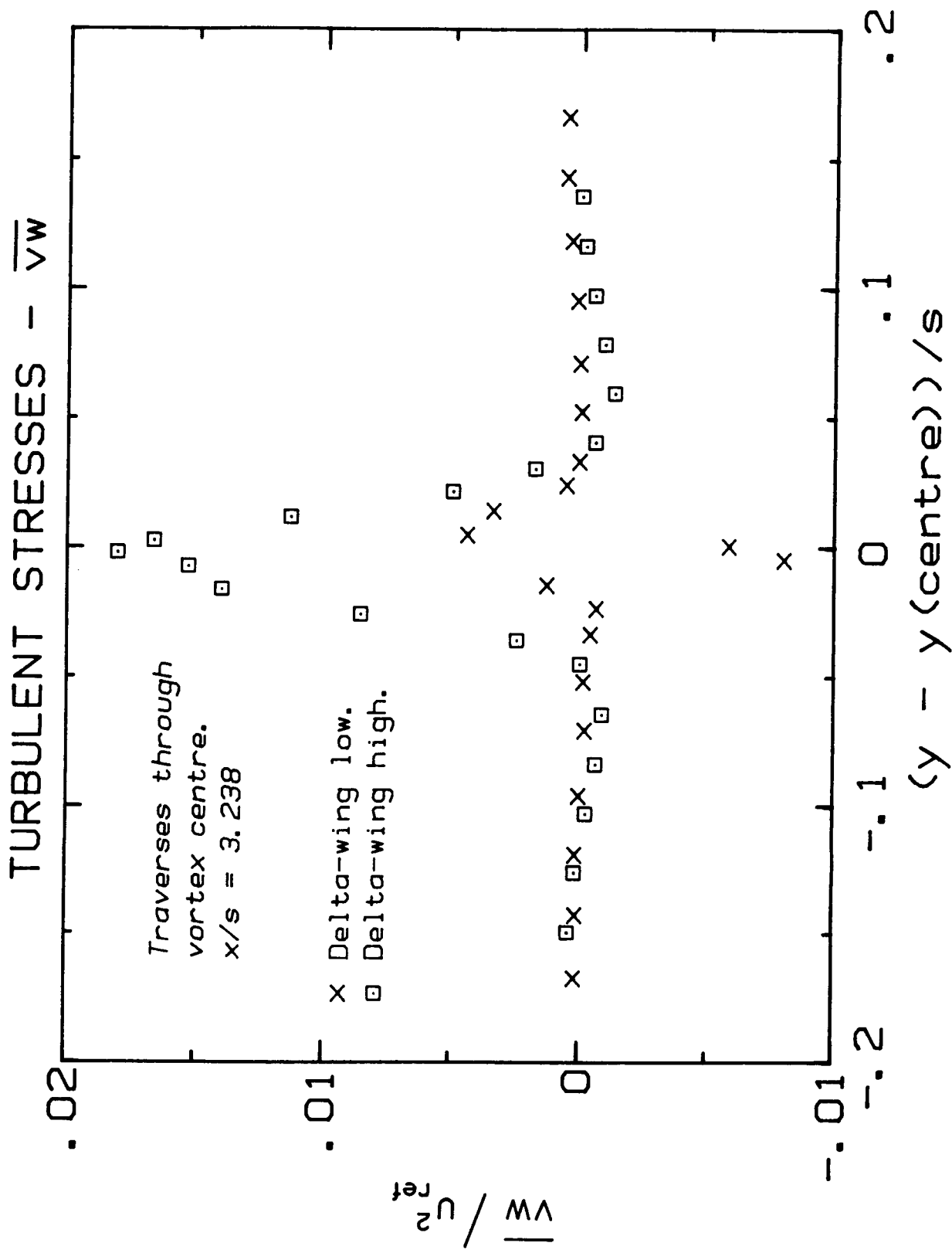


# TURBULENT STRESSES - $\overline{w^2}$









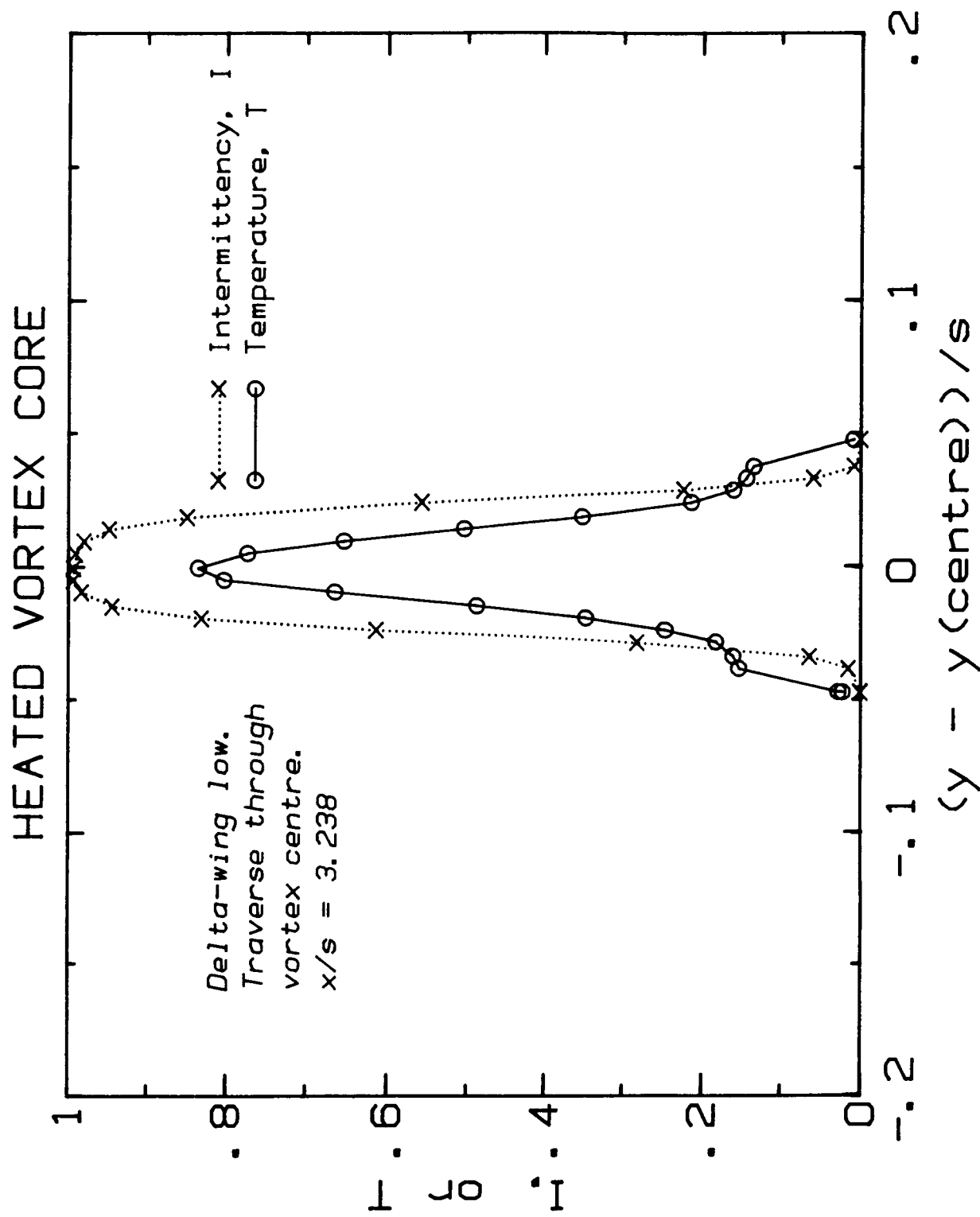


Figure 38. Profiles of non-dimensionalised temperature  $(T_h - T_c)/T_{ref}$  and intermittency I through the vortex centre.

\*\*\*Figures 39-44 Further derived results.\*\*\*

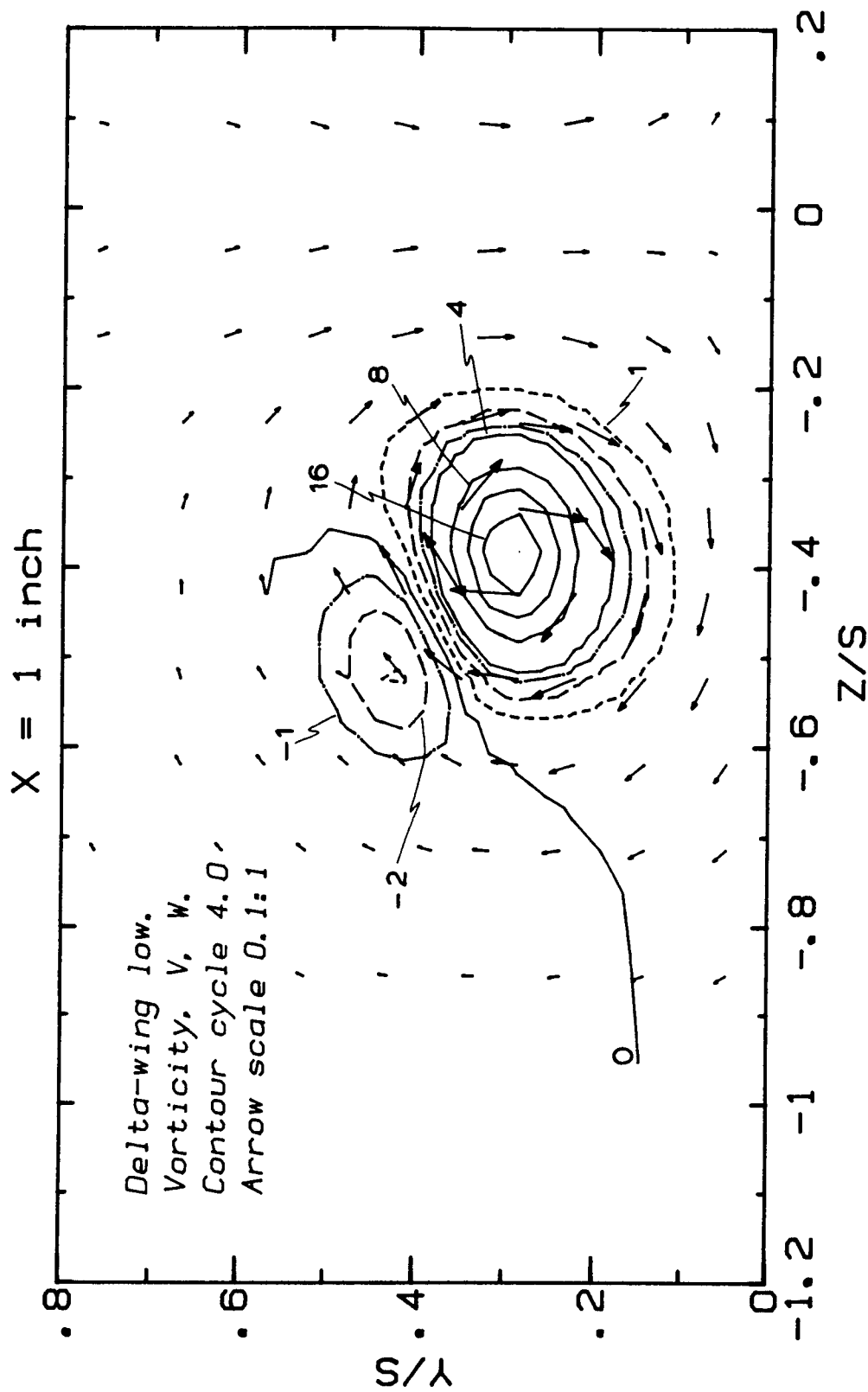
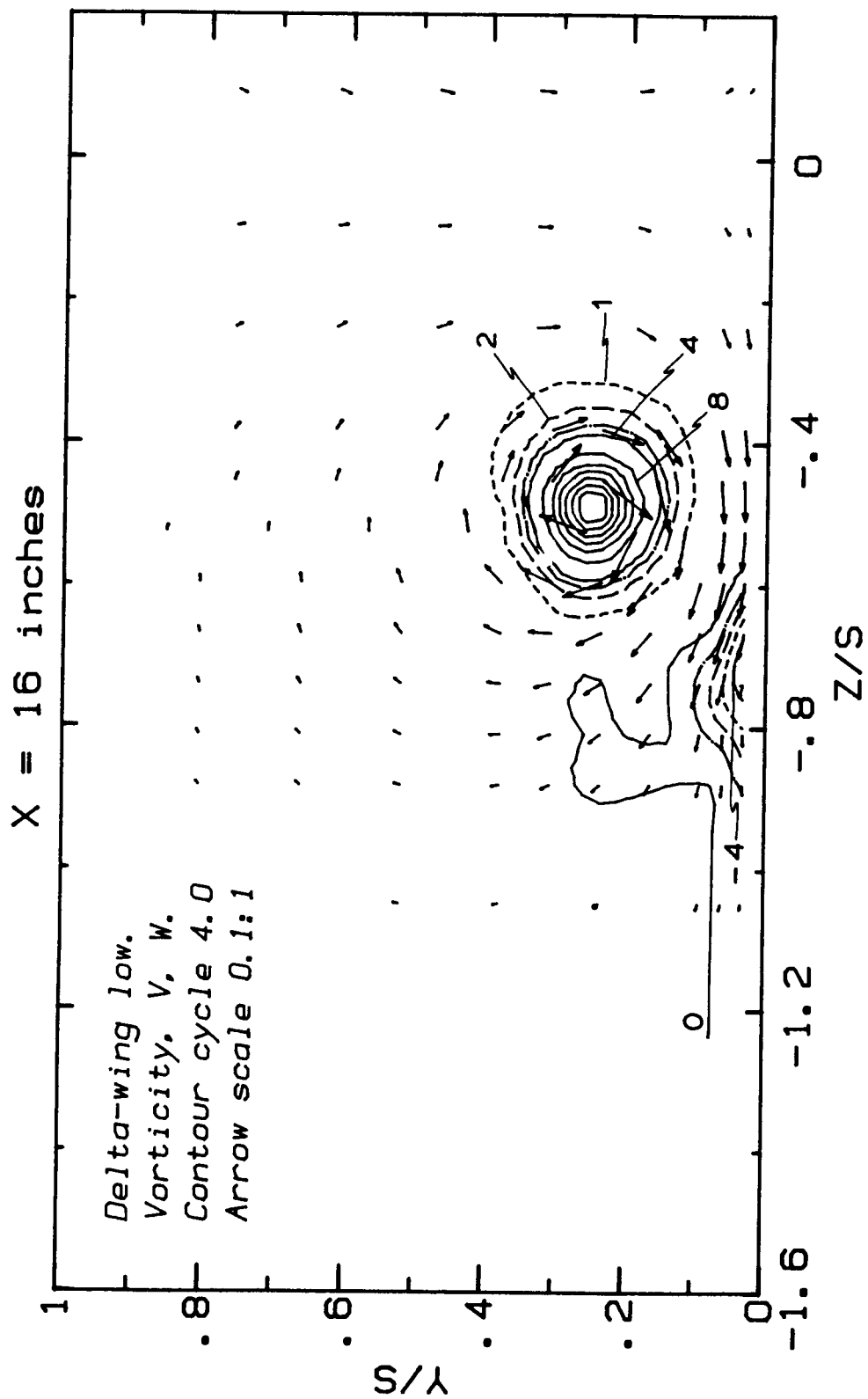
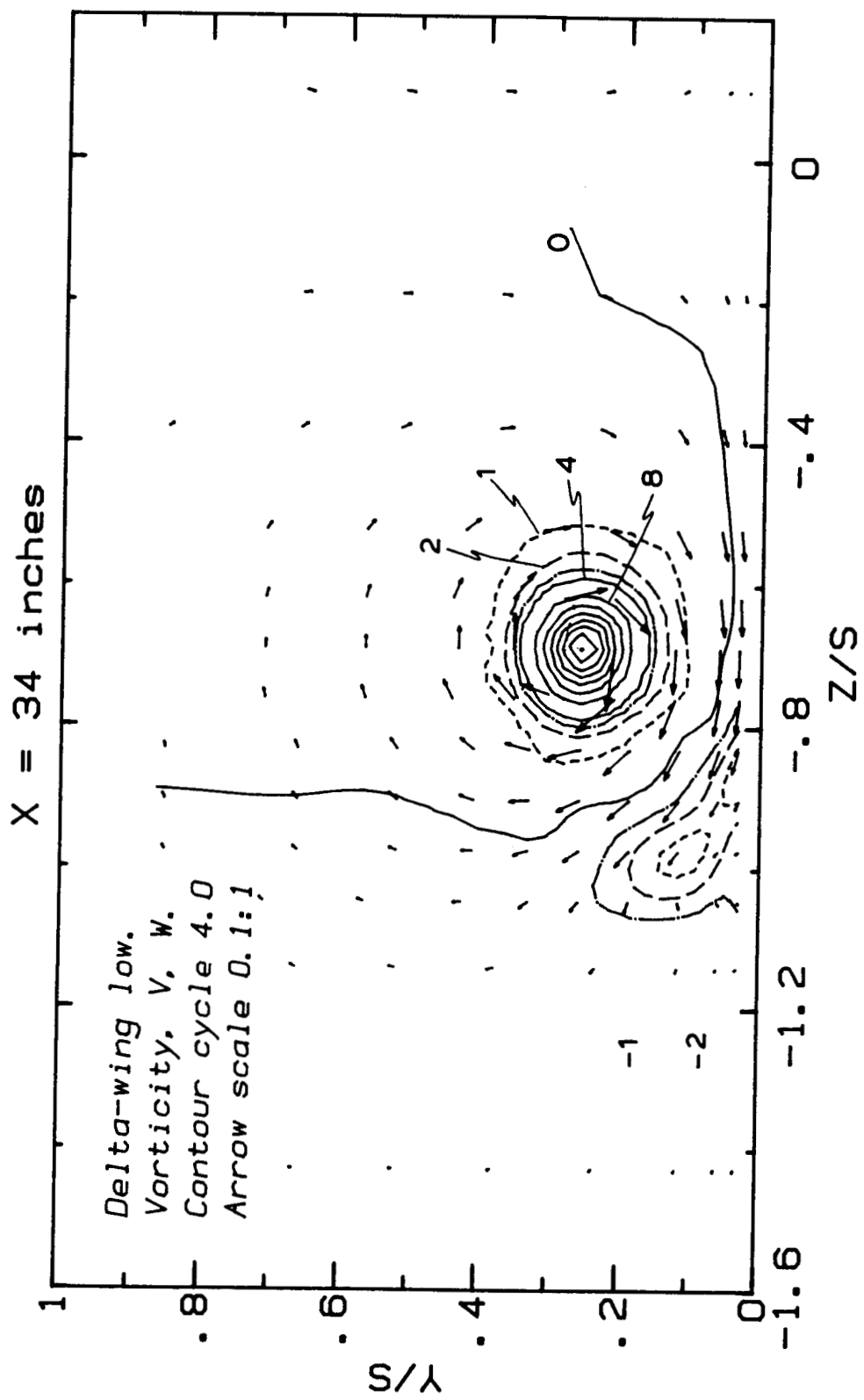


Figure 39. Contours of longitudinal vorticity and secondary mean velocity vectors for the "delta-wing low" case:

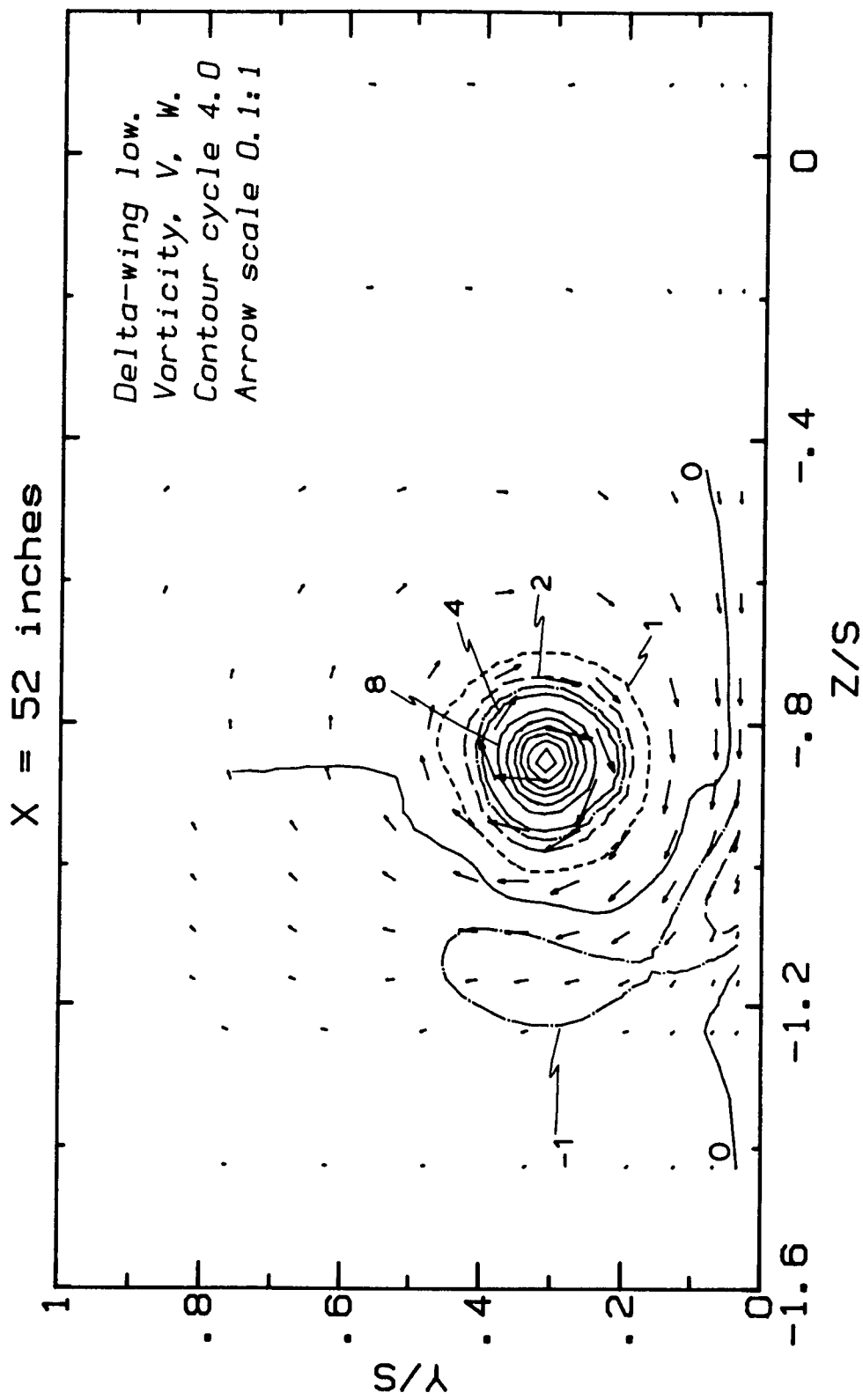
39(a)  $x/s = 0.095$



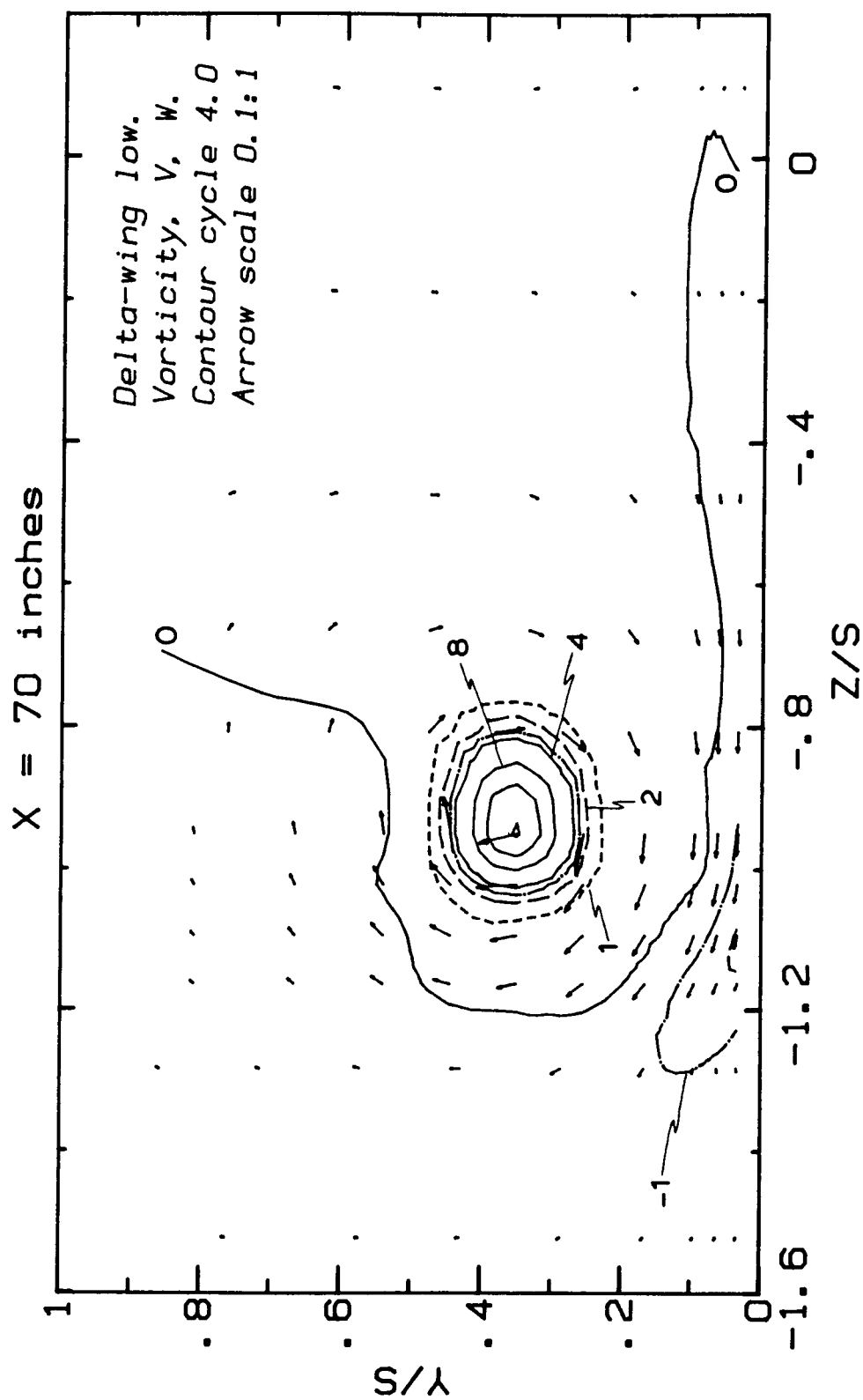
39(b)  $x/s = 1.524$



39(c)  $x/s = 3.238$



39(d)  $x/s = 4.952$



39(e)  $x/s = 6.667$

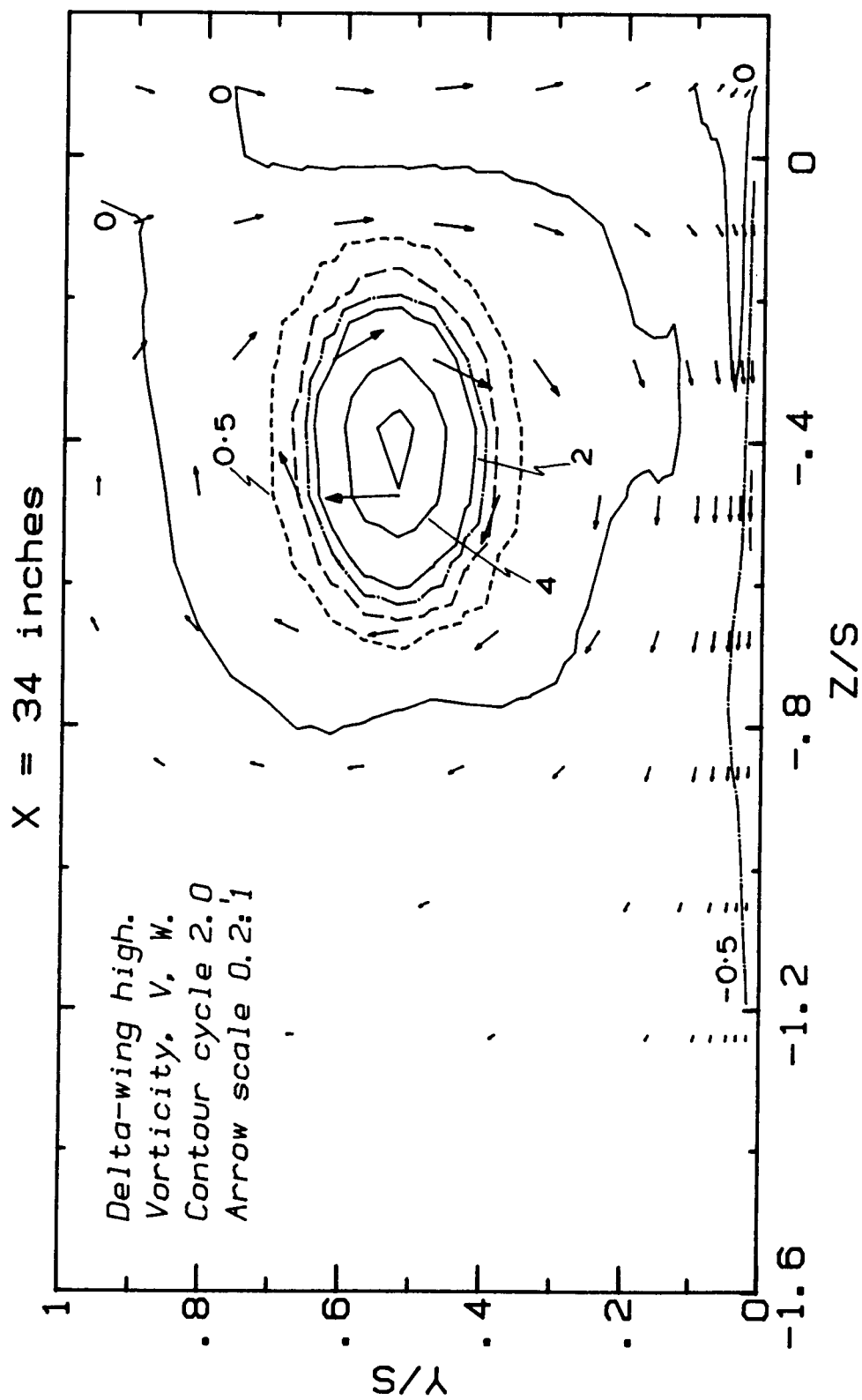
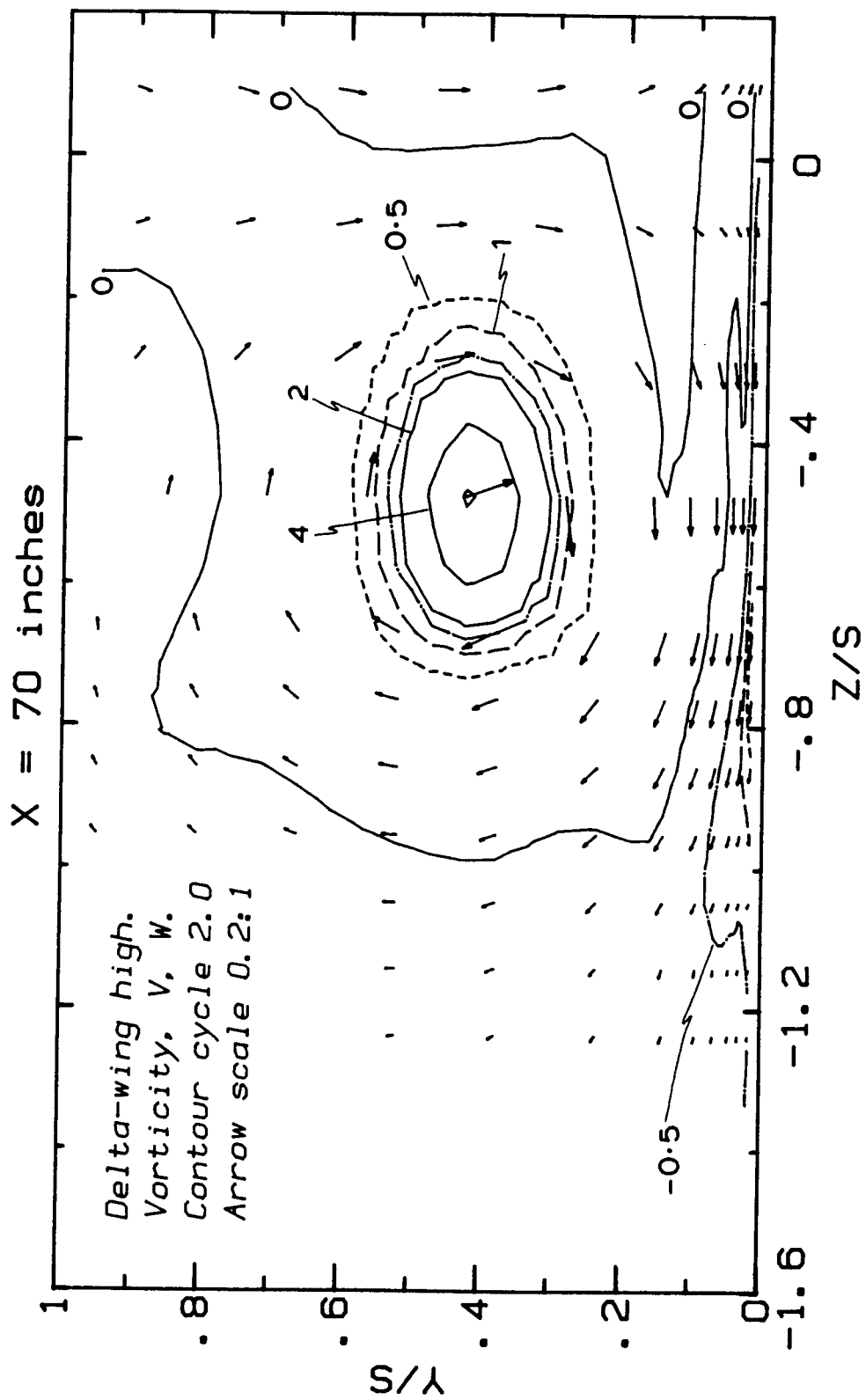


Figure 40. Contours of longitudinal vorticity and secondary mean velocity vectors for the "delta-wing high" case:

40(a)  $x/s = 3.238$



40(b)  $x/s = 6.667$

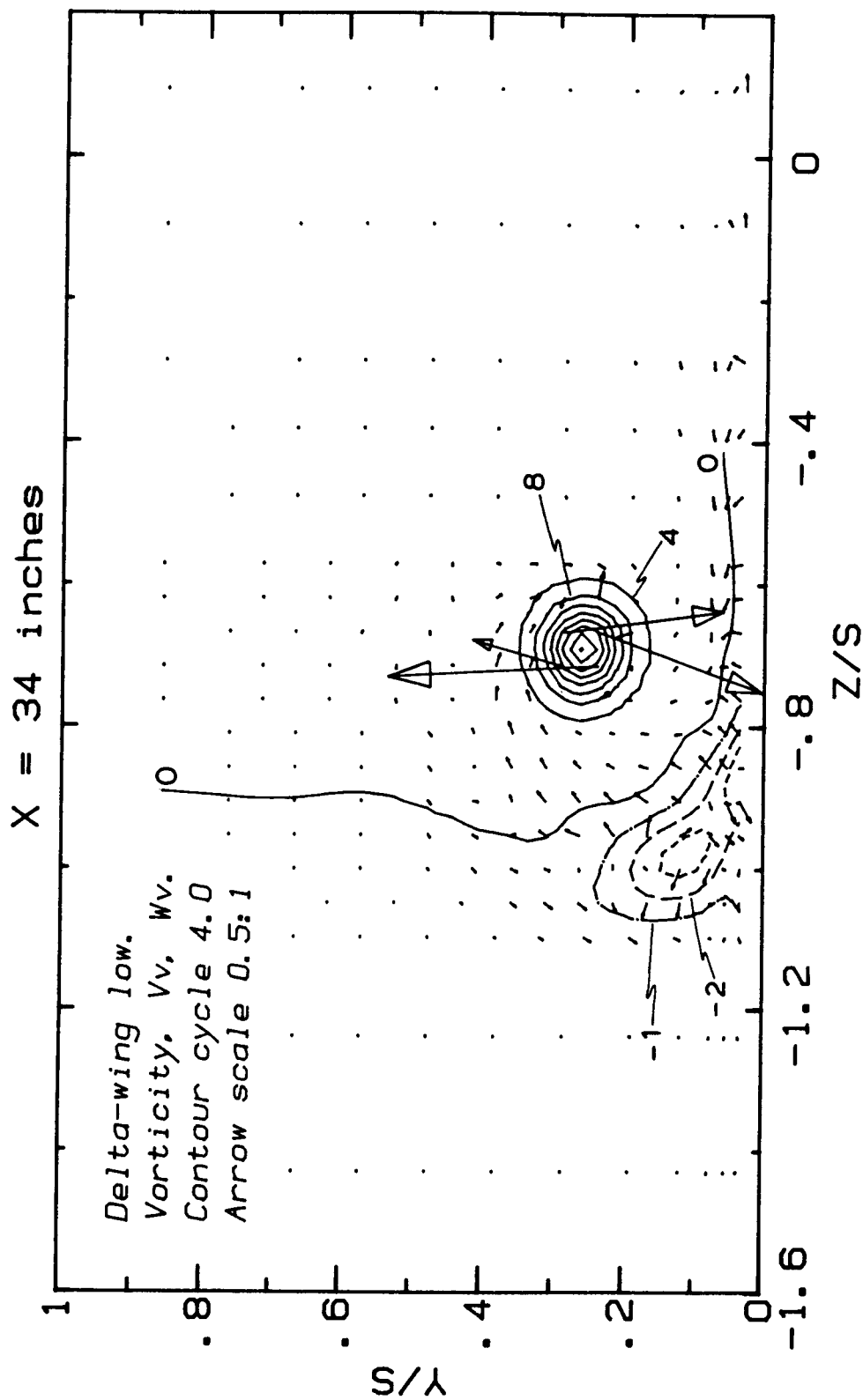
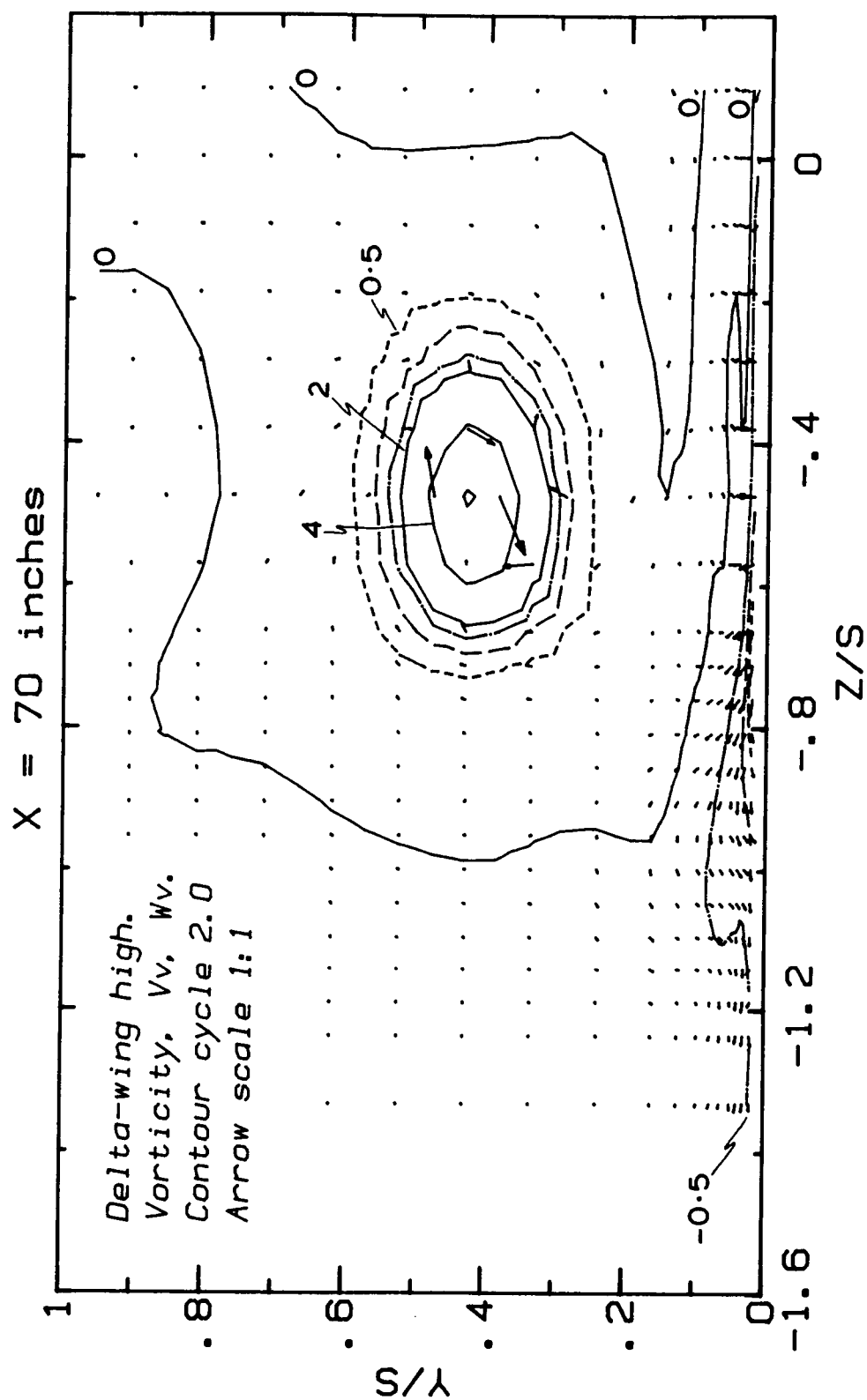


Figure 41. Contours of longitudinal vorticity and vectors with y component 2 and z component 3:

41(a) "delta-wing low" case at  $x/s = 3.238$



41(b) "delta-wing high" case at  $x/s = 6.667$ .

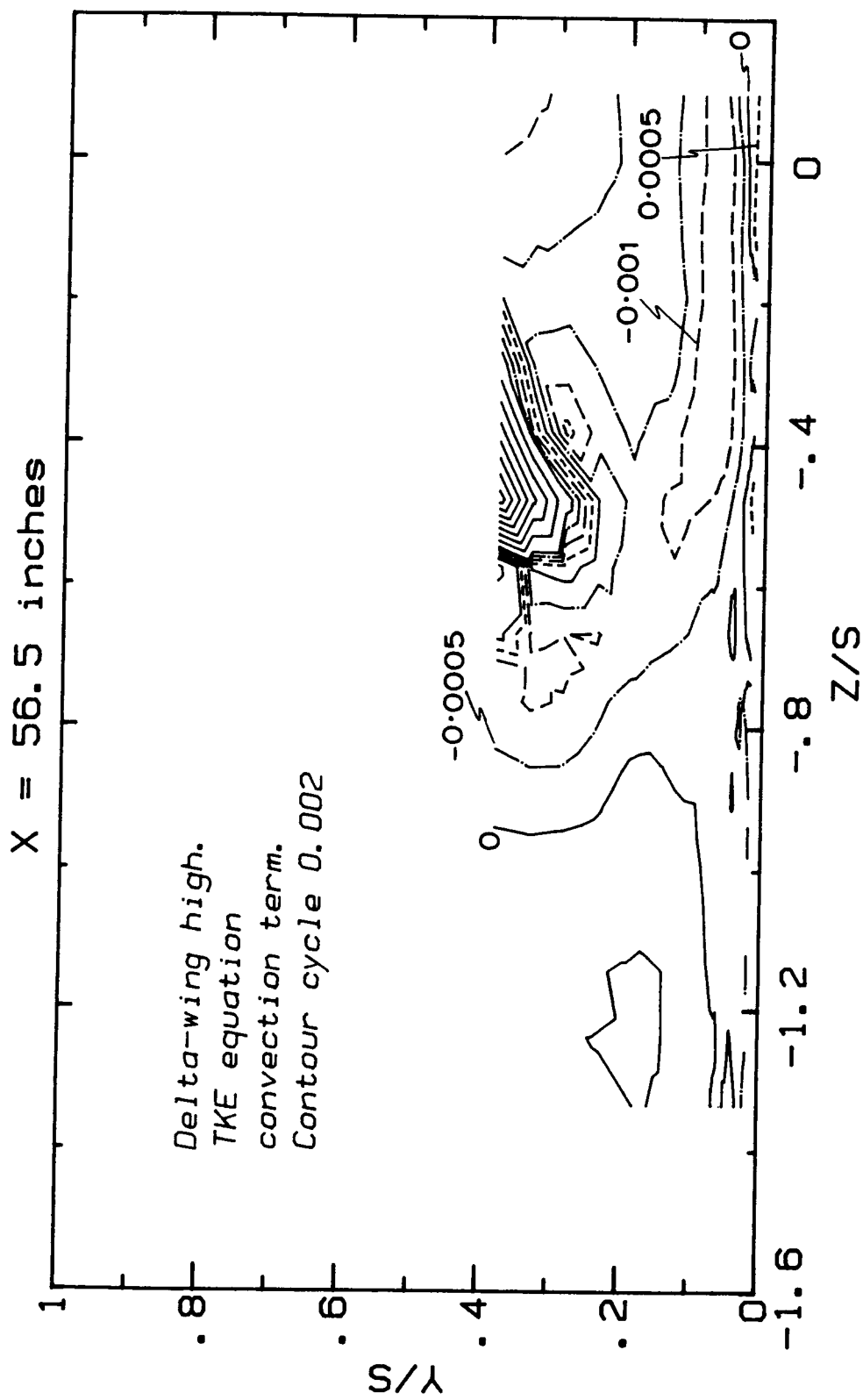
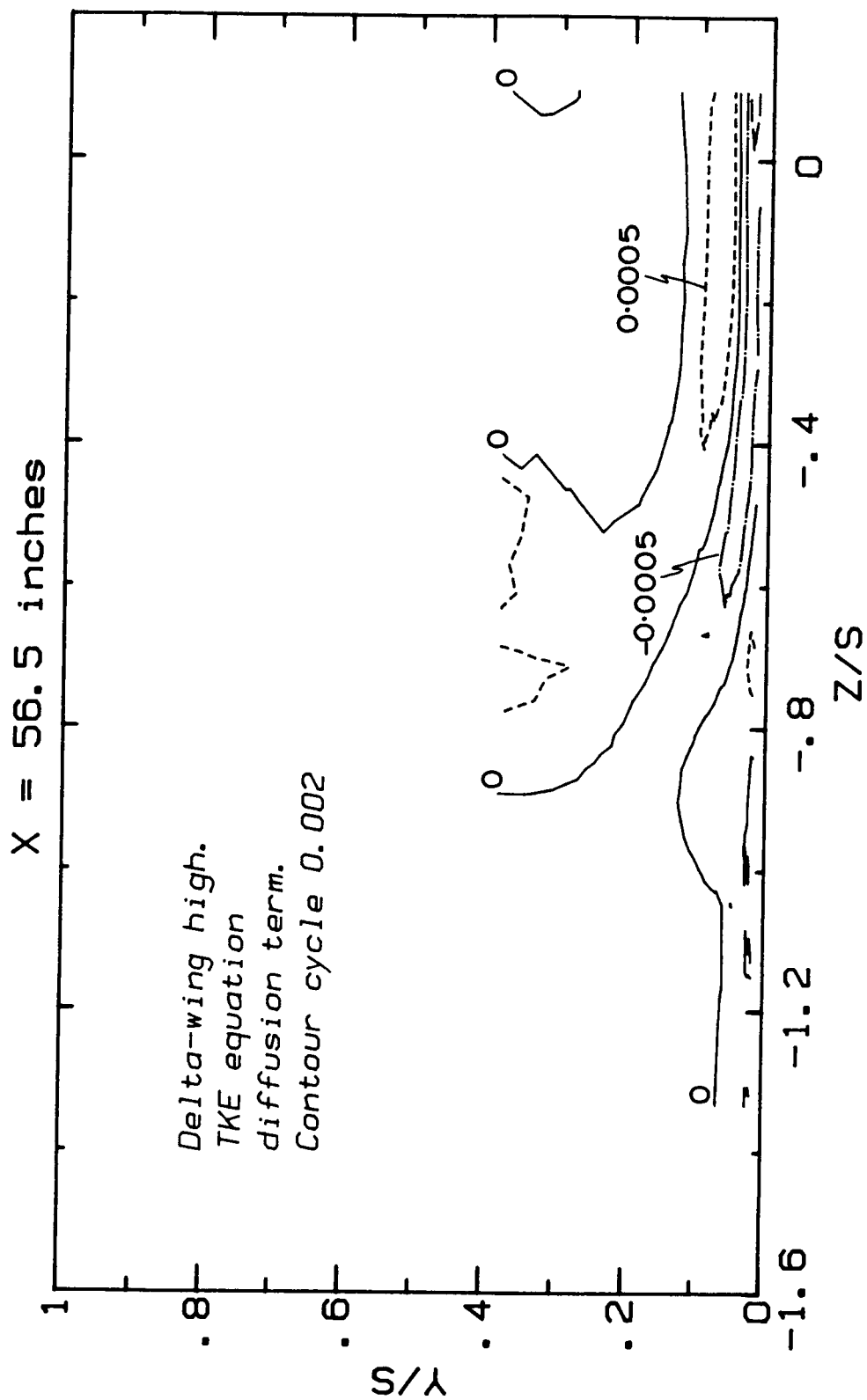
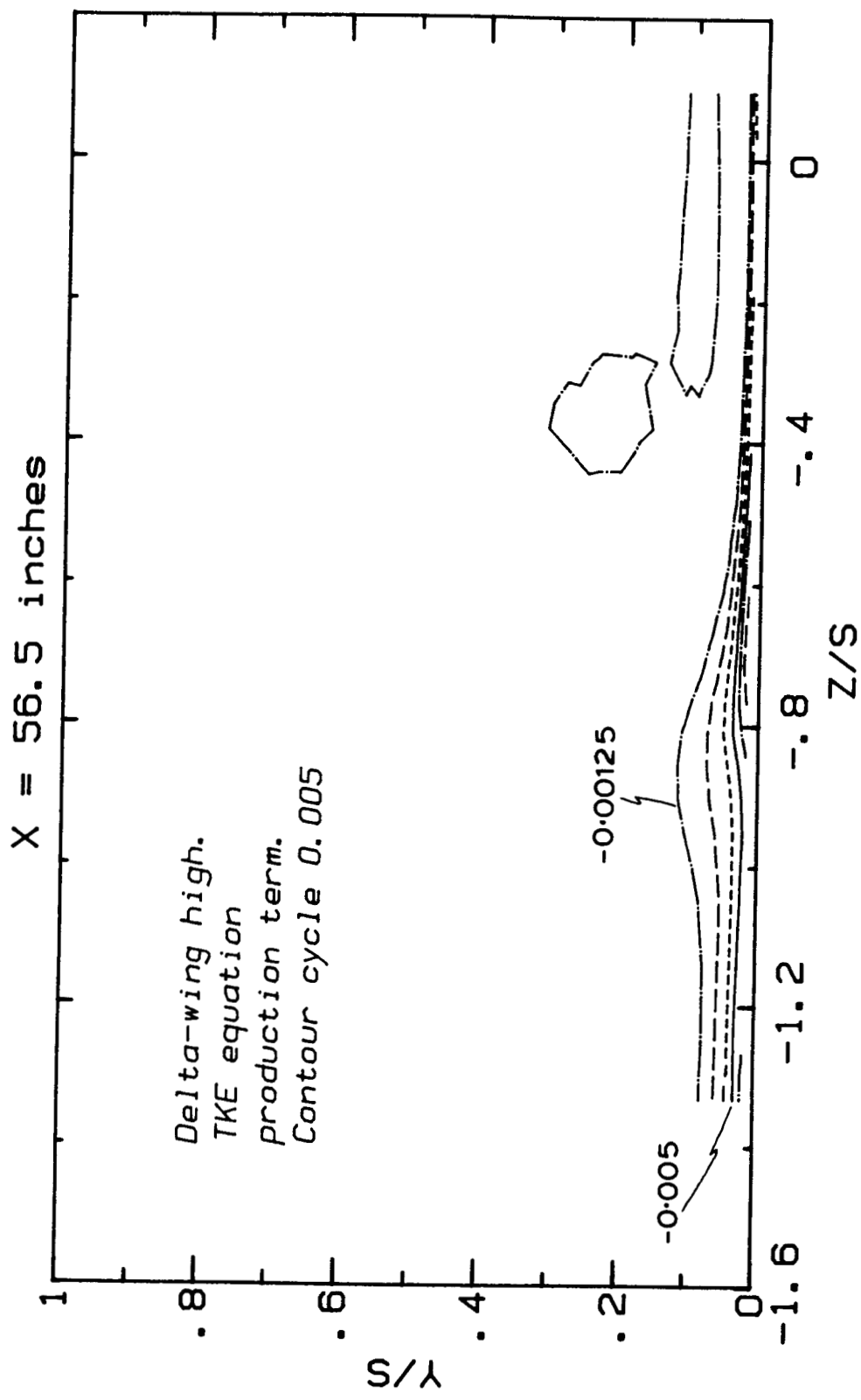


Figure 42. Contours of terms of the turbulent kinetic energy equation at  $x/s = 5.381$  for the delta-wing high case:

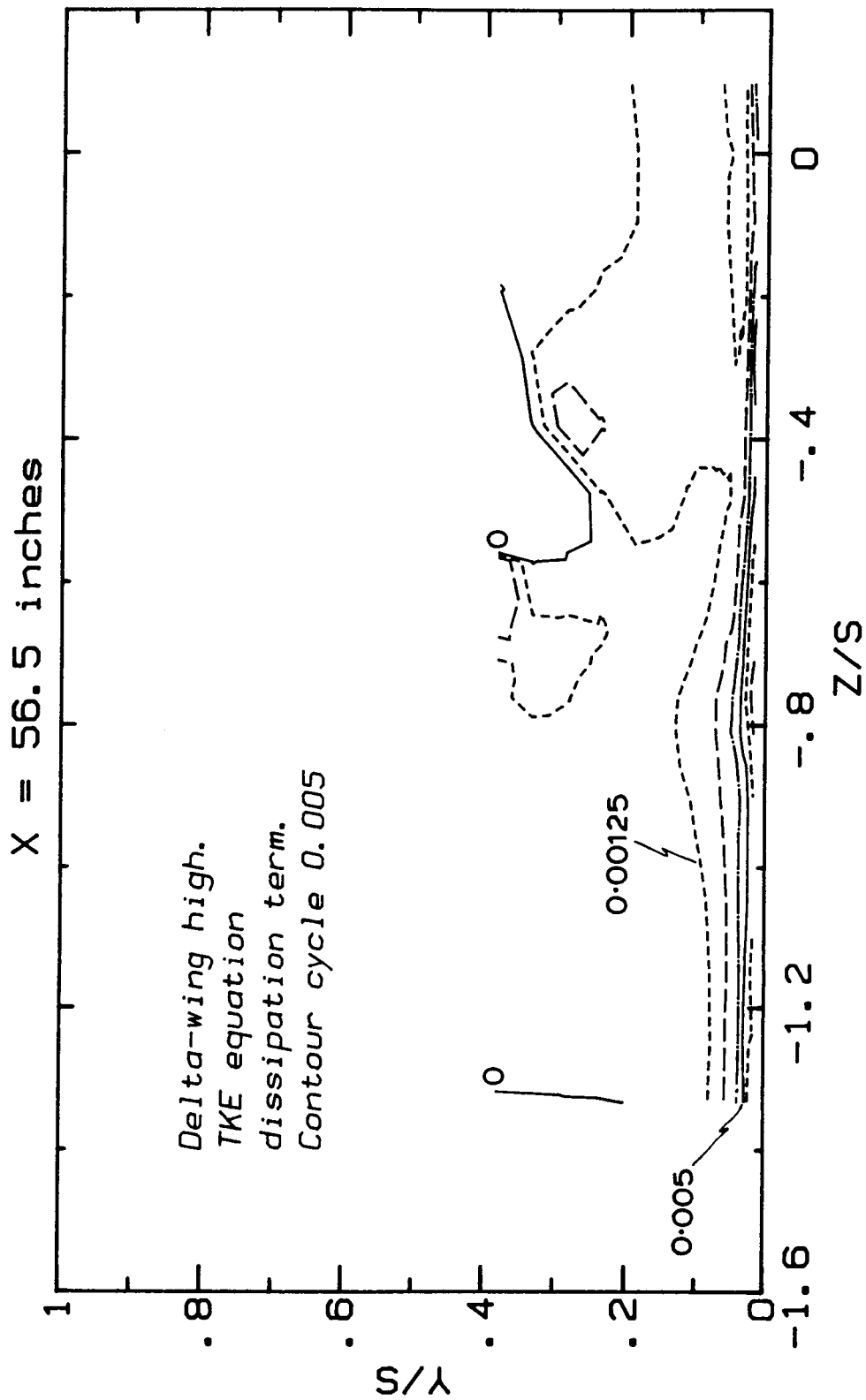
42(a) convection



42(b) diffusion



42(c) production



42(d) dissipation

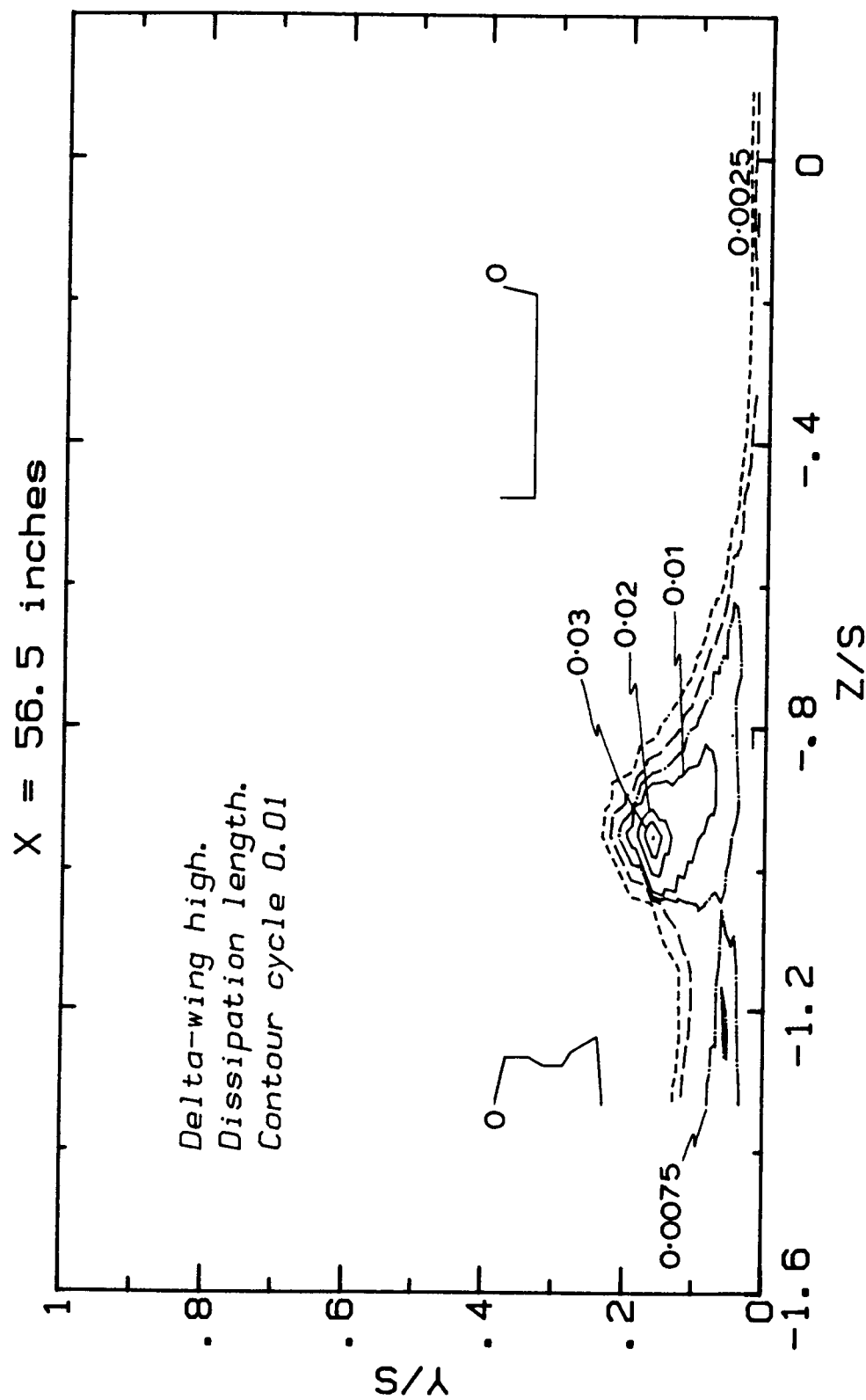


Figure 43. Contours of the dissipation length  $L = (-\bar{u}'\bar{v}')^{3/2}$  (dissipation) at  $x/s = 5.381$  for the delta-wing high case.

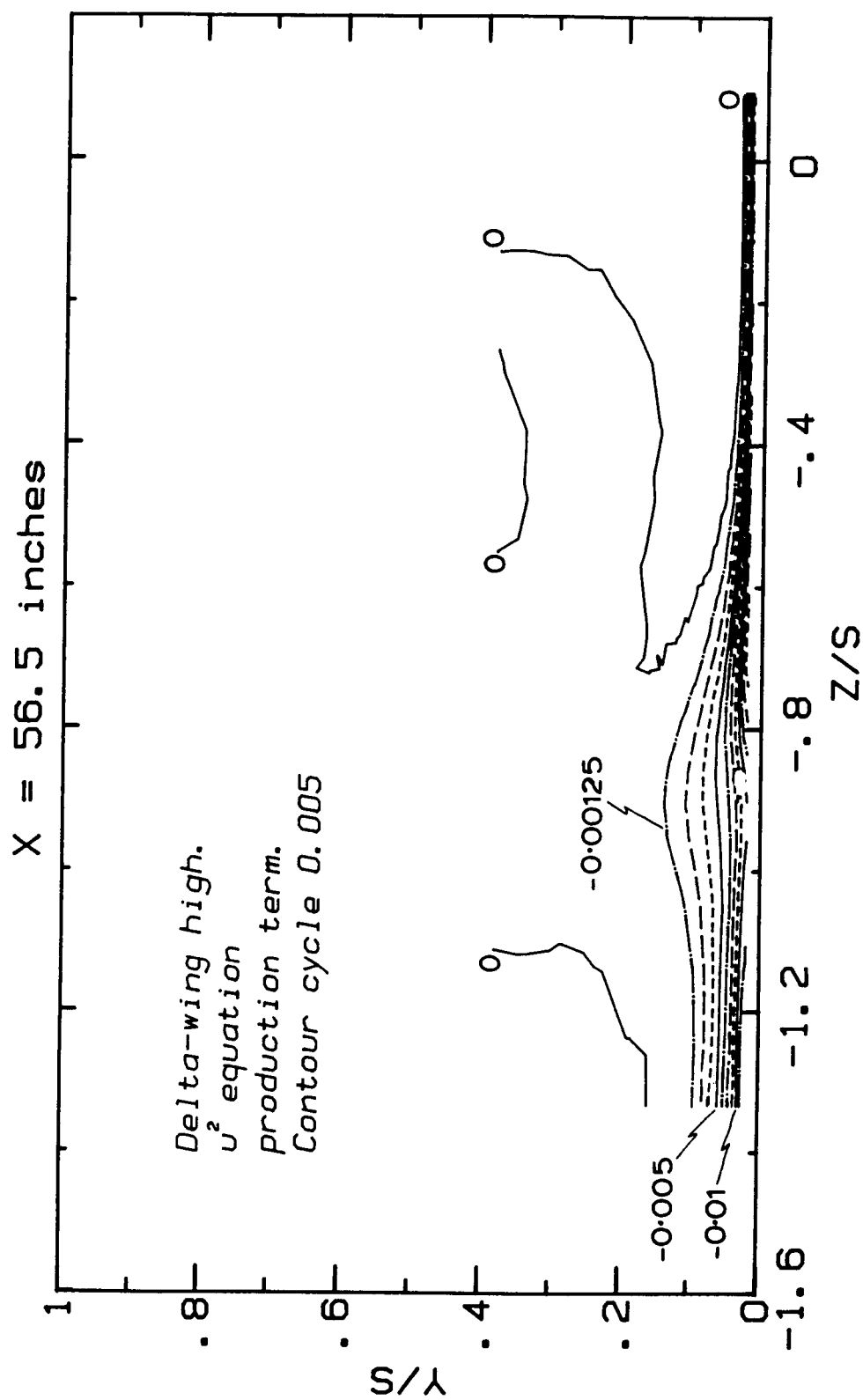
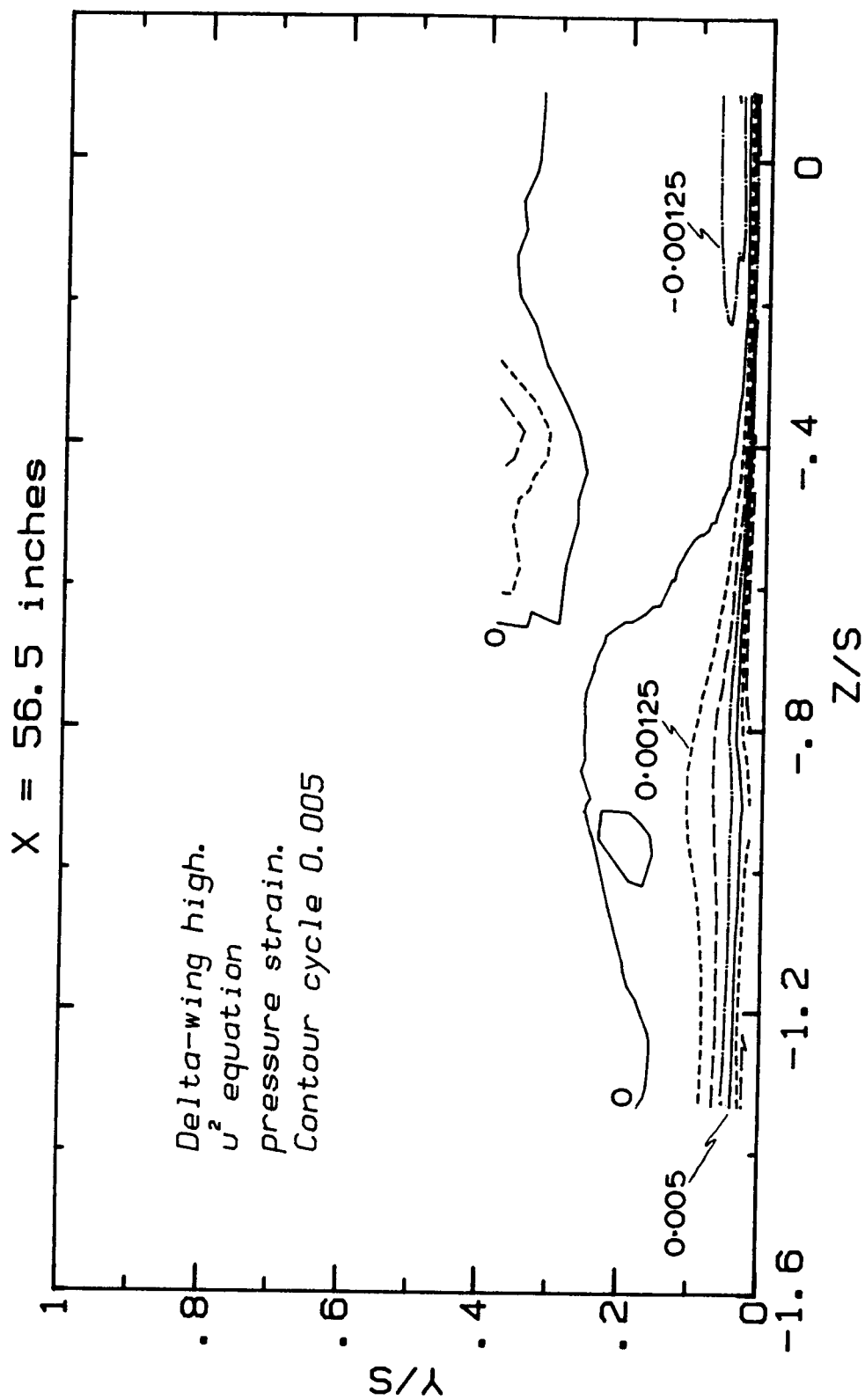
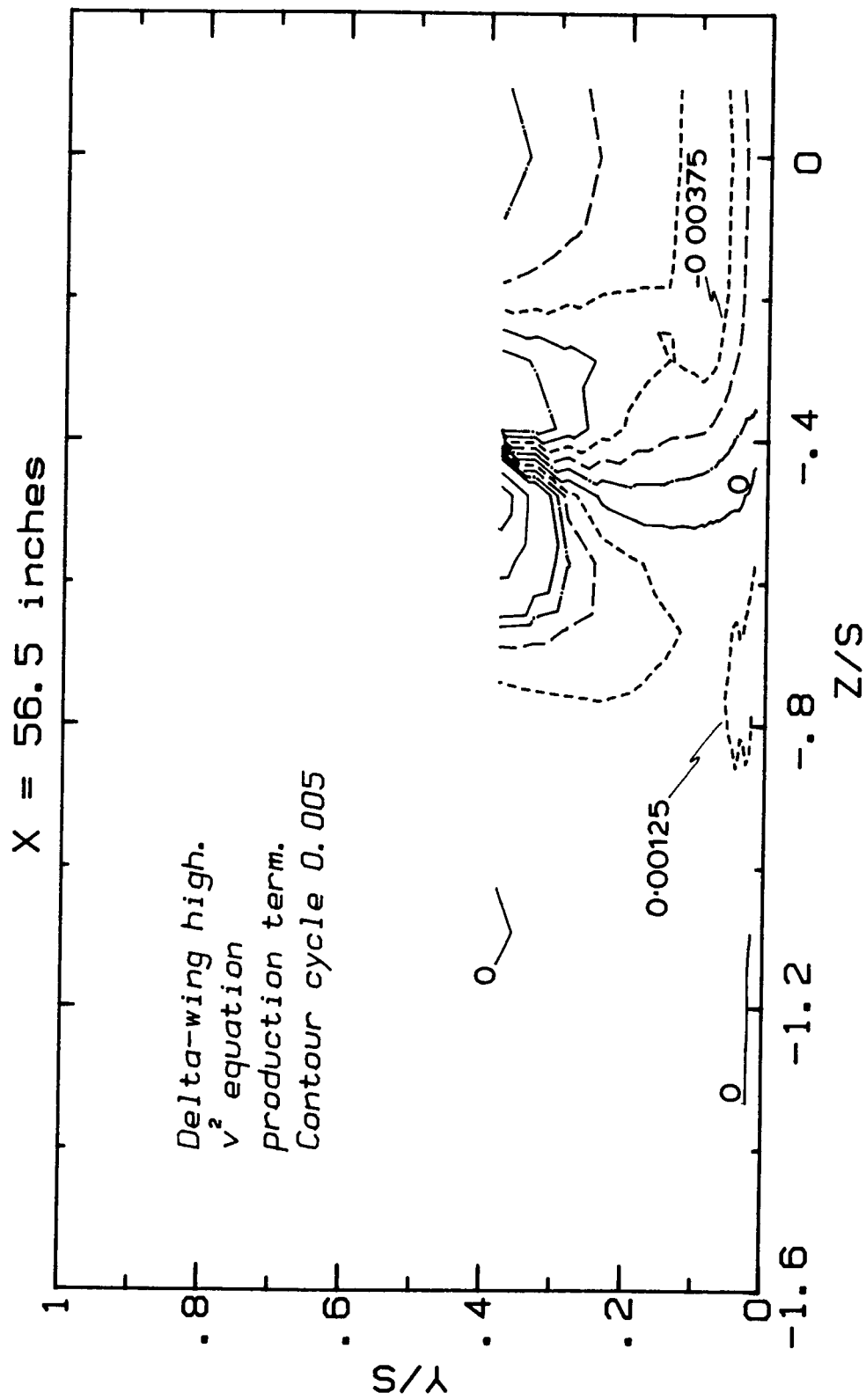


Figure 44. Contours of terms in the Reynolds stress transport equations:

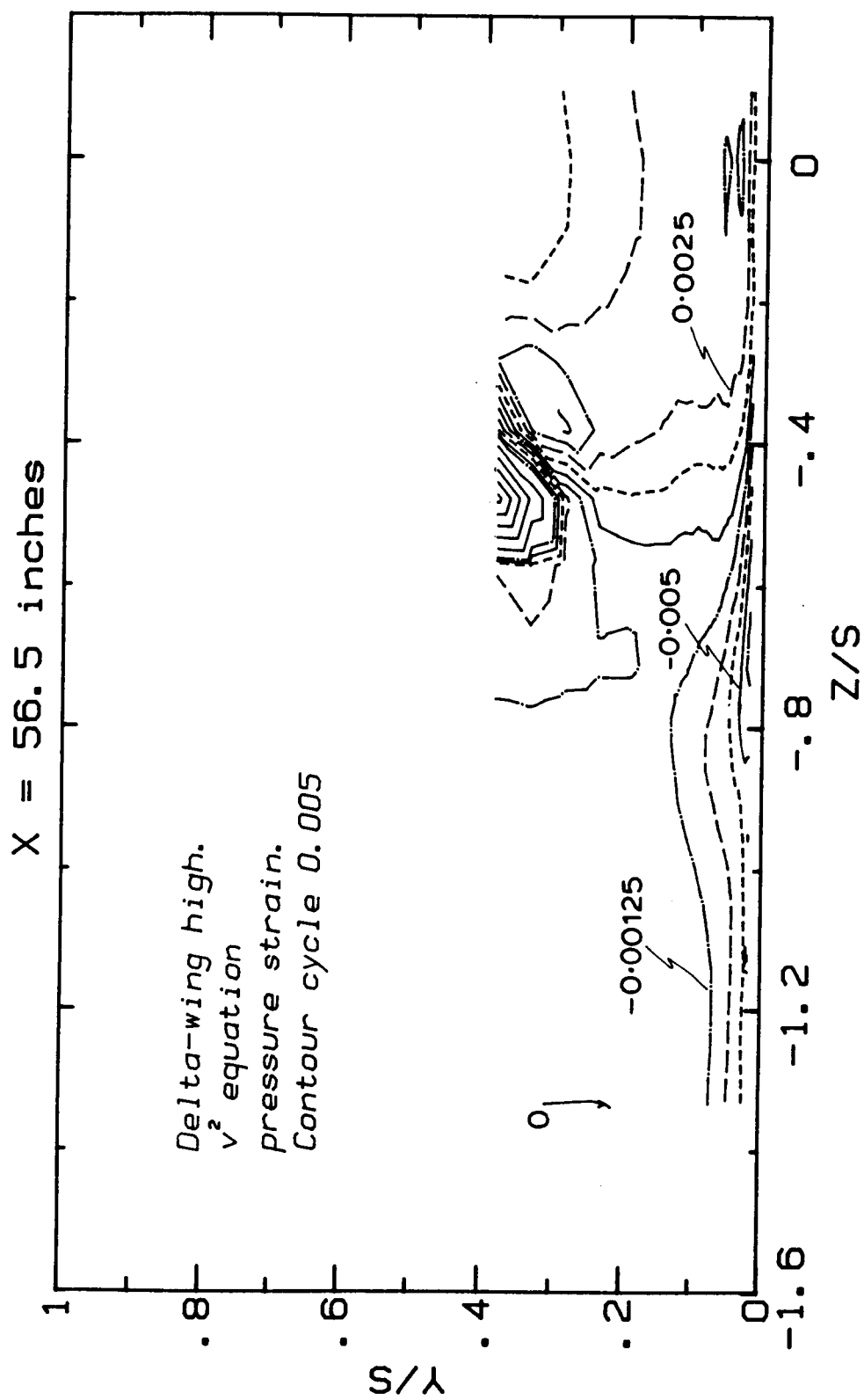
44(a)  $\overline{u^2}$  production

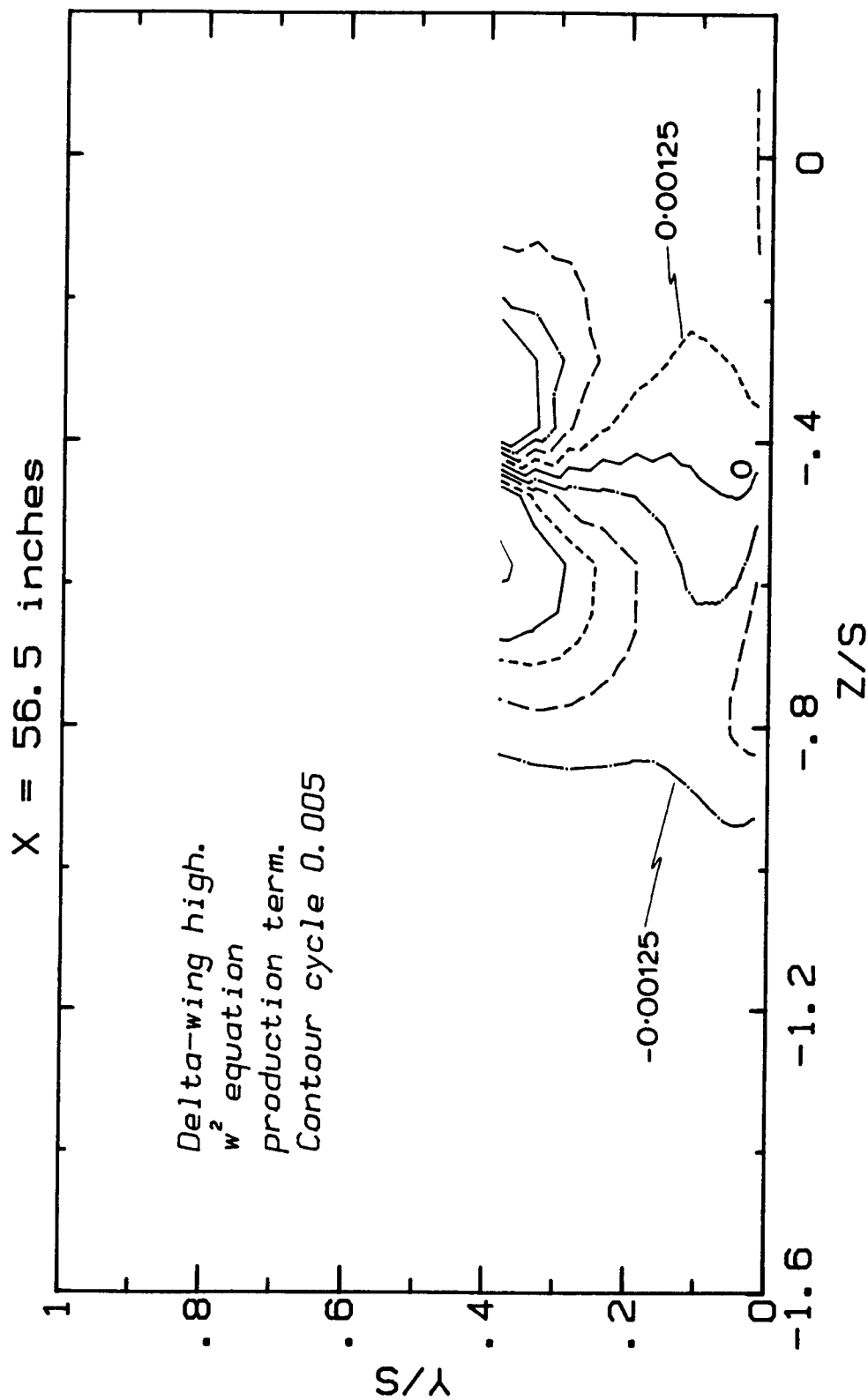


44(b)  $\overline{u^2}$  pressure-strain

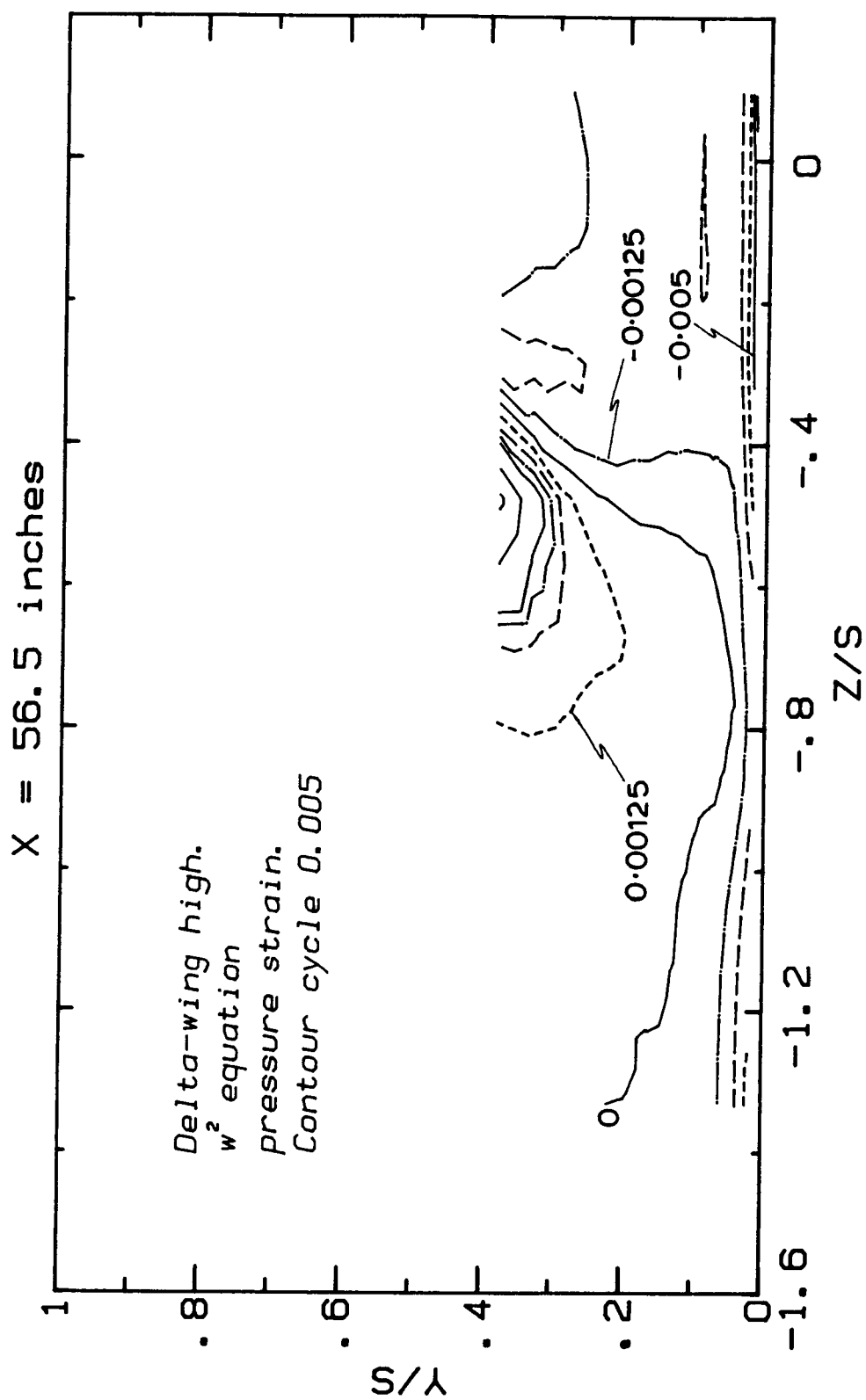


44(c)  $\bar{v}^2$  production

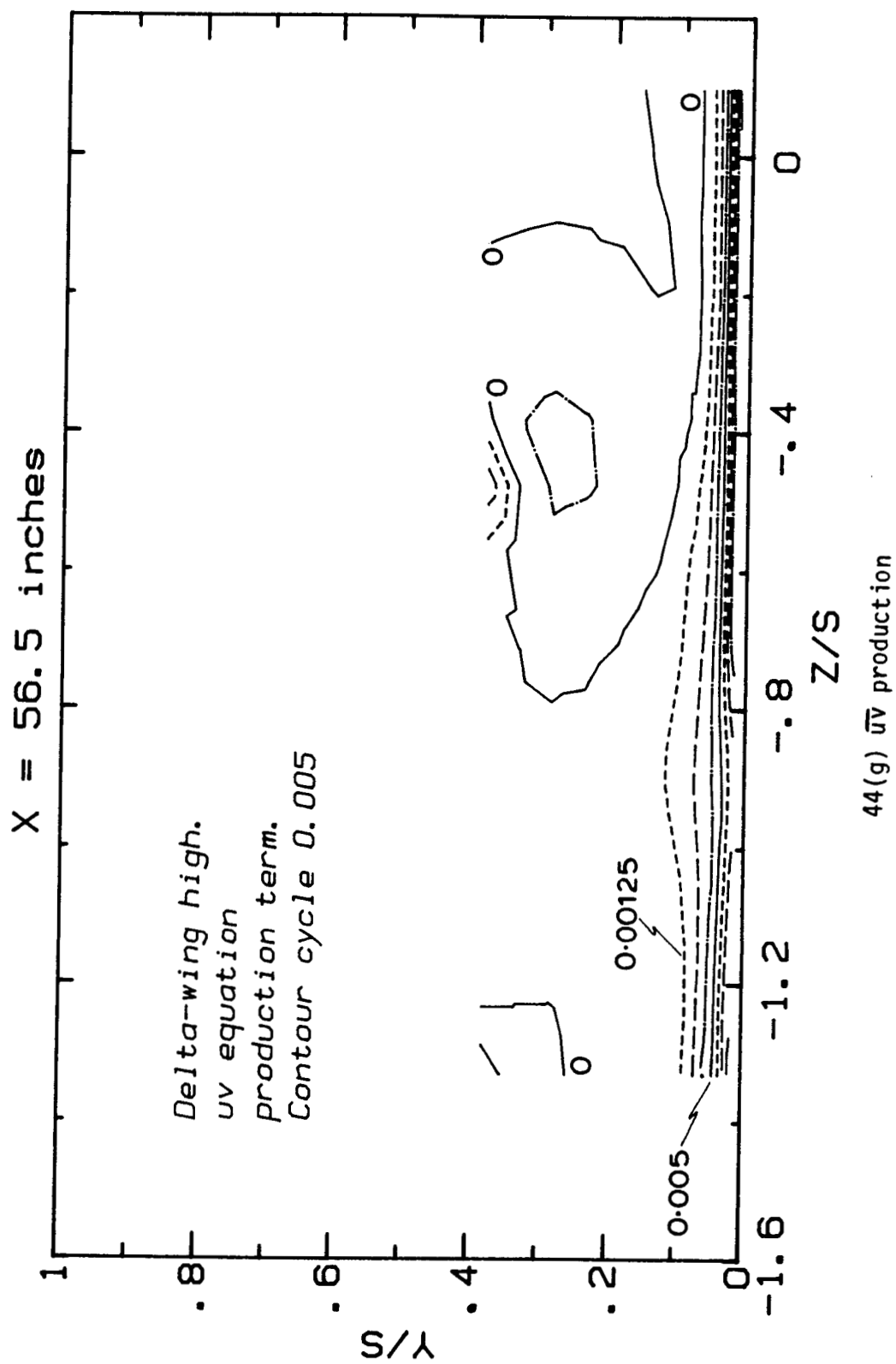


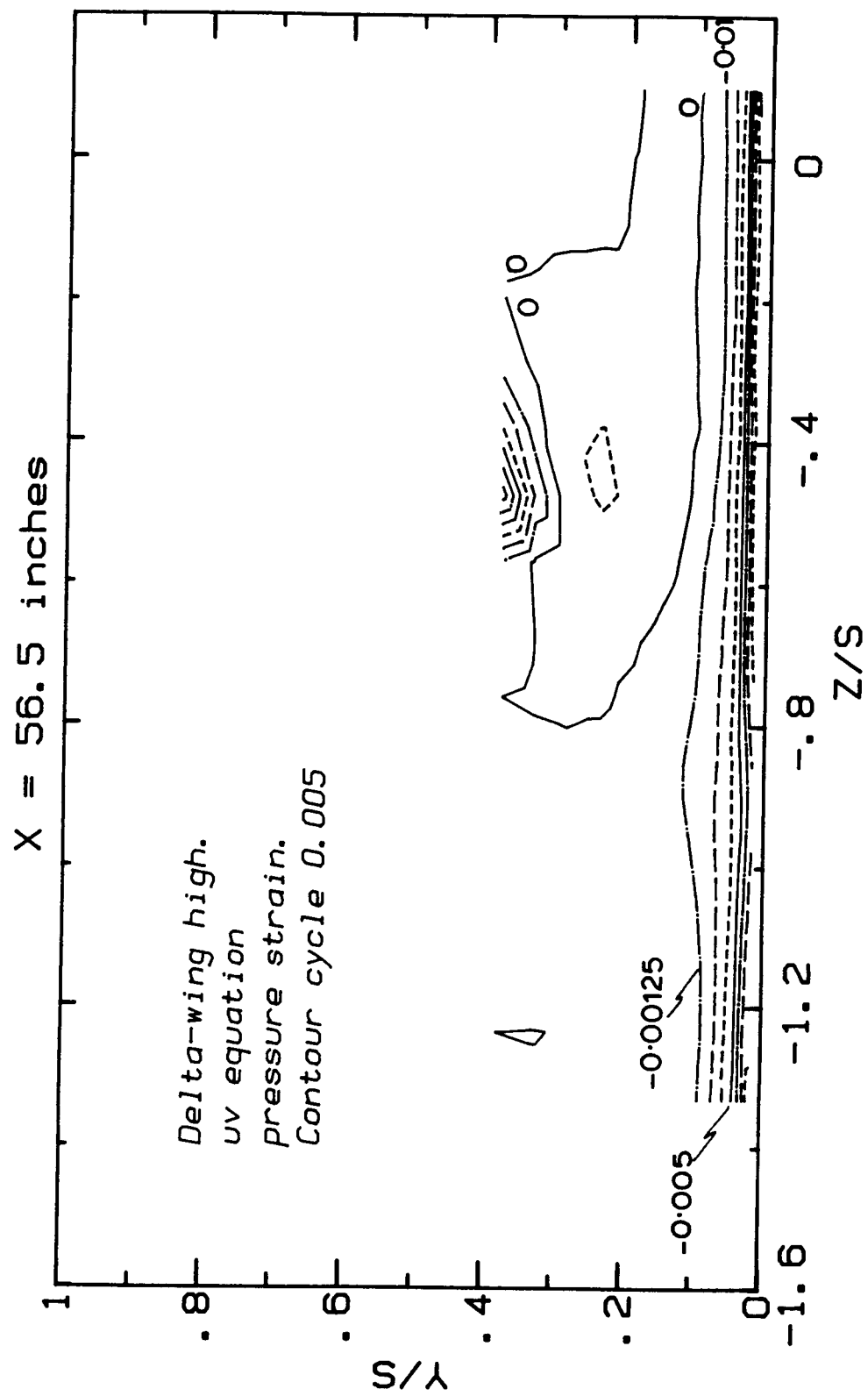


44(e)  $\overline{w^2}$  production

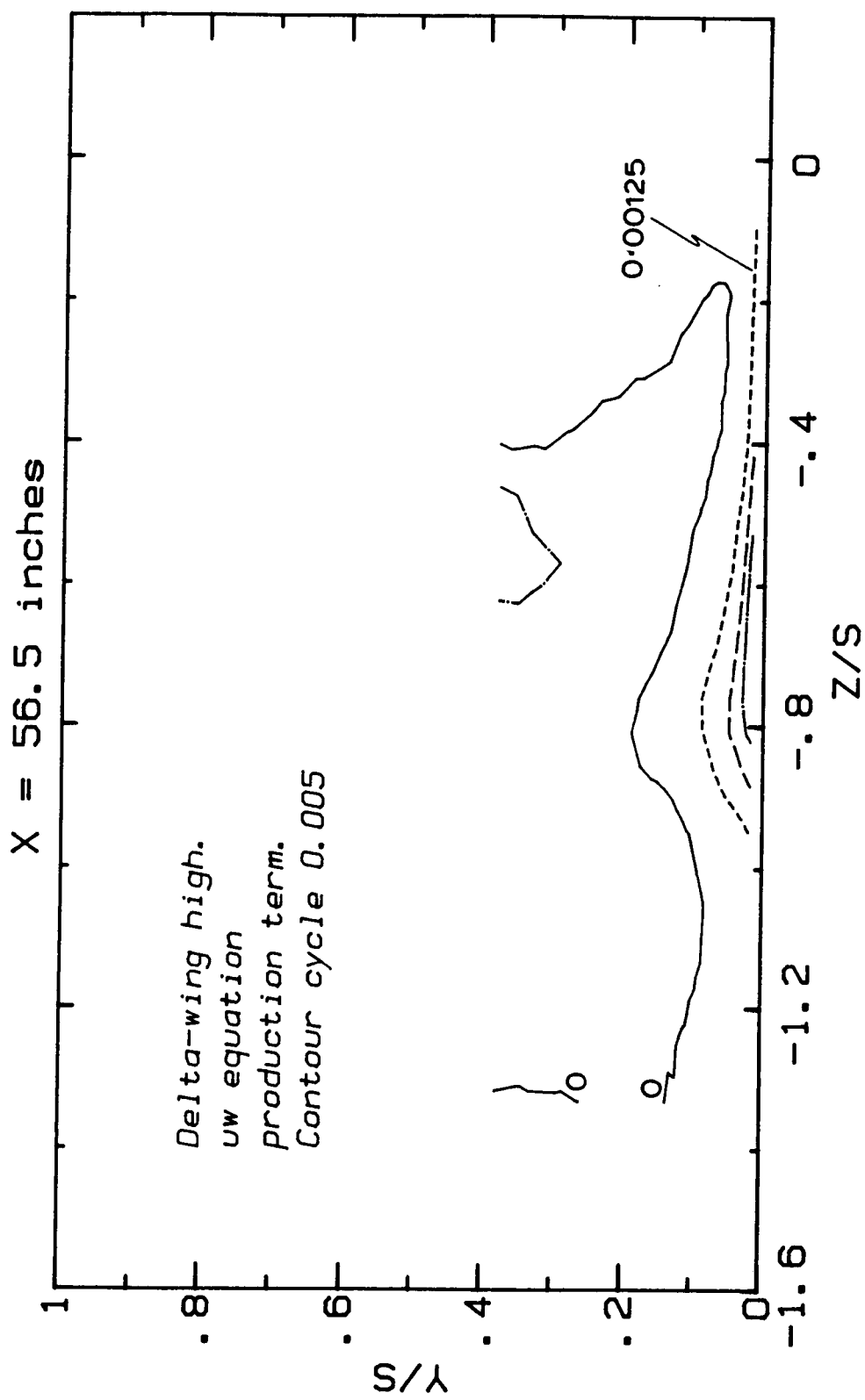


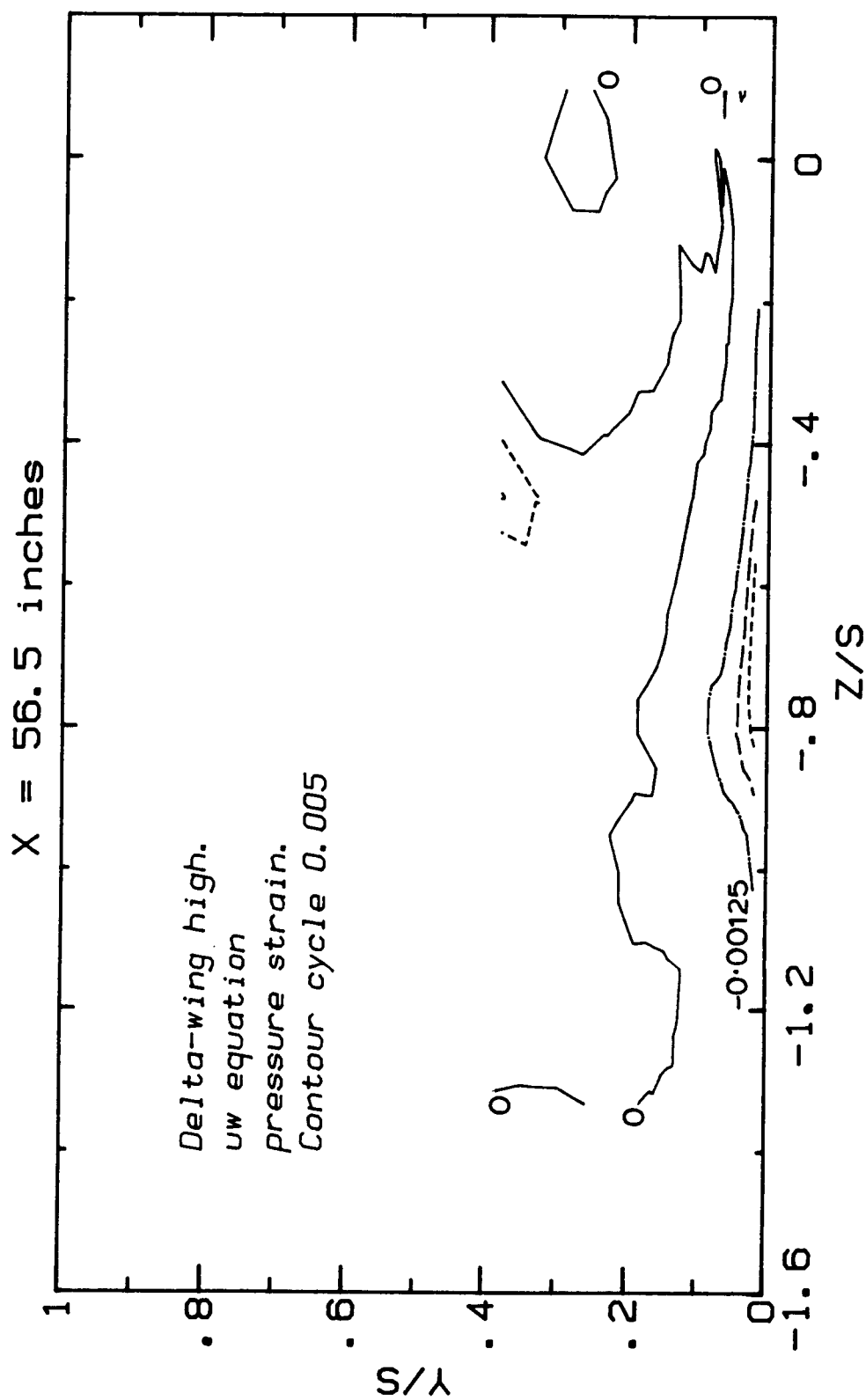
44(f)  $\overline{w^2}$  pressure-strain



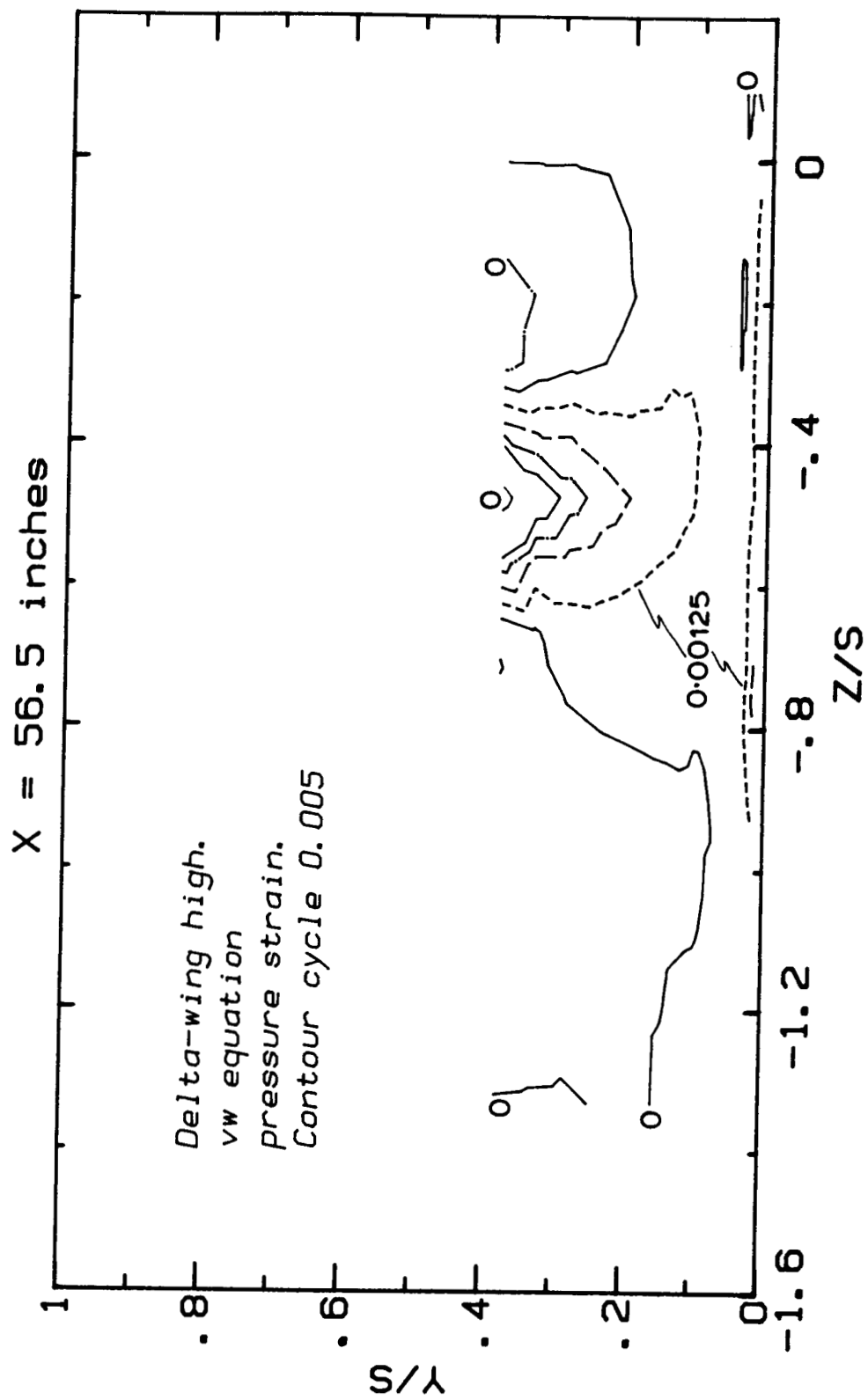


44(h)  $\sigma \epsilon$  pressure-strain

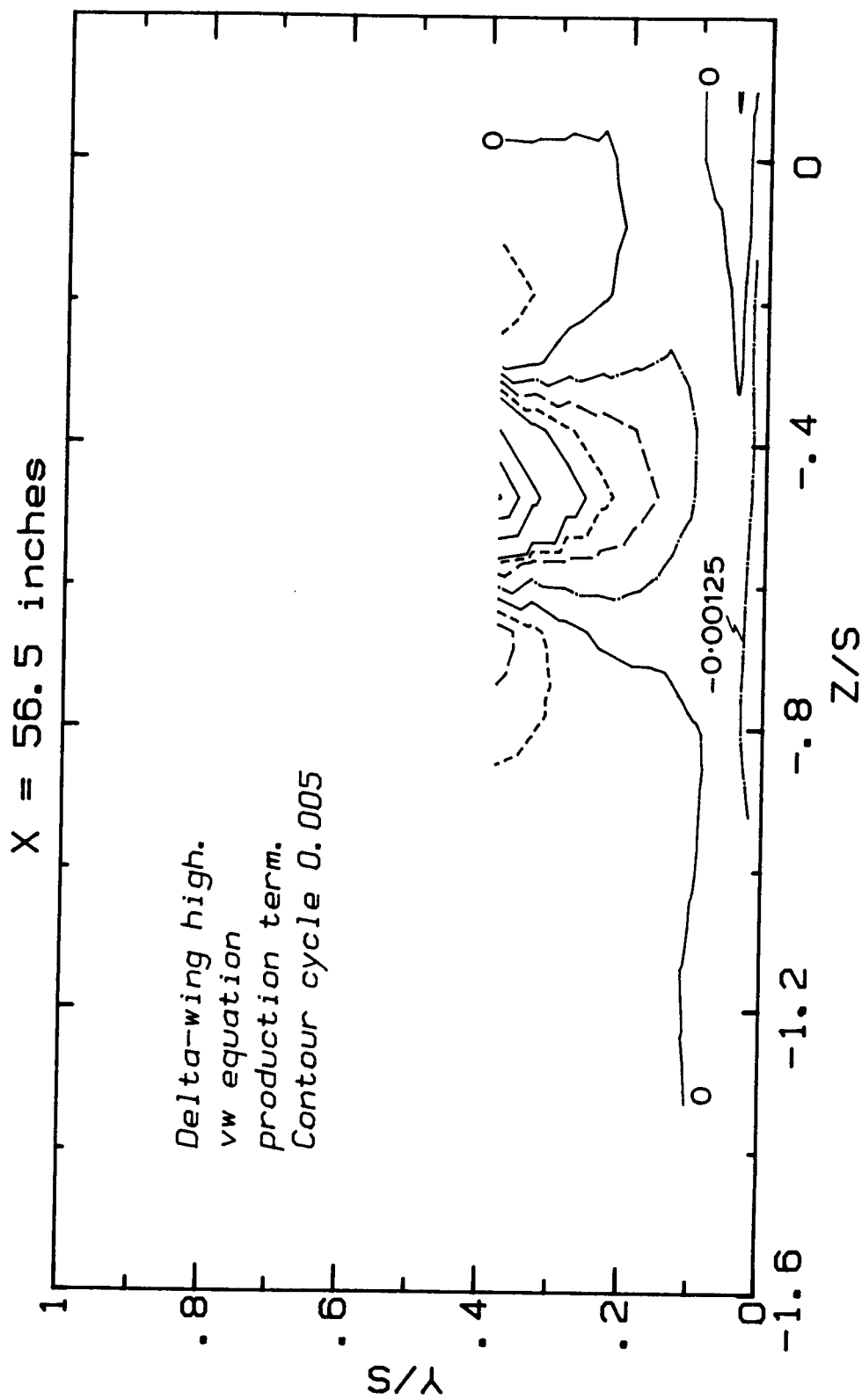




44(j)  $\overline{uw}$  pressure-strain



44(k)  $\nabla w$  production



44(1)  $\overline{vw}$  pressure-strain